01 Apr 1968

The dynamic behavior of steel frame and truss buildings

Dixon Rea

Jack G. Bouwkamp
Missouri University of Science and Technology

R. W. Clough

BULLETIN No. 9, APRIL, 1968—*Rea, Bouwkamp, Clough*—THE DYNAMIC BEHAVIOR OF STEEL FRAME AND TRUSS BUILDINGS

STEEL RESEARCH for construction

THE DYNAMIC BEHAVIOR OF STEEL FRAME AND TRUSS BUILDINGS

—*Dixon Rea*

J. G. Bouwkamp

R. W. Clough

Committee of Structural Steel Producers • Committee of Steel Plate Producers

american iron and steel institute

BULLETIN No. 9, APRIL, 1968

STRUCTURES AND MATERIALS RESEARCH
DEPARTMENT OF CIVIL ENGINEERING
DIVISION OF STRUCTURAL ENGINEERING
AND STRUCTURAL MECHANICS

THE DYNAMIC BEHAVIOR OF STEEL FRAME AND TRUSS BUILDINGS

A Report of an Investigation

by

DIXON REA
Assistant Specialist

J. G. BOUWKAMP
Associate Professor of Civil Engineering

R. W. CLOUGH
Professor of Civil Engineering

to

American Iron and Steel Institute, New York

College of Engineering
OFFICE OF RESEARCH SERVICES
University of California
Berkeley, California

September 1966

Printed in U.S.A. 468 3000

TABLE OF CONTENTS

Table of Contents – (Cont.)

ABSTRACT

This report describes experimental and analytical studies of the dynamic behavior of the East Building of the University of California's new Medical Center at San Francisco, California. It also describes experimental tests conducted on the East Building's mechanical service tower and on an adjacent elevator tower.

Experimental tests on the East Building were conducted in the summers of 1964 and 1965. Vibrations were produced by eccentric-mass-type vibration generators. Frequency responses, time responses, and mode shapes were observed. In the summer 1964 tests, the first mode east-west had 2% of critical damping and the first mode north-south had 1.8%; the values of damping for the higher modes lay in the range 0.4% to 0.9% of critical. In the summer 1965 tests, the damping capacity measurements were mostly in the range 5 to 10% of critical. The cause of this increase in damping capacity was investigated in the fall 1965 tests.

The fall 1965 tests showed that although the East Building was designed as free-standing, it was dynamically coupled to its adjacent buildings. The relatively large damping capacity of this coupled system has been attributed to the Coulomb damping provided by non-structural connections between buildings.

An analytical model of the East Building was formulated to provide behavior corresponding to the summer 1964 test results. A standard open-frame-type model was found capable of representing the dynamic behavior of the real structure. The analytical model was subjected to the El Centro earthquake ground acceleration record in a digital computer analysis. With 5% critical damping in the first few modes, no members of the frame yielded, but when the intensity of the earthquake was increased by a factor of 1.3, some members did yield.

LIST OF FIGURES

List of Figures – (Cont.)

List of Figures – (Cont.)

LIST OF TABLES

CHAPTER 1

INTRODUCTION

1.1 GENERAL

High-speed digital computers and matrix algebra analytical techniques have made feasible the computation of the response of complex structures to earthquake loading. The analytical and computational techniques have been refined to the point where confidence in the design is limited only by a lack of accuracy in basic input data. (For example, the damping capacity of a structure cannot be calculated in the design stages, and values of damping capacity must be assumed for any refined analysis.) The main purpose of this research program has been to increase the state of knowledge about the basic dynamic properties of multi-story frame and trussed steel buildings.

American Iron and Steel Institute recognized that this lack of basic experimental data was hampering further refinements in design techniques, and they agreed to sponsor a research program to investigate the dynamic properties of three multi-story buildings of the new structural complex at the University of California's Medical Center in San Francisco. The new complex consists of two multi-story buildings, a service tower associated with each, and an elevator tower. Of these structures, the east multi-story building, its service tower, and the elevator tower were tested. There were numerous reasons why these buildings were suitable for this test program:

i. The buildings are of modern design, and the results will be applicable to similar buildings which will be constructed in the future.
ii. All the buildings had two axes of symmetry, which meant translational and torsional modes could be excited independently.
iii. The University of California was willing to grant permission to conduct the tests.
iv. The location of the buildings was convenient to the Berkeley Campus.

The scope of the investigation embraced both an experimental study and an analytical study. The experimental study consisted of measuring the resonant frequencies,mode shapes and damping capacities of the buildings. In the analytical study, the experimental results for the East Building were used in the formulation of a model which would behave in a manner dynamically similar to the real structure. Such a model is of great value in aseismic design because it can be subjected to known earthquake ground acceleration records, and the response of the real structure under similar earthquakes can be predicted.

1.2 ACKNOWLEDGMENT

The authors of the report would like to thank the following organizations and individuals for their contributions to the project:

The Committees of Structural Steel and Steel Plate Producers of American Iron and Steel Institute, New York, for funding the research project.

The University of California for its permission to test the buildings.

Reid, Rockwell, Banwell and Tarics, Architects and Engineers, San Francisco, for their help in planning the tests.

The Office of Architects and Engineers of the University of California, San Francisco, for their cooperation in arranging the tests.

The Dinwiddie Construction Company, San Francisco, for its assistance with practical problems during the experimental work.

The Office of Architecture and Construction, Department of General Services, State of California, for making available the vibration generators.

The California Institute of Technology for lending four accelerometers.

The following students who worked on the project at various times: R. Engelhart, I. King, D. MacKenzie, N. Mostaghel and J. Nadherny.

CHAPTER 2

DESCRIPTION OF FACILITIES

2.1 GENERAL

The new structural complex at the Medical Center of the University of California in San Francisco consists of two multi-story buildings, two mechanical service towers and an elevator tower. One mechanical service tower is associated with each multi-story building and the elevator tower serves all buildings through a connecting corridor as shown in Fig. 2.1. The Main East Building and its service tower are identical in plan to their West counterparts, although the West Building is one story higher than the 15-story East Building. In this test program the East Building, its associated service tower, and the elevator tower were tested, and these buildings are described individually below. In addition, the connections between these buildings are also described because they were found to have considerable effect on the dynamic response of both the East Building and its service tower.

2.2 EAST BUILDING

The East Building is 195 ft. (15 stories) high, and its outside plan dimensions are 107 ft. by 107 ft. The steel columns of the moment-resistant steel frames (see Fig. 2.2) are placed 10 ft. in from the perimeter of the building and are located on center distances of 30 ft. 1½ in., 33 ft. 4 in., and 30 ft. 1½ in. along each side. The schedule of the interior columns and the story heights is shown in Fig. 2.3, and the schedule of the corner columns is shown in Fig. 2.4. The girder-to-column connections have been described by Bouwkamp (1965), and the steel layout of a typical floor is shown in Fig. 2.5. The reinforced slabs were cast in situ using lightweight concrete.

2.3 SERVICE TOWER AND ELEVATOR TOWER

The mechanical service tower and elevator towers are constructed of vertical steel trusses stiffened by encasing them entirely in concrete. Fig 2.6 shows the bare steel truss of the east service tower, and Fig. 2.7 shows the completed service tower of the West Building. The height of both the east service tower and the elevator tower is approximately 200 ft. The plan of these buildings is also shown in Fig. 2.1, the elevator tower being 30 ft. x 30 ft., and the service tower 20 ft. x 36 ft.

The central section of each mechanical service tower is occupied by a stairwell, and the spaces on either side of the stairwell by piping and ventilation ducts.

The elevator tower contains 6 elevator shafts for vertical traffic flow. It serves both main buildings through a connecting corridor which leads into corridors around the central core of each main building. The connecting corridor also provides access to the previously existing buildings, as shown in Fig. 2.1.

2.4 CONNECTIONS BETWEEN BUILDINGS

Although the buildings have been designed as free-standing structures, there are two types of non-structural connections which exist on every floor level at points of access from one building to another. First, bellows-type aluminum ducts run the whole height of the buildings for weatherproofing purposes (Fig. 2.8); secondly, in order to permit traffic between buildings, steel plates bolted to ledges on the service tower and to the floor slabs of the connecting corridor span the gap to the East Building, where they rest freely on the floor slabs (see Figs. 2.8 and 2.9).

Furthermore, structural connections between the East Building and its service tower are present at the ground floor level (labeled floor no. 2, as in Fig. 3.6), and at the foundation level. These connections consist of reinforced concrete beams and slabs as shown in Fig. 2.10.

CHAPTER 3

EXPERIMENTAL TESTS

3.1 EXPERIMENTAL APPARATUS

3.1.1 Vibration Generators.

Forced vibrations were produced by two vibration generators or shaking machines, one of which is shown in Fig. 3.1. These machines were developed at the California Institute of Technology under the supervision of the Earthquake Engineering Research Institute for the Office of Architecture and Construction, State of California. Each machine consists of an electric motor driving two pie-shaped baskets or rotors, each of which produces a centrifugal force as a result of the rotation. The two rotors are mounted on a common vertical shaft and rotate in opposite directions so that the resultant of their centrifugal forces is a sinusoidal rectilinear force. When the baskets are lined up in the position shown in Fig. 3.1, a peak value of the sinusoidal force will be exerted. The structural design of the machines limits the peak value of force to 5,000 lbs. This maximum force may be attained at a number of combinations of eccentric mass and rotational speed, since the output force is proportional to the square of the rotational speed as well as the mass of the baskets and the lead plates inserted in the baskets. The maximum force of 5,000 lbs. can be reached for a minimum rotational speed of 2.5 cps when all the lead plates are placed in the baskets. At higher speeds the eccentric mass must be reduced in order not to surpass the maximum force of 5,000 lbs. The maximum operating speed is 10 cps, and the minimum practical speed is approximately 0.5 cps. At 0.5 cps with all lead plates in the baskets, a force of 200 lbs. can be generated. The relationship between output force and frequency of rotation of the baskets for different basket loads is shown in Fig. 3.2.

The speed of rotation of each motor driving the baskets is controlled by an Electronic Amplidyne housed in a control unit (see Fig. 3.1). The control unit allows the machines to be synchronized or operated 180° out-of-phase. This makes it convenient to excite, in structures with a line of symmetry, either pure torsional or pure translational vibrations without changing the position of either machine. A complete description of the vibration generators is given by Hudson (1962).

3.1.2 Accelerometers.

The transducers used to detect horizontal floor accelerations of the buildings were Statham Model A4 accelerometers. In the 1964 tests ±1-g accelerometers had sufficient sensitivity to give large traces on the recording paper, but in all subsequent tests ± 0.25-g accelerometers were required because the vibration amplitudes had become much smaller.

3.1.3 Equipment for measurement of frequency.

Vibration excitation frequencies were determined by measurement of the speed of rotation of the electric motor driving the baskets. A tachometer attached to a rotating shaft driven by a transmission belt from the motor, generated a sinusoidal signal of frequency 300 times the frequency of rotation of the baskets. The maximum accuracy of frequency measurements was thus ± 1 count in the total number of counts in a period of 1 second (the gating period), i.e., ± 1/3 of 1% at 1 cps and ± 1/9 of 1% at 3 cps.

3.1.4 Equipment for measurement of phase angles.

In order to determine the phase relationship between the excitation and response, it was necessary to obtain a signal indicating the basket position. This signal was obtained by attaching a small magnet to one basket and a coil of wire to the stationary structure supporting the baskets so that the magnet's circular path passed close to the coil. Each time the magnet passed the coil, a small electrical pulse was generated which was recorded alongside the acceleration traces on the oscillograph. The pulse signal could be generated for whatever instantaneous basket position was desired by proper positioning of the magnet on the basket.

3.1.5 Recording equipment.

The electrical signals from all accelerometers and the pulse indicating the basket position were fed to amplifiers and then to a Honeywell Visicorder ultraviolet recorder with 6''-wide chart. In frequency-response tests, the counter reading was observed and recorded manually on the chart alongside the associated traces.

3.2 EXPERIMENTAL PROCEDURE AND REDUCTION OF DATA

3.2.1 Frequency response

Experimental data for frequency-response curves were collected for a number of basket load combinations over their effective frequency ranges. For each value of eccentric mass, the rotational speed of the baskets was increased until the acceleration traces on the chart were large enough for measurement. Above this frequency the excitation frequency was increased in steps until the speed limit of the machines for that eccentric mass was reached. Near resonance, where the slope of the frequency-response curve is changing most rapidly, these steps were made as small as the speed control system would allow, but were relatively large in regions away from resonance. Each time the frequency was set at a particular value, the vibration response was given sufficient time to become steady-state, and then the acceleration traces were recorded. At the same time, the frequency of vibrations as displayed by the digital counter was observed and written on the chart with its corresponding traces.

These experimental data are displayed in this report in the form of normalized acceleration responses from which both resonant frequencies and damping capacities were derived. The recording acceleration amplitudes were normalized by dividing them by their corresponding frequency squared, which for the case of linear stiffness and damping, makes the frequency response equivalent to one that would have been obtained for a constant exciting force. In the summer and fall of 1964 the frequency responses were normalized with respect to 1 cps, but in the summer and fall of 1965, for reasons of arithmetic convenience, they were normalized with respect to 1000 counts (3.33 cps). This means the 1964 normalized acceleration frequency responses are equivalent to the acceleration frequency responses that would have been obtained by a constant exciting force of magnitude equal to that which occurred at 1 cps. Similarly, the 1965 acceleration frequency responses are equivalent to those for a constant force of magnitude equal to that which occurred at 3.33 cps. Resonant frequencies (frequencies corresponding to maximum responses) were read directly from these curves.

The damping capacity was calculated from the resonance curves by means of the following formula:

$$\zeta = \frac{\Delta f}{2f}$$

where ζ = damping factor

f = resonant frequency

Δf = difference in frequency of the two points on the resonant curve with amplitudes $1/\sqrt{2}$ times the resonant amplitudes (see Fig. 3.3).

The above expression for ζ is applicable to the displacement resonance curve of a linear, single

degree of freedom system with a small amount of viscous damping. The error in applying it to acceleration frequency responses instead of displacement frequency responses is small and comparable to errors in other violations of the basic assumptions for which the expression was derived. Some displacement resonance curves were calculated, and the difference in damping capacity as measured from displacement or acceleration curves was at most 10%.

A few frequency responses are also shown in the form of Kennedy and Pancu plots (Kennedy and Pancu, 1949). In Kennedy and Pancu plots the phase angle between the excitation and response is plotted as argument, and the amplitude of vibration as modulus in an Argand diagram (see Fig. 3.4). The phase angles were calculated from the relative positions of the peaks in the acceleration traces and the pulses indicating the basket position. The damping ratio ζ is again given by

$$\zeta = \frac{\Delta f}{2f}$$

where f = resonant frequency

Δf = difference in frequency of the two points lying at arguments of 45° and 135°.

3.2.2 Time response.

Time responses were obtained by vibrating the structure at a resonant frequency and recording the transient vibration when the machines were switched off. Theoretically, only that part of a transient after the baskets had stopped rotating should be used in calculating the damping capacity, but often the vibration itself had ceased by that time. Therefore, it was assumed that the frequency of the exciting force decreased sufficiently from the resonant frequency during the beginning of the transient so that the latter part was nearly a free vibration. The damping capacity was estimated in the usual manner as described below.

The experimental data are shown in the form of logarithmic decay curves, Fig. 3.5, where the logarithm of vibration amplitude is plotted against the number of elapsed cycles. The slope of this curve is equal to the logarithmic decrement, δ . If the damping capacity is independent of vibration amplitude, the logarithmic decay curve will be a straight line and δ may be calculated from:

$$\delta = \frac{1}{n} \log_e \frac{y_o}{y_n}$$

y_o = amplitude of first cycle

y_n = amplitude of nth cycle

n = number of cycles between y_o and y_n.

The damping ratio (ζ) is related to the logarithmic decrement as follows:

$$\zeta = \frac{\delta}{2\pi}$$

3.2.3 Mode shapes.

The method of measuring mode shapes in the summer of 1964 differed from that employed in all subsequent tests. In the summer 1964 tests, two accelerometers were placed on the roof and one on each of the 14th, 11th, 8th, and 5th floors. The building was vibrated at each resonant frequency in turn and the accelerometer readings were recorded. This method had to be modified in the 1965 tests because only four accelerometers were available (see section 3.1.2). Also, it was decided that more displacement amplitudes were necessary in order to describe the mode shape to the desired accuracy.

Because only four accelerometers were available in the 1965 tests, it was necessary to stop the machines after the first four measurements had been recorded. Three accelerometers were then moved to three different floors, while the fourth one was kept at a convenient floor to serve as a "control" accelerometer. The building

was vibrated at resonance once more and the accelerations at the new positions recorded. This procedure was repeated until a sufficient number of floor accelerations had been recorded.

The accelerometers were cross-calibrated dynamically before and after the determination of each mode shape. The cross-calibration consisted of putting all the accelerometers together in one place and in the same direction, so that they would all record equal accelerations. Any difference in magnitudes of the recorded traces were attributable to differences in the calibration factors of the accelerometers. Absolute calibration was not required, so the accelerometers were calibrated statically only approximately, by tilting them through a known angle.

The control accelerometer enabled adjustments to be made to the recorded accelerations to compensate for any differences in the magnitude of vibrations between measurements for each set of three floors. The cross-calibration enabled differences in calibration factors between accelerometers to be eliminated. Both of these adjustments were made to the readings of accelerations measured from the chart. The mode shape was then normalized by making the amplitude of the roof equal to unity.

3.3 EXPERIMENTAL RESULTS

In this section the experimental results are described in chronological order.

3.3.1 Summer 1964

The Main East Building was tested for the first time in the summer of 1964. At this time the concrete floor slabs had been cast in the East Building, and the steel frame of the east mechanical tower had been erected but was not yet encased in concrete.

Two vibration generators were mounted on the roof of the East Building as shown schematically in Fig. 3.6. The machines were run in phase, first in the N–S direction, and then in the E–W direction. Finally, by running the machines 180° out-of-phase, torsional vibrations were induced in the building.

During the N–S vibration, four of the six 1-g accelerometers used in this test series were placed on the roof of the building above the column caps on the south side of the structure (numbers 1, 2, 3 and 4 in Fig. 3.6). The two remaining accelerometers (numbers 5 and 6) were placed along the center line of the roof. The latter two transducers were removed after the initial tests, since their traces were affected by secondary motions due to vertical slab vibrations. Information for several acceleration frequency-response curves was obtained with results shown in Figs. 3.7 through 3.11.

Fig. 3.7 is a plot showing the N–S normalized acceleration response of the building from 0.5 to 7.5 cps, and Figs. 3.8 through 3.11 are individual (non-normalized) acceleration resonance curves for the first few modes.

Non-normalized frequency-response curves for the first three modes of translational vibrations in the E–W direction are shown in Figs. 3.12 and 3.13. Torsional frequency responses are shown in Figs. 3.14 and 3.15.

The resonant frequencies and damping capacities of all modes were found from the resonance curves. The resonant frequencies for E–W and N–S translational modes as well as for torsional modes are presented in Table 3.1. Table 3.2 shows the damping capacities of the same modes.

TABLE 3.1

Resonant Frequencies of East Building, Summer 1964

Direction	Resonant Frequencies (cps)				
	Mode				
	1	2	3	4	5
E–W	0.85	2.25	3.90	5.55	7.20
N–S	0.85	2.25	3.90	5.55	7.20
Torsion	1.3	2.9	4.9	–	–

TABLE 3.2

Damping Capacities of East Building as Measured from Resonance Curves, Summer 1964

Direction	Damping Ratios (% Critical)				
	Mode				
	1	2	3	4	5
E–W	2.0	0.9	0.6	–	–
N–S	1.8	0.7	0.4	0.5	0.4
Torsion	–	1.3	0.7	–	–

After the resonant frequencies were established, the mode shapes at resonance were determined. In this case, the amplitudes at the roof, 14th, 11th, 8th and 5th-floor levels were measured; the resulting mode shapes are presented in Figs. 3.16 through 3.19 for both N–S and E–W vibration. In these figures the frequency (ω) at which a mode shape was measured and the acceleration double amplitude of the roof ($\ddot{Y}$) are also recorded.

Some vibration decay curves for the East Building were also observed at this time. They were obtained by vibrating the building at resonance, stopping the exciter quickly, and then recording the subsequent free vibrations. The results are plotted in the form of logarithmic decay curves in Fig. 3.20 (E–W vibrations) and Fig. 3.21 (N–S vibrations). The curves indicate the damping is nearly independent of amplitude, and the values of damping capacity as measured from the initial straight portions are shown in Table 3.3.

In the summer of 1964 transient vibrations of the bare steel frame of the service tower were also recorded. Vibrations were produced by men standing in the East Building and shaking the service tower frame by hand. After a suitable amplitude was reached, the shaking was stopped and the subsequent free vibrations were recorded. A logarithmic decay curve is shown in Fig. 3.22. The damping capacity was highly dependent on amplitude, varying from 0.8% to 3.2% of critical over the range tested. The resonant frequency was measured from the decay curve and found to be 0.2 cps.

TABLE 3.3

Damping Capacities of East Building as Measured from Decay Curves, Summer 1964

Direction	Damping Ratios (% Critical)				
	Mode				
	1	2	3	4	5
E–W	–	0.7	1.0	–	–
N–S	–	0.6	0.7	–	0.9

3.3.2 Fall 1964

The mechanical service tower and the elevator tower were tested in the fall of 1964 after their steel frames had been encased in concrete.

The response of the service tower to forced vibrations was complex and the results were not satisfactory. One vibration generator was bolted to the 17th floor of the service tower, and it was planned to vibrate the tower in both the N–S and E–W directions. However, it was found that the service tower would only vibrate in a torsional mode and that the Main East Building vibrated as well, indicating that some link existed between these buildings. Fig. 3.23 shows the response of the 17th floor of the service tower to N–S excitation and the simultaneous N–S response of the East Building. From this graph, the resonant frequency of the first mode was found to be 1.18 cps and its damping capacity 6% of critical. Fig. 3.24 shows the

vibration amplitudes of different service tower floors near the first mode resonance. The damping capacities measured from these curves are about 5% of critical.

The forced vibration results for the elevator tower were also unsatisfactory. In the N–S direction, the first two resonant frequencies were found at 2.2 and 3.8 cps (see Figs. 3.25 and 3.26). In the E–W direction there was a resonant frequency at 3.7 cps (see Fig. 3.27). In the N–S direction the resonance curves yielded an average value of 5% for the damping capacity.

3.3.3 Summer 1965

The Main East Building was tested for the second time in the period July–August 1965. The following work had been done since the summer of 1964:

i. The windows had been installed in the East Building;
ii. Floors 4 through 8 of the East Building had been equipped with ventilation ducts and some partitioning;
iii. Piping had been installed throughout both the East Building and the mechanical service tower;
iv. The steel frame of the mechanical service tower had been encased in concrete (between summer and fall of 1964).

For the summer 1965 test series, the vibration generators were bolted to the 16th floor of the East Building in order to protect them from the weather, because when the machines were on the roof during the previous summer, moisture in the electrical connectors had caused "shorting". The exciter positions on the 16th floor in the summer of 1965 are shown in Fig. 3.28.

As soon as this series of tests commenced, it was apparent that the response of the building was much smaller than it had been the previous summer. Another vibration generator was installed in the center of the building midway between the other two, but even with 3 machines, the maximum trace on the chart produced by the original 1-g accelerometers was only about 1 inch with full amplifier gain. Therefore, two ± 0.20-g and two ± 0.25-g accelerometers were borrowed from the California Institute of Technology. These accelerometers gave traces of sufficient size for accurate measurement.

The building was tested first in the E–W direction, and the results for E–W translational vibration are shown in Figs. 3.29 through 3.35. Fig. 3.29 shows the acceleration measured at column B (Fig. 3.28) on the 16th floor for the cases of empty baskets, and basket loads L–1, L–2 and L–4. The normalized form of this plot is shown in Fig. 3.30. In this graph, the recorded accelerations have been divided by the square of their corresponding count number (proportional to frequency squared), regarding 1000 counts as unity, as described in Section 3.2.1. Those portions of the normalized frequency responses close to a resonant frequency are reproduced to a different scale in Figs. 3.31 through 3.35. In particular, Fig. 3.31 shows the frequency responses measured at three columns of the west line of columns normal to the direction of excitation. Fig. 3.32 shows the normalized acceleration frequency responses of column B on the 16th-floor level for different vibration amplitudes. Figs. 3.33 through 3.35 are resonance curves for the 2nd, 3rd and 5th modes, respectively.

The East Building was tested also in the N–S direction, and the resulting frequency responses are shown in Figs. 3.36 through 3.40. Fig. 3.36 shows the acceleration frequency response in the range 1–5 cps for a variety of loads, and Fig. 3.37 is the normalized version of this plot. Figs. 3.38 through 3.40 show the normalized resonance curves for the first three modes.

The values of resonant frequencies and damping capacities derived from the above graphs are shown in Tables 3.4 and 3.5, respectively.

Some of the resonance curves described above are shown in Figs. 3.41 and 3.42 in the form of Kennedy and Pancu plots.

TABLE 3.4

Resonant Frequencies of East Building, Summer 1965

Resonant Frequencies (cps)					
Direction	Mode				
	1	2	3	4	5
E–W	1.0	2.4	4.5	–	7.7
N–S	1.1	2.6	4.3	–	–

TABLE 3.5

Damping Capacities of East Building, Summer 1965

Damping Ratios (% Critical)					
Direction	Mode				
	1	2	3	4	5
E–W	7	8	13	–	5
N–S	9	7	7	–	–

The mode shapes at frequencies close to the resonant frequencies for the first two E–W modes are shown in Fig. 3.43 and for the first three N–S modes in Fig. 3.44.

A logarithmic decay curve for the first mode is shown in Fig. 3.45, giving a value of 6.7% critical for the damping capacity at higher amplitudes. Decay curves for modes other than the first were affected by some first-mode response excited when the speed of rotation of the baskets passed through the first resonant frequency as the speed was being reduced to zero.

3.3.4 Fall 1965, Tests I and II

The summer 1965 tests showed that a significant increase in both damping and stiffness of the East Building had occurred since the first tests in the summer of 1964. The fall 1965 I and II test series were carried out in an attempt to discover the cause of these increases. The only changes in the building from the summer of 1965 were the addition of more partitions and facilities in floors 3 through 8 of the main building. Furthermore, the installation of ventilation ducts in the service tower was almost complete. The vibration generators were placed again on the 16th floor as in the summer of 1965, and the ± 0.25-g and ± 0.20-g accelerometers were used to measure accelerations.

It was suspected that one cause of the increase of damping between the summers of 1964 and 1965 was the frictional energy losses which occurred in relative movements between the main building and its adjacent buildings. In relative movements of the buildings, the steel plates spanning the gaps between buildings and resting on the floor slabs of the East Building slid over the floor slabs, and energy was dissipated by a Coulomb friction mechanism. An attempt was made to reduce this energy loss by inserting small grease plate sandwiches beneath the steel plates. The grease plate sandwiches consisted of two small steel plates 3/4" x 3/4" x 1/16" with a layer of grease between them. In the case of the three 10-ft.-long plates spanning from the service tower at every floor level, a sandwich was placed at each end and one in the middle of every plate. A sandwich at each end of the plates spanning from the connecting corridor was sufficient, since these plates were only 5 ft. in length. It was hoped that all relative movement of the buildings would take place by a shearing action at the greased interface where the coefficient of friction was small.

The East Building was tested first without the grease plate sandwiches (test series I) and then with them in position (test series II) to see if any change in response could be detected because of the reduction in the coefficient of friction. The results obtained in the fall of 1965 are presented in Figs. 3.46 through 3.61. Figs. 3.46 through 3.51 are frequency responses for E–W vibration, and Figs. 3.52 through 3.57 are frequency responses for N–S vibration. The mode shapes

of the East Building and the vibration shapes of the service tower measured at the same resonant frequency are shown in Figs. 3.58 through 3.61 (E–W direction) and in Figs. 3.62 through 3.65 (N–S direction). The results obtained in the fall of 1965, series II (with grease plates) are presented in similar fashion in Figs. 3.66 through 3.83.

Torsional frequency responses of the East Building with the grease plates in place are shown in Figs. 3.84 through 3.86. Fig. 3.87 shows the vibration amplitudes at col. J (Fig. 3.6) in both the N–S and E–W directions when the building was vibrating in its first torsional mode in the fall 1965 test series I. Figs. 3.88 and 3.89 are similar to 3.87, except that they are for the 1st and 2nd torsional modes in the fall 1965 test series II.

The resonant frequencies and damping capacities of the East Building were measured from the above resonance curves. The results are shown in Tables 3.6 and 3.7, respectively. Table 3.6 compares the resonant frequencies obtained in the fall 1965 test series I and II, and Table 3.7 is a comparison of the damping values obtained in these tests.

TABLE 3.6

Resonant Frequencies of East Building, Fall 1965

Resonant Frequencies (cps)					
Direction and test	Mode				
	1	2	3	4	5
E–W I	1.0	2.5	4.5	–	7.7
E–W II	0.95	2.3	4.5	–	7.6
N–S I	1.1	2.5	4.5	–	7.7
N–S II	1.0	2.4	4.4	–	7.6
Torsion II	2.6	4.6	6.3	–	–

TABLE 3.7

Damping Capacities of East Building, Fall 1965

Damping Ratios (% Critical)					
Direction and test	Mode				
	1	2	3	4	5
E–W I	5	*	*	–	*
E–W II	7	6	*	–	*
N–S I	12	10	*	–	3
N–S II	12	9	9	–	4
Torsion II	–	7	4	–	–

* DAMPING LARGE: NO "RESONANCE CURVE"
– MODE NOT EXCITED

3.4 DISCUSSION OF EXPERIMENTAL RESULTS

The experimental results obtained for the East Building were mode shapes, resonant frequencies and damping capacities. These results are discussed below. In addition, the transmission of energy from the East Building to other buildings is also discussed, since this factor affected the results considerably.

3.4.1 Mode Shapes

Experimental mode shapes of the East Building for the tests in the summer of 1964 are shown in Figs. 3.16 through 3.19. For the summer of 1965 the mode shapes are shown in Figs. 3.43 and 3.44; for the fall of 1965 they are shown in Figs. 3.58 through 3.65 and in Figs. 3.78 through 3.83.

The most striking feature of these translational mode shapes was the constancy in the position of the nodal points. It was found that the nodes in the shape of a particular mode lay

at very nearly the same height regardless of the test series during which they were measured, or whether the vibration was N–S or E–W. The nodal points of the second, third and fifth mode shapes were as follows:

i. For the second mode shape, the node was close to the 13th floor;
ii. For the third mode shape, one node was close to the 9th floor and the other midway between the 14th and 15th floors;
iii. In the case of the fifth mode shape, the nodes were close to the 6th floor, midway between the 9th and 10th floors, slightly above the 13th floor and slightly above the 16th floor.

It was expected that the nodes for corresponding N–S and E–W mode shapes would be at similar heights because of the geometry of the building; however, some changes in nodal point positions might have been expected between the summer 1964 tests and subsequent tests because of the significant increases in resonant frequencies and large increases in damping capacities between the summer of 1964 and the summer of 1965.

The constancy in the position of the nodal points was further illustrated by the fact that during the 1965 tests when the machines were operated on the 16th floor, the fourth mode in neither the N–S or E–W direction could be excited (see Figs. 3.29, 3.36 and 3.52). This indicates that during the summer 1965 and fall 1965 test series I and II, a node point of the 4th mode shape was located at the 16th-floor level. A node point of the 4th mode was also found to lie close to the 16th floor during the summer of 1964 when the machines were operated on the roof (see Figs. 3.17 and 3.19).

Although the node points remained very close to the same positions for each determination of a particular mode shape (either N–S or E–W vibration), there were, except in the case of the first mode, considerable differences in the normalized amplitudes of floor displacements close to anti-nodes. In general, such differences may be caused by two factors:

i. errors in the measurement of the acceleration amplitudes;
ii. sensitivity of a mode shape to changes in forcing frequency near resonance.

The measurement of mode shapes does not require absolute calibration of accelerometers, and the cross-calibration procedure and subsequent adjustments to the recorded data kept errors due to calibration within a few percent. The only error the cross-calibration did not compensate was the efficiency of fixing the accelerometers to the floors. However, any errors from this source must have been quite small, because a 50-lb. weight was set on the base plate of each accelerometer, which kept any relative movement between accelerometer and floor very small.

Since the measurement of accelerations was accurate, only the sensitivity of mode shapes to changes of forcing frequency can explain the differences in normalized amplitudes of floors near anti-nodes. Figs. 3.51 and 3.57 show that the maximum amplitudes of the top floors and roof of the 5th resonant frequency did not occur simultaneously. Thus, the shape of the 5th mode of vibration depended on the frequency at which it was measured. Since the modes were measured at slightly different frequencies on each occasion (N–S and E–W, in summers 1964 and 1965, and fall 1965 I and II), this accounts for the discrepancies between various determinations of a particular mode. The rate of change of mode shape was greatest near the 5th resonant frequency and negligible at the first, so that the experimental mode shapes become less meaningful as their resonant frequencies increase. This problem is well known in resonance testing and is discussed in detail by Gauzy (1959) and Bishop and Gladwell (1961). Therefore only a brief explanation will be given here.

Normal modes were not being excited in the structure, and hence the maximum amplitudes of each floor did not occur at the same frequency. This resulted in inaccurate mode shapes as described above. The excitation of

damped normal modes requires: (see, e.g., Gauzy)

i. The damping matrix for the structure to be of a type that does not couple the modes, and

ii. The excitation to be such that it balances the damping force at all times at all points of the structure.

Nothing can be done about the first requirement except to hope that the damping does not couple the modes, or that if it does, it will be too weak to do so effectively.

Requirement (ii) implies employing the same number of exciters as degrees of freedom of the structure. Gauzy points out that this requirement is not essential in practice if the locations of the exciter stations are chosen judiciously. He suggests that if it is desired to excite a particular mode, the exciters should be deployed to feed a maximum input of energy to this mode, and a minimum energy input to its neighboring modes, since only these will affect appreciably the response of that particular mode. This last consideration has considerable bearing on the results of a test with only one excitation point, as was the case in this project.

3.4.2 Transmission of energy from East Building to its adjacent buildings.

During the forced vibration tests on the service tower in the fall of 1964, it was noticed that the East Building was vibrating also. At this time the vibration generators were installed on the 17th floor of the service tower (see Fig. 3.6). In Fig. 3.23 the responses of the 17th floors of both the service tower and East Building at this time are shown. Similarly, during the summer of 1965, when the vibration generators were on the 16th floor of the East Building, the service tower was found to vibrate. However, the service tower vibrations were not recorded. Because it was felt that the service tower may have caused either the increase of damping or the increase of resonant frequencies, or both, which occurred between the summers of 1964 and 1965, a more detailed study of the service tower vibrations was made in the series of tests conducted in the fall of 1965.

Since it is at resonance that the interaction of the buildings would have greatest effect on each other, the vibration shape of the service tower in these tests was observed when the East Building was at resonance. The vibration shape of the service tower and the simultaneous mode shape of the East Building were measured both with (Figs. 3.58 through 3.65) and without (Figs. 3.78 through 3.86) the grease plate sandwiches inserted beneath the steel plates spanning the gap between the buildings. The grease plate sandwiches did not affect appreciably the response of either building except in the case of the 2nd resonant mode in the N–S direction. This and other results from these tests are described below:

1. In the first resonant modes, in both E–W and N–S directions, the service tower vibrated mainly in the same direction as the East Building. However, there was also vibration in the direction at right angles to the exciting force direction (see Figs. 3.58, 3.62, 3.78 and 3.81). The vibration of the service tower in the direction of the main building vibration was in phase with, and of approximately the same amplitude as, the vibration of the main building. The first torsional resonant frequencies of the service tower must be approximately equal to the first translational resonant frequencies of the East Building.
2. In contrast to the first resonant frequency, the interaction between the East Building and its service tower near the second resonant frequency was complicated, and the behavior in the N–S direction differed from that in the E–W direction. In addition, the grease plate sandwiches appeared to alter the behavior for both directions. It is not certain that the grease plate sandwiches were responsible for the changes in vibration shapes which took place after they were inserted, because in both directions the tests were conducted at slightly different frequencies.

Without grease plates the vibrations of the two buildings were in-phase or 180° out-of-phase (depending on floor level) for N-S vibration, but 90° out-of-phase for E-W vibration. In both cases, the magnitude of the service tower vibrations was much smaller than, and almost entirely of the same direction as, the corresponding vibrations in the East Building (see Figs. 3.59 and 3.63). After the grease plates were inserted beneath the steel plates, the magnitude of the E-W vibrations of the East Building increased, those of the service tower decreased, and the vibrations of the buildings were still 90° out-of-phase (see Fig. 3.79). In this second case (with grease plates) the amplitudes of vibration of the East Building also increased for N-S vibration, but the vibrations of the buildings became 90° out-of-phase (see Fig. 3.82). The tests without grease plates were conducted at 2.6 cps and 2.5 cps for E-W and N-S directions, respectively. The corresponding frequencies with grease plates were 2.4 cps and 2.4 cps.

3. In the third resonant mode, in both E-W and N-S directions, the only appreciable vibration of the service tower was again in the same direction as the East Building's vibration. The results before and after inserting the grease plate sandwiches were similar. The magnitudes of the service tower amplitudes, E-W, were much smaller than, and, depending on the floor, either in-phase or 180° out-of-phase with the vibration of the East Building (see Figs. 3.60 and 3.80). In this case, the service tower vibrated in its second mode. In the N-S direction the amplitudes of vibration of the service tower were extremely small and 90° out-of-phase with the East Building (see Figs. 3.64 and 3.83). Clearly, the 3rd resonant frequency of the East Building was not close to a resonant frequency of the service tower in this direction. (The service tower is rectangular in plan [see Fig. 2.1] and hence its N-S and E-W resonant frequencies are different).
4. When the East Building was vibrating in its fifth resonant mode, the vibration shape was measured only for the case when no grease plates were beneath the steel plates (Figs. 3.61 and 3.65). For vibrations in both the N-S and E-W direction, the service tower vibration was small and in-phase or 180° out-of-phase with the East Building's vibration. The service tower vibrated in its third mode N-S and its second mode E-W.

It is now clear that a different system was tested in the summer and fall of 1965 to that tested in the summer of 1964. In the summer of 1964 the steel frame of the service tower had not been encased in concrete and its first resonant frequency was very low -- 0.2 cps. So, although the steel frame was connected to the East Building at the foundation and ground floor levels, it was not capable of exercising much influence on the dynamic behavior of the East Building. Thus, the East Building was tested virtually in isolation. However, after the steel frame of the service tower had been encased in concrete, the mass and stiffness of the service tower were large enough to influence the behavior of the East Building. Therefore, in the summer and fall of 1965 a new system, consisting of the East Building coupled to its service tower, was tested.

Initially, it was thought that the steel plates spanning the gap between the service tower and the main building may have contributed to this coupling. In any relative motion between the buildings, a frictional force exists which would tend to excite vibrations in the service tower. However, it may be seen in Figs. 3.58 through 3.65 and Figs. 3.78 through 3.83 that in all cases where it was possible to measure the amplitudes of vibration of the bottom few stories of the service tower, these amplitudes were in-phase with the amplitudes of the corresponding floors in the main buildings. In the upper floors, however, the vibrations of corresponding floors were in-phase for some modes but out-of-phase for others. This would suggest that the steel

plates did not couple the buildings, but that the reinforced concrete beams and slabs at the 2nd floor and foundation levels provided the coupling. Fig. 3.90 is a diagrammatic model of the new system tested in the summer of 1965 and afterwards.

Not only did the service tower vibrate while the East Building was being vibrated, but other adjacent buildings vibrated also. The vibrations in the elevator tower and connecting corridor were small and more of a random nature than harmonic. However, there were harmonic vibrations in the Main West Building which are of some interest.

The vibrations in the West Building were mainly in the same direction (for both E-W and N-S vibrations) as the source vibration in the East Building. They were measurable only in the frequency range 1.8 - 2.0 cps. They were in phase with, and of approximately the same amplitude as, the vibration in the East Building. Evidence of this resonant mode may be seen in Fig. 3.46, where a small resonance peak appears to occur just below the second resonant frequency. The source of the coupling between the East Building and the West Building is unknown also, but energy may have been transmitted through the ground, or alternatively through the intervening buildings to the West Building.

3.4.3 Resonant frequencies.

The Main East Building was tested on three occasions. First in the summer of 1964, then in the summer of 1965, and finally in the fall of 1965. The final test series was in two parts; first, the building was tested as it was designed (fall 1965 I), and second, with grease plate sandwiches inserted beneath the steel plates connecting the service tower and the connecting corridor to the East Building (fall 1965 II). Table 3.8 shows the resonant frequencies of the first 5 modes in the E-W direction obtained in each test series. Table 3.9 shows the corresponding resonant frequencies for the N-S direction. Before drawing conclusions from these tables, a discussion of the errors in the determination of the resonant frequencies is pertinent.

Table 3.8
E-W Resonant Frequencies of East Building for All Tests

Resonant Frequencies (cps)					
Test	Mode				
	f_1	f_2	f_3	f_4	f_5
Summer 1964	0.85	2.25	3.90	5.55	7.20
Summer 1965	1.00	2.4	4.5	--	7.7
Fall 1965 I	1.00	2.5	4.5	--	7.7
Fall 1965 II	0.95	2.3	4.5	--	7.6

Table 3.9
N-S Resonant Frequencies of East Building for All Tests

Resonant Frequencies (cps)					
Test	Mode				
	f_1	f_2	f_3	f_4	f_5
Summer 1964	0.85	2.25	3.90	5.55	7.20
Summer 1965	1.1	2.6	4.3	--	--
Fall 1965 I	1.1	2.5	4.5	--	7.7
Fall 1965 II	1.0	2.4	4.4	--	7.6

There were numerous difficulties in assigning values of resonant frequencies to the vibration modes, and each of these led to some error. These difficulties were caused by (a) heavy

damping, (b) nonlinear stiffness, and (c) complex vibration modes. Their effect on the resonance curves is discussed below:

a. Heavy Damping

In the summer 1964 tests, the damping was small, resulting in sharp resonance curves from which resonant frequencies could be read accurately. However, in subsequent tests, the damping capacity in all modes had increased greatly so that the resonance curves were blunt. In some cases, resonance curves of the usual type did not even exist. Thus, estimating resonant frequencies from the summer and fall 1965 resonance curves involved considerable personal judgment.

b. Nonlinear Stiffness

The decrease of resonant frequency with vibration amplitude in the 2nd mode E-W, summer 1965, is clearly seen in Fig. 3.32. This spring softening non-linearity was evident to a lesser extent in several other modes of the summer and fall 1965 tests and was even slightly evident in the test results of the summer of 1964. Thus, values of resonant frequencies depend on vibration amplitude, and for modes excited at more than one amplitude, the values refer to some average peak vibration amplitude.

c. Complex Vibration Modes

Figs. 3.51 and 3.57 show that normal modes were not excited at the 5th resonant frequency N-S and E-W, and that the maximum amplitudes of the top floors and roof occurred at different frequencies. Thus, again it was necessary to estimate some mean value of resonant frequency. The errors caused in exciting a mixture of modes instead of a normal mode were greatest in magnitude for the 5th mode, and decreased with the order of the mode to the first mode, where it was negligible.

These considerations show that the values of resonant frequencies given in Tables 3.8 and 3.9 are not very precise. It is probable, however, that resonance occurred within a range of ± 0.05 cps of the values in Tables 3.8 and 3.9 for the summer 1964 tests, and within a range of ± 0.1 cps for tests at other times. Despite the lack of accuracy in the values of resonant frequency, the following conclusions may be drawn:

i. In the summer 1964 tests the value of the resonant frequency for any E–W mode was equal, within the limits of experimental error, to the value for the corresponding N-S mode.

ii. The resonant frequencies of all modes both E–W and N-S increased between the summer of 1964 and the summer of 1965. The percentage increase is shown in Table 3.10. (The value of the 4th resonant frequency was not obtained in the summer and fall 1965 tests for reasons given in Section 3.4.1).

Table 3.10

Percentage Increases in Resonant Frequencies Between the Summers of 1964 and 1965

Direction	Mode			
	f_1	f_2	f_3	f_5
E - W	18	7	15	7
N - S	29	16	10	7

iii. In the summer and fall tests of 1965, the value of the first resonant frequency N–S was slightly greater than the first resonant frequency E–W. Although the difference in resonant frequency lies within the limits of experimental error given above, the experimental error is smallest for this first mode. Therefore, since this result was obtained in three tests, it is considered correct.

iv. The values of resonant frequency for most modes in the fall 1965 II tests are slightly smaller than the corresponding values for the fall 1965 I and summer 1965 tests. The decrease lies well within the range of experimental error, and it is

not thought attributable to the grease plate sandwiches. If the grease plate sandwiches had been responsible for the 5–10% decrease in frequencies, it would imply that they had decreased the stiffness of the system of 10–20%. Since this is inconceivable, it is probable that this decrease of frequency was caused by a systematic type of error in the data reduction.

There are two possible explanations for the increase in resonant frequencies between the summers of 1964 and 1965:

a. As described previously in Section 3.4.2, the structure tested in the summer of 1964 differed from that tested in 1965. It is thus possible that the virtually isolated East Building tested in the summer of 1964 had lower resonant frequencies than the 1965 system, composed of the East Building coupled to its service tower. There is one piece of evidence supporting this theory. When vibrating the service tower in the fall of 1964, it was found that the East Building was vibrating also. This means that the test in the fall of 1964 was on the coupled system with the point of excitation in the service tower. The first resonant frequency was found at 1.16 cps (Fig. 3.23), which agrees fairly well with the value of 1.1 cps found in 1965 with the machines on the East Building.

b. Alternatively, the increase in stiffness in the East Building could be attributed to the stiffening effect of the steel window frames and the glass. The stiffness of the windows was estimated and a value for the effective stiffness of the glass was taken from the test data presented in a report by Skidmore, Owings and Merrill (1958). The total increase in stiffness was distributed as an increase in the moment of inertia (I) of the columns, but in no case was I increased by more than 1%. It was, therefore, concluded that the installation of the windows could not account for the observed increase in resonant frequencies.

Table 3.11

E-W Damping Capacities of East Building for All Tests

Damping Ratios (% Critical)					
Test	Mode				
	1	2	3	4	5
Summer 1964	2.0	0.9	0.6	--	--
Summer 1965	7	8	13	--	--
Fall 1965, I	5	*	*	--	--
Fall 1965, II	7	6	*	--	--

*RESPONSE AMPLITUDE DID NOT DECREASE SUFFICIENTLY BEYOND RESONANCE FOR DAMPING TO BE MEASURED.

Table 3.12

N-S Damping Capacities of East Building for All Tests

Damping Ratios (% Critical)					
Test	Mode				
	1	2	3	4	5
Summer 1964	1.8	0.7	0.4	0.5	0.4
Summer 1965	9	7	7	--	--
Fall 1965, I	12	10	*	--	3
Fall 1965, II	12	9	9	--	--

*RESPONSE AMPLITUDE DID NOT DECREASE SUFFICIENTLY BEYOND RESONANCE FOR DAMPING TO BE MEASURED.

3.4.4 Damping Capacities.

The damping capacities of the East Building are shown for E-W and N-S vibration in Tables 3.11 and 3.12, respectively. In the summer of 1964, the first mode E-W had 2% of critical damping and the first mode N-S had 1.8%. At this time, the values of damping for higher

modes were in the range of 0.4% to 0.9% of critical. In the tests in the summer and fall of 1965, the damping capacity of every mode was in the range 3-13% of critical. Thus, a large increase in damping capacity of all modes occurred between the summers of 1964 and 1965. Also, in Tables 3.11 and 3.12, it can be seen that a smaller, but distinct, increase in damping occurred between the summer and fall of 1965.

The exact causes of the increase in damping capacity between the summers of 1964 and 1965 are unknown. However, possible sources of energy loss present in the summer 1965 test, but absent in the first test, are listed below and subsequently discussed:

1. The coupled system of the East Building and its service tower may have inherently greater damping capacity than the isolated East Building. In a sense, since the coupling is somewhere at the lower floors, the service tower may be regarded as an energy sink for the East Building's vibrations.
2. The relative displacements of adjacent floors must have been accommodated by movement of the glass panes relative to their frames. If this movement involved slippage between the glass and its neoprene gasket (see Fig. 3.91), then considerable energy may have been lost by Coulomb friction.
3. Shrinkage cracks in the floor slabs, running N–S and E–W between columns, had developed between the summers of 1964 and 1965. When the building was vibrating, the floor slabs vibrated vertically, opening and closing the shrinkage cracks—a process which could result in considerable dissipation of energy.
4. The steel plates spanning the gaps between the East Building and its adjacent buildings rested on the East Building's floor slabs, and in relative movements of corresponding floors energy was dissipated by Coulomb friction.
5. Ventilation ducts, partitions, pipes, etc., installed in the East Building between the summers of 1964 and 1965 may have increased the damping capacity of the building.

The only source of energy loss amenable to test variation was the frictional damping of the steel plates. It was attempted to reduce the coefficient of friction by inserting grease plate sandwiches between the steel plates and the floor slabs. The coefficient of friction was then due to greased steel on greased steel, instead of steel on concrete. The fall 1965 II series of tests refers to the tests conducted on the main building with the grease plates in place, and the fall 1965 I series of tests refers to the tests conducted without the grease plates. Any difference in these two test series should be attributable to the reduction in the coefficient of friction.

The largest difference in these two test series was in the damping capacity of the 2nd mode E–W. In test series I the response continued to increase after the exciter frequency passed the second resonant frequency and there was no resonance curve from which to measure damping (see Fig. 3.49). But in test series II there was a resonance curve which yielded a value of 6% critical (Fig. 3.68). In the 2nd mode N–S, the damping reduced from 10% to 9% critical (Figs. 3.55 and 3.74, respectively), and in the 3rd mode N–S it was 9% with the grease plates in place, when previously without grease plates there was not a resonance curve from which damping could be measured (Figs. 3.75 and 3.50, respectively). It is, therefore, concluded that the grease plate sandwiches caused a small decrease in damping in the 2nd and 3rd modes.

The effect on the damping capacity of a reduction in this coefficient of friction was estimated also. The results are summarized in Table 3.13 for the first 3 modes in both N–S and E–W directions.

The relative accelerations of corresponding floors of the East Building and the service tower were measured from the mode shapes shown in Figs. 3.58 through 3.65. The sum of these relative accelerations for each mode is shown in column (2) of Table 2.13, and the relative

displacements (accelerations divided by circular frequency squared) are shown in column (3). Columns (4) and (5) are the generalized accelerations and velocities, respectively, of each mode, taking the displacement of the roof as the generalized coordinate. Column (6) shows the generalized masses calculated from:

$$M_n^* = \Sigma M_i \phi_{in}^2$$

where ϕ_{in} = amplitude of i th floor in the n th normalized mode shape.

M_i = mass of i th floor.

Column (7) is the energy stored in the steady-state vibration,

$$W_n = \tfrac{1}{2} \dot{Y}_n^2 \; M_n^*$$

The energy absorbed per cycle (ΔW_f) by Coulomb friction is:

$$\Delta W_f = 4 \mu F x$$

where μ = coefficient of friction

F = normal reaction

x = displacement amplitude (sum of relative displacements of all floors)

The damping capacity ζ is given by:

$$\zeta = \frac{\Delta W'}{4\pi(W'_{EB} + W'_{ST})} = \frac{\Delta W_{in} + \Delta W_f}{4\pi(W_{EB} + W_{ST})}$$

where ΔW_{in} = energy absorbed by East Building

ΔW_f = energy absorbed by friction

W'_{EB} = energy stored in East Building

W_{ST} = energy stored in service tower

Assuming the vibrational energy stored in the service tower (W_{ST}) is small in comparison with the vibrational energy stored in the East Building (this is true for all modes except the first, in which the amplitude of vibration of the service tower and East Building were approximately equal), then:

$$\zeta \doteq \zeta_{EB} + \Delta \zeta_f$$

where ζ_{EB} = damping capacity of isolated East Building

$\Delta \zeta_f$ = change in damping capacity caused by a change in the coefficient of friction between the steel plates and floor slabs.

The values of $\Delta\zeta_f$ for a change in magnitude of μ of 0.5 and a normal reaction (F) of 500 lbs. due to the weight of the plates are shown in column (8) of Table 3.13. (In estimating (F), the weight of the plates from the connecting corridor to the East Building was neglected, since this weight is small in comparison to the weight of the plates from the service tower.)

The values of $\Delta\zeta_f$ (Table 3.13) show that the large increase of damping between the summers of 1964 and 1965 may have been caused by the steel plates rubbing on the concrete floor slabs. An increase in the coefficient of friction during the period between the summer and fall I tests of 1965 would then explain the slight increase of damping which occurred at this time. This increase in the coefficient of friction may have been caused by an accumulation of grit between the plates and concrete slab. Finally, the insertion of the grease plate sandwiches could have reduced the value of the coefficient of friction and caused the decrease in damping between the fall 1965 I and II tests.

An attempt was made to determine if there was any slippage taking place between the neoprene gaskets and window panes. A layer of stress coat was sprayed over the junction of the gasket and glass at different points of several

TABLE 3.13

Estimated Increase of
Damping Caused by Steel Plates

(1)	(2)	(3)	(4)	(5)	(6)	(7)	(8)
MODE	Σ rel. acc. amplitudes ($x\ 10^{-3}g$)	Σ rel. displ. amplitudes (ins)	$\ddot{Y}_n$ ($x\ 10^{-3}g$)	$\dot{Y}_n$ ins/sec	M^*_n ($x\ 10^3$)	W_n lbs in.	$\triangle\zeta_f$ (% crit)
E-W							
1	0.7	.0066	0.83	.052	16.1	21.8	2.4
2	27.2	.0406	3.40	.080	14.5	46.0	7.0
3	16.2	.0066	5.20	.066	5.1	9.4	5.6
N-S							
1	1.3	.0086	0.84	.042	13.6	12.1	5.6
2	24.3	.0378	2.70	.066	21.6	46.7	6.4
3	24.0	.0124	4.33	.067	6.9	15.4	6.4

windows. No cracks were formed in the stress coat, which indicates any relative slippage must have been very small. The energy loss at this source is assumed to have been correspondingly small.

No attempt could be made to estimate the energy loss caused by the shrinkage cracks in the floor slabs, or energy absorbed in the vibration of ventilation ducts, partitions, etc.

It is therefore concluded that there were two main sources of energy dissipation responsible for the large increase of damping between the summers 1964 and 1965. These were: first, the energy dissipated in Coulomb friction between the steel plates and floor slabs, and second, the energy dissipated in the service tower itself. The relative importance of these two mechanisms is unknown, but it is thought that together they account for most of the increase in damping. In the first mode (both for N-S and E-W vibration) the amplitudes of vibration in the service tower and East Building were comparable, and it could be expected that the dissipation of energy by the service tower affected the first modes considerably. In higher modes the vibration of the service tower was small and it is probable that the Coulomb friction between the steel plates and floor slabs played the more important role.

CHAPTER 4

FORMULATION OF ANALYTICAL MODEL

4.1 GENERAL

The analytical model of the East Building was formulated from the experimental results obtained during the summer of 1964. The formulation consisted of adjusting the stiffness, mass, and damping characteristics until the model's response to harmonic excitation matched that of the real structure. Since resonant frequencies depend primarily on mass and stiffness properties, and resonant amplitudes primarily on damping properties, it was possible to develop the model in two stages. First, the estimated mass and stiffness were adjusted in order to match the resonant frequencies of the model and prototype, and then the damping capacities of the first five modes were varied until the model's resonant amplitudes equalled those of the real structure for equivalent excitation.

All computations in the formulation of the analytical model were performed by an IBM 7090/7094 Direct Coupled System using the programs FRMDYN, DINFRA and NONLIN, which were developed in the Division of Structural Engineering and Structural Mechanics, Department of Civil Engineering at Berkeley. The programs were used for the following purposes:

FRMDYN — To compute the translational vibration mode shapes, natural frequencies and steady-state response of the model in the various stages of its formulation. Also, to compute the linear response of the model to ground acceleration records.

DINFRA — To compute torsional mode shapes and natural frequencies of the model.

NONLIN — To compute the nonlinear translational response of the model after yielding had occurred in some of the members.

These programs are restricted to structures composed of a number of parallel rectangular frames with horizontal girders and vertical columns. They assume:

i. The geometry of the structure is defined by center-line to center-line dimensions,
ii. The mass of the structure and lateral forces are concentrated at the floor levels.

The input data concerning the structure are similar in all three programs. The first set of data cards describes the structure generally, and subsequent sets give the properties of the girders and beams in each frame. In the case of FRMDYN and NONLIN, the load data which follow next were in these particular computations presented in the form of ground acceleration records.

The output differed considerably between programs, and a list of the printed output for each program is given below:

FRMDYN
1. Input data
2. Mode shapes and frequencies
3. Maximum values and their distribution versus time for
   a. Lateral displacements
   b. Total story shears
   c. Total story moments
4. Maximum values for
   a. End moments in all girders
   b. Top and bottom moments, shear and axial forces in all columns

DINFRA
1. Input data
2. Mode shapes and frequencies

NONLIN

1. Input data
2. Maximum lateral story displacements and the time of their occurrence
3. Girder and column moment ratios; a comparison of the maximum moment to the yield capacity of the element
4. Maximum axial force in each column
5. Girder and column ductility ratios; the maximum ratio of plastic rotation to elastic rotation capacity of each element.

4.2 MATCHING RESONANT FREQUENCIES

Resonant frequencies of a structure are determined primarily by its stiffness and mass characteristics, and most of the data required to assemble the stiffness and mass matrices of the building were known to a high degree of accuracy; e.g., the geometry of the structure, flexural rigidity and mass of structural members, etc. However, there were some quantities which were not known to sufficient accuracy, and errors in their assigned values might have significant effect on the resonant frequencies. These were:

i. Effective length of columns,
ii. Width of floor slab acting compositely with the girders,
iii. Density of the lightweight concrete in floor slabs.

The first two quantities affect the stiffness matrix, and the third affects the mass matrix. The changes in resonant frequencies resulting from variations in these quantities were computed by means of FRMDYN and these changes are discussed below.

4.2.1 Effective Length of Columns

The 42"-deep girders increased the column stiffness over the girder depth, reducing the effective length of the columns to some length less than the story length of 13', and it was

Table 4.1

Effect on Resonant Frequencies of
Changes in Column Lengths

Description	Natural Frequency (cps) and (Percent of Difference)					Remarks
	f_1	f_2	f_3	f_4	f_5	
h = 11 ft. b* = 8 ft. w = 107 p.c.f.	.811	2.34	4.07	5.88	7.90	Control Model
h = 9 ft. at 1^{st} floor only	.830 (2.2)	2.38 (1.7)	4.15 (2.0)	6.00 (2.0)	8.11 (1.9)	Slab unchanged base fixity Influence
h = 13 ft	.765 (-5.7)	2.20 (-5.1)	3.78 (-7.1)	5.41 (-8.0)	7.25 (-8.2)	h = 13 ft. = Story Height

therefore necessary to consider the column length as a parameter in the model's formulation. However, the column lengths could not be varied directly since any variation in column lengths would alter the center-line geometry of the structure and the dynamic forces, as well as the column stiffness. Therefore, the column length parameter was varied by introducing equivalent changes in the flexural rigidity of the columns (inversely proportional to the effective length cubed), always maintaining the column length of the model as 13'.

The control for investigating the effect on the resonant frequencies of changes in column lengths was a model having effective column length of 11 ft., slab width of 8' (16t where t = slab thickness = 6") acting with the girder, and a concrete density of 107 lbs/cu. ft. The results of this investigation are shown in Table 4.1. The natural frequencies decreased by 5 to 8 percent for a change in effective column length from 11 to 13 ft.

4.2.2 Effective Slab Width

The flexural rigidity of the steel girders was increased by composite action with the floor slab, and the effect of this composite action on the resonant frequencies was investigated by assuming various widths of floor slab to act with the girders. The control model was the same as that used to investigate the effective column lengths. Table 4.2 shows that a reduction in effective slab width from 8 ft. to 4 ft. resulted in a decrease of natural frequencies of 4 to 5%; an increase in effective slab width from 8 ft. to 16 ft. increased the natural frequencies from 3 to 4%.

The elastic modulus of the lightweight concrete in the floor slabs was not known accurately, but was assumed to be 2.9 x 10^6 lbs/in^2 (modular ratio of 10). Any variations in the modulus, however, are equivalent to changes in effective slab width and may thus be considered incorporated in the slab width parameter.

Table 4.2

Influence of Composite Action
Between Floor Slabs and Girders

Description	Natural Frequency (cps) and (Percent of Difference)					Remarks
	f_1	f_2	f_3	f_4	f_5	
L = 11 ft. b = 8 ft. w = 107 p.c.f.	.811	2.34	4.07	5.88	7.90	Control model
b = 4 ft.	.776 (-4.3)	2.24 (-4.5)	3.87 (-4.8)	5.64 (-4.1)	7.62 (-3.5)	L = 11 ft. w = 107 p.c.f.
b = 16 ft.	.845 (4.1)	2.43 (3.9)	4.21 (3.4)	6.05 (2.9)	8.11 (2.8)	L = 11 ft. w = 107 p.c.f.

Table 4.3

Influence of Concrete Density

Description	Natural Frequency (cps) and (Percent of Difference)					Remarks
	f_1	f_2	f_3	f_4	f_5	
L = 11 ft. b = 8 ft. w = 107 ft.	.811	2.34	4.07	5.88	7.90	Control model
w = 100 p.c.f.	.858 (5.8)	2.48 (6.0)	4.33 (6.4)	6.25 (6.3)	8.40 (6.3)	L = 11 ft. b = 8 ft.
w = 130 p.c.f.	.760 (-6.3)	2.19 (-6.3)	3.82 (-6.2)	5.55 (-5.6)	7.46 (-4.3)	L = 11 ft. b = 8 ft.

4.2.3 Density of Concrete

The density of the lightweight concrete in the floor slabs was not known exactly, and it was also treated as a parameter. Using the same control model as previously, a decrease in density from 107 to 100 p.c.f. increased the natural frequencies by about 6%, and an increase in density from 107 to 130 p.c.f. decreased the natural frequencies by about 6% (see Table 4.3).

4.2.4 Final Choice of Model

Clearly, there is no unique combination of values for effective length of columns, effective slab width, and concrete density for which the resonant frequencies of the model will match those of the real structure. Thus, a number of combinations of these parameters was found to match the experimental resonant frequencies equally well. In matching the model's resonant frequencies to the experimental resonant frequencies, particular attention was paid to the 2nd and 3rd resonant frequencies, since these were considered the most accurate. The final choice of values for the parameters is a matter for engineering judgment and the combination chosen was:

effective column length for all stories = 11 ft.
effective slab width = 8 ft.
density of lightweight concrete = 120 p.c.f.

Table 4.4 compares the resonant frequencies of the model and real structures.

Table 4.4

Comparison of Resonant Frequencies of Model and Prototype

	Resonant Frequencies (cps)				
	f_1	f_2	f_3	f_4	f_5
Prototype (N-S)	0.85	2.25	3.90	5.55	7.20
Model (N-S)	0.78	2.25	3.92	5.68	7.62
Prototype (E-W)	0.85	2.25	3.90	5.55	7.20
Model (E-W)	0.79	2.25	3.92	5.68	7.64

4.3 MATCHING RESONANT AMPLITUDES

The second phase in the formulation of the analytical model consisted of adjusting the values of damping capacity in the first 5 modes to give equal resonant amplitudes in the model and prototype for equivalent sinusoidal excitation. The exciter force was simulated in the model by applying a horizontal force $\omega^2 P \sin \omega t$ to the roof. In the first trial, the damping capacity of the first 5 modes of the model was made equal to the corresponding experimental values found in the building in the summer of 1964. The circular frequency ω was increased from zero to a frequency above the 5th resonant frequency, then the model's resonant amplitudes were compared with those found experimentally in the summer 1964 tests. The damping values were adjusted; the resonant amplitudes recomputed, and compared with the experimental results. This process was continued until the resonant amplitudes of the model matched the experimental resonant amplitudes of the building to the required degree of accuracy. Table 4.5 compares the value of damping capacity derived for the model with those found in the building in the summer 1964 tests.

Table 4.5

Comparison of Model's Damping Ratios with Those Found for the East Building in the Summer 1964 Test

Mode	N-S		E–W	
	Model	Exp.	Model	Exp.
1	1.70	1.8	1.05	2.0
2	0.35	0.7	0.40	0.9
3	0.38	0.4	0.40	0.7
4	0.50	0.5	0.45	–
5	0.75	0.7	–	

4.4 CHECKING MODEL AGAINST EXPERIMENTAL RESULTS

The shape of the resonance curves and vibration modes were not used to formulate the model. They thus provide a means of checking the model's accuracy. Experimental points of the resonance curves of the real structure are plotted on the resonance curves of the first 3 E-W modes of the model in Figs. 4.1 through 4.3. The first two E-W mode shapes of the model and prototype are compared in Figs. 4.4. The discrepancy between the computed and experimental mode shapes is attributable to inaccuracies in the experimental results as discussed in Section 3.4.1.

Similarly, a comparison of the computed and experimental torsional resonant frequencies serves to check the accuracy of the model. The torsional resonant frequencies of the model were computed by means of DINFRA, and they are compared with the experimental torsional resonant frequencies in Table 4.6. The agreement between the computed and experimental results is considered satisfactory.

Table 4.6

Comparison of Computed and Experimental Torsional Resonant Frequencies

Mode	Resonant Frequencies (cps)	
	Computed	Experimental
1	1.36	1.32
2	3.22	2.92
3	5.39	4.89

Overall, the analytical model was considered to simulate the behavior of the prototype realistically, and hence the response of the real structure to earthquake ground accelerations could be predicted reliably from this analytical model.

4.5 RESPONSE OF ANALYTICAL MODEL TO GROUND ACCELERATIONS

The analytical model for the N-S direction was subjected to ground acceleration records in order to assess the behavior of the real structure in an earthquake. A linear analysis was employed at first, but since it was found for certain cases of damping that the yield moments of some members was being exceeded, a nonlinear analysis was also conducted.

4.5.1 Linear Analysis

The computer program FRMDYN was used for the linear analysis. This program employs the mode superposition procedure, and in this case the first 6 modes were considered. The response of the model was computed for two earthquakes: El Centro of May 18, 1940 (N-S direction), and Taft of 1952 (N69W). Figs. 4.5 and 4.6 show, for the first 15 sec. of El Centro and Taft, respectively, the variation with time of roof displacement, base shear and base overturning moment.

The stresses generated in the model by the ground acceleration are compared with those predicted by the Uniform Building Code in Table 4.7. As has been found in many previous analyses, the U.B.C. stresses are much smaller than these calculated theoretically. It should be remembered, however, that the values of damping employed in the computer calculations are experimental values for very small amplitudes. It is reasonable to expect, therefore, that in the larger stress amplitudes that would occur in an earthquake, the values of damping capacity would be substantially larger than the ones used in this calculation.

Table 4.7 also shows that for an earthquake of El Centro intensity, yielding should be expected to occur if the damping values were of the same magnitude as measured in the summer 1964 tests. Yielding would occur first in the flanges of the intermediate columns around their weak axes. On increasing the values of damping capacity to 5% of critical in all modes, yield stresses were not reached in any part of the structure. The yield mechanism of the structure under earthquake loading was studied by means of the program NONLIN.

4.5.2 Nonlinear Analysis

The response of the model to ground acceleration when yielding of the members occurred was computed by means of NONLIN. This program employs a step-by-step numerical integration procedure to solve the differential equations governing the motion of the structure.

It was necessary to consider only one quarter of the model structure in the analysis since the structure has two axes of symmetry. The quarter structure analyzed is shown in Fig. 4.7(a), and for the purposes of this analysis, the two frames AB and CD were linked to form an equivalent plane frame shown in Fig. 4.7(b).

The equivalent plane frame of the East Building with zero damping was subjected to the El Centro ground acceleration. The resulting yield mechanism is shown in Fig. 4.8. The ductility ratio shown beside each yielding member is defined as: the maximum ratio of plastic rotation to elastic rotation capacity of that element. Yielding was severest between floor levels 11 and 13 around the weak axis of the interior columns.

When the damping was increased to 5% of critical in the first mode, the yield moment of no member was exceeded.

In order to cause yielding with 5% of critical damping in the first mode, the acceleration ordinates of the El Centro record were all increased by a factor of 1.3. Under these conditions, the maximum lateral story displacements were approximately equal to those for the case of zero damping described above (a maximum roof displacement of approximately 8 ins). However, the maximum story-to-story displacements were substantially reduced from the zero damping case; the maximum ductility factors were associated with the interior columns between floor levels 11 and 13 (see Fig. 4.9).

Table 4.7

Maximum Response Values for Vertical and Horizontal Loads, East Building

Description		Vertical	Horizontal (N-S)			
				Dynamic		
			U.B.C.	El Centro		Taft
		Static	(earthquake)	Case I*	Case II**	Case I
Max. Roof Displacement (*in.*)		-	1.45	7.09	5.53	4.44
Max. Overturning Moment (*k-in.*)		-	1.22×10^6	6.80×10^6	5.52×10^6	4.05×10^6
Max. Base Shear (*k*)		-	934	6760	3760	4595
Bending Stresses (*ksi*)	Corner Column (Strong Direction)	1.93	5.23	31.8	20.3	
	Intermediate Column (Strong Direction)	2.91	3.39	23.4	13.5	
	Intermediate Column (Weak Direction)	3.24	6.39	46.2	25.8	
Shear Stresses (*ksi*)	Corner Column (Strong Direction)	0.01	0.68	18.2	10.0	
	Intermediate Column (Strong Direction)	1.00	2.16	15.9	8.8	
	Intermediate Column (Weak Direction)	0.06	2.30	6.0	3.3	

*Case I 1.70, 0.35, 0.38, 0.58, 0.75% CRITICAL DAMPING IN FIRST 5 MODES.

**Case II: 5% CRITICAL DAMPING IN FIRST 5 MODES.

CHAPTER 5

SUMMARY AND CONCLUSIONS

5.1 GENERAL SUMMARY

The experimental results from dynamic tests conducted on the new buildings at the University of California's Medical Center in San Francisco have been presented in Chapter 3. The results obtained for the East Building were used in the formulation of a model of that building, and this analytical work has been described in Chapter 4. In this chapter, the experimental work, the interaction of the buildings which had considerable effect on the experimental results, and the analytical work are discussed. Finally, the conclusions are summarized.

5.2 EXPERIMENTAL WORK

The experimental work consisted of three test series conducted on the East Building over a period of 18 months, and some tests on the mechanical service tower and the elevator tower conducted mainly in the fall of 1964.

The experimental equipment was found to be completely satisfactory for measuring the properties of the first two modes of vibration. However, it was found that one exciter station was not sufficient to excite good approximations to normal modes in the higher modes of vibration; the structure did not respond as a single degree of freedom system in the 3rd, 4th and 5th modes. Such a multi-degree of freedom system could only be excited satisfactorily in its higher modes by deploying more vibration generators over the height of the building. However, in future testing, if more vibration generators are not available, then consideration should be given to testing each mode individually with the vibration generators placed at the optimum position for that mode.

Resonant frequencies were obtained by reading the frequencies at which maximum responses occurred in the frequency-response curves. In general, this method in itself was satisfactory and did not impose a limit to the accuracy of the resonant frequencies. Instead, the precision of the resonant frequencies was limited by two other factors:

i. The structure behaved nonlinearly as a spring-softening system with a weak nonlinearity. The resonant frequencies thus decreased with amplitude so that the values which have been quoted are for an average of the amplitudes at which the tests were conducted.

ii. In the case of higher modes of vibration, the excitation was not suitable for exciting good approximations to normal modes. The resonant peaks of different floors occurred at slightly different frequencies, thus reducing the precision of evaluating the resonant frequencies.

The method of measuring mode shapes described in Chapter 2 was found to be satisfactory. The first two mode shapes were determined accurately, but the lack of appropriate excitation for the higher modes led to inaccuracies in their mode shapes. Because the structure was not behaving entirely as a single degree of freedom system in the higher modes, these mode shapes varied rapidly with frequency near resonance. Hence, the mode shape depended considerably on the frequency at which it was measured.

Damping capacities were measured by both the bandwidth method and the logarithmic decay method.

The bandwidth method was found to be applicable over the complete range of damping

capacities and frequencies investigated. However when the damping capacity was below 1% of critical, some difficulties were encountered in observing sufficient points on the resonance curve to define it accurately. These difficulties arose because of insufficient control of the motor speed when the damping capacity of the structure was small. Above 8% critical damping capacity, the resonance curves became ill-defined, and in some cases resonance curves in the normal sense did not exist. Some Kennedy and Pancu plots were drawn but, since the resonant frequencies were well separated, this method had no advantage over the normal bandwidth method.

In the summer 1964 tests when the damping was small, the logarithmic decay method was found to be convenient and accurate, and could be used for all the modes. In the 1965 tests this method could be employed only for the first mode. By 1965 the damping had increased so much that when the vibration generators' rotational speed was being turned down to zero from the resonant frequency of a higher mode, the first mode would be excited and interfere with the higher-mode response.

The experimental results of the first two modes of vibration for the East Building were determined to a satisfactory accuracy. Although the results for the higher modes of vibration were not so accurate, they are still of significant value. The experimental results, however, will not be of as much value in the design of this type of building as was hoped originally because of the interaction of the East Building with its adjacent service structures. This interaction between the buildings is discussed in the next section.

5.3 INTERACTION OF BUILDINGS

The large change in dynamic properties of the East Building which occurred between the summers of 1964 and 1965 is one of the most striking features of the experimental results. In the summer of 1964, the damping capacities were in the range 0.4 to 2.0% of critical. However, in subsequent tests, they were in the range of 5 to 13% of critical. In the same period the resonant frequencies of all modes increased by amounts varying from 7 to 29%. At first it was thought that these changes had been caused by the insertion of windows and partitions in the building. But, after the detailed study of the behavior of the service tower in the fall 1965 tests, it was realized that the changes had occurred because of the interaction between the East Building and its service tower.

The tests in the fall of 1965 showed the East Building was coupled to its service tower in some complex manner. The coupling was caused by the reinforced concrete beams and slabs at the ground floor and basement levels. Thus, a different system was tested in 1965 from that tested in the summer of 1964, and it is therefore reasonable to expect a difference in dynamic properties between the 1964 and 1965 tests.

It was not surprising that the coupled system had somewhat higher resonant frequencies than the isolated East Building; however, it was difficult at first to understand the causes of the large increase in damping capacity. But it has been shown that this increase in damping capacity is mainly attributable to the energy dissipated in Coulomb friction between the concrete floor slabs of the East Building and the steel plates which span the gaps at every floor level to both the service tower and the connecting corridor.

This unforeseen dynamic coupling of the buildings had a number of effects on the research program:

1. The schedule of testing had to be modified after the fall of 1964, when it was no longer possible to test the mechanical service tower and the elevator tower in isolation. The effect and cause of the connections between the buildings then became important and had to be fully investigated.
2. The damping capacity of the connected system of buildings was much larger than that of the isolated East Building as tested

in 1964. The response of the system was small and hence was more difficult to measure. It was also necessary to monitor the response of many points in the connected system of buildings in order to understand the system's behavior. Thus, after the buildings became connected, the experimental work was more difficult and laborious.

3. The damping capacity results from the 1965 tests were for a system of connected buildings, and they were influenced greatly by the type of connection which existed between the buildings. Thus, the measured damping capacities are only of direct applicability to systems with this type of connection and will not be as useful in design as those from the isolated buildings would have been. Therefore, in choosing buildings for testing in future, attention should be paid to any such peculiarities in construction which might limit the applicability of the damping capacity results.

5.4 ANALYTICAL WORK

The formulation of the analytical model was quite straightforward. The main difficulties encountered were in determining the effective column lengths and effective slab widths. The values of both these parameters were estimated, and then adjustments were made to these values until the resonant frequencies of the model coincided with the experimental resonant frequencies. The damping capacity of the model was adjusted until the resonant amplitudes of model and prototype were equal for the same excitation. The standard open-frame model formulated in this way was found to reproduce accurately the dynamical behavior of the real structure.

The model of the building was subjected to both the El Centro (1940) and Taft (1952) earthquake ground accelerations. This linear model indicated that yielding would occur in the intermediate columns around their weak axes in an earthquake of El Centro intensity if the damping was of the same magnitude as in the summer of 1964 (1.70, 0.35, 0.38, 0.58, and 0.75% critical in the first 5 modes, respectively). However, when the damping was 5% in all modes (corresponding approximately to the damping capacities in the summer of 1965), no yielding occurred at all. In the Taft earthquake, yielding did not occur even in the case of the lower damping capacities.

The yield mechanism of the model as caused by the El Centro earthquake record was studied in a nonlinear analysis. For zero damping capacity yielding was quite severe. The highest ductility ratios were found at the 11th and 12th floors (2.43 and 2.11, respectively), in the interior columns resisting bending around their weak axes. With 5% damping in the first mode, yielding did not occur in any member. To cause yielding in the 5% damping case, the acceleration amplitudes of El Centro were increased by a factor of 1.3. In this case, the highest ductility factors were found in the same members as before, but yielding was not so severe or widespread.

This nonlinear analysis illustrated the important role of damping in enabling structures to withstand earthquakes.

5.5 SUMMARY OF CONCLUSIONS

1. The experimental equipment was found to be capable of exciting the first 5 translational modes of the East Building. However, because there was only one exciter station, the excitation of the higher modes of vibration was not entirely satisfactory.
2. The experimental techniques of measuring the dynamic properties of the structure did not, in themselves, impose a limit on the accuracy of the results. Instead, the quantities being measured were often of an imprecise nature due to the characteristics of the structure, and in the case of the higher modes, this effect was accentuated by a lack of proper excitation.

3. The logarithmic decay method of measuring damping was found very convenient and accurate if the damping capacities were small—less than 1% of critical. For higher damping capacities, this method lost some of its advantages, and when the damping capacity was between 1% and 5% of critical the bandwidth method was found more suitable as a method of measuring damping.
4. The steel frame of the service tower had very little effect on the dynamic behavior of the East Building in the summer of 1964, and the East Building was tested virtually in isolation. However, when the steel frame had been encased in concrete, the service tower did affect the behavior of the East Building; in fact, both buildings then formed a new structural system. This interconnected system had much larger damping capacity than any of the isolated buildings, and it was correspondingly more difficult to test.
5. The increase of damping after the summer of 1964 was caused mainly by the connections between buildings. Thus, the resulting damping capacity, as measured in 1965, can only be applied directly to buildings with similar connections. In selecting buildings for future testing, consideration should be given to any such peculiar features which, although they may be ignored for design purposes, have a large influence on the building's dynamic response.
6. A standard open-frame model was found to reproduce accurately the dynamical behavior of the East Building. This model was subjected to the ground acceleration record of the El Centro earthquake. It was found that the amount of damping in the model played an important role in determining the extent to which yielding occurred.
7. More resonance tests of the type discussed in this report should be conducted in order to accumulate data on the damping capacity and other dynamic properties of all types of structures.

BIBLIOGRAPHY

Bishop and Gladwell (1961)

An Investigation into the Theory of Resonance Testing. Phil. Trans. R. Soc. Series A 255: 1055, 1963.

Bouwkamp (1965)

An Investigation for the Earthquake Resistant Design of Large-Size Welded and Bolted Girder to Column Connections. Proc. of the Third World Conference on Earthquake Engineering, IV/B/19, New Zealand 1965.

Gauzy (1959)

Measurement of Inertia and Structural Damping. Manual on Aeroelasticity, Vol. IV, 1959.

Hudson (1962)

Synchronized Vibration Generators for Dynamic Tests of Full-Scale Structures, Earthquake Engineering Research Laboratory Report, California Institute of Technology, 1962.

Kennedy and Pancu (1949)

Use of Vectors in Vibration Measurement and Analysis. Journ. of Aero. Sci. 14:11, 1947.

Skidmore, Owings and Merrill (1958)

An Evaluation of the Effect of Earthquake Cracking on a Neoprene Glazing Bead. Private Communication.

FIGURES

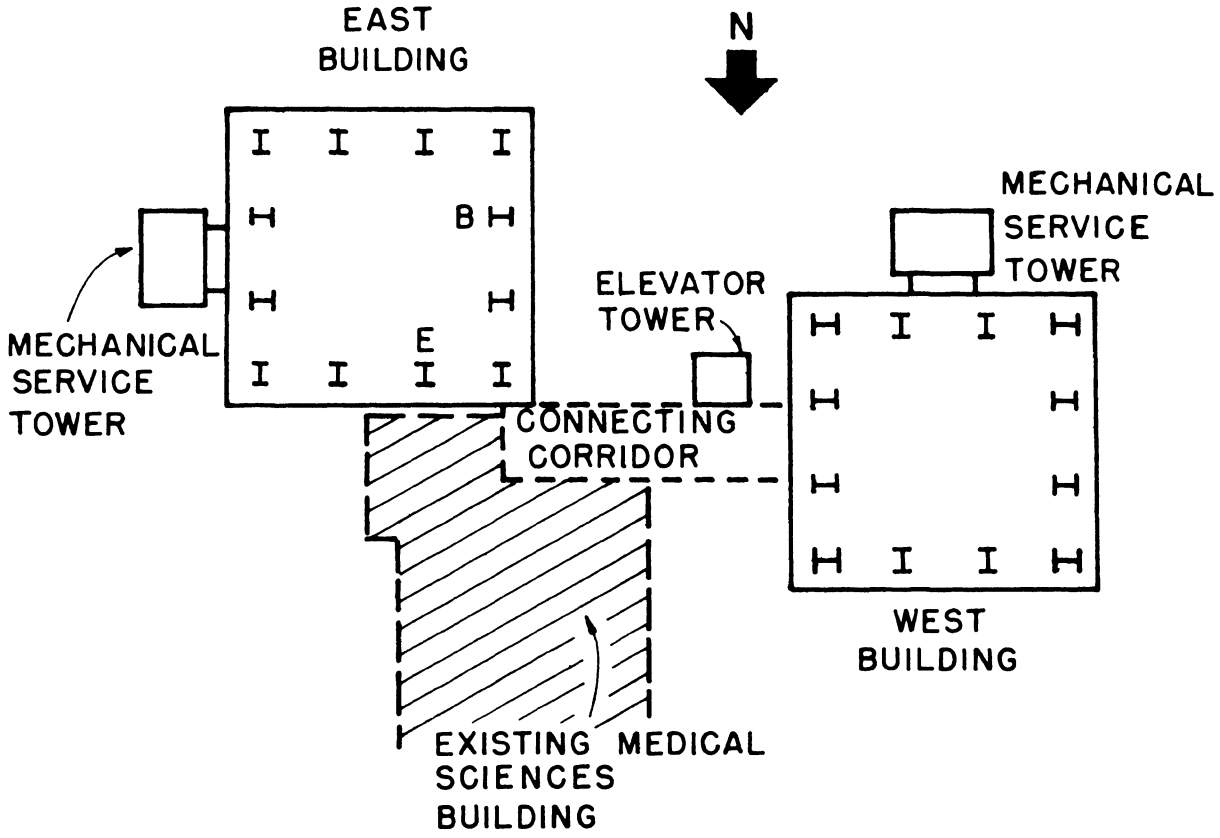

FIG. 2.1 – GENERAL PLAN OF BUILDINGS

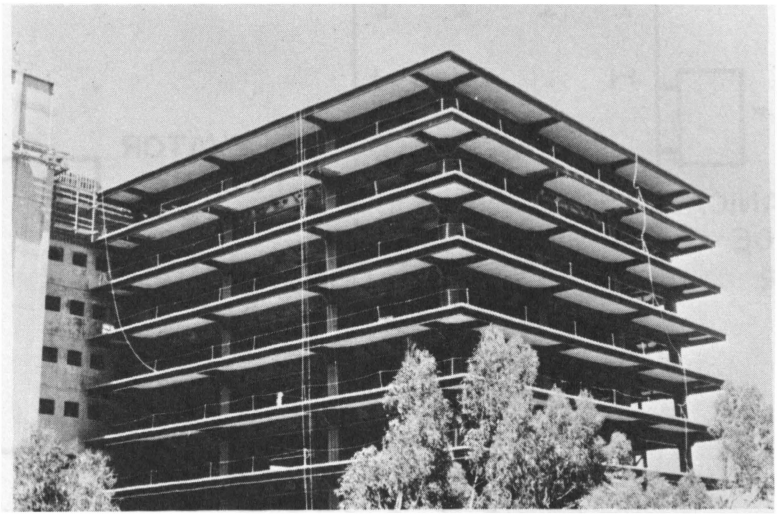

FIG. 2.2 – UPPER FLOORS OF EAST BUILDING

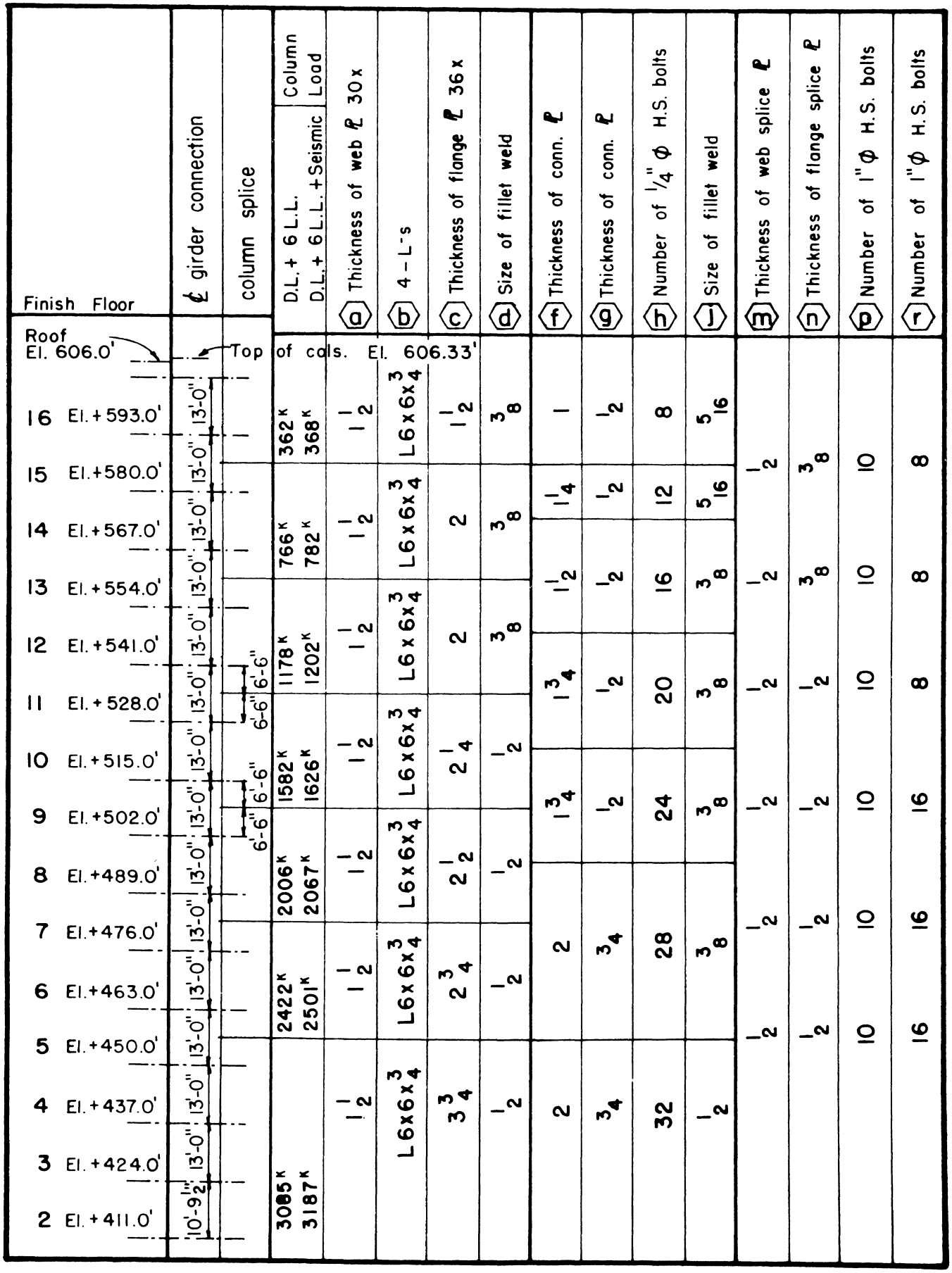

FIG. 2.3 — INTERMEDIATE COLUMN SCHEDULE

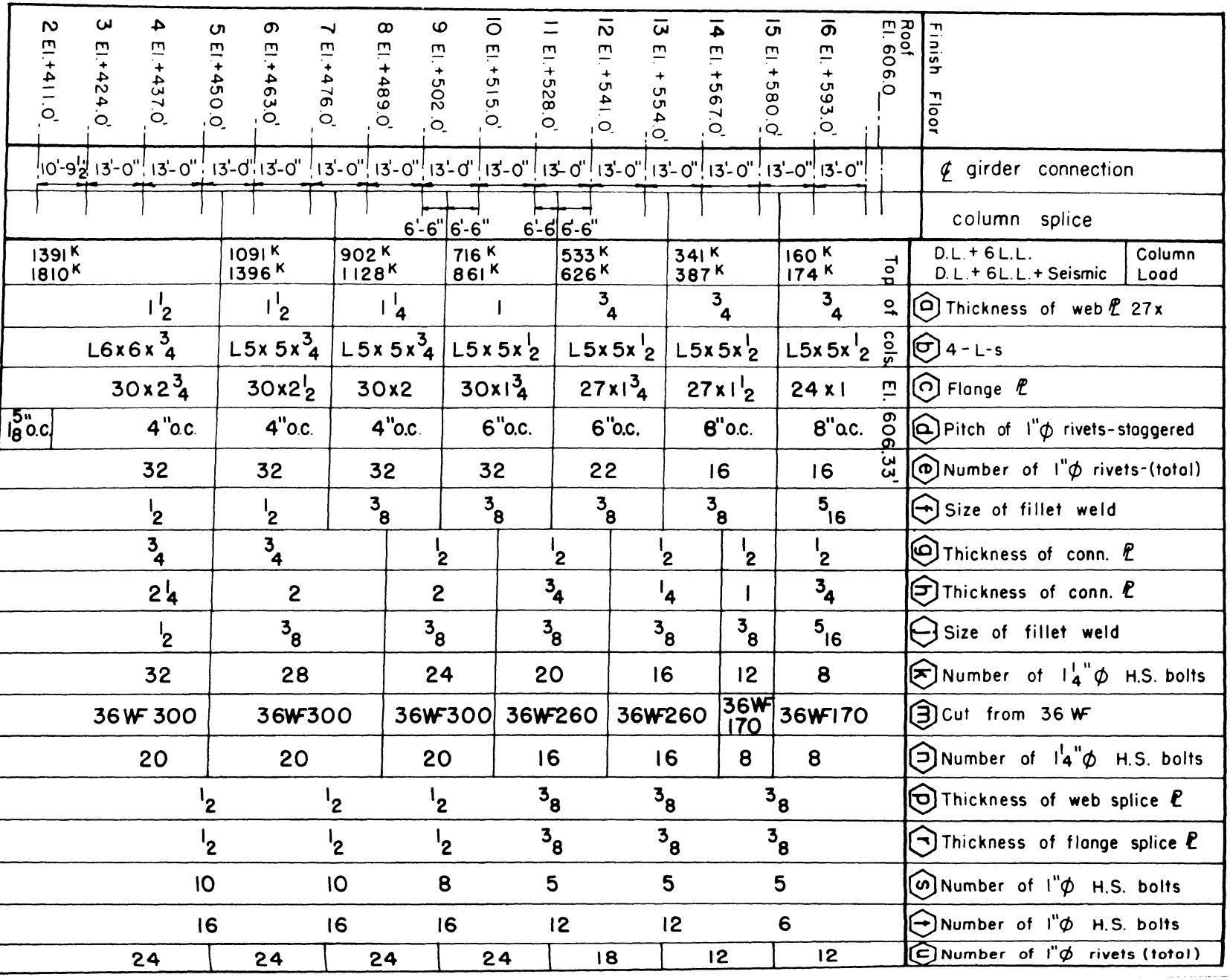

Finish Floor	2 El.+411.0'	3 El.+424.0'	4 El.+437.0'	5 El.+450.0'	6 El.+463.0'	7 El.+476.0'	8 El.+489.0'	9 El.+502.0'	10 El.+515.0'	11 El.+528.0'	12 El.+541.0'	13 El.+554.0'	14 El.+567.0'	15 El.+580.0'	16 El.+593.0'	Roof El. 606.0	
℄ girder connection	10'-9½"	13'-0"	13'-0"	13'-0"	13'-0"	13'-0"	13'-0"	13'-0"	13'-0"	13'-0"	13'-0"	13'-0"	13'-0"	13'-0"	13'-0"		
column splice								6'-6"	6'-6"	6'-6"	6'-6"						
D.L. + 6 L.L. D.L. + 6 L.L. + Seismic — Column Load				1391 K 1810 K			1091 K 1396 K		902 K 1128 K		716 K 861 K		533 K 626 K		341 K 387 K		160 K 174 K
(a) Thickness of web ℄ 27x				$1\frac{1}{2}$			$1\frac{1}{2}$		$1\frac{1}{4}$		1		$\frac{3}{4}$		$\frac{3}{4}$		$\frac{3}{4}$
(b) 4 - L-s				L6x6x$\frac{3}{4}$			L5x5x$\frac{3}{4}$		L5x5x$\frac{3}{4}$		L5x5x$\frac{1}{2}$		L5x5x$\frac{1}{2}$		L5x5x$\frac{1}{2}$		L5x5x$\frac{1}{2}$
(c) Flange ℄				30x2$\frac{3}{4}$			30x2$\frac{1}{2}$		30x2		30x1$\frac{3}{4}$		27x1$\frac{3}{4}$		27x1$\frac{1}{2}$		24x1
(d) Pitch of 1"ϕ rivets-staggered	$\frac{5}{8}$"o.c.	4"o.c.			4"o.c.			4"o.c.			6"o.c.		6"o.c.		8"o.c.		8"o.c.
(e) Number of 1"ϕ rivets-(total)		32			32			32			32		22		16		16
(f) Size of fillet weld		$\frac{1}{2}$			$\frac{1}{2}$			$\frac{3}{8}$			$\frac{3}{8}$		$\frac{3}{8}$		$\frac{3}{8}$		$\frac{5}{16}$
(g) Thickness of conn. ℄		$\frac{3}{4}$			$\frac{3}{4}$			$\frac{1}{2}$			$\frac{1}{2}$		$\frac{1}{2}$	$\frac{1}{2}$			$\frac{1}{2}$
(h) Thickness of conn. ℄		$2\frac{1}{4}$			2			2			$\frac{3}{4}$		$\frac{1}{4}$	1			$\frac{3}{4}$
(j) Size of fillet weld		$\frac{1}{2}$			$\frac{3}{8}$			$\frac{3}{8}$			$\frac{3}{8}$		$\frac{3}{8}$	$\frac{3}{8}$			$\frac{5}{16}$
(k) Number of $1\frac{1}{4}$"ϕ H.S. bolts		32			28			24			20		16	12			8
(m) Cut from 36 WF		36WF 300			36WF300			36WF300			36WF260		36WF260	36WF 170			36WF170
(n) Number of $1\frac{1}{4}$"ϕ H.S. bolts		20			20			20			16		16	8			8
(p) Thickness of web splice ℄			$\frac{1}{2}$			$\frac{1}{2}$			$\frac{1}{2}$			$\frac{3}{8}$			$\frac{3}{8}$		
(r) Thickness of flange splice ℄			$\frac{1}{2}$			$\frac{1}{2}$			$\frac{1}{2}$			$\frac{3}{8}$			$\frac{3}{8}$		
(s) Number of 1"ϕ H.S. bolts			10			10			8			5			5		
(t) Number of 1"ϕ H.S. bolts			16			16			16			12			12		
(u) Number of 1"ϕ rivets (total)		24			24			24			24		18		12		12

FIG. 2.4 – CORNER COLUMN SCHEDULE

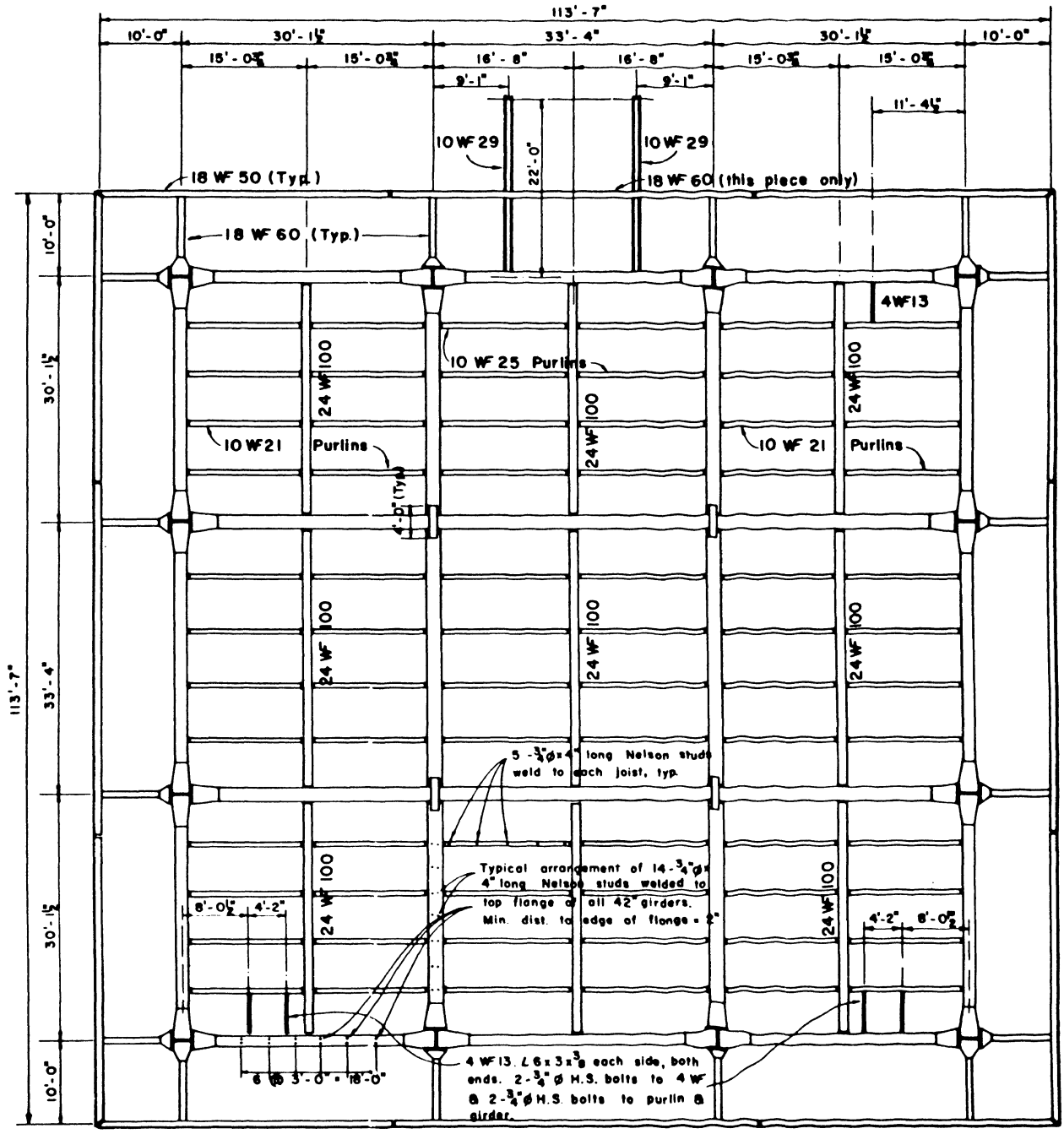

FIG. 2.5 – TYPICAL FLOOR FRAMING PLAN FROM THIRD FLOOR UP INCLUDING THE ROOF

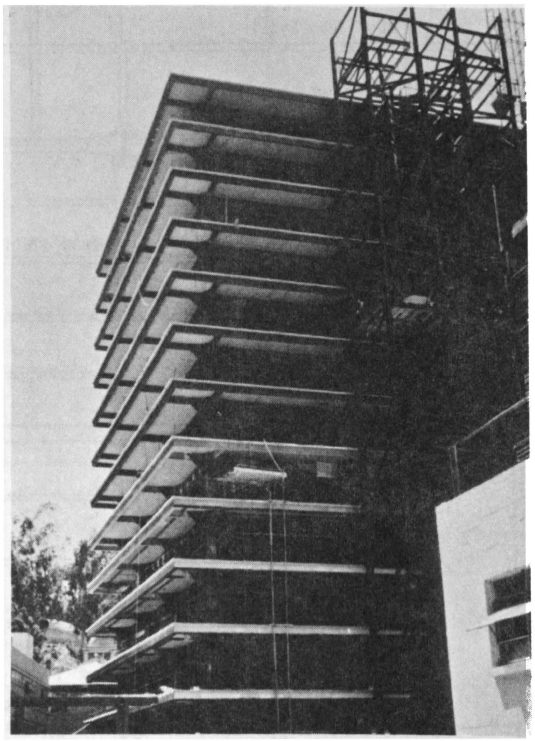

FIG. 2.6 – STEEL TRUSS OF EAST MECHANICAL SERVICE TOWER

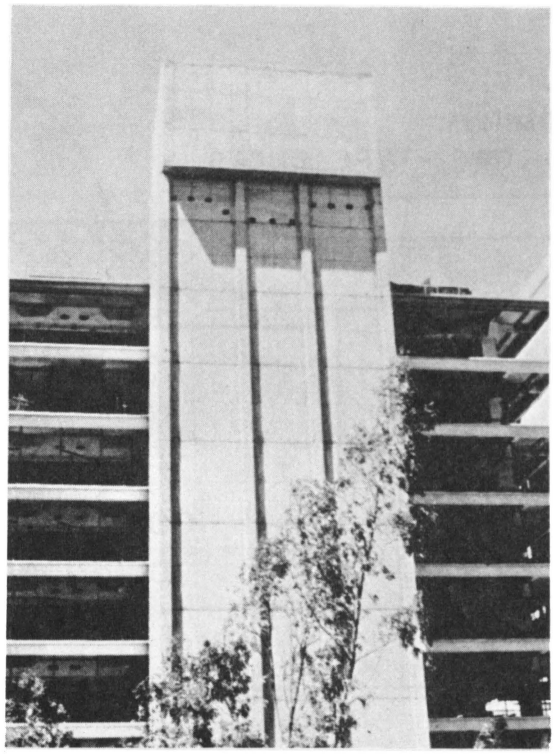

FIG. 2.7 – COMPLETED WEST MECHANICAL SERVICE TOWER

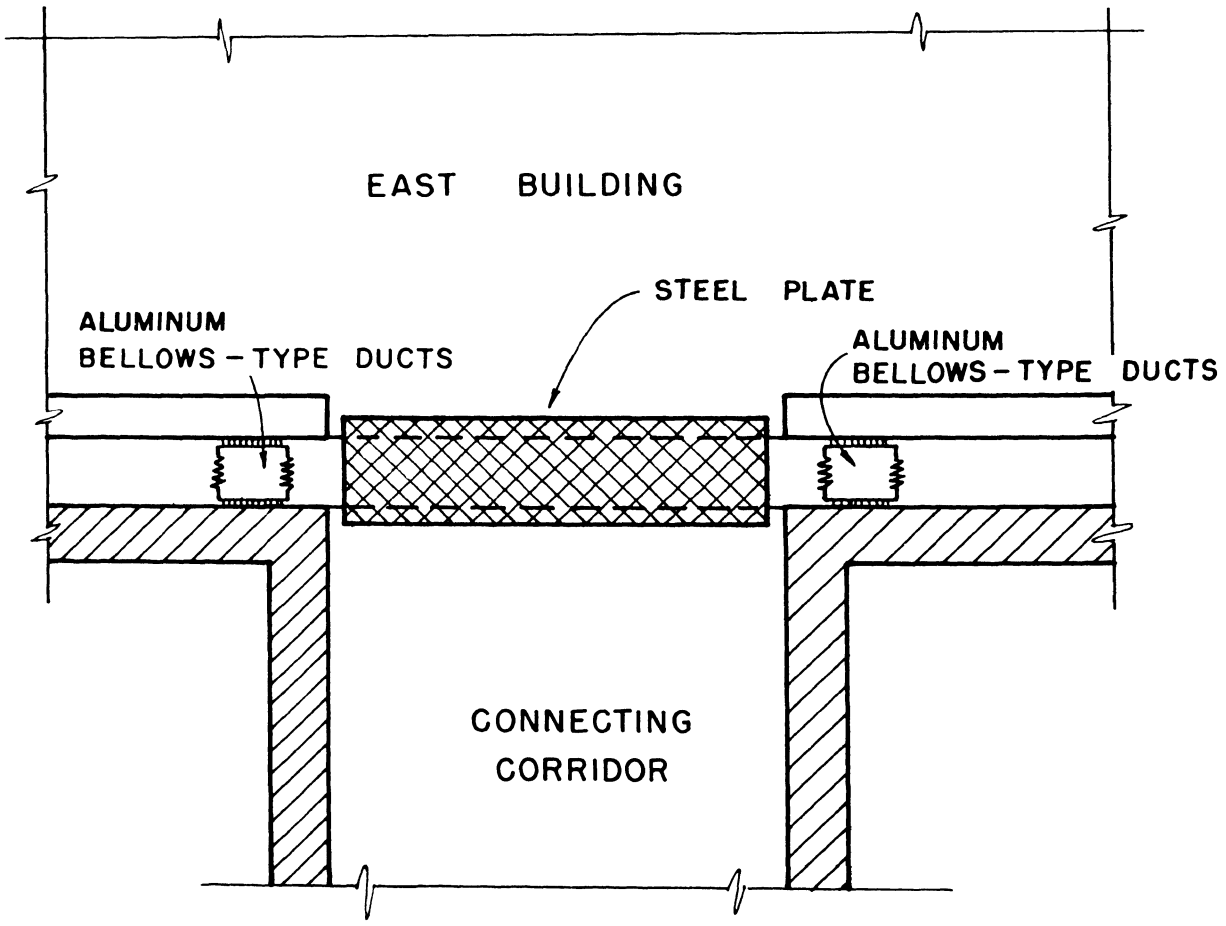

FIG. 2.8 – CONNECTION BETWEEN BUILDINGS AT ENTRANCE FROM CONNECTING CORRIDOR TO EAST BUILDING

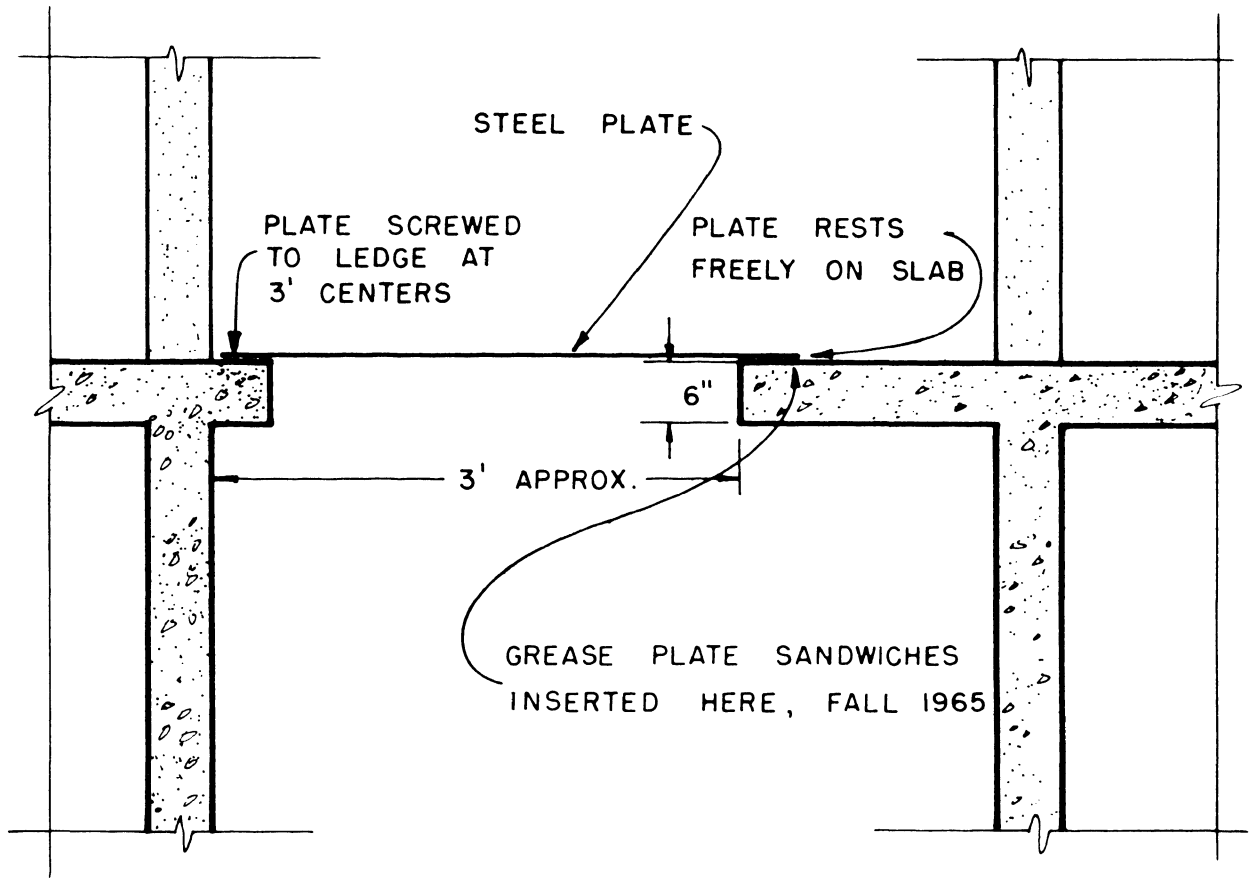

SECTION: NOT TO SCALE

FIG. 2.9 – STEEL PLATE PROVIDING ACCESS FROM EAST BUILDING TO SERVICE TOWER AT EVERY FLOOR

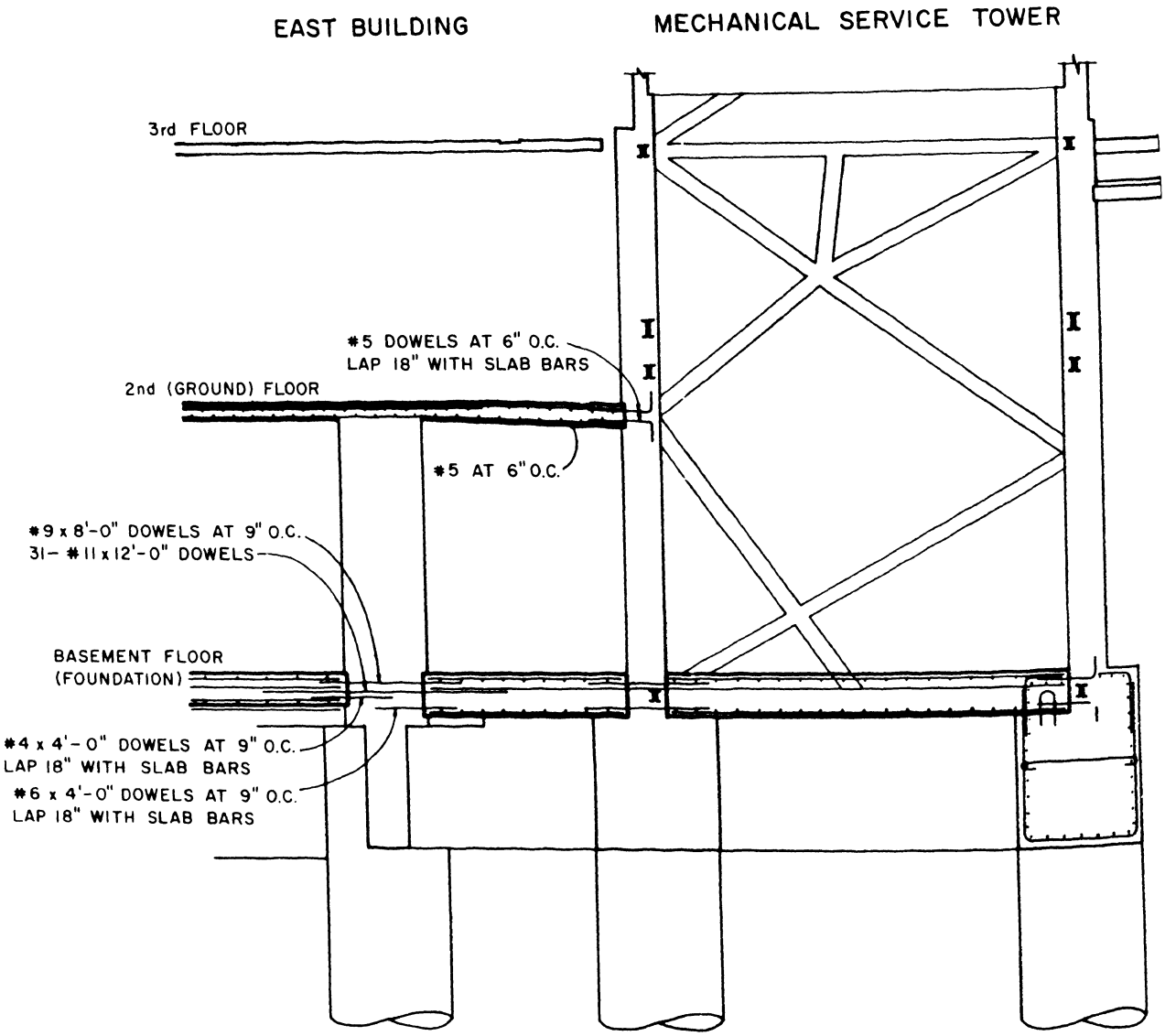

FIG. 2.10 – REINFORCED CONCRETE CAISSONS, COLUMNS, WALLS, BEAMS AND SLABS BETWEEN EAST BUILDING AND SERVICE TOWER

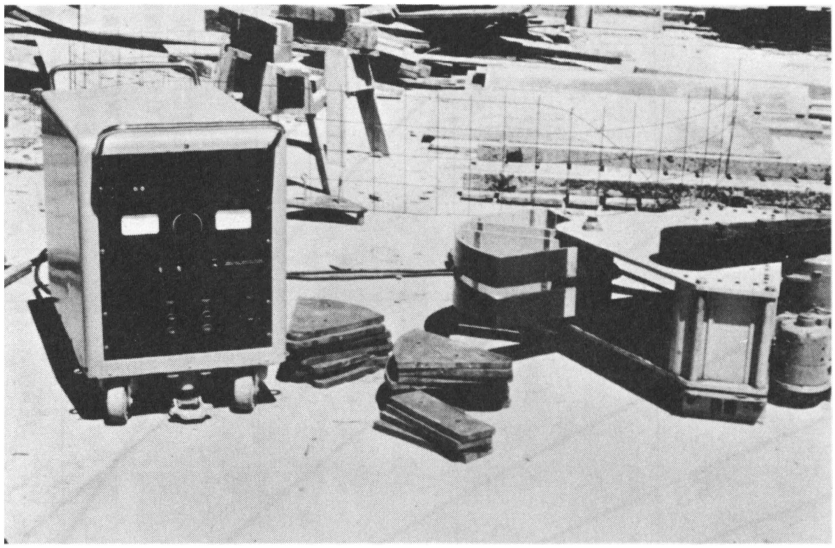

FIG. 3.1 – VIBRATION GENERATOR

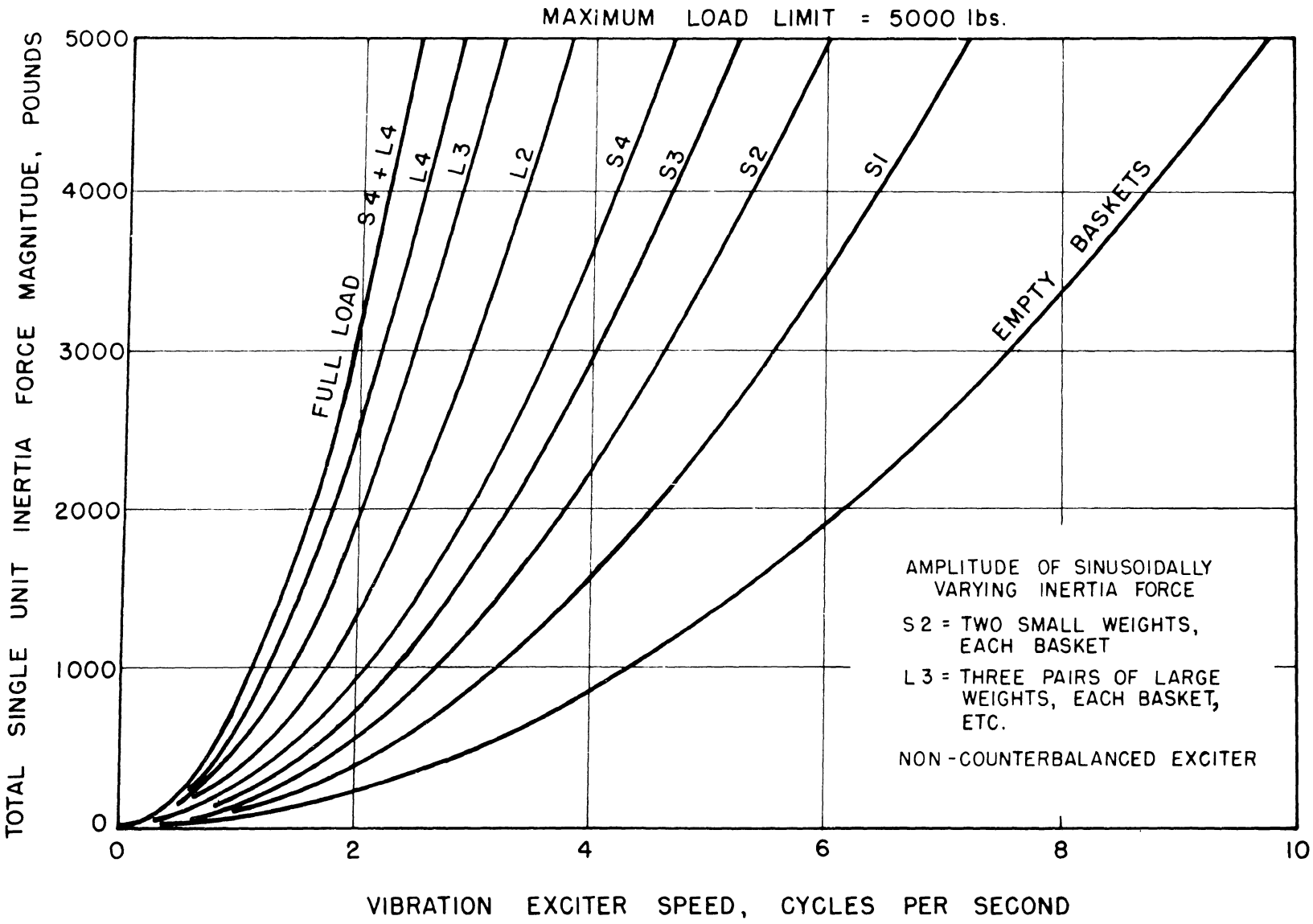

FIG. 3.2

VIBRATION GENERATOR FORCE OUTPUT vs. SPEED — NON-COUNTERBALANCED
(AFTER HUDSON 1962)

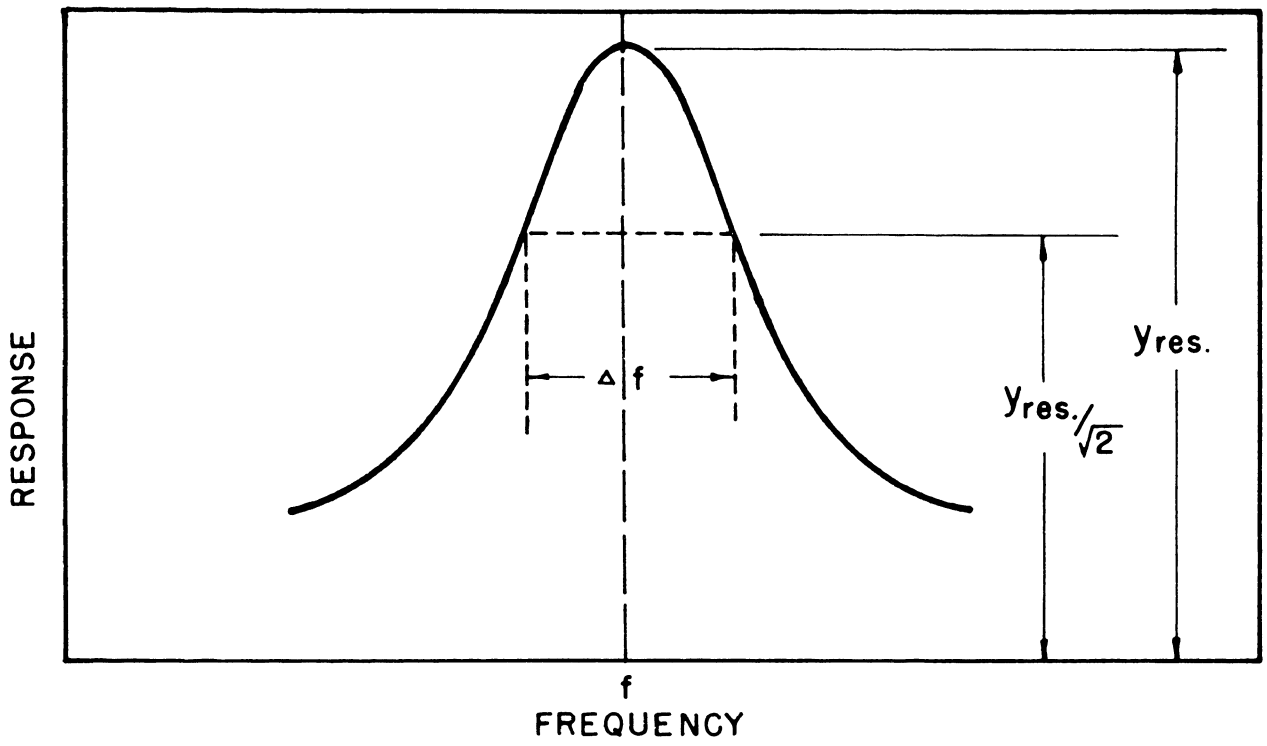

FIG. 3.3 – TYPICAL RESONANCE CURVE

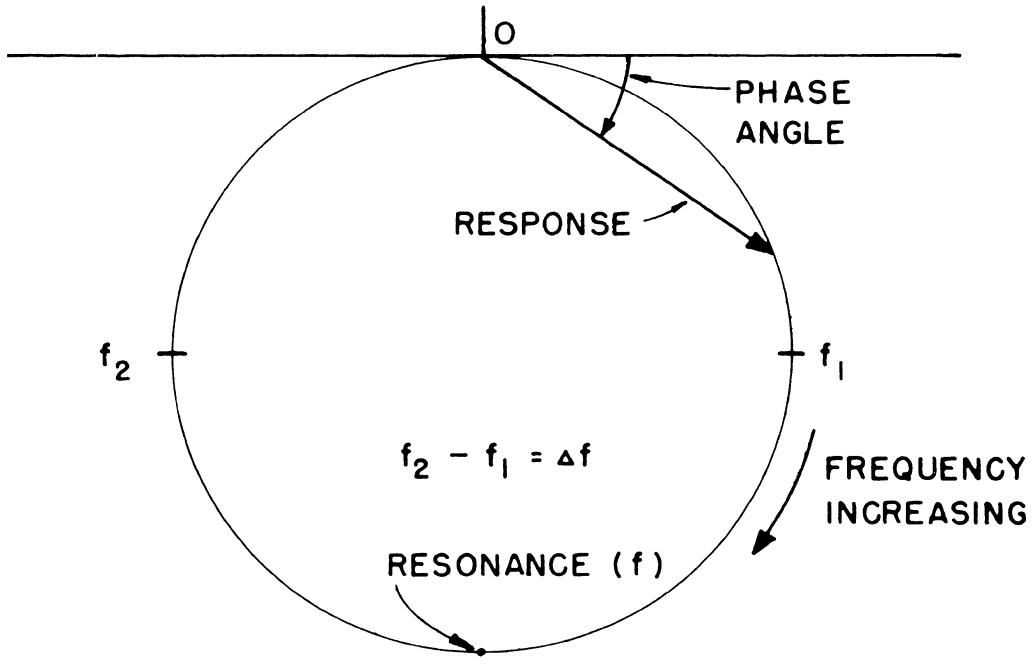

FIG. 3.4 – KENNEDY AND PANCU PLOT

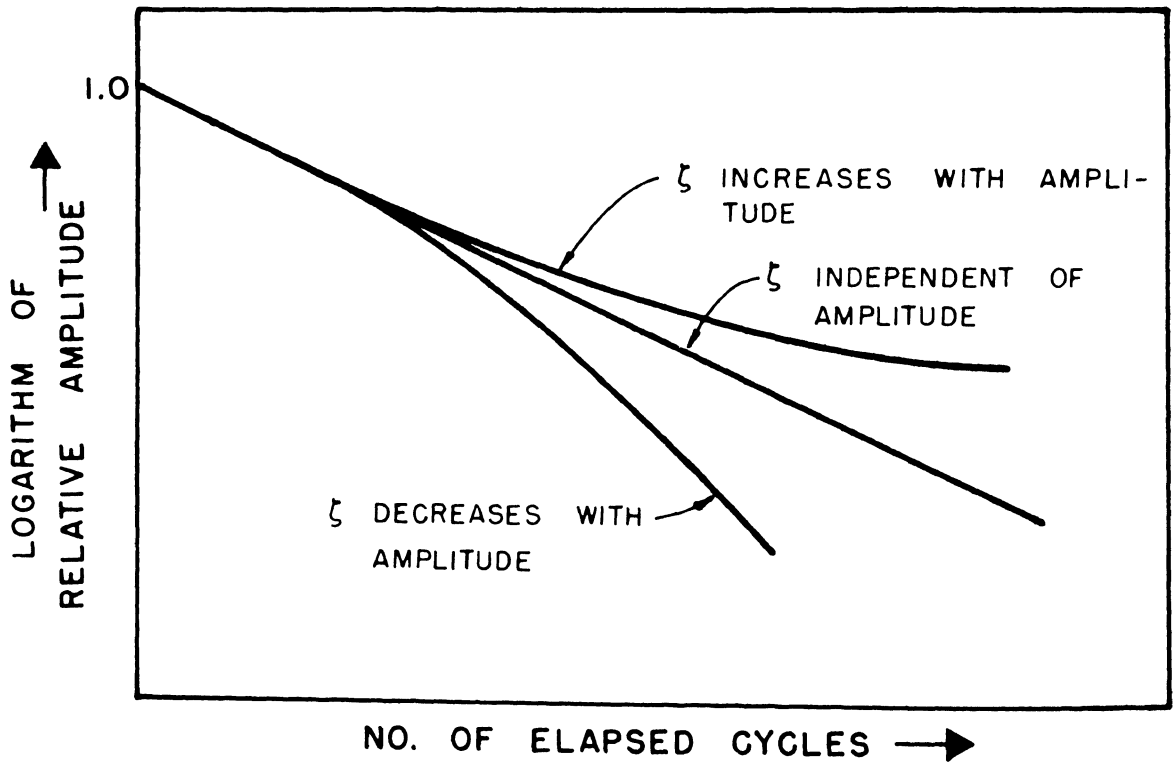

FIG. 3.5 – LOGARITHMIC DECAY CURVE

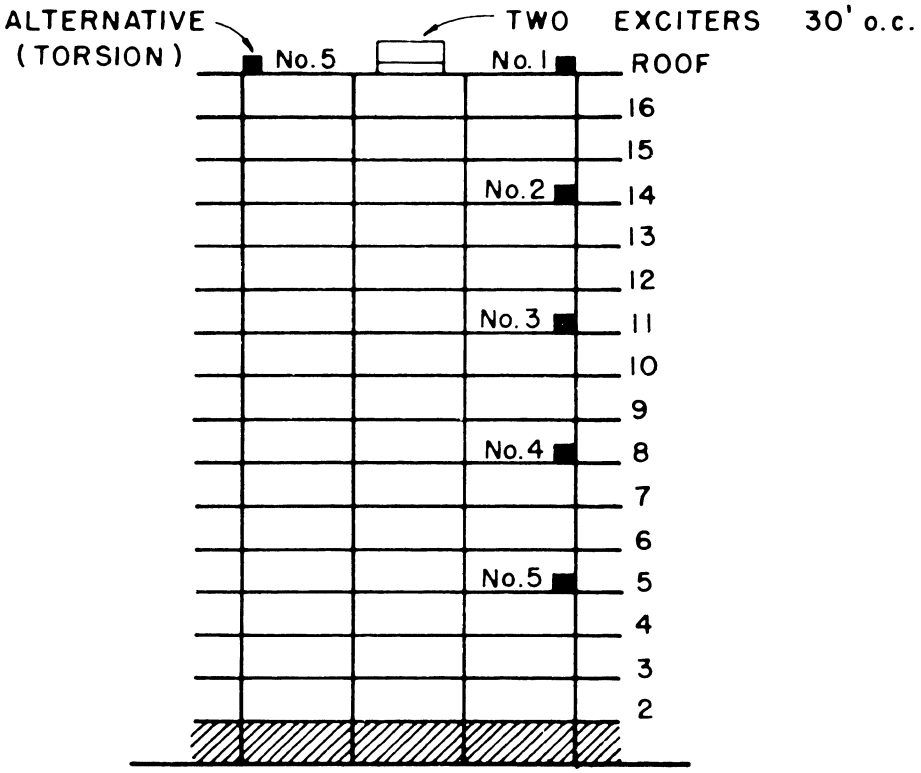

EAST BUILDING ELEVATION

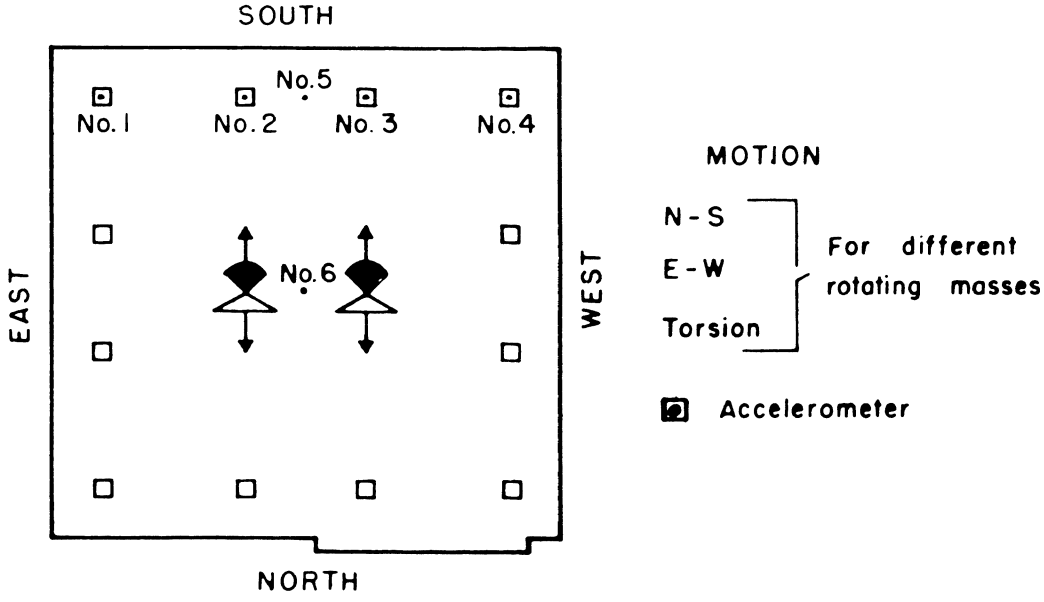

EAST BUILDING ROOF PLAN

FIG. 3.6 – POSITION OF VIBRATION GENERATORS AND ACCELEROMETERS; SUMMER 1964

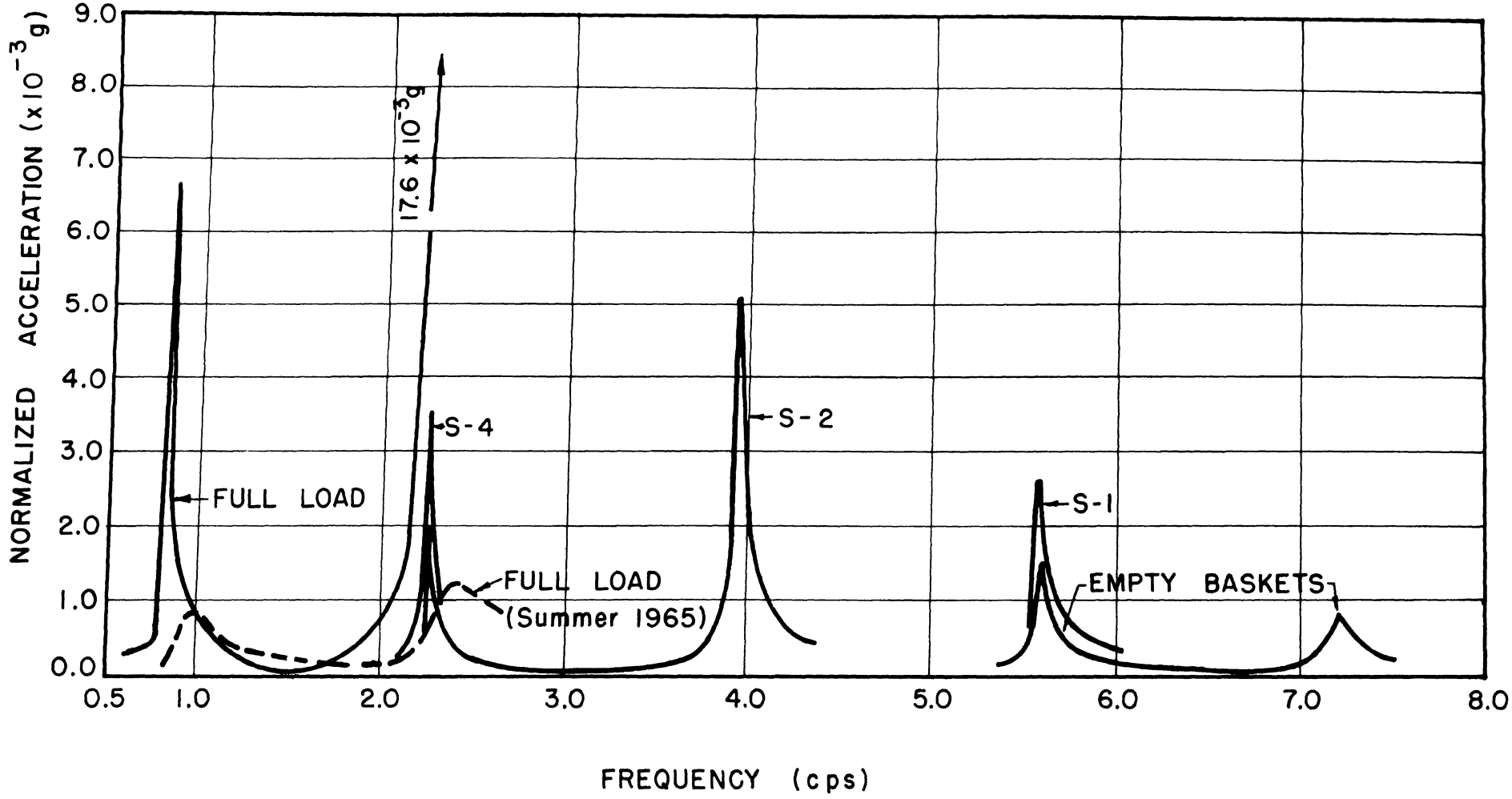

FIG. 3.7

FREQUENCY RESPONSE OF EAST BUILDING, N–S, SUMMER 1964

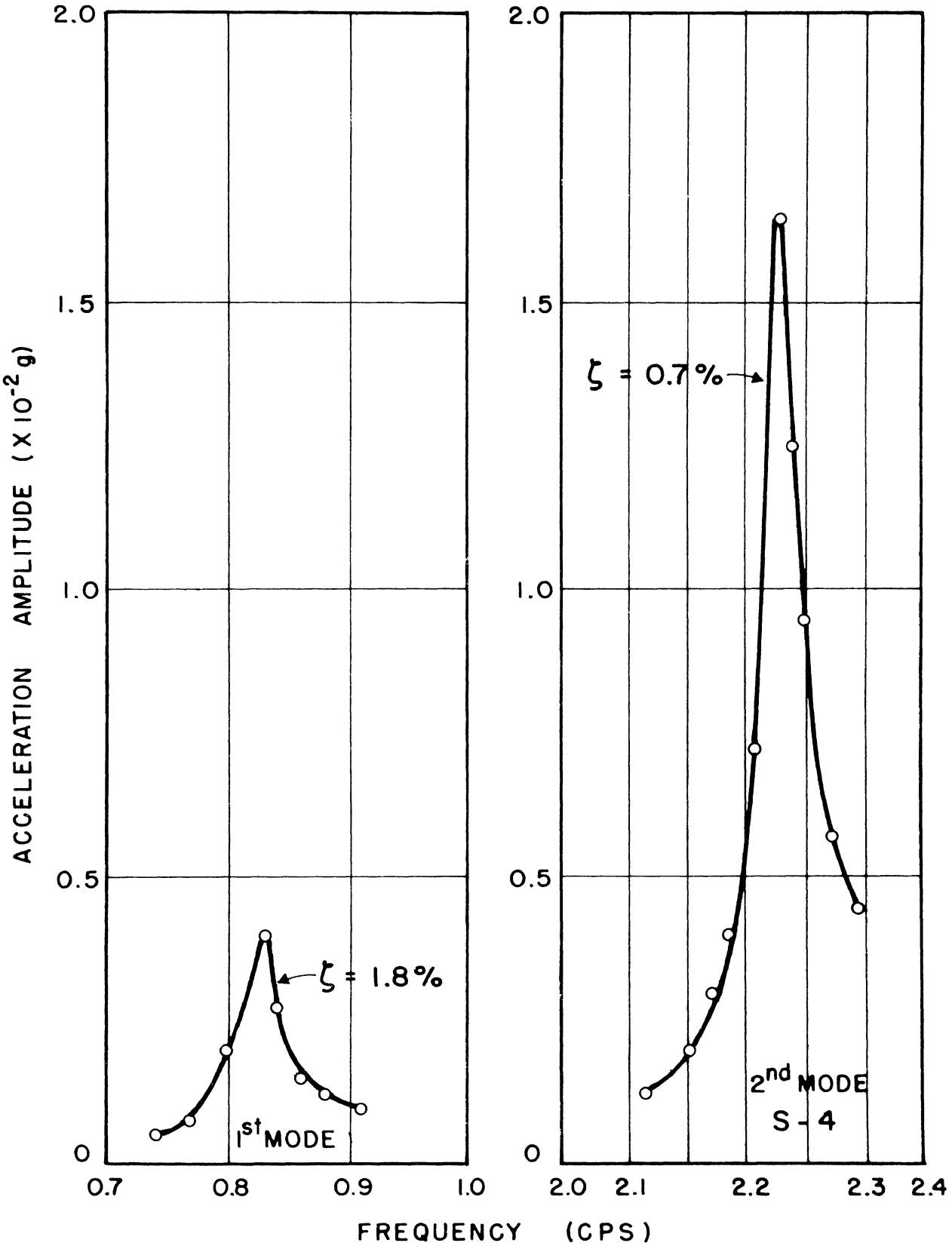

FIG. 3.8 – FREQUENCY RESPONSE, N–S, SUMMER 1964

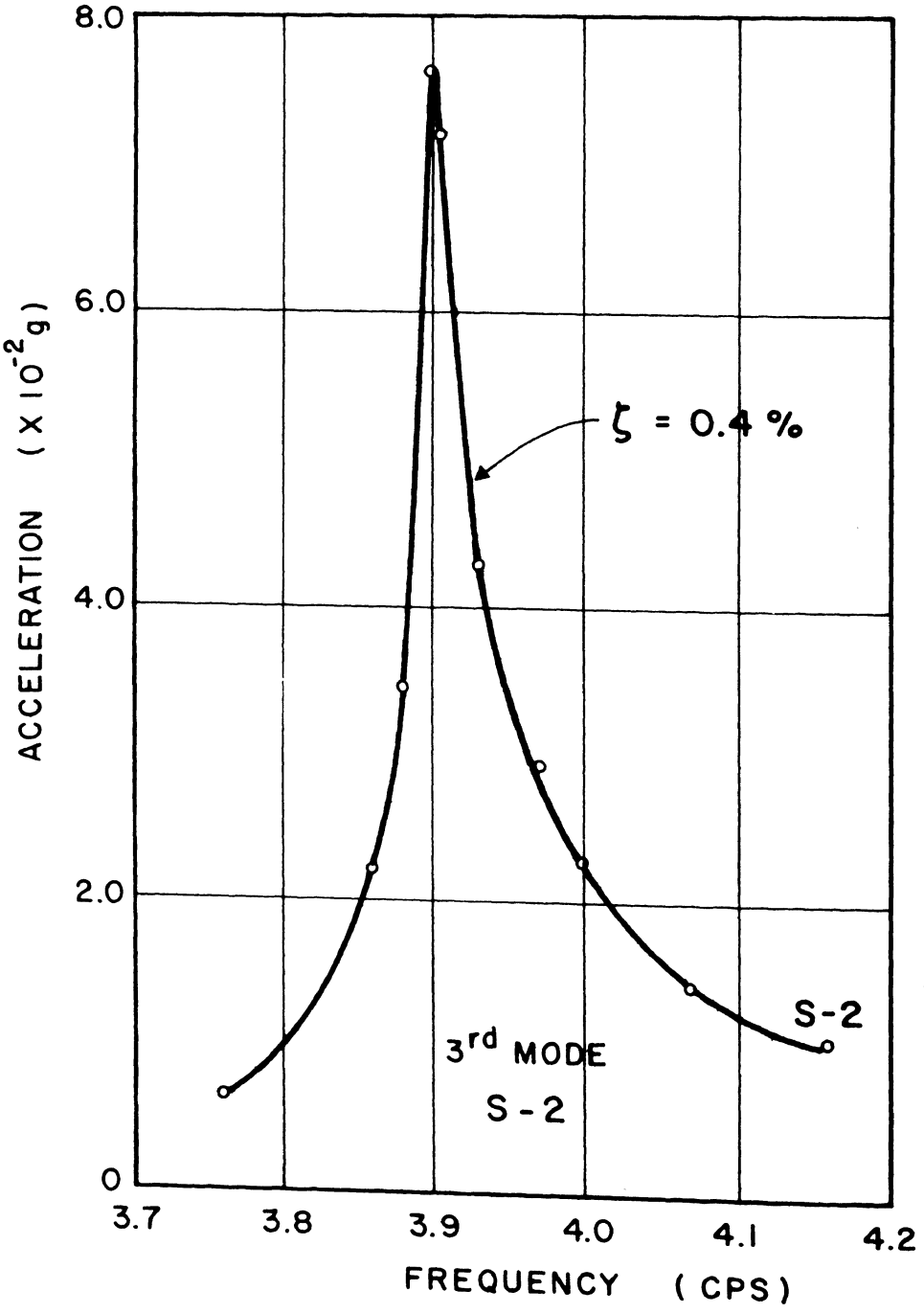

FIG. 3.9 – FREQUENCY RESPONSE, N–S, SUMMER 1964

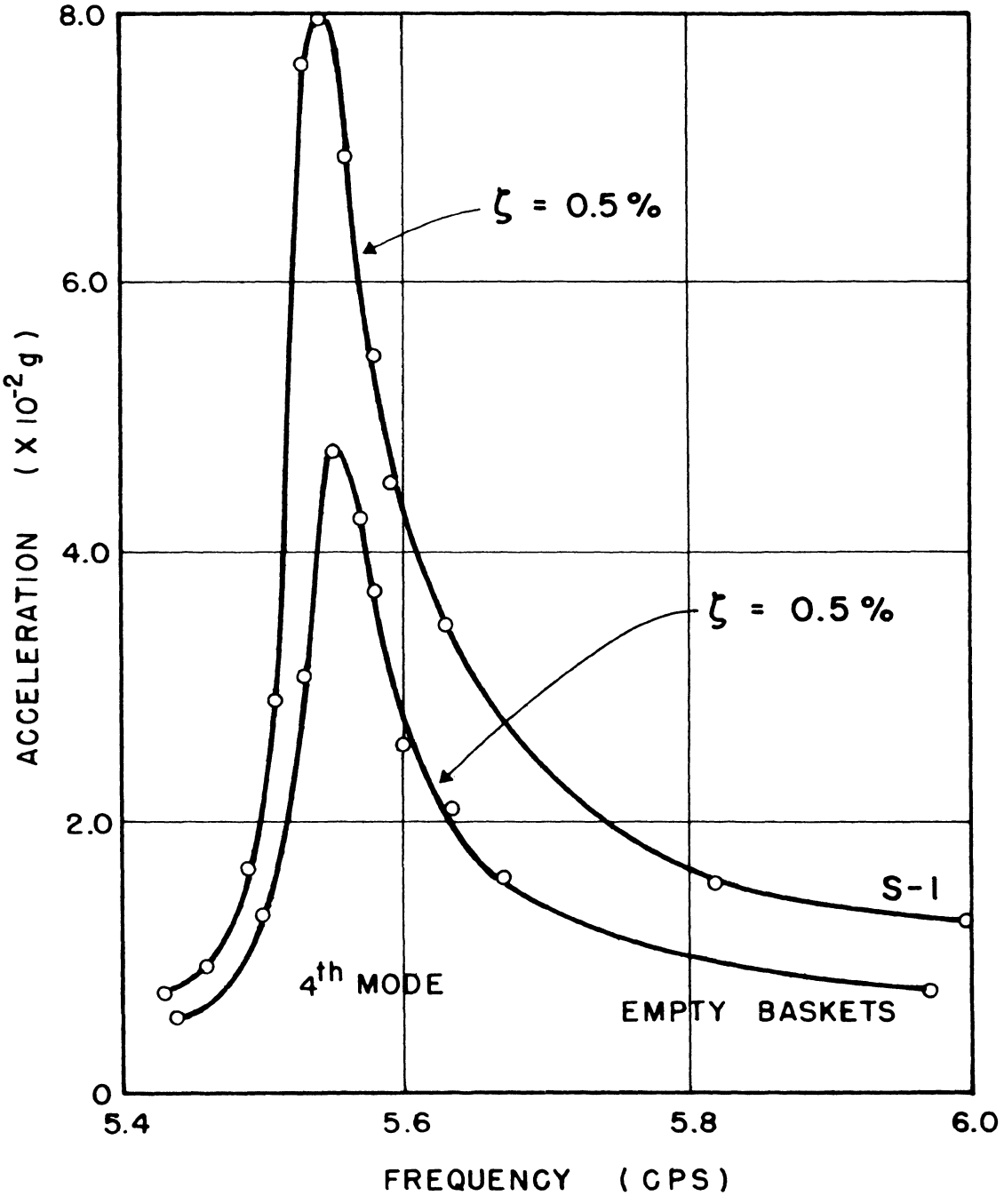

FIG. 3.10 – FREQUENCY RESPONSE, N–S, SUMMER 1964

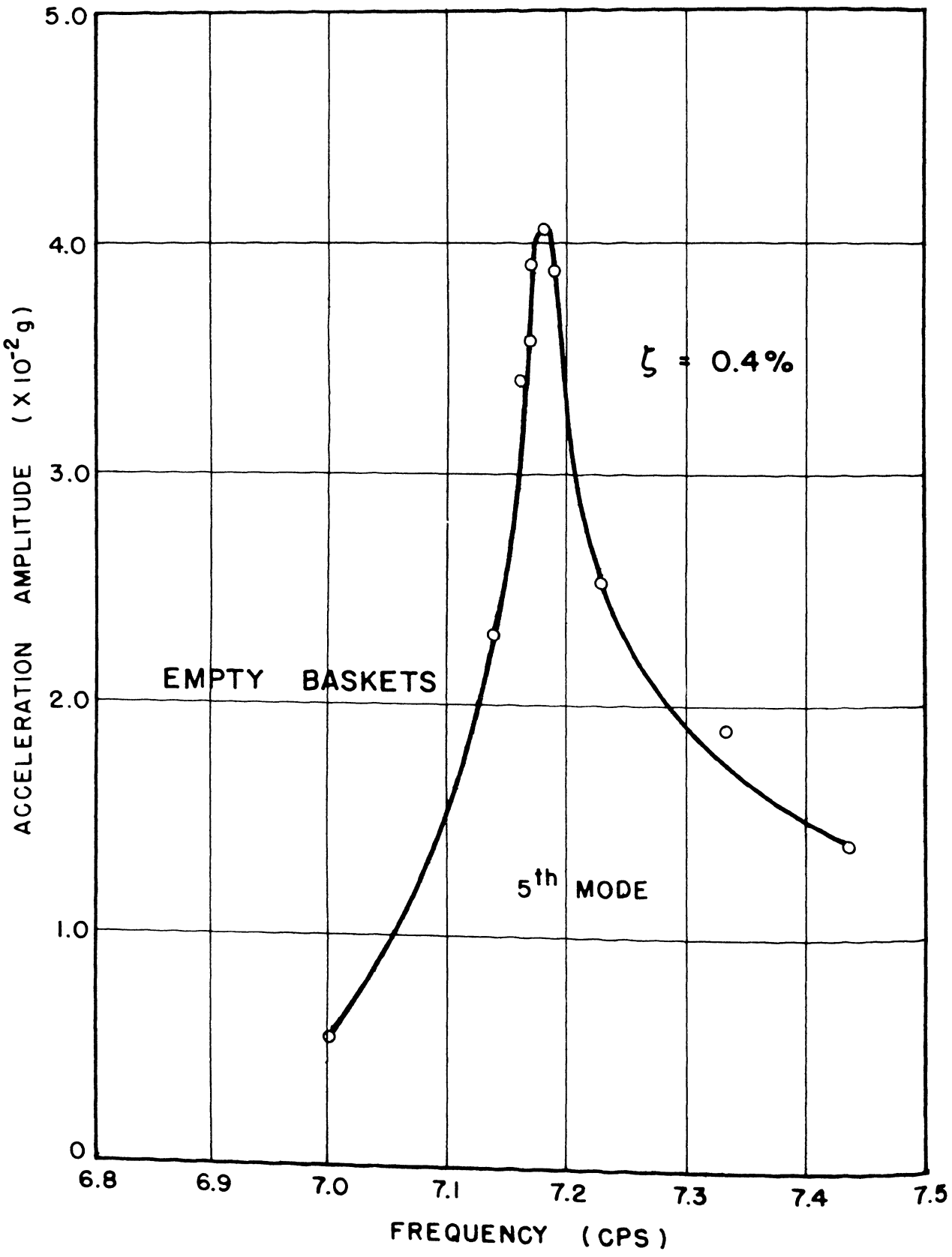

FIG. 3.11 – FREQUENCY RESPONSE, N–S, SUMMER 1964

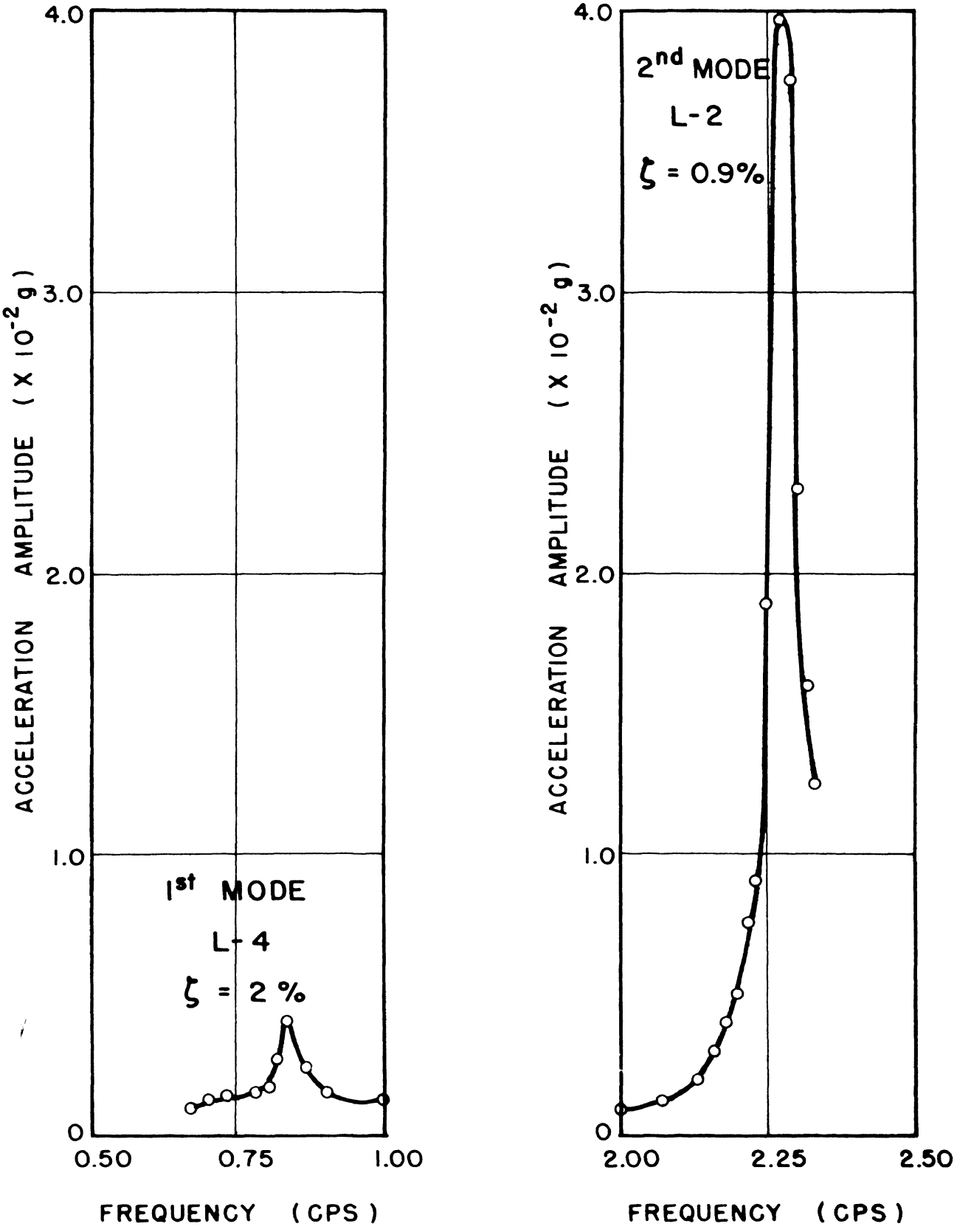

FIG. 3.12 – FREQUENCY RESPONSE, E–W, SUMMER 1964

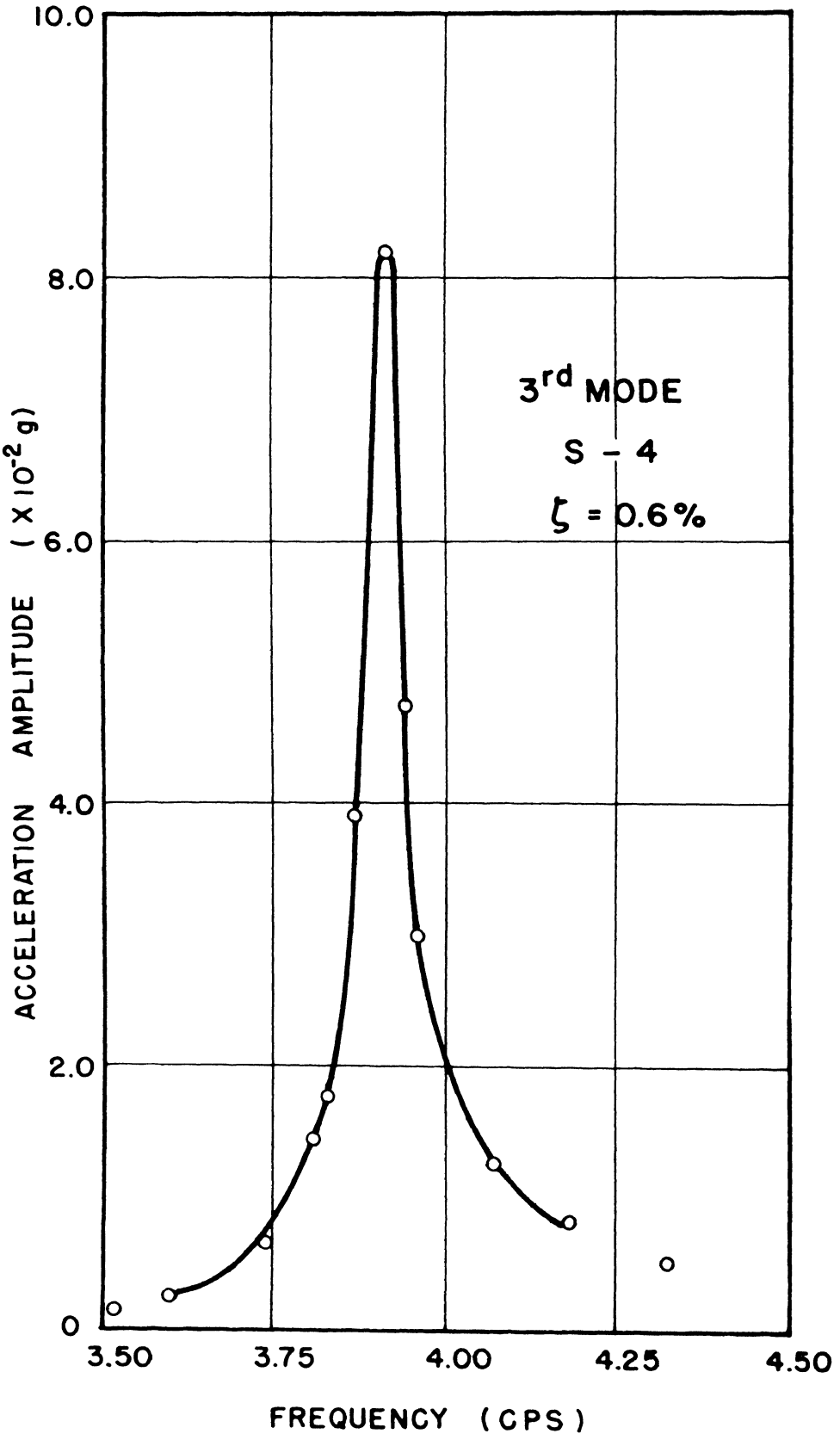

FIG. 3.13 – FREQUENCY RESPONSE, E–W, SUMMER 1964

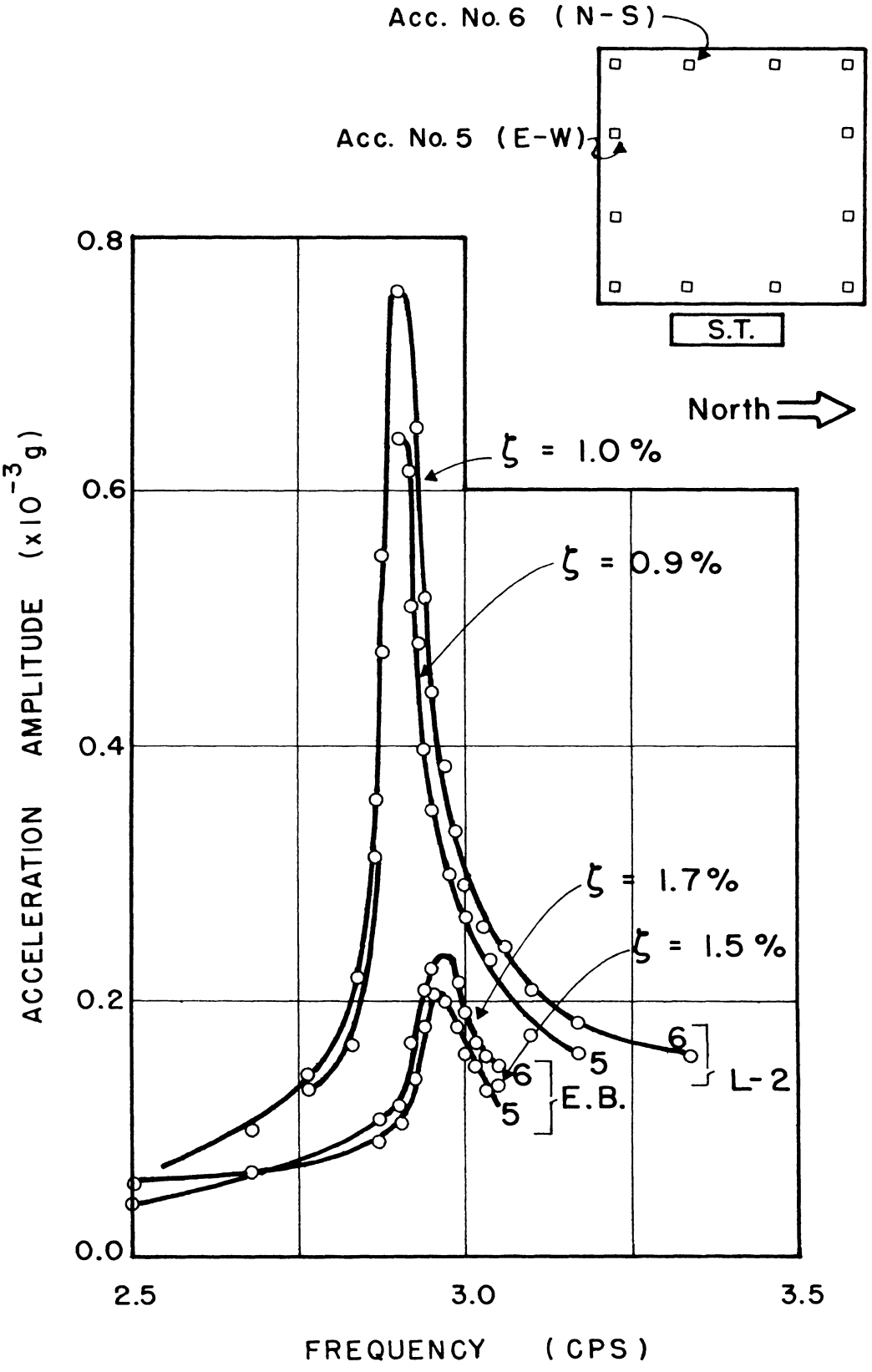

FIG. 3.14 – TORSIONAL RESPONSE, SUMMER 1964

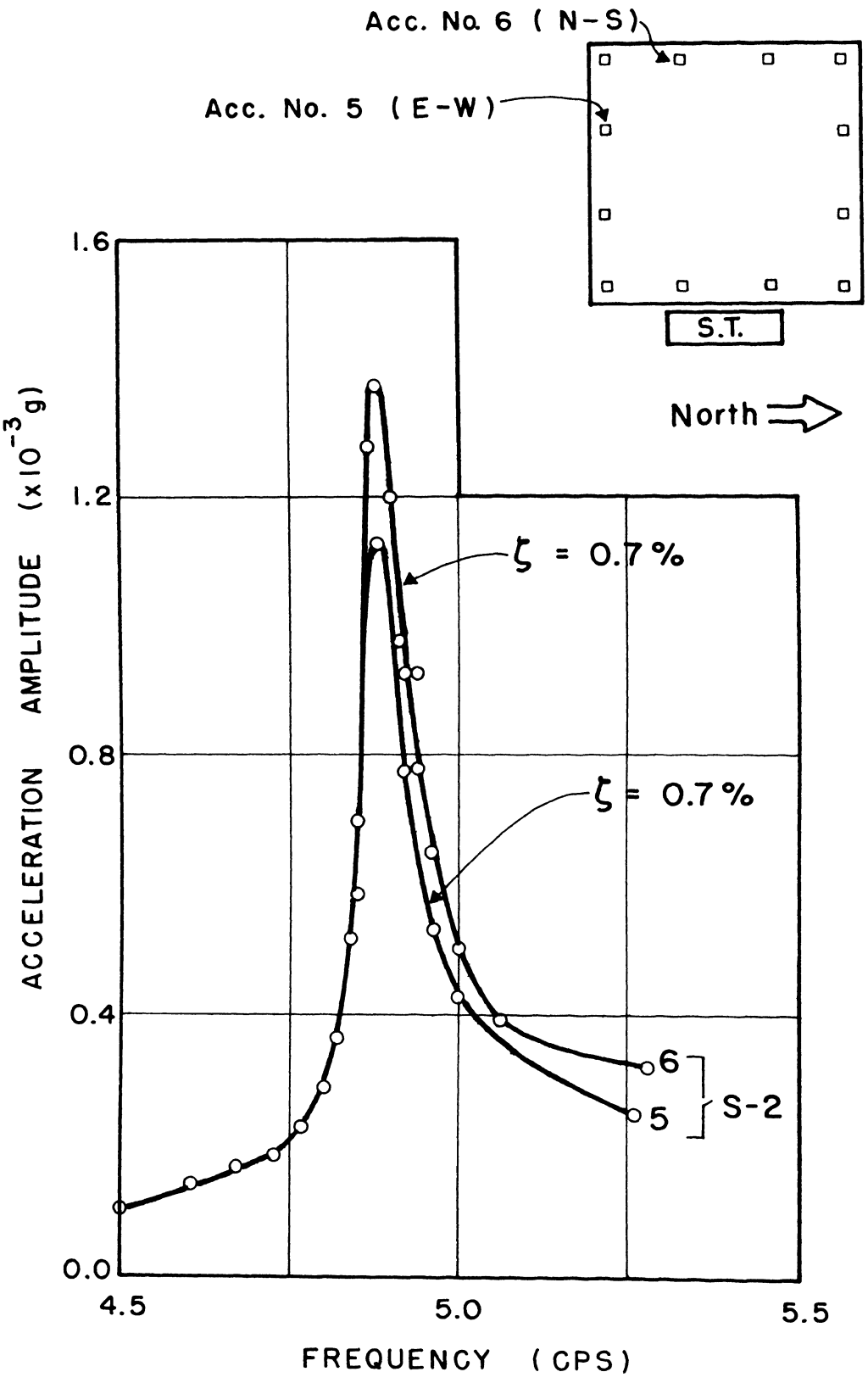

FIG. 3.15 – TORSIONAL RESPONSE, SUMMER 1964

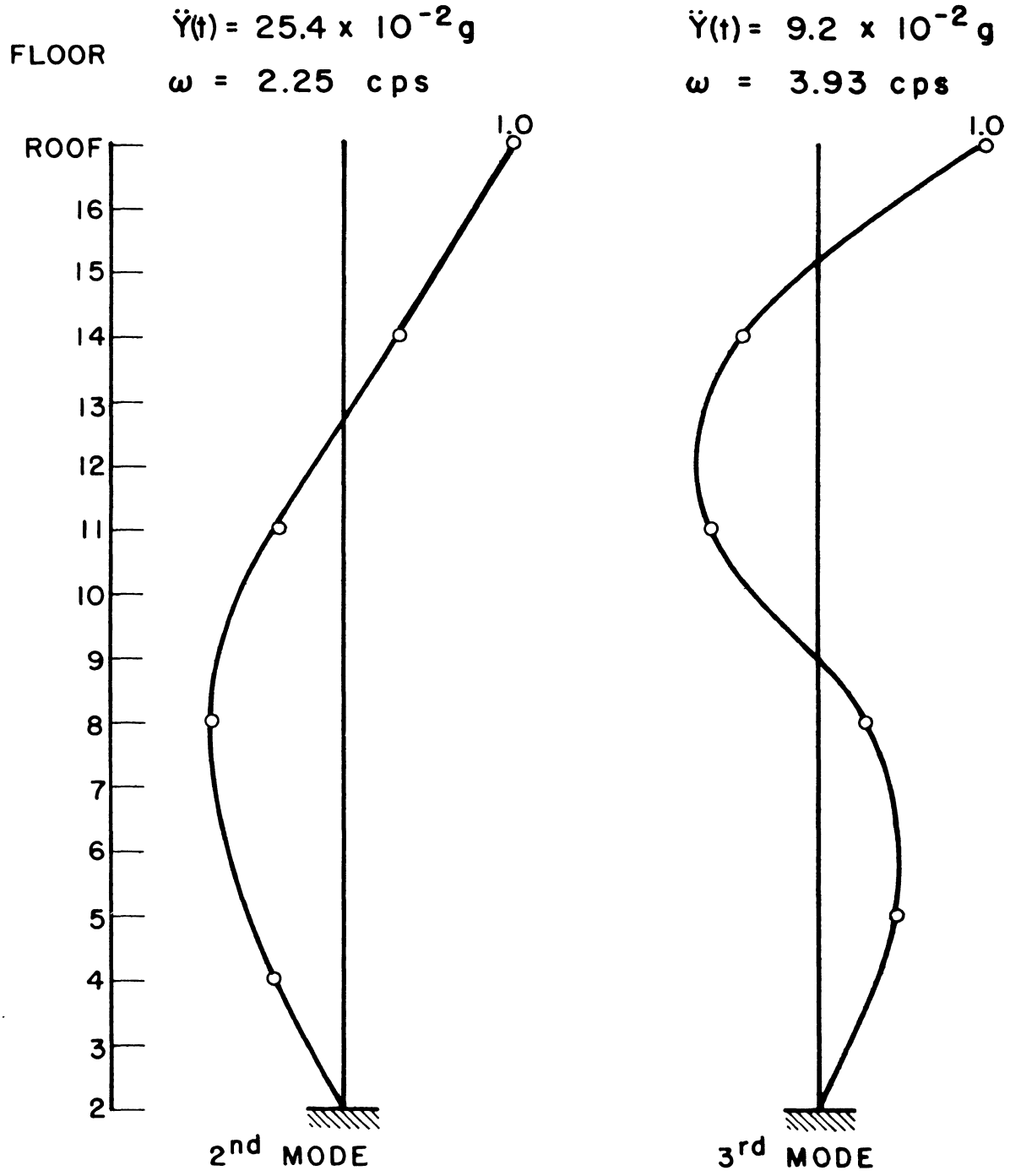

FIG. 3.16 – N–S MODE SHAPES, SUMMER 1964

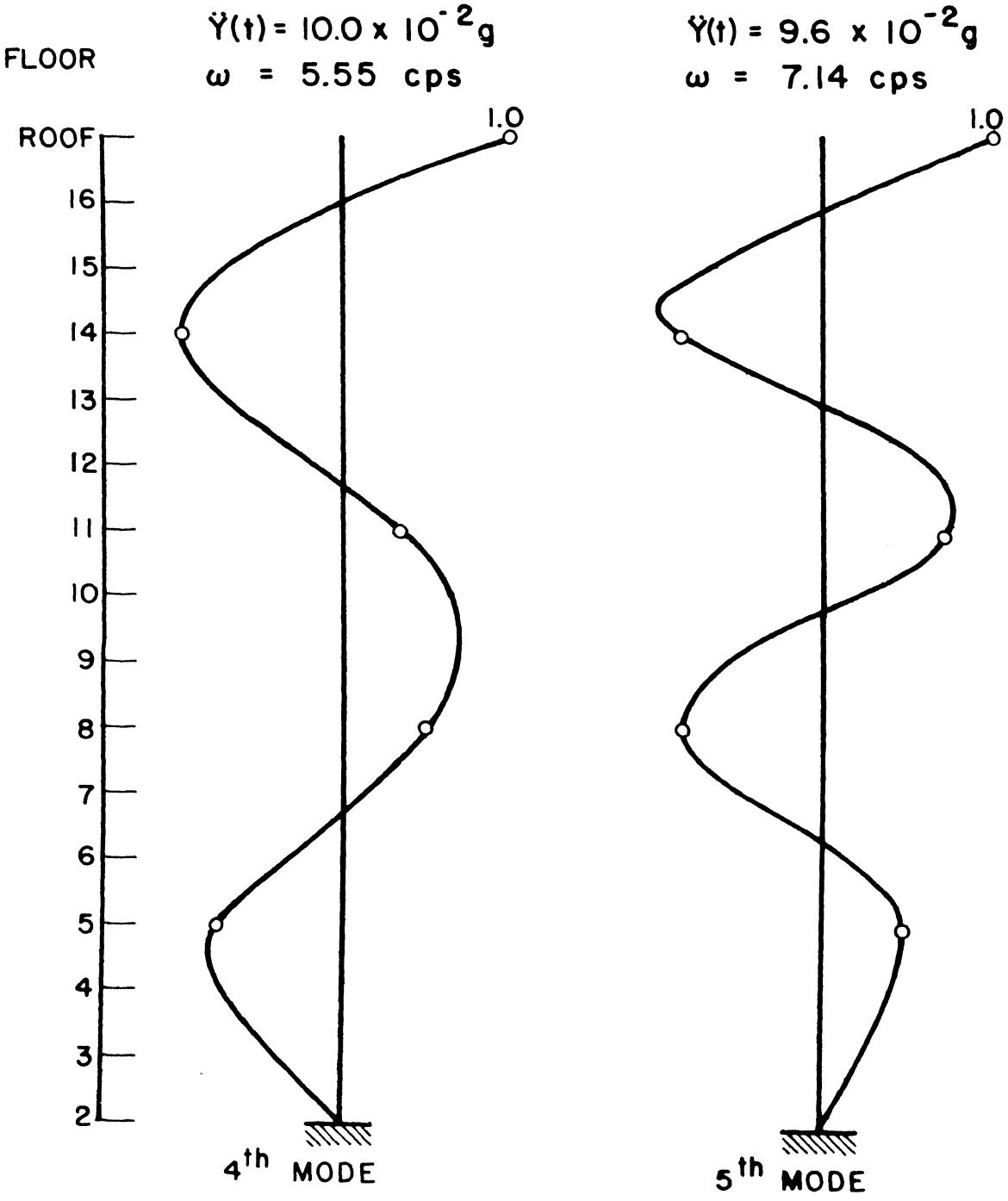

FIG. 3.17 – N–S MODE SHAPES, SUMMER 1964

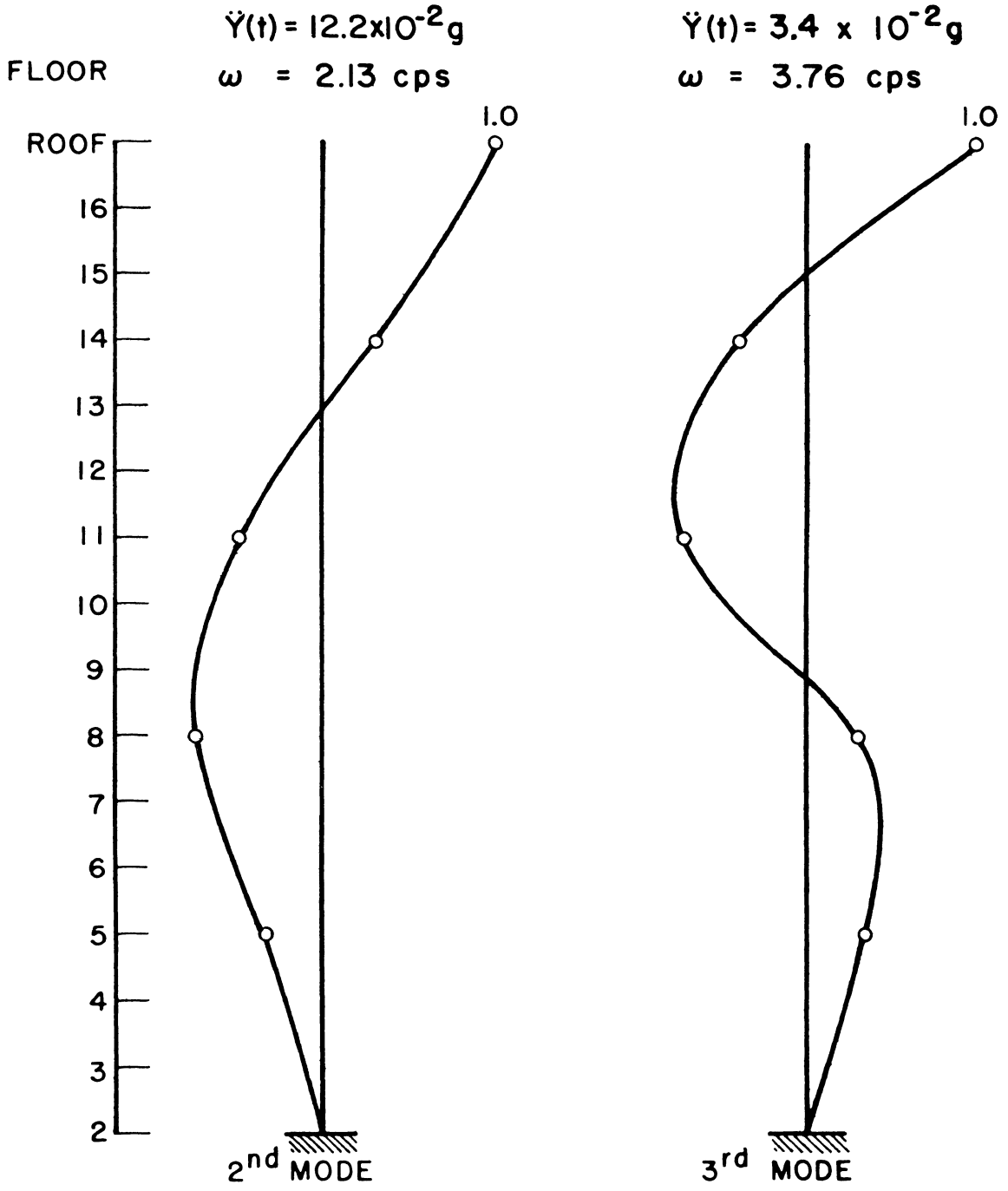

FIG. 3.18 – E–W MODE SHAPES, SUMMER 1964

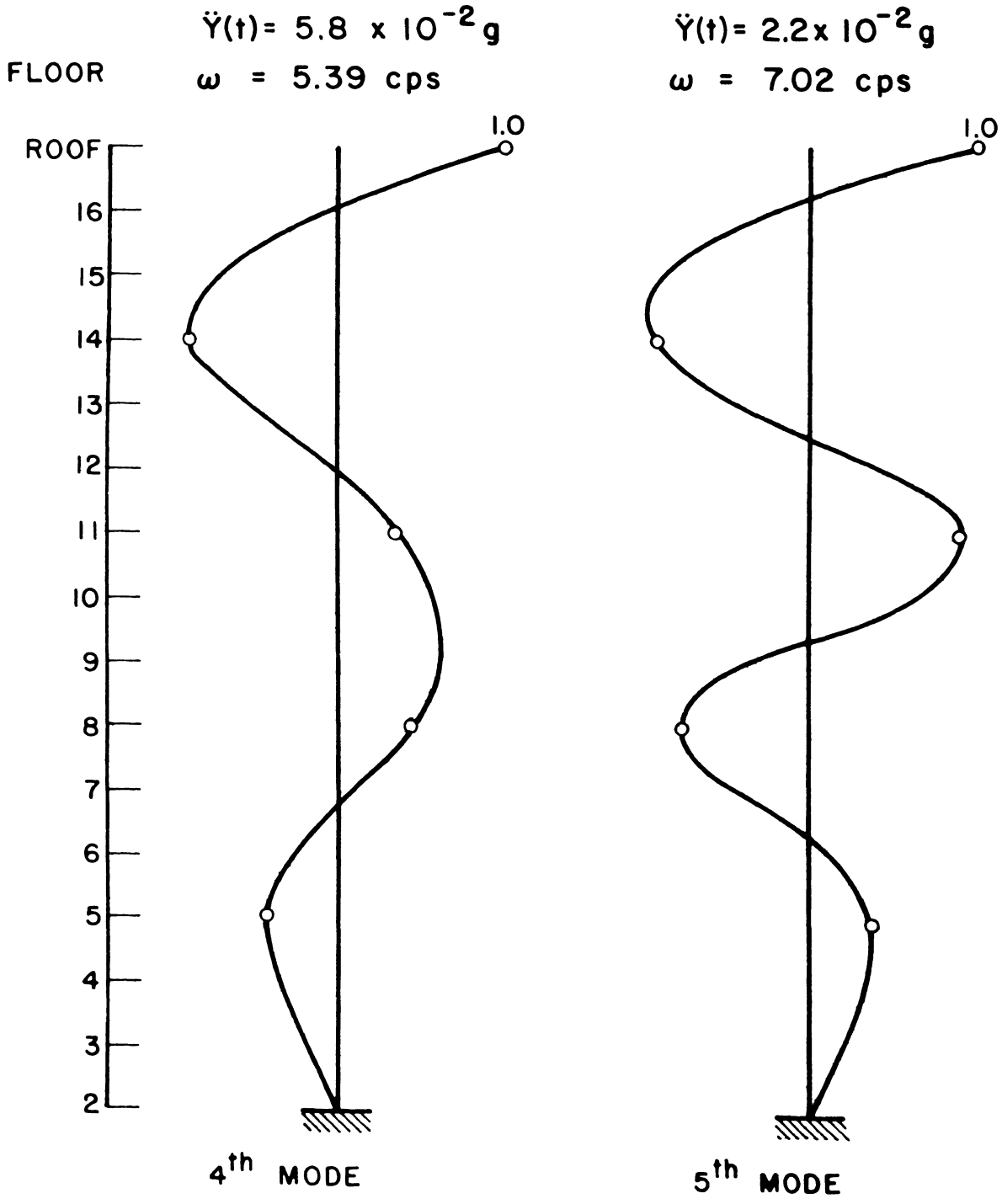

FIG. 3.19 – E–W MODE SHAPES, SUMMER 1964

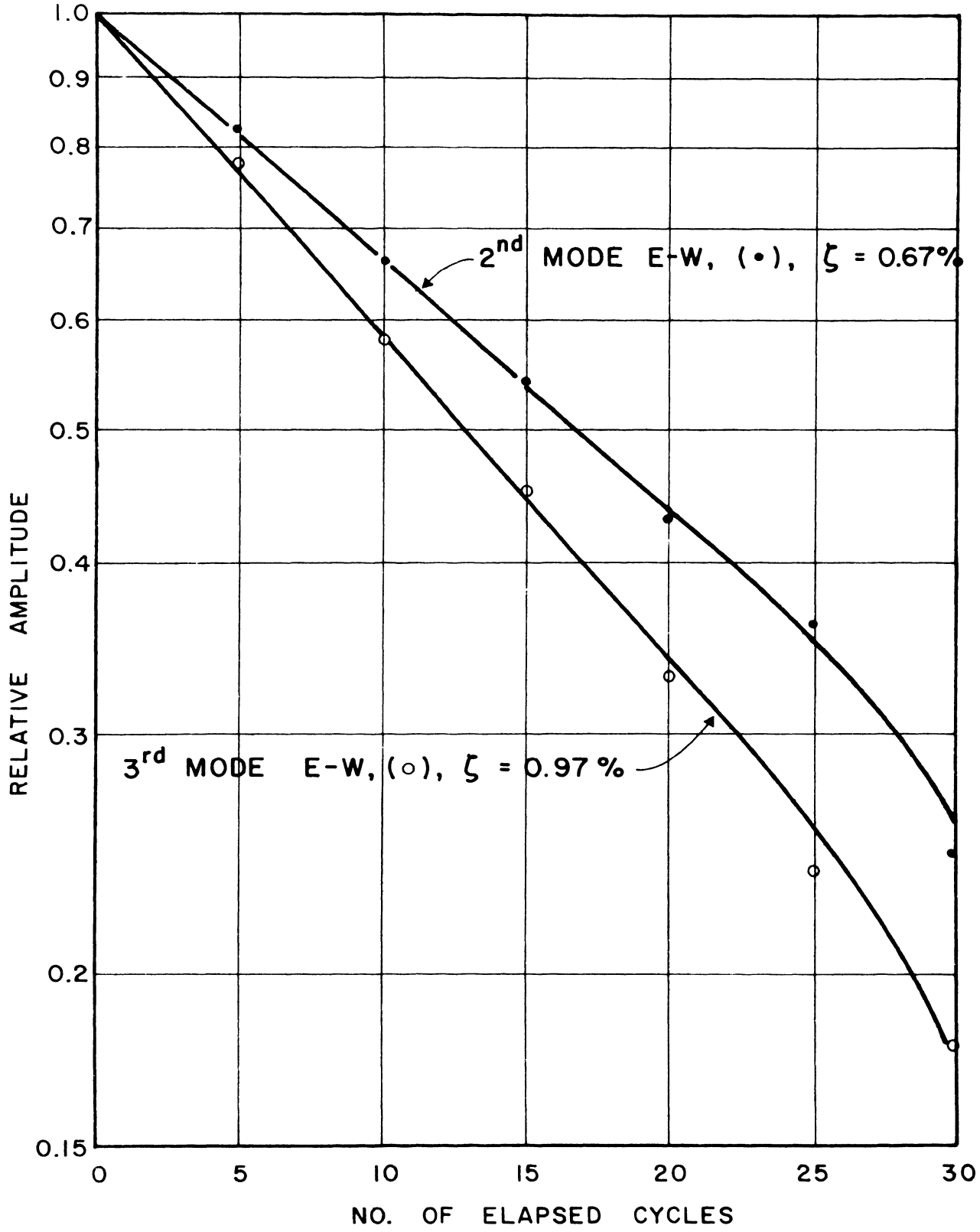

FIG. 3.20 – LOGARITHMIC DECAY CURVE FOR EAST BUILDING
SUMMER 1964, 2nd AND 3rd MODES E–W

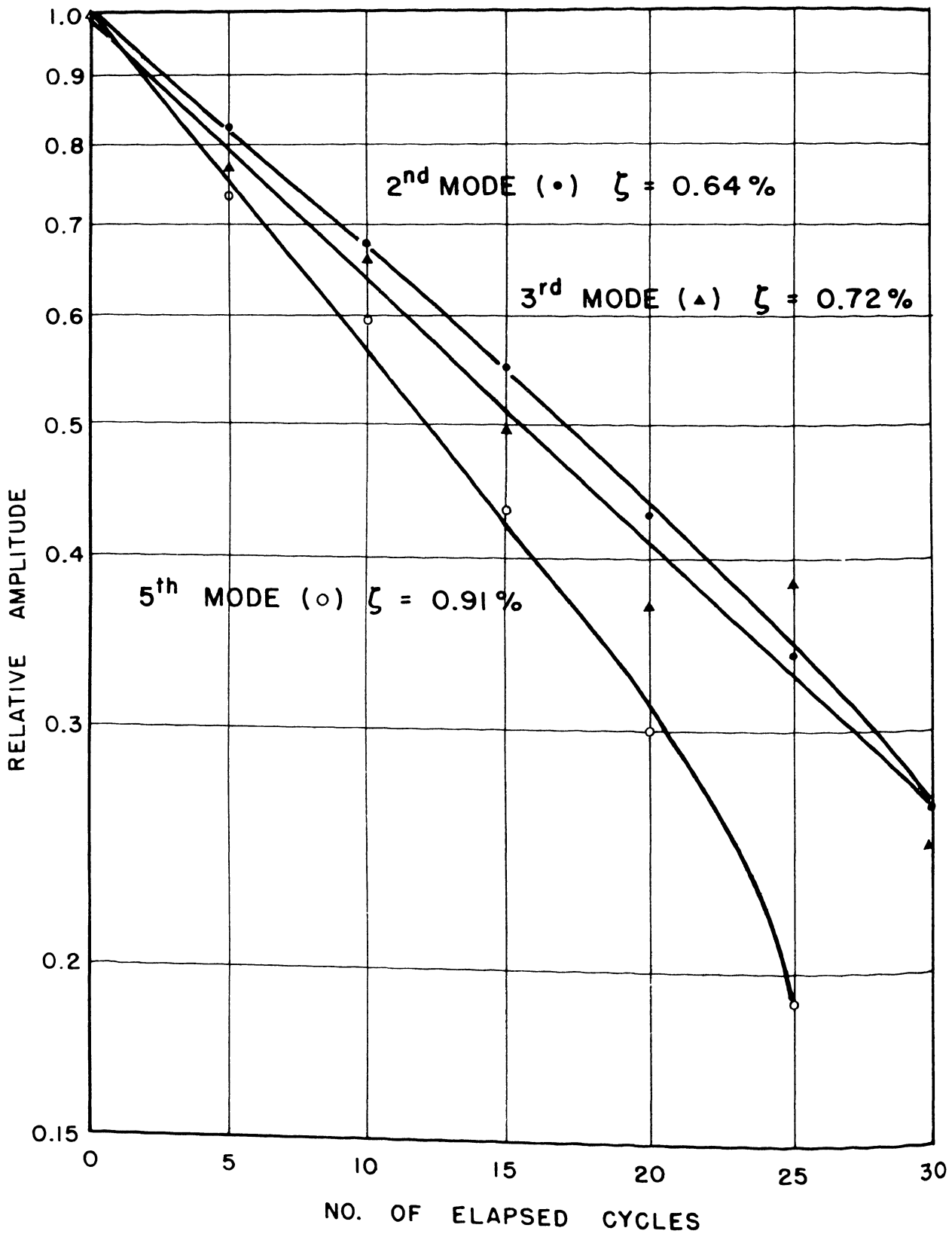

FIG. 3.21 – LOGARITHMIC DECAY CURVE FOR EAST BUILDING
SUMMER 1964, 2nd, 3rd AND 5th MODES N–S

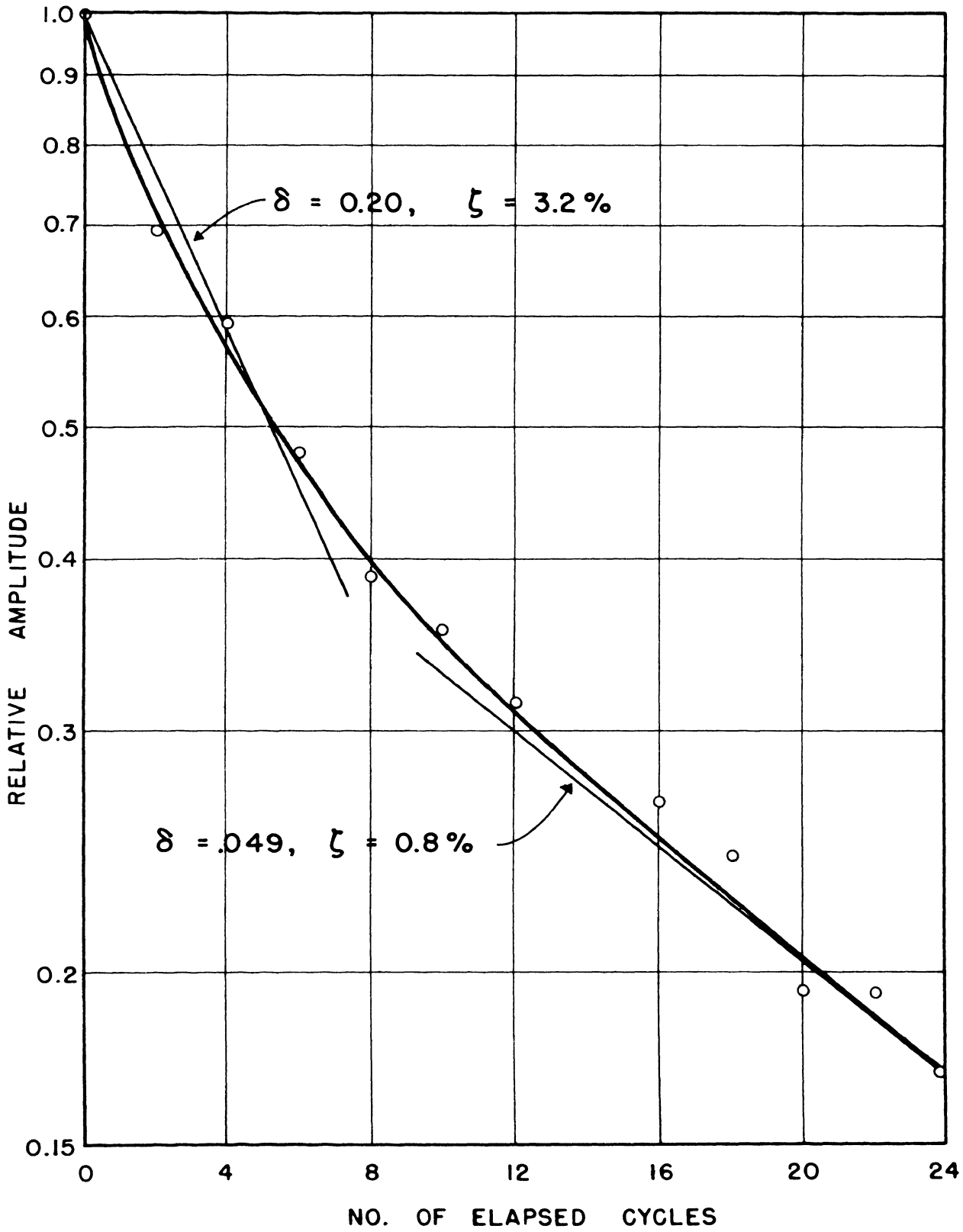

FIG. 3.22 – LOGARITHMIC DECAY CURVE FOR SERVICE TOWER
SUMMER 1964

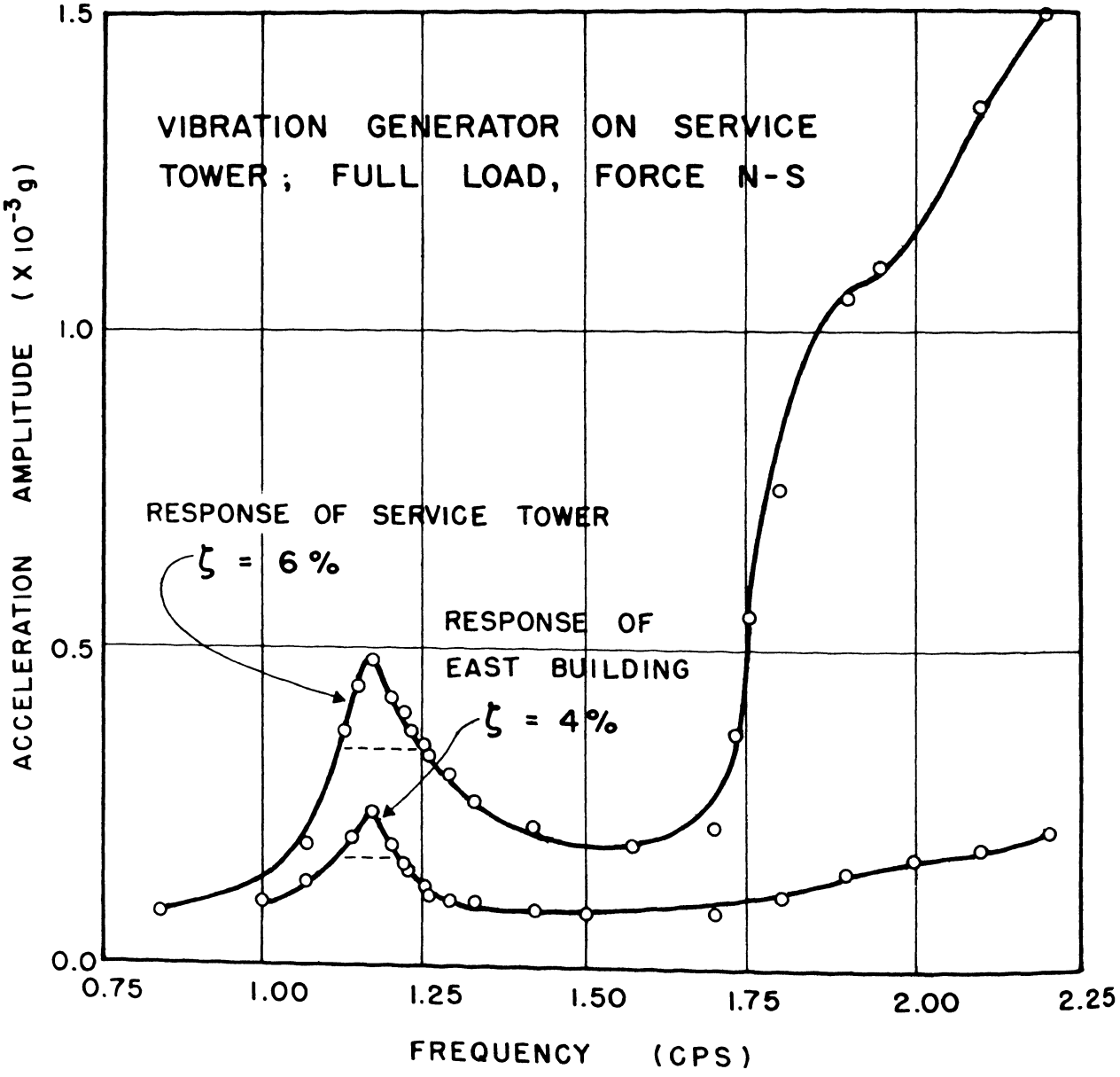

FIG. 3.23 – RESPONSE OF SERVICE TOWER AND EAST BUILDING, N–S, FALL 1964

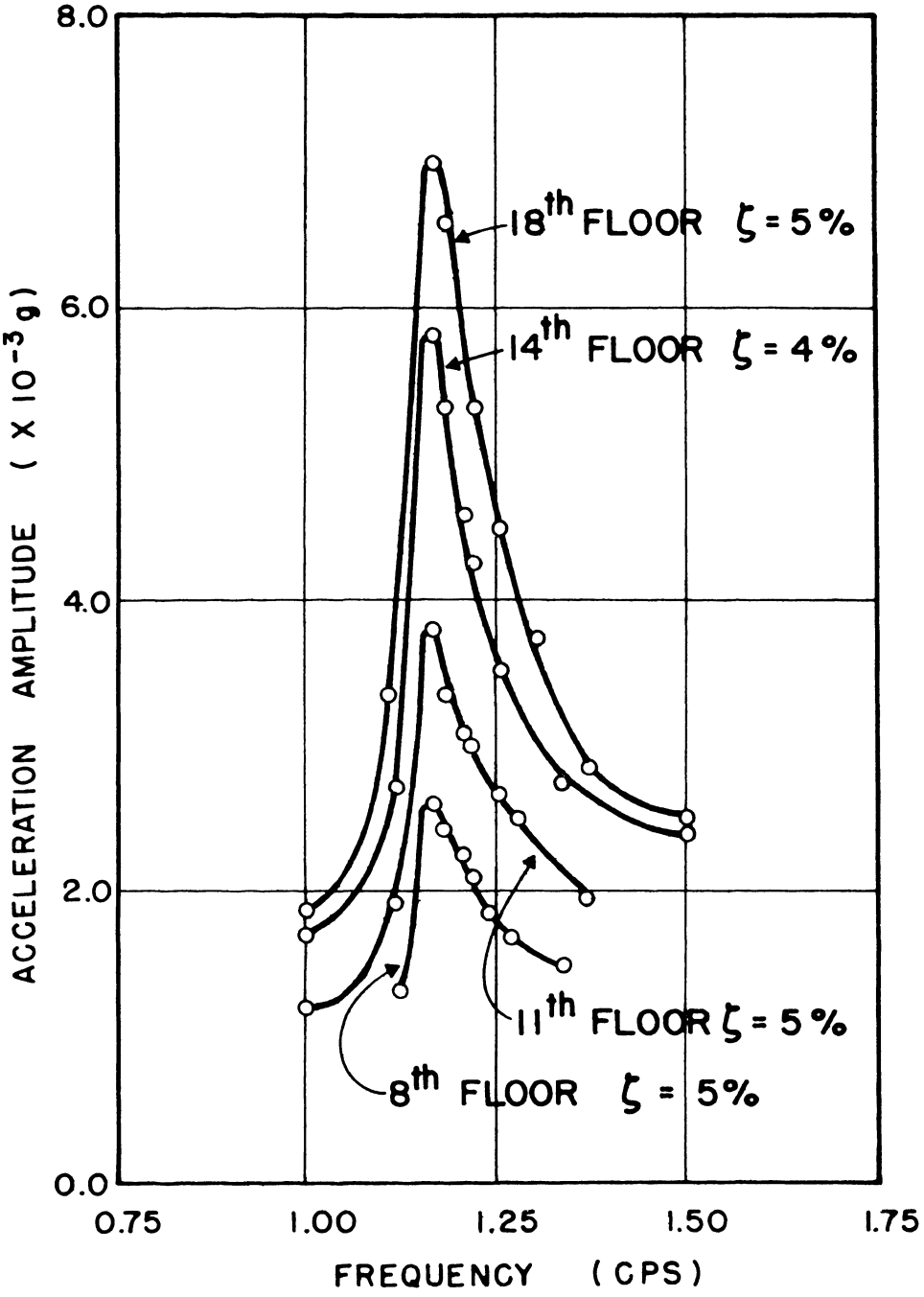

FIG. 3.24 – FREQUENCY RESPONSE OF SERVICE TOWER, N–S, FALL 1964

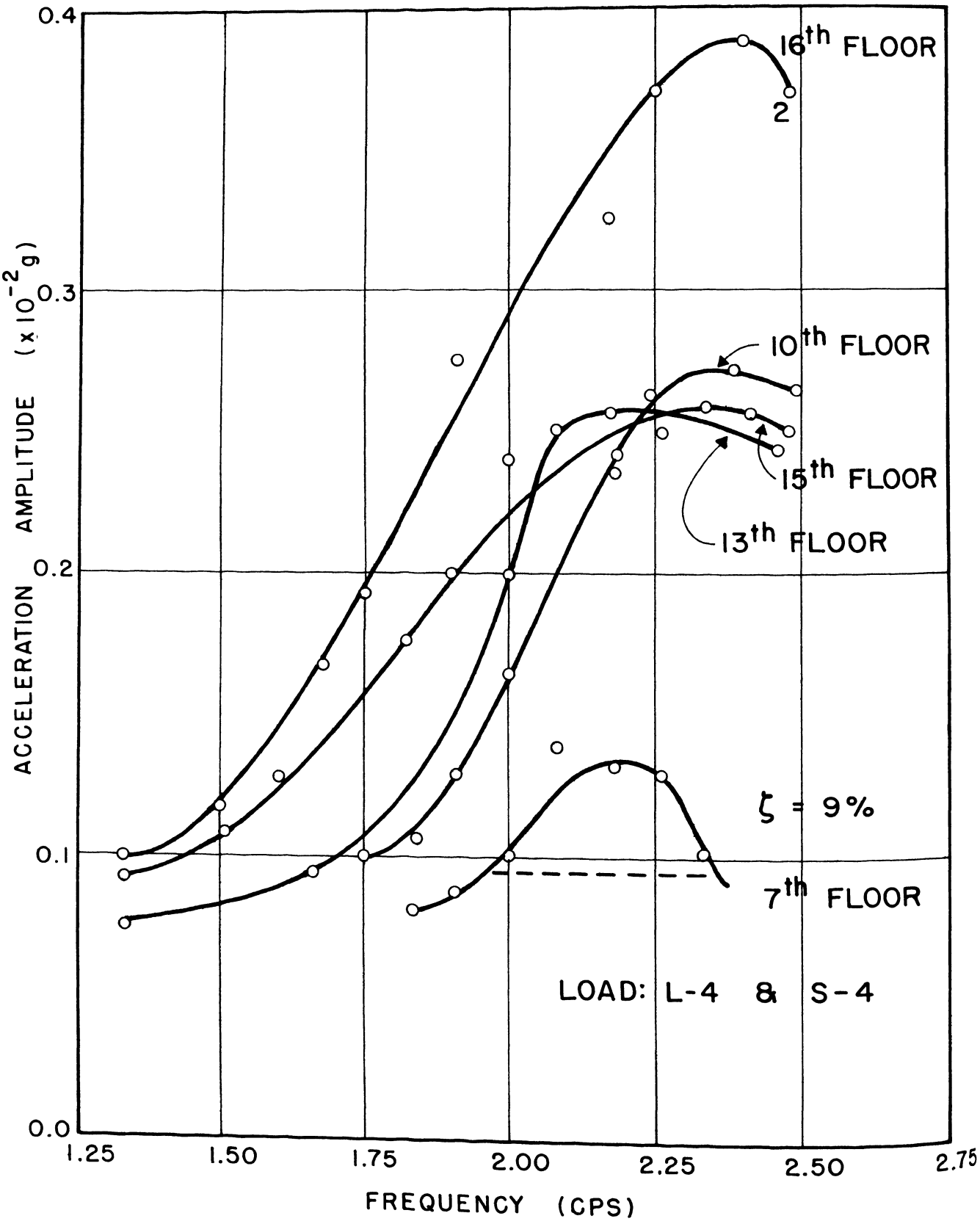

FIG. 3.25 – FREQUENCY RESPONSE OF ELEVATOR TOWER, N–S, FALL 1964

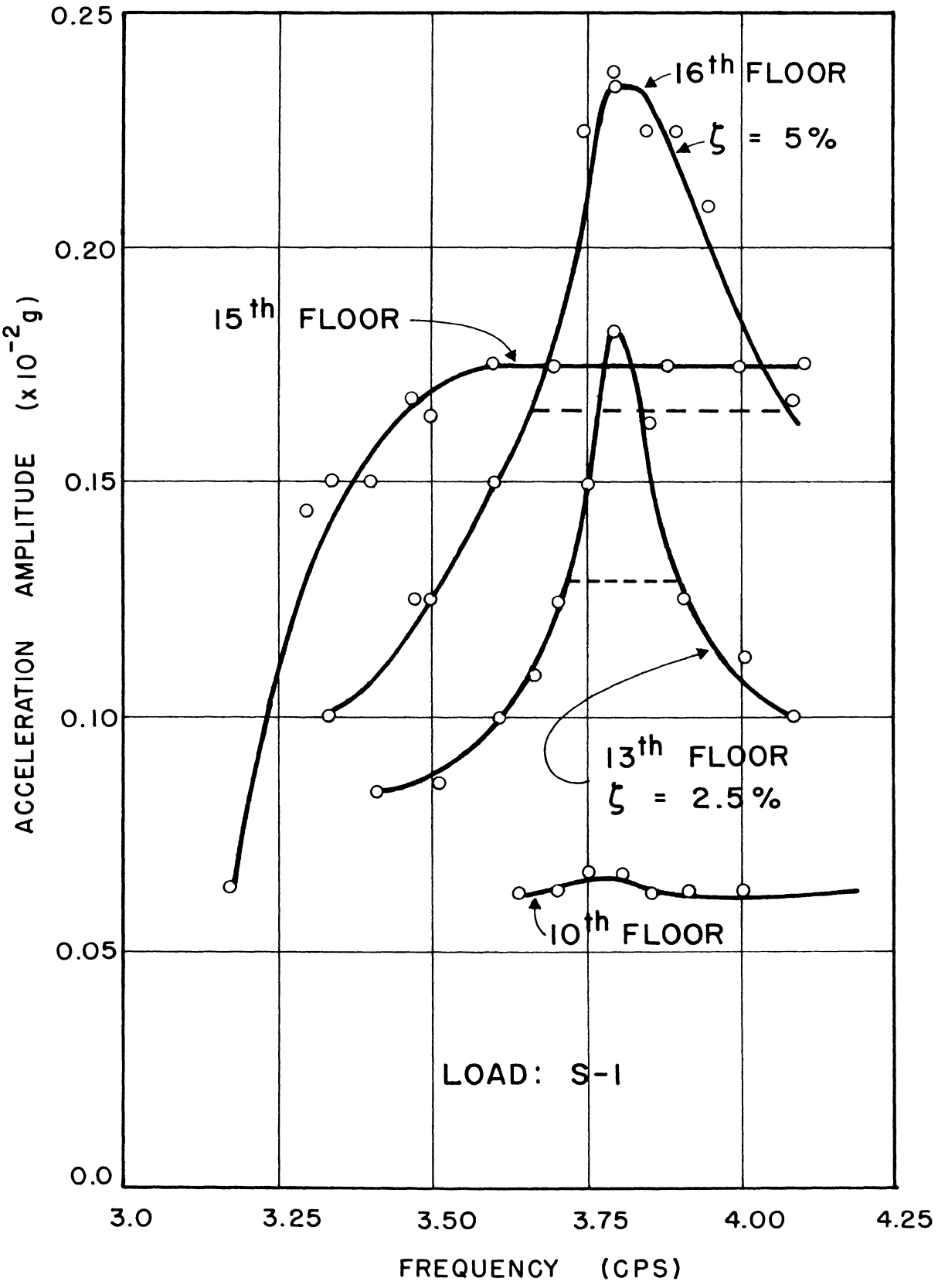

FIG. 3.26 – FREQUENCY RESPONSE OF ELEVATOR TOWER, N–S, SUMMER 1964

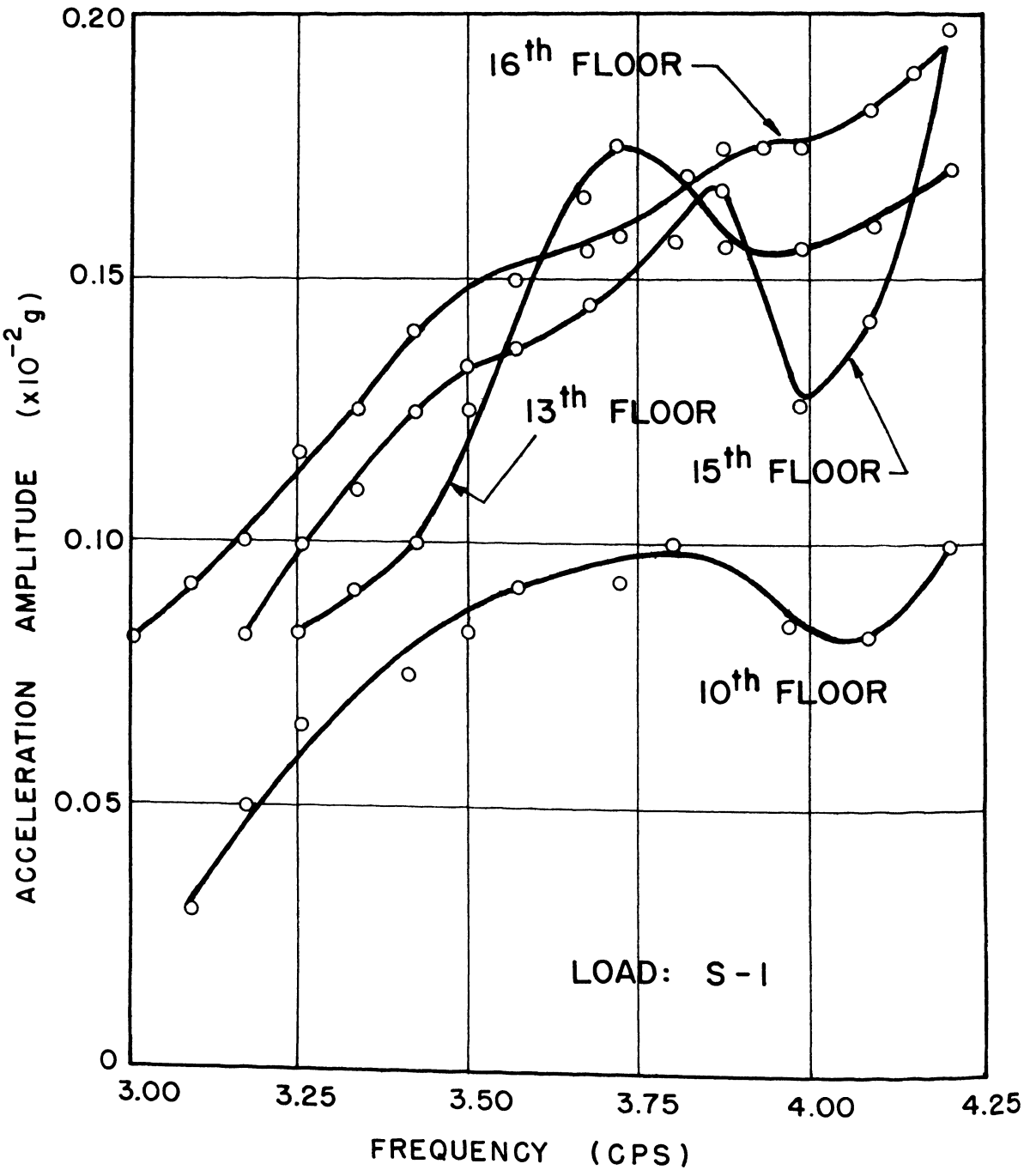

FIG. 3.27 – FREQUENCY RESPONSE OF ELEVATOR TOWER, E–W, FALL 1964

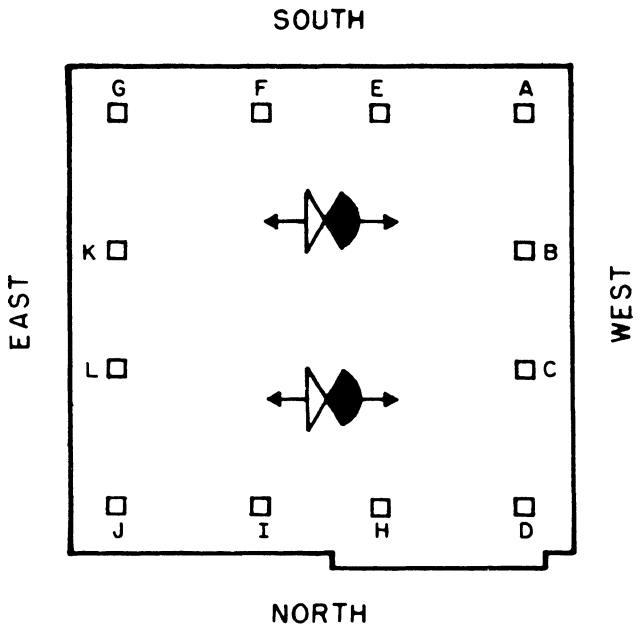

16th-FLOOR PLAN

FIG. 3.28 – POSITION OF EXCITERS IN 1965 TESTS

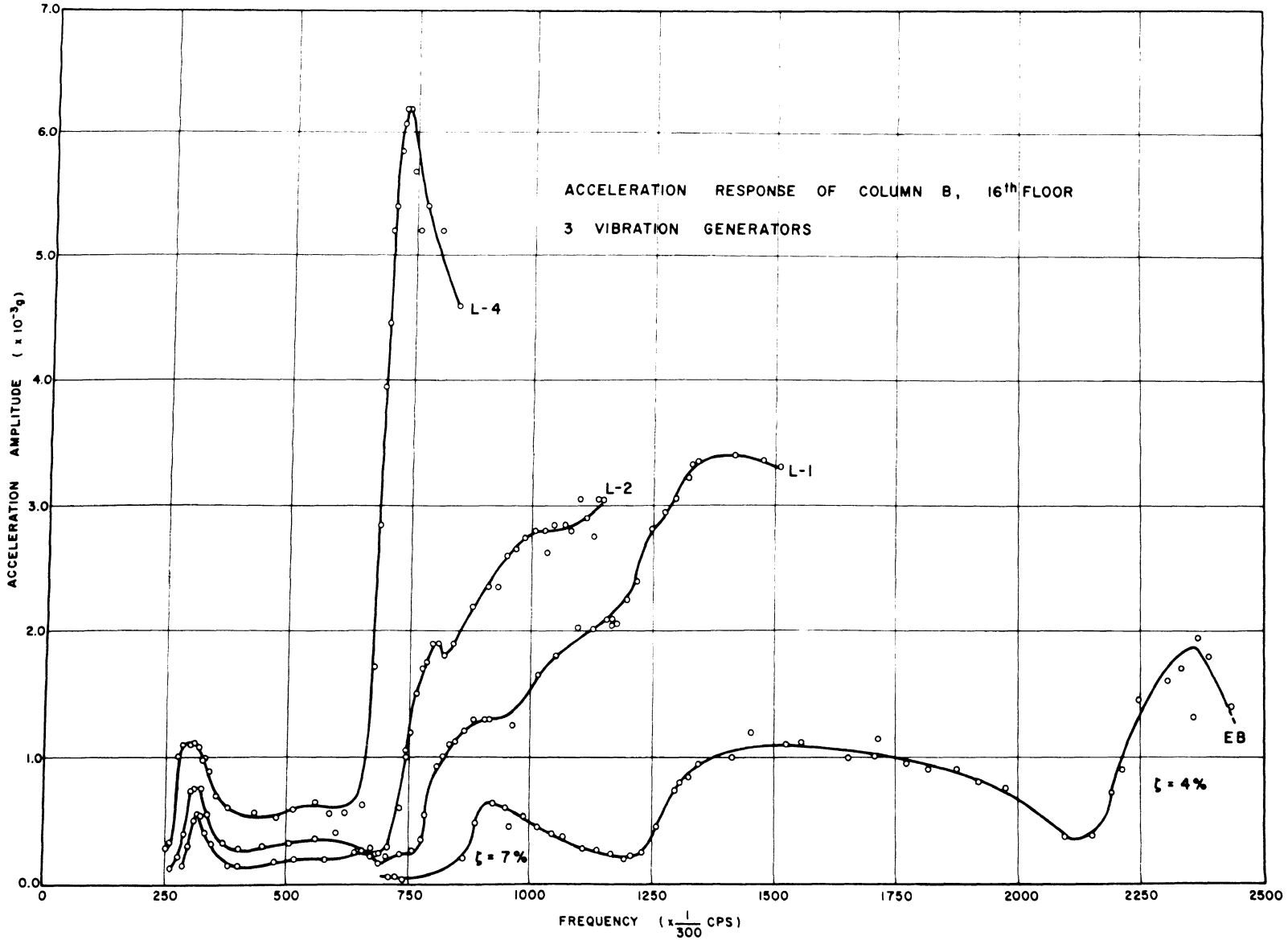

FIG. 3.29

E–W ACCELERATION FREQUENCY RESPONSE, SUMMER 1965

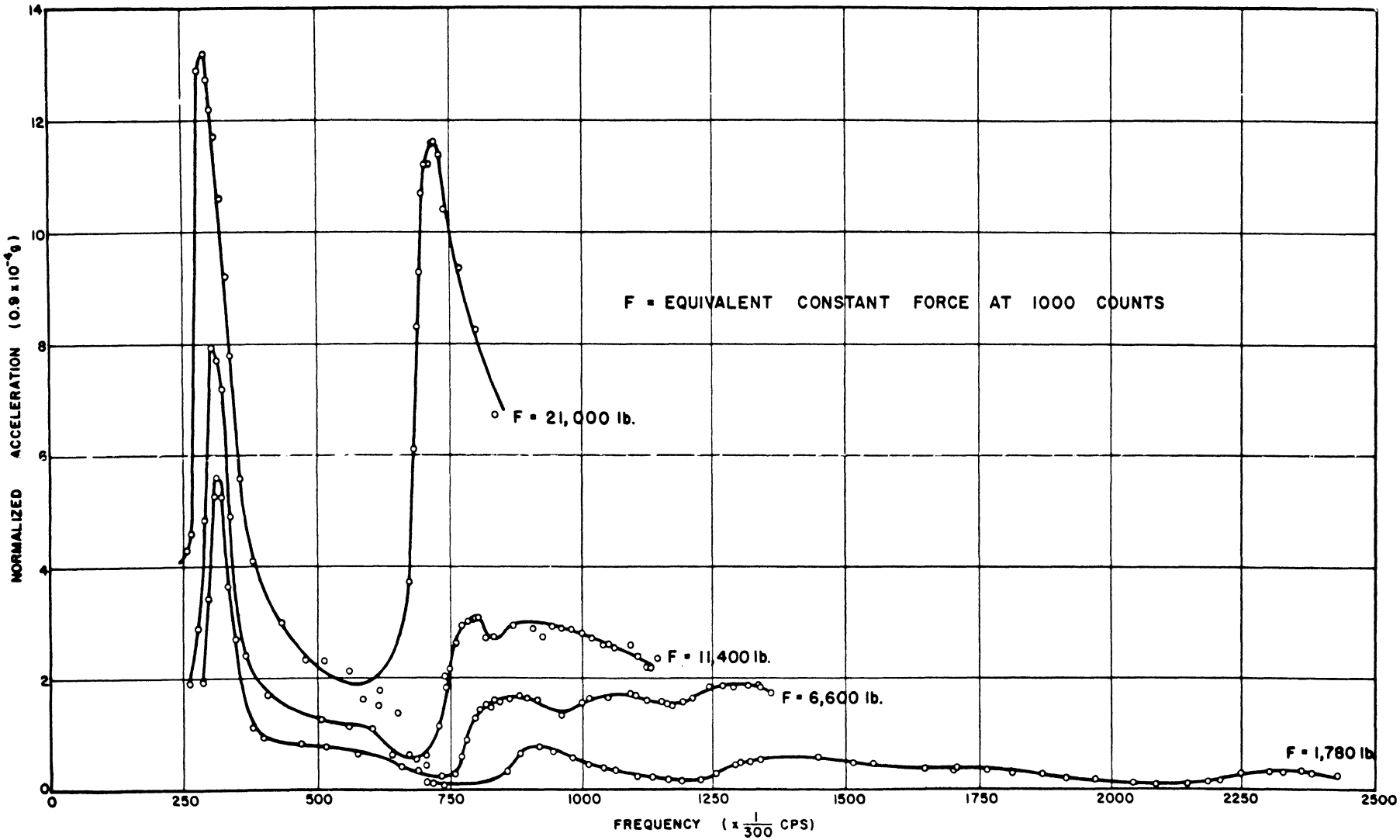

FIG. 3.30

NORMALIZED ACCELERATION FREQUENCY RESPONSES, E–W,
SUMMER 1965

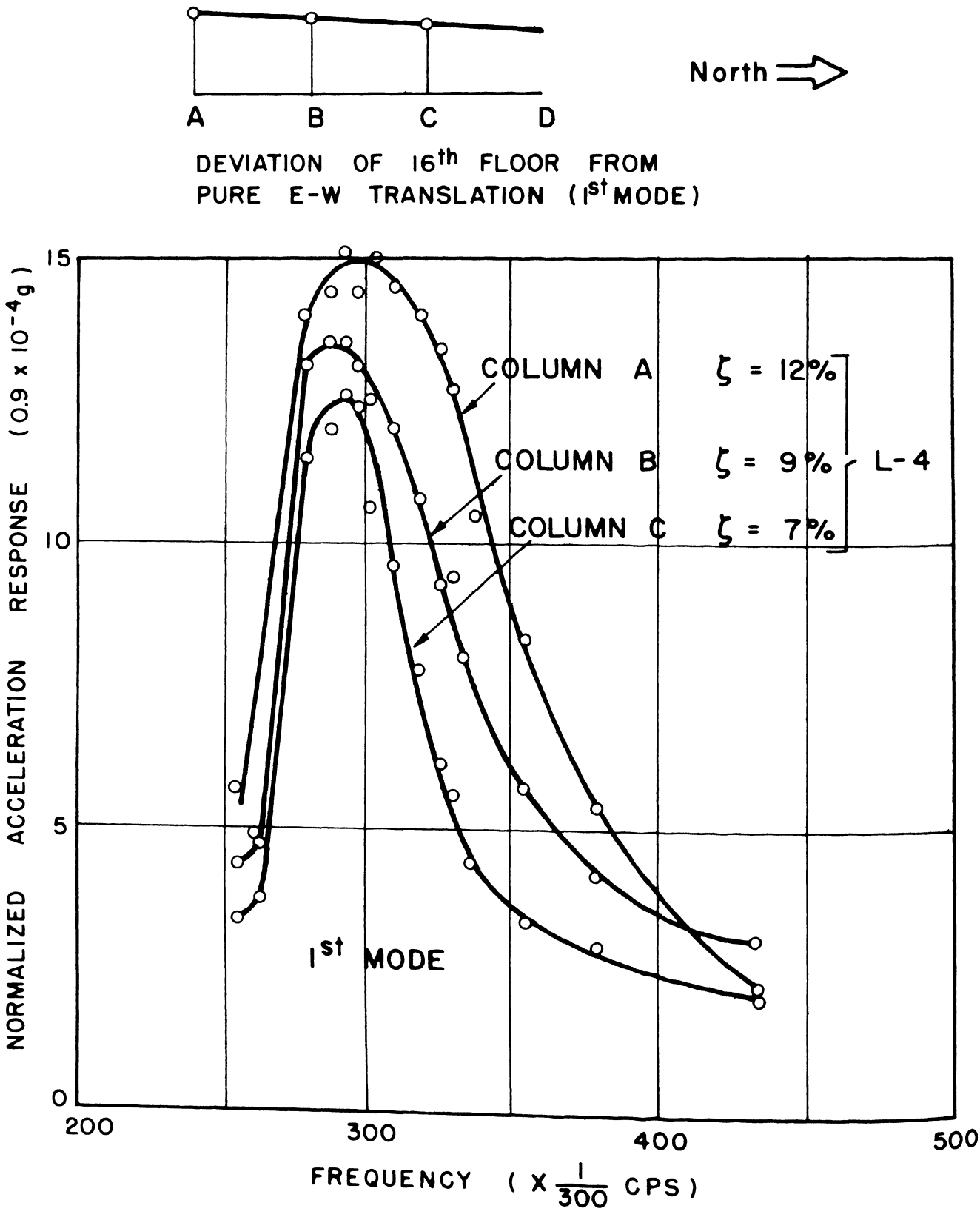

FIG. 3.31 – FREQUENCY RESPONSE OF 16th FLOOR E–W, SUMMER 1965

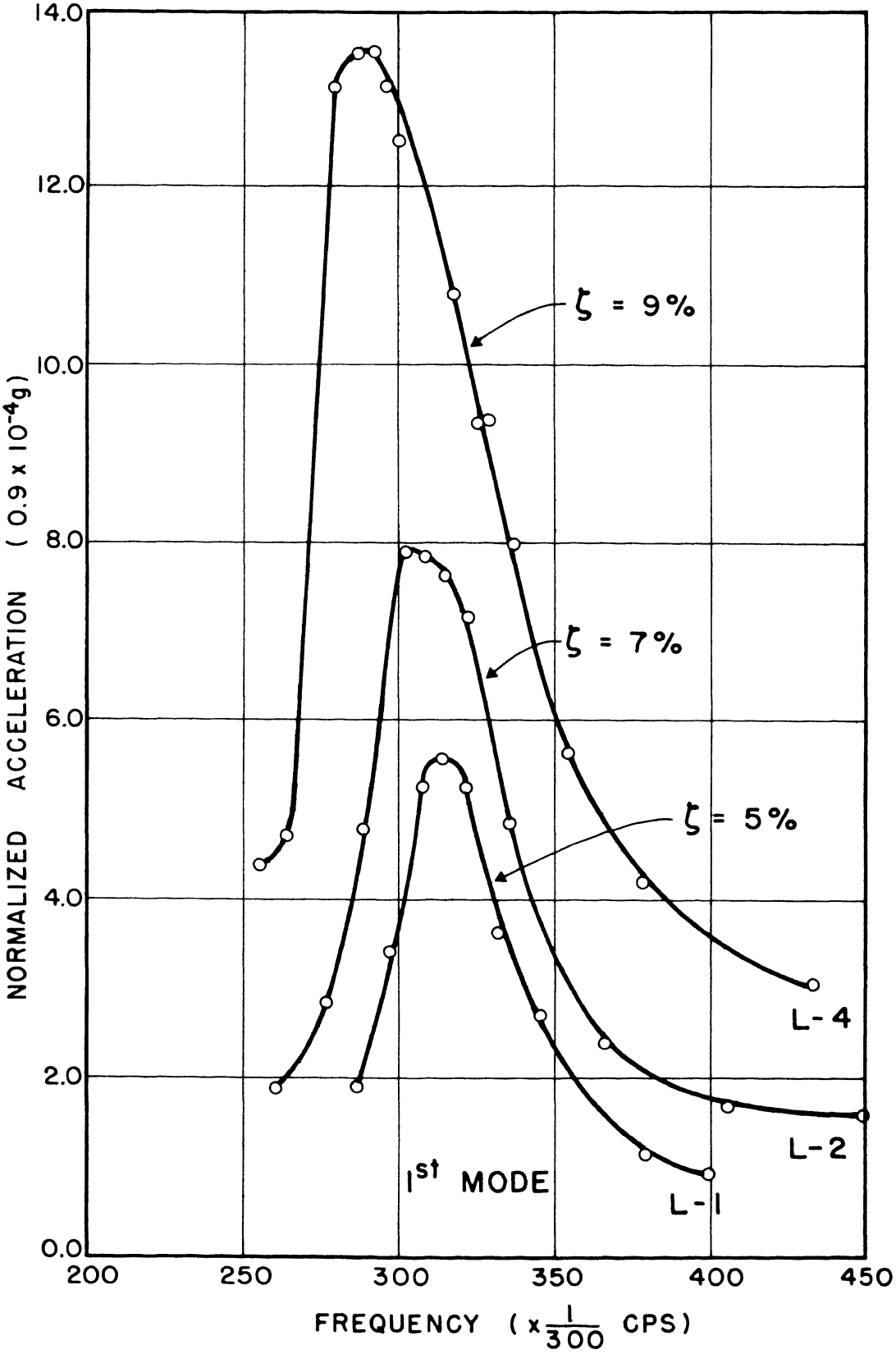

FIG. 3.32 – FREQUENCY RESPONSE COLUMN B, 16th FLOOR E–W, SUMMER 1965

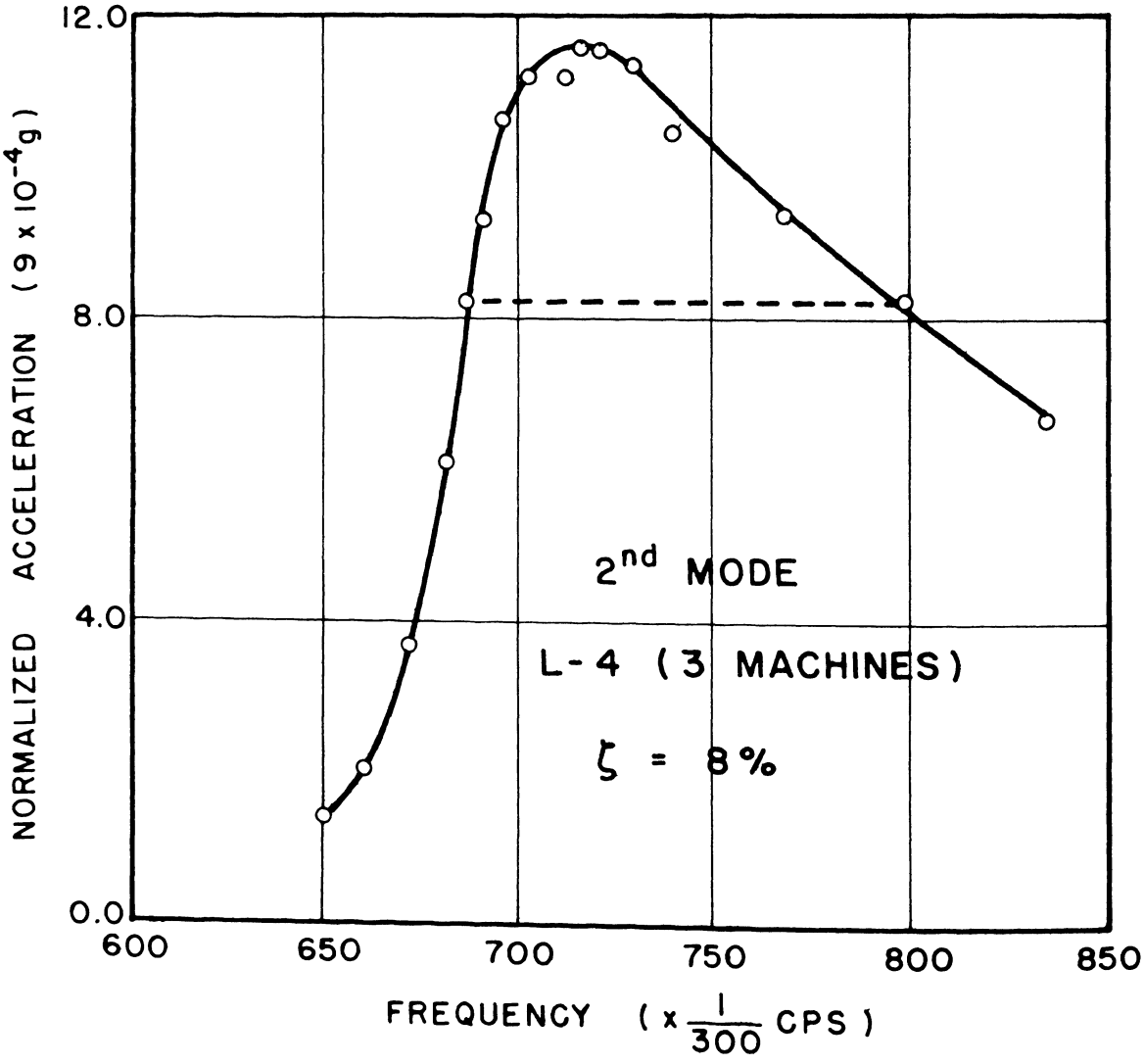

FIG. 3.33 – FREQUENCY RESPONSE COLUMN B, E–W
SUMMER 1965

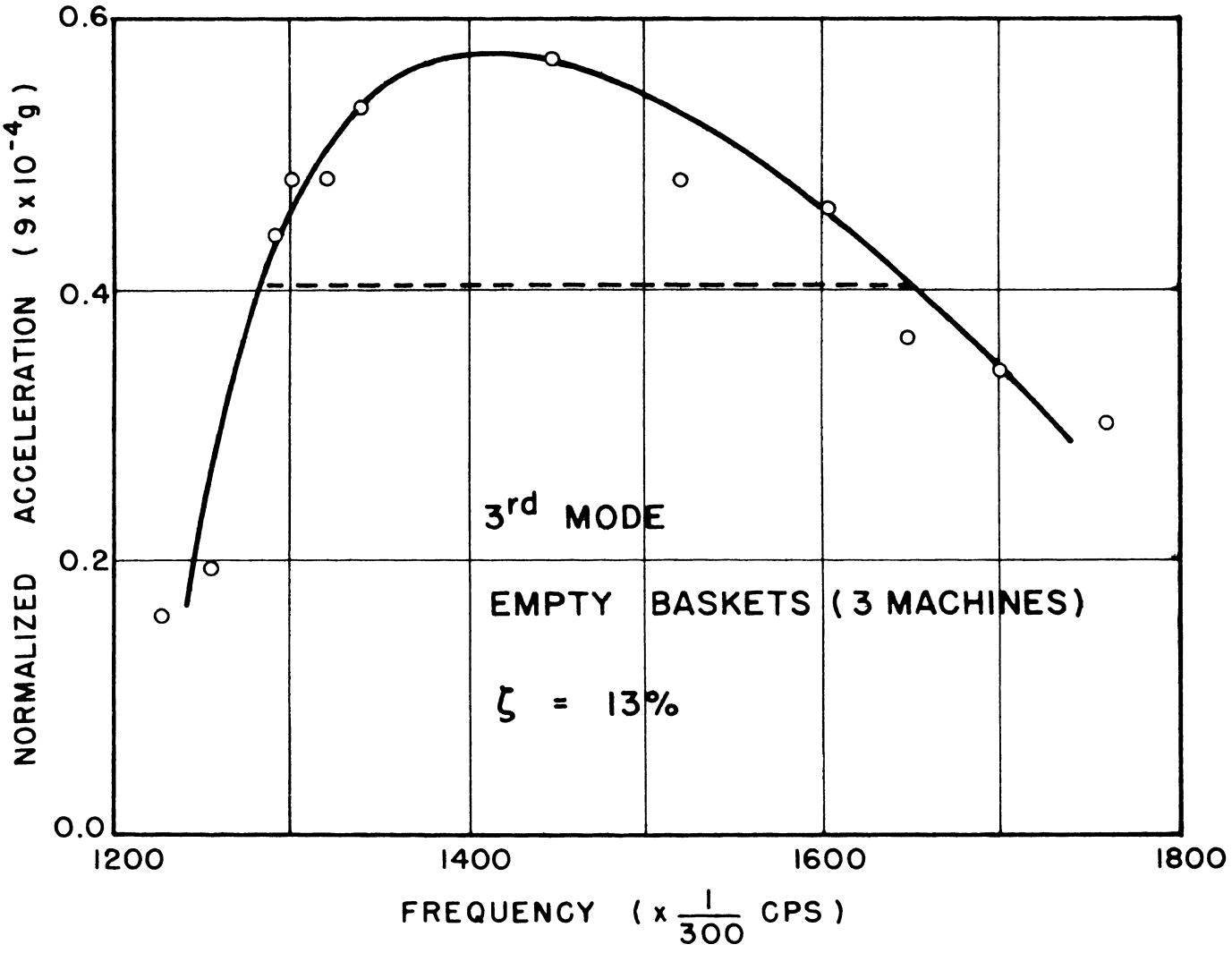

FIG. 3.34 – FREQUENCY RESPONSE COLUMN B, E–W
SUMMER 1965

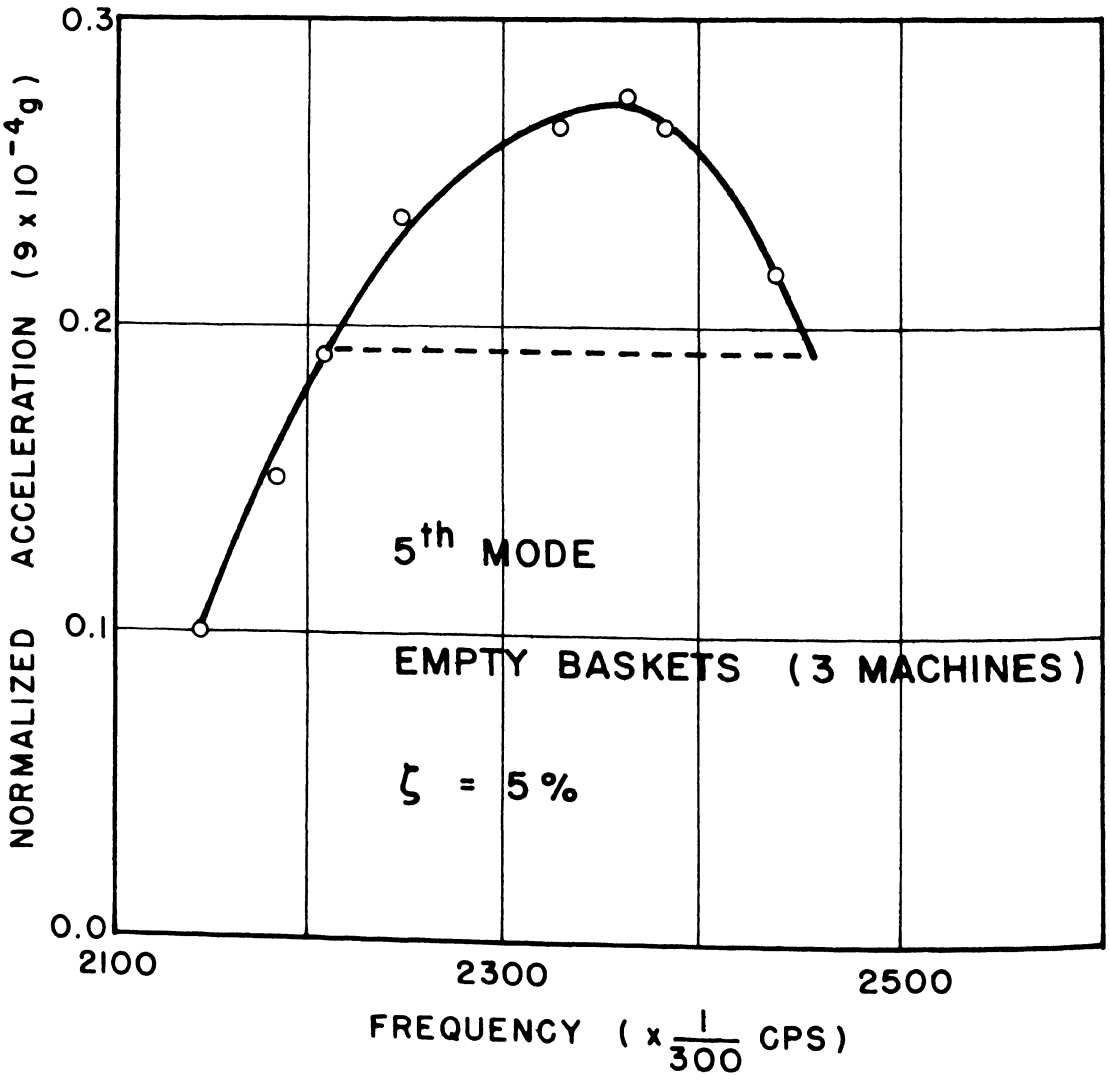

FIG. 3.35 – FREQUENCY RESPONSE COLUMN B,E–W, SUMMER 1965

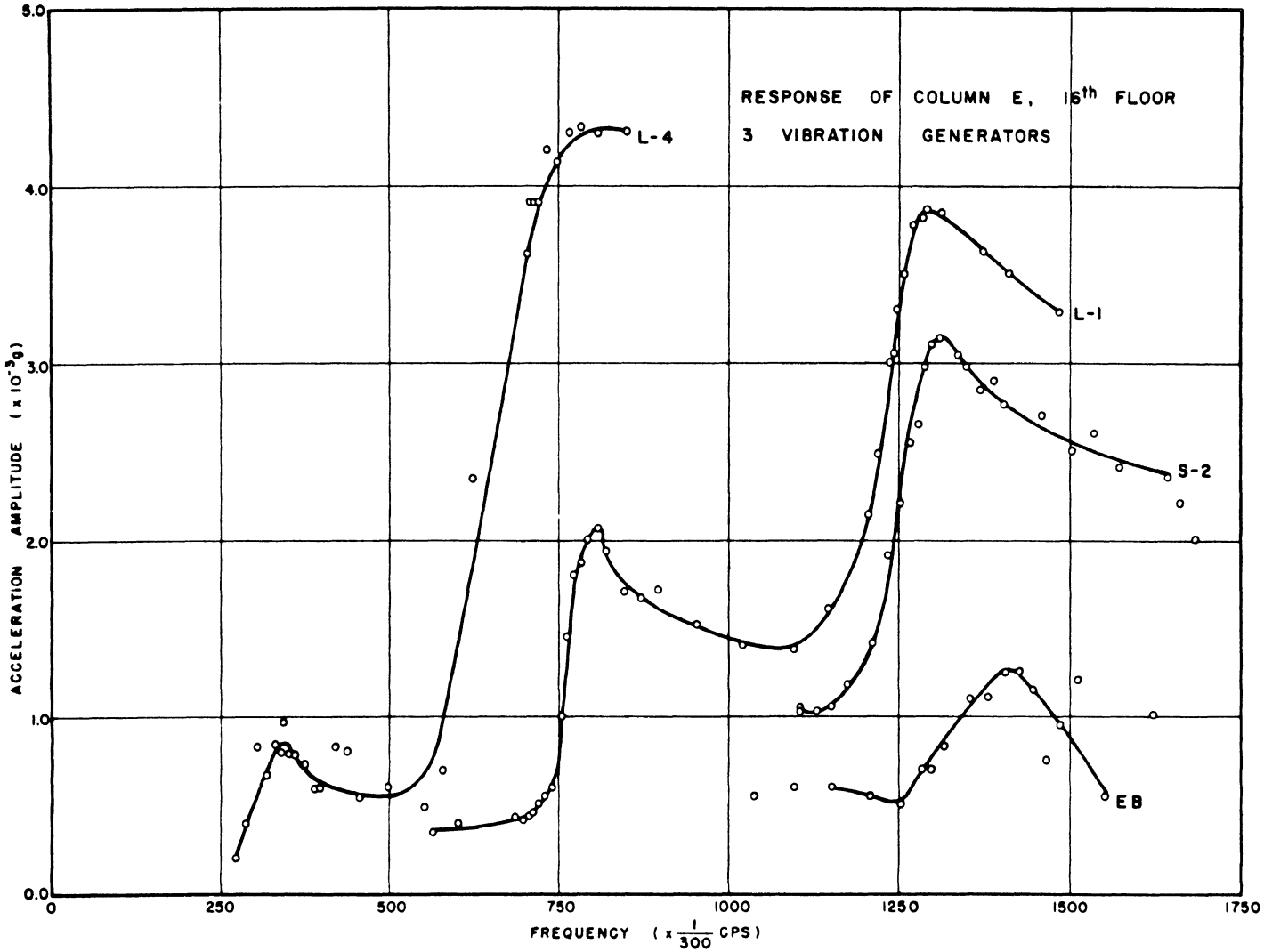

FIG. 3.36

ACCELERATION FREQUENCY RESPONSES, N–S, SUMMER 1965

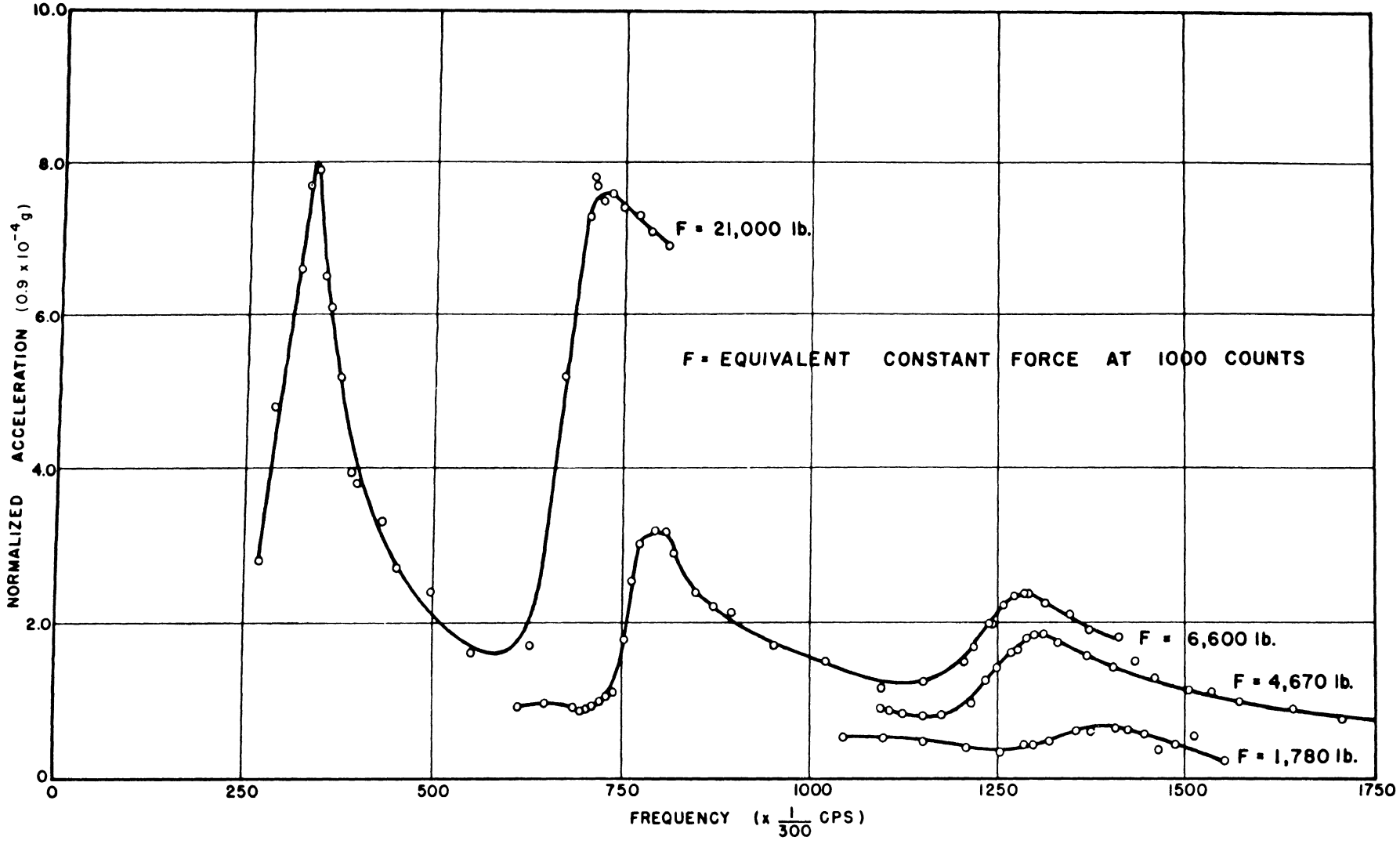

FIG. 3.37

NORMALIZED ACCELERATION FREQUENCY RESPONSE, N–S,
SUMMER 1965

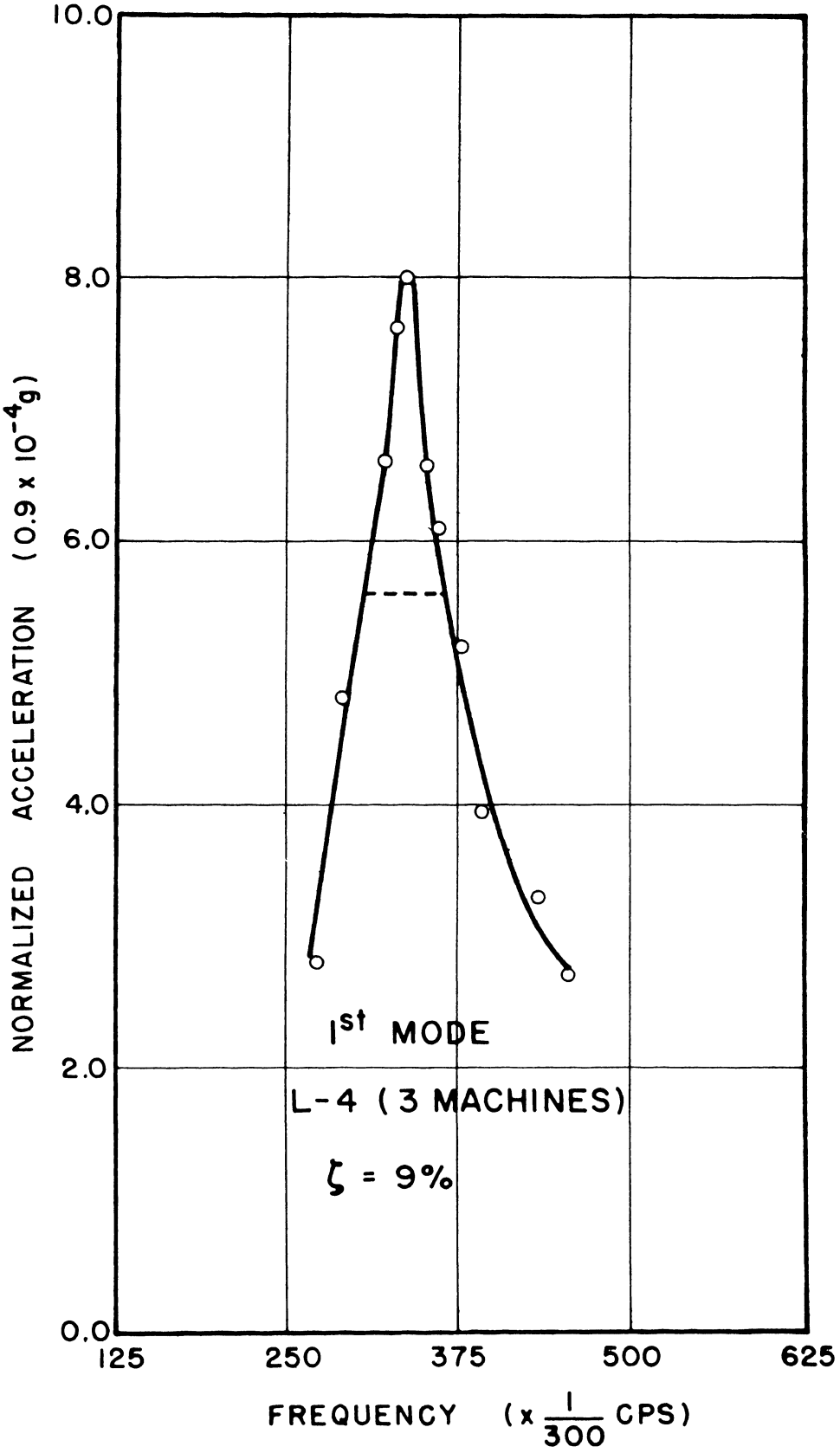

FIG. 3.38 – NORMALIZED FREQUENCY RESPONSE COLUMN E, N–S, SUMMER 1965

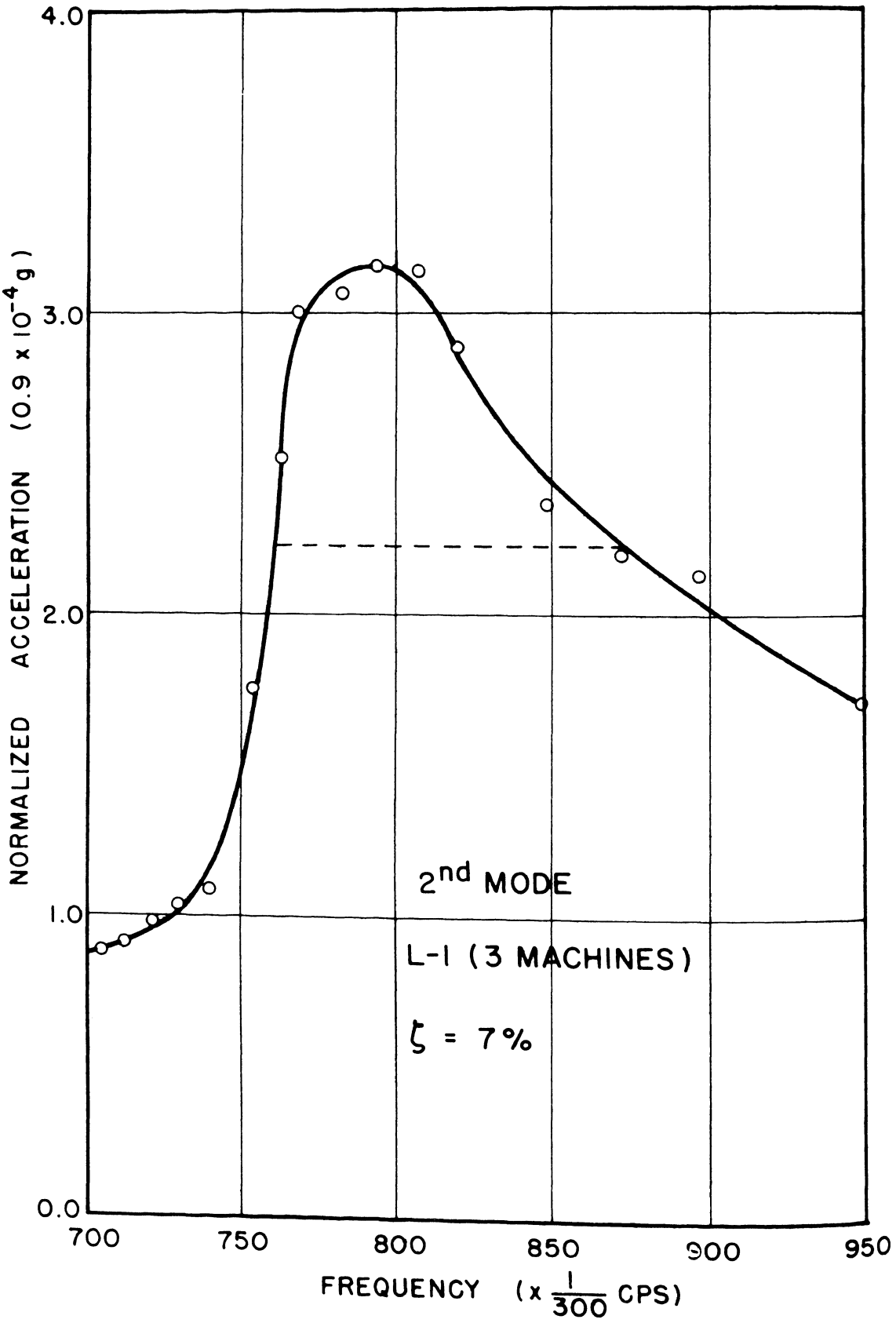

FIG. 3.39 – NORMALIZED FREQUENCY RESPONSE COLUMN E, N–S, SUMMER 1965

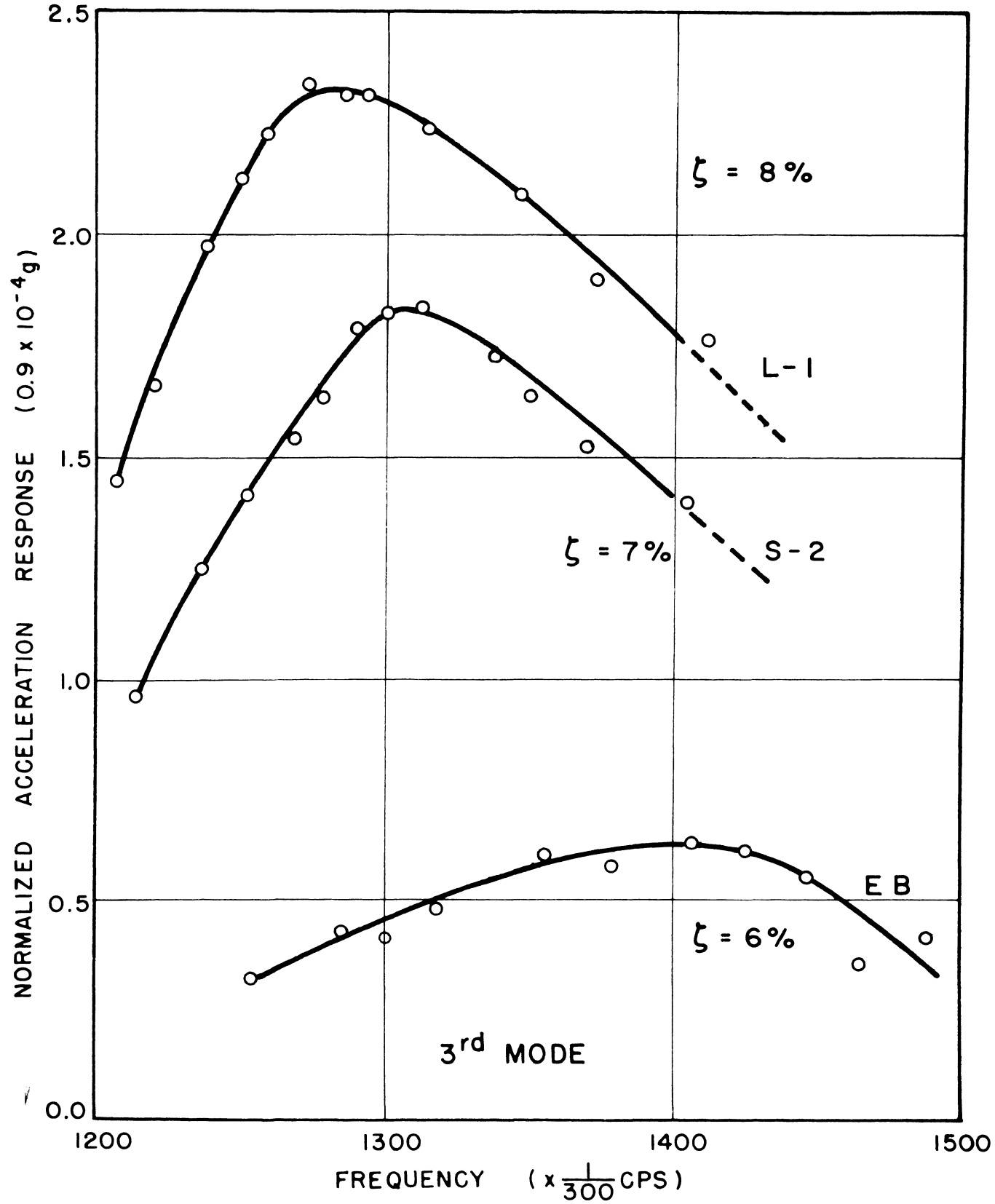

FIG. 3.40 – NORMALIZED FREQUENCY RESPONSE COLUMN E
16th FLOOR, N–S, SUMMER 1965

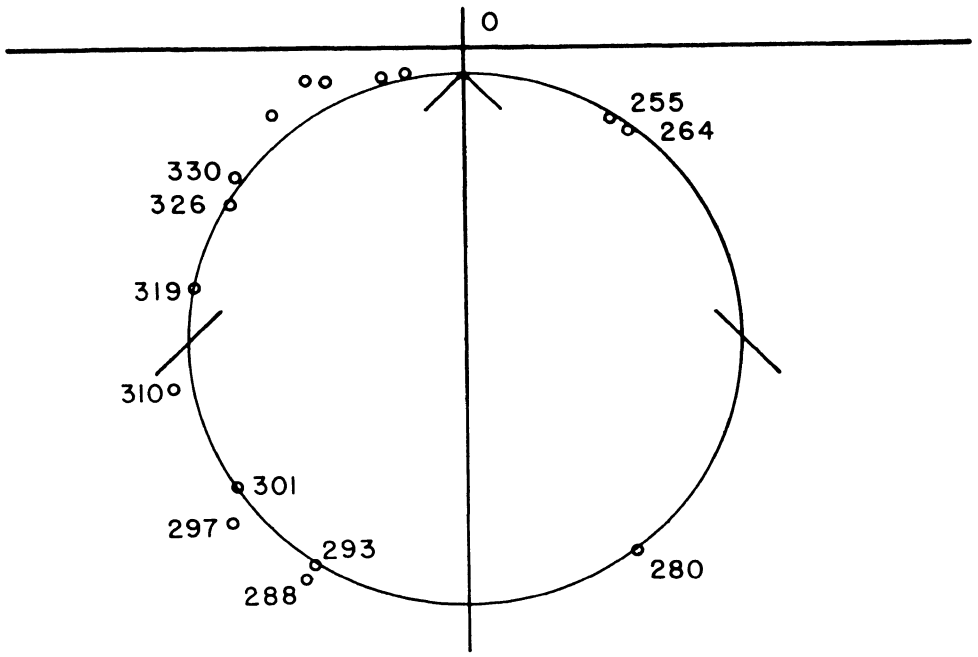

FIG. 3.41 – K AND P PLOT, 1st MODE E–W, SUMMER 1965

FIG. 3.41

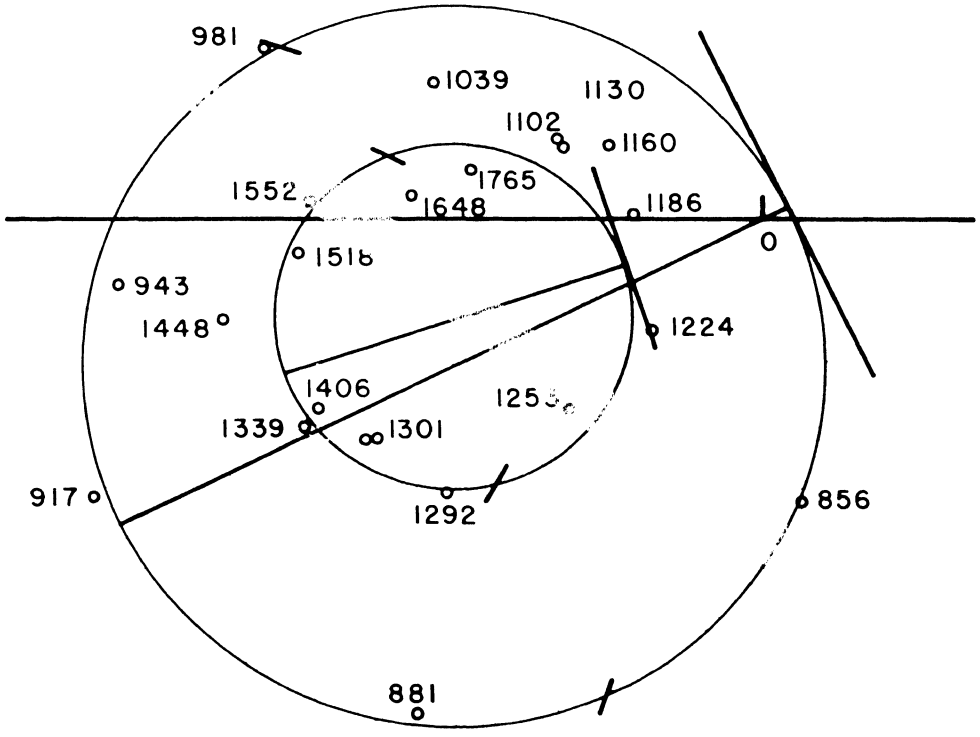

FIG. 3.42 – K AND P PLOT, 2nd AND 3rd MODES E–W, SUMMER 1965

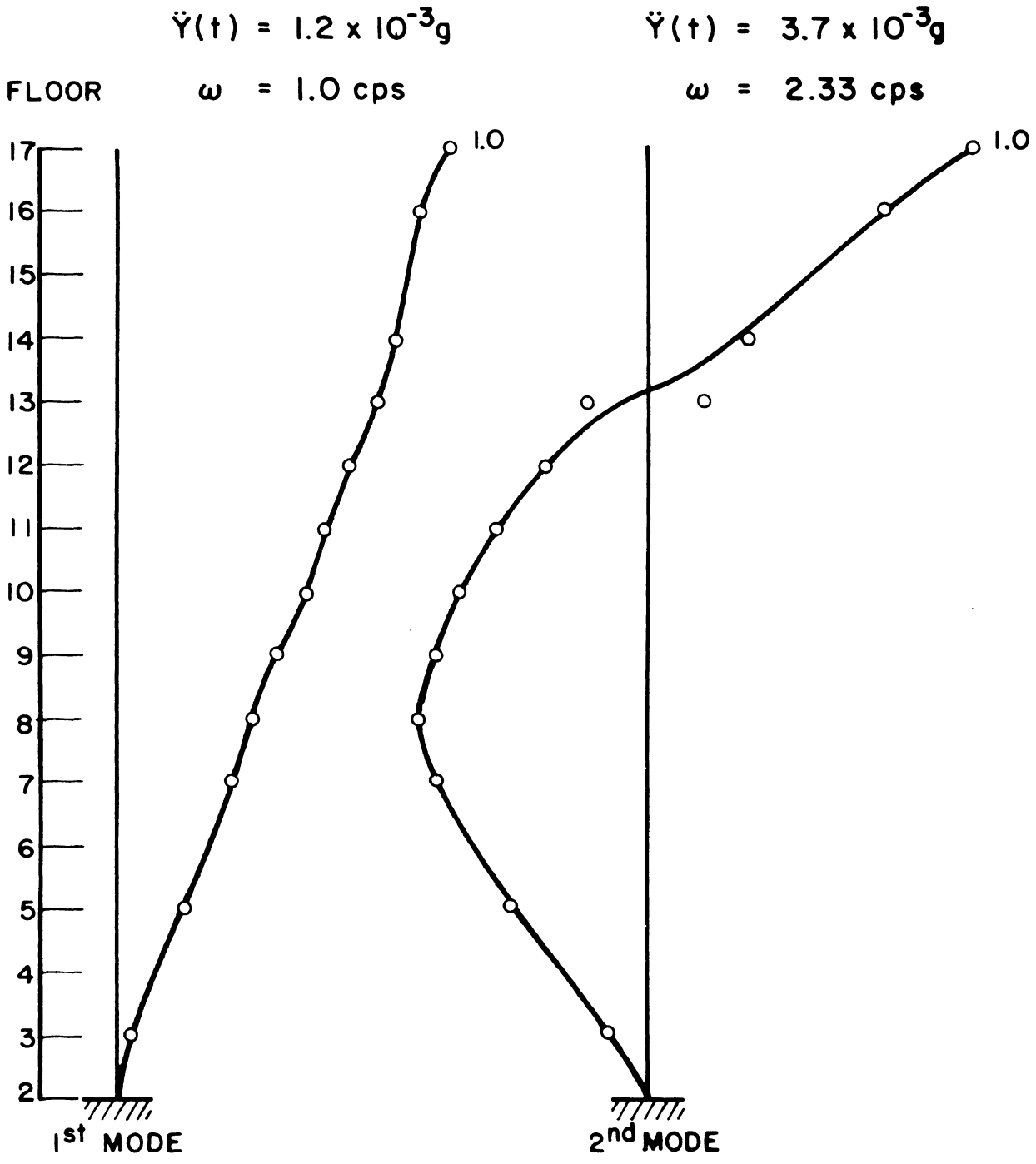

FIG. 3.43 – E–W MODE SHAPES, SUMMER 1965

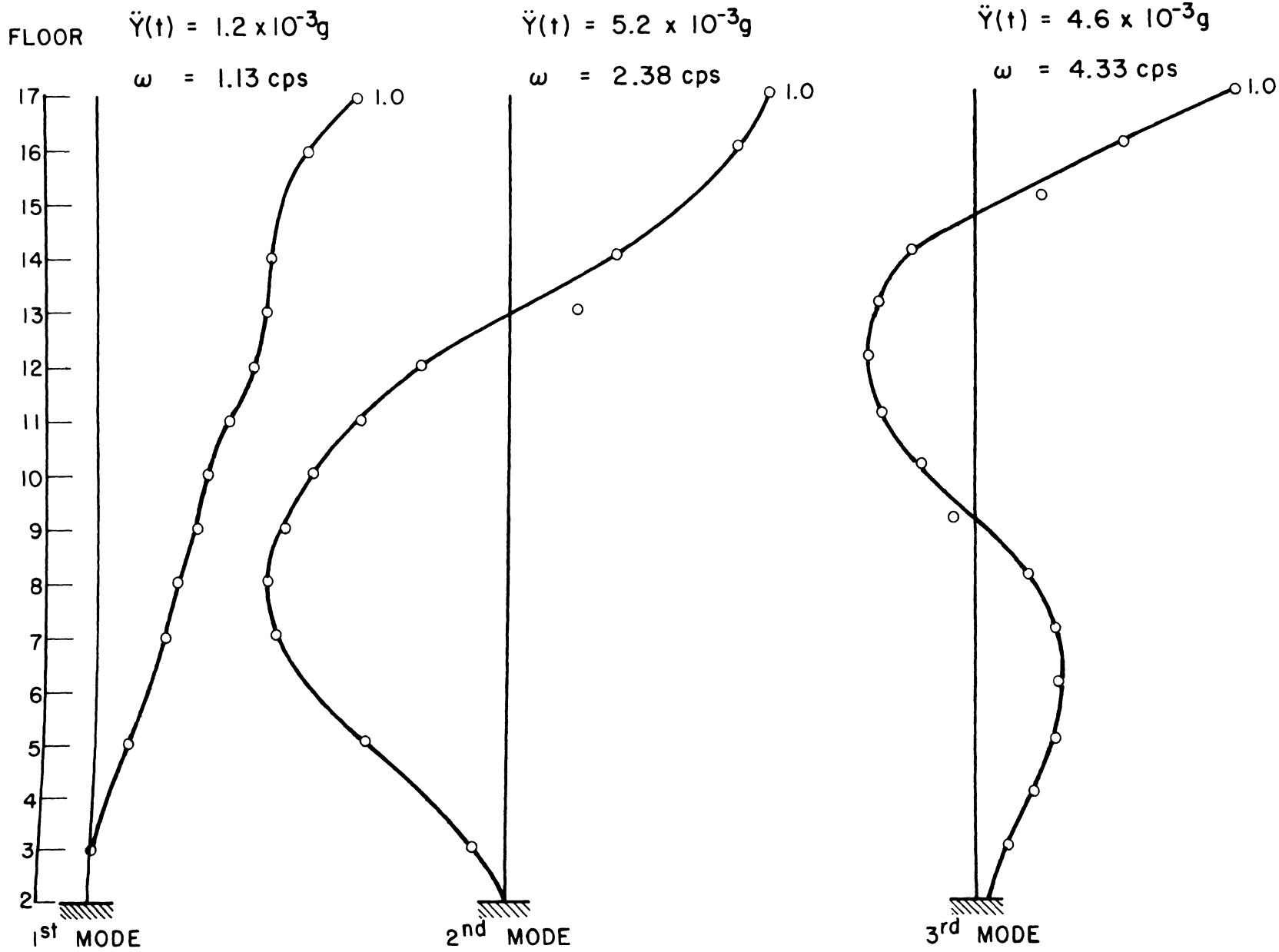

FIG. 3.44

N–S MODE SHAPES, SUMMER 1965

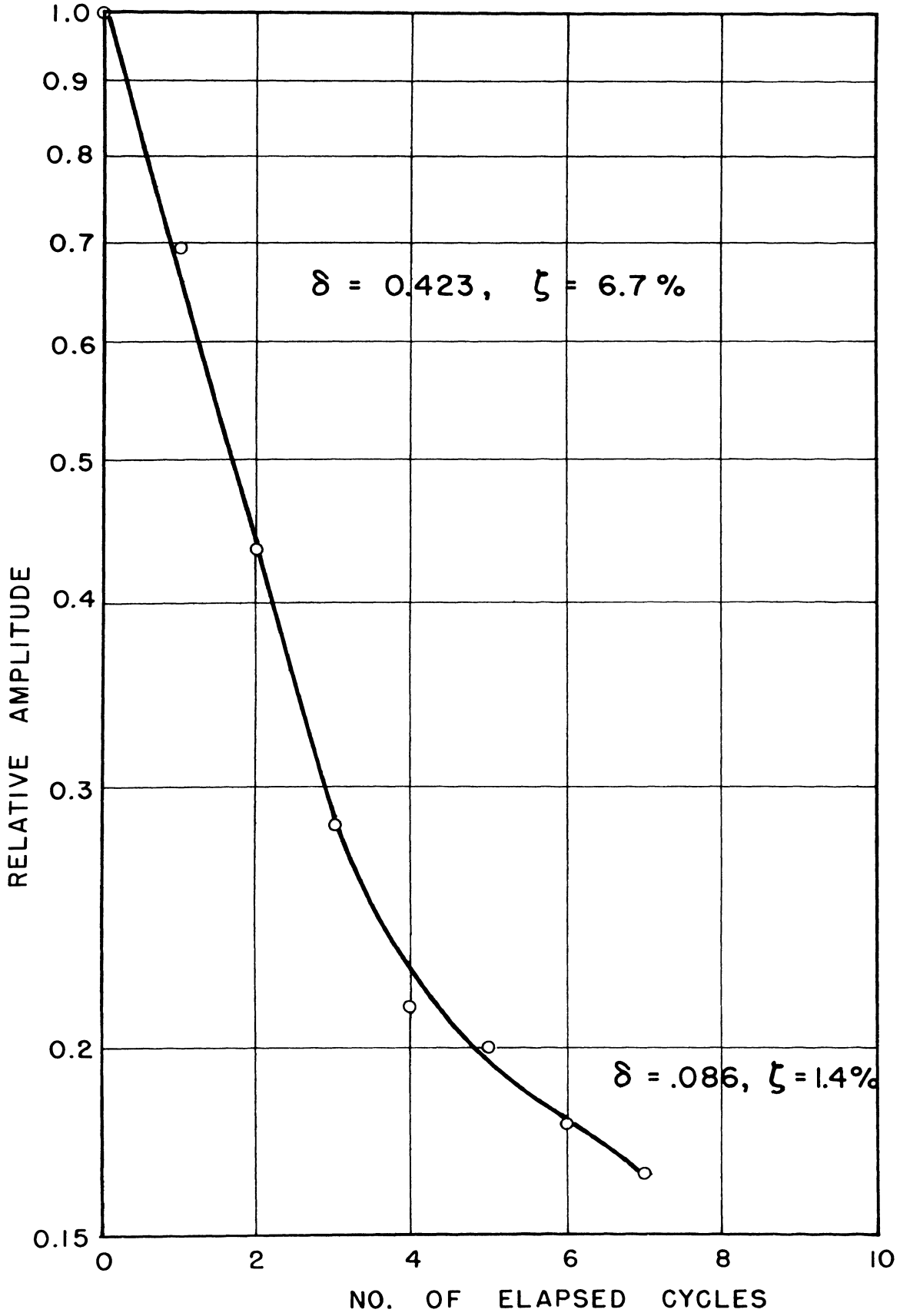

FIG. 3.45 – LOGARITHMIC DECAY CURVE OF FIRST MODE E–W
SUMMER 1965

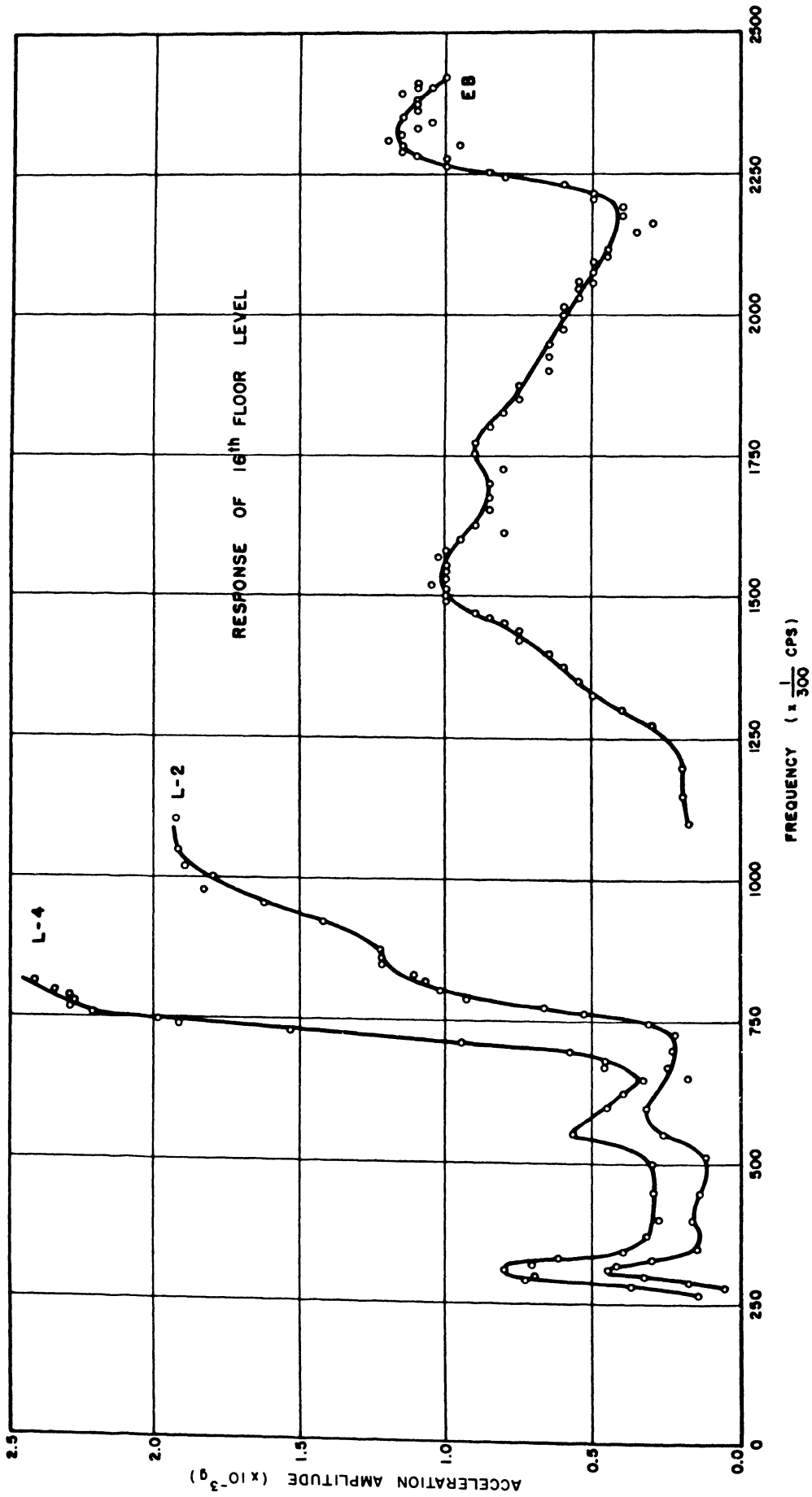

ACCELERATION FREQUENCY RESPONSES, E–W, FALL 1965 I

FIG. 3.46

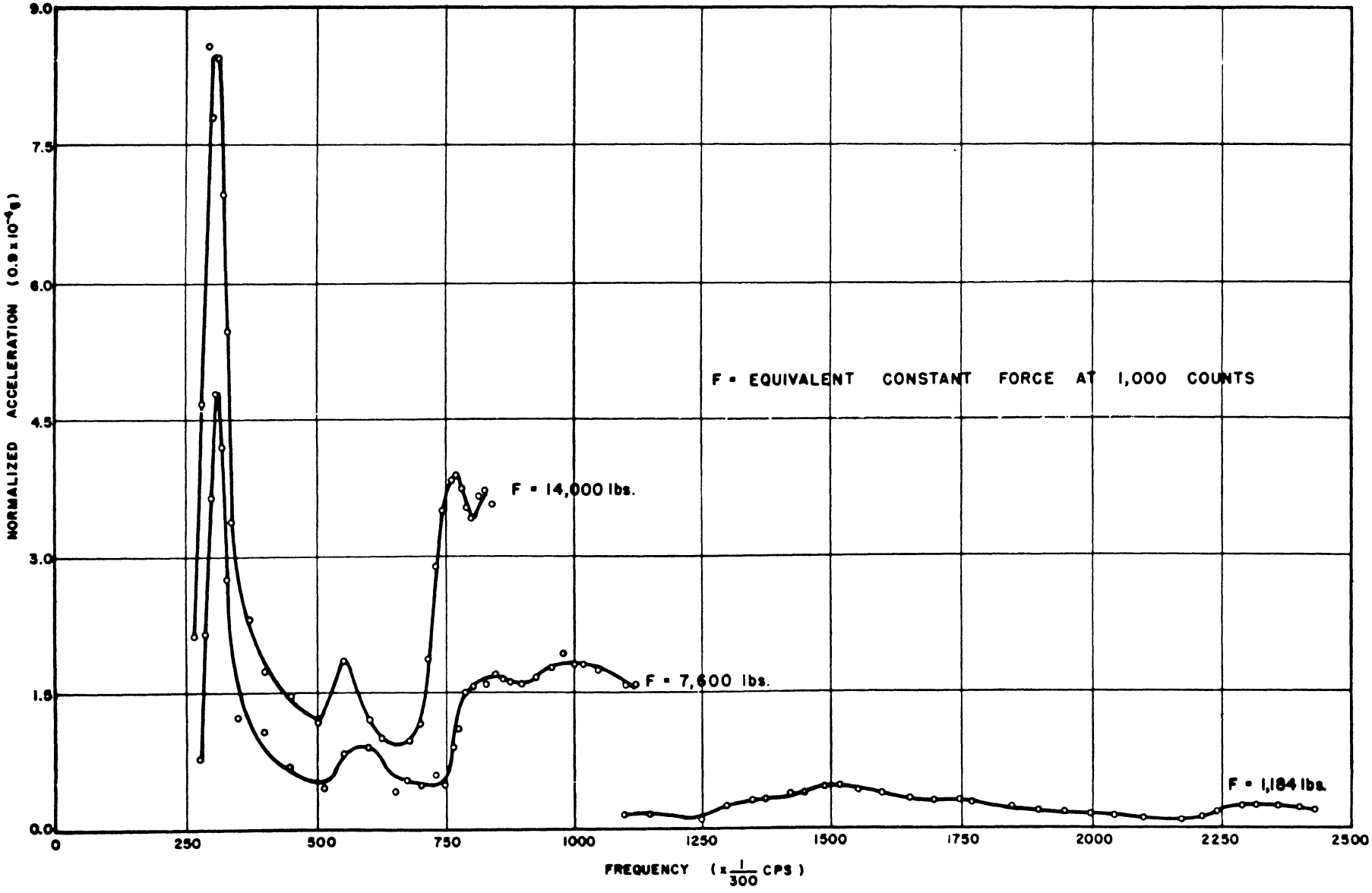

FIG. 3.47

NORMALIZED ACCELERATION FREQUENCY RESPONSES, E–W FALL 1965 I

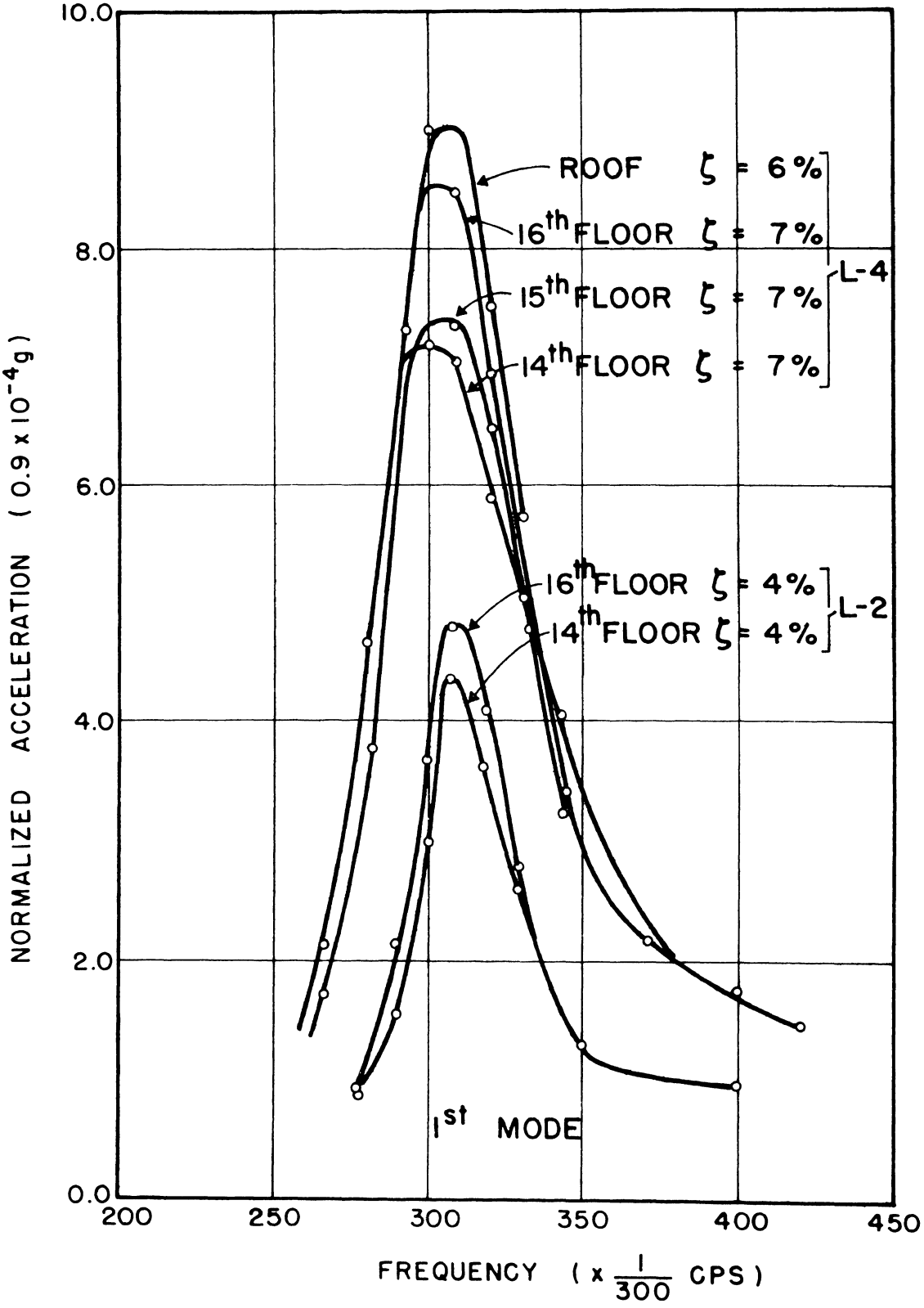

FIG. 3.48 – FREQUENCY RESPONSES, COLUMN B, E–W, FALL 1965 I

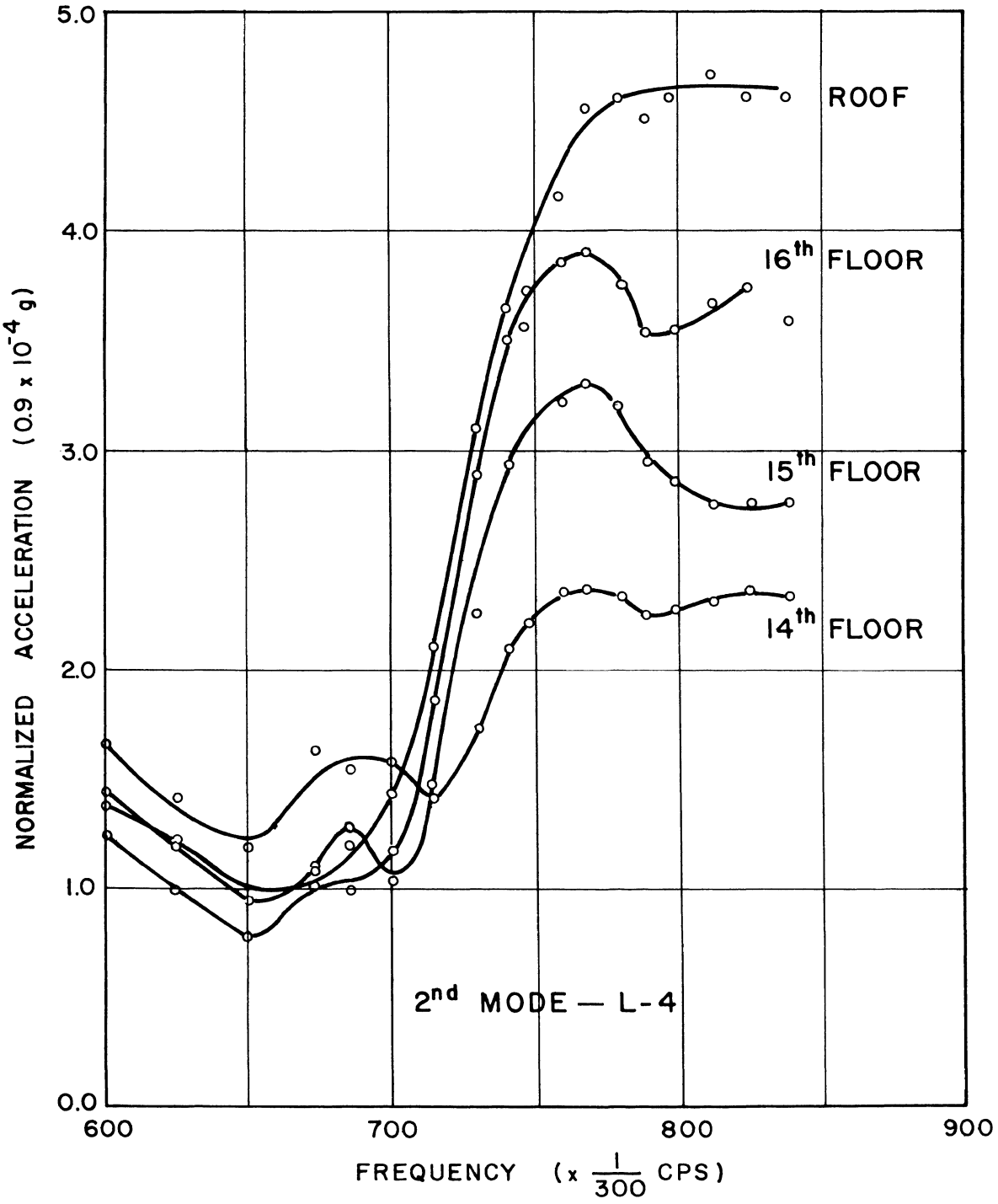

FIG. 3.49 — FREQUENCY RESPONSES, COLUMN B, E—W, FALL 1965 I

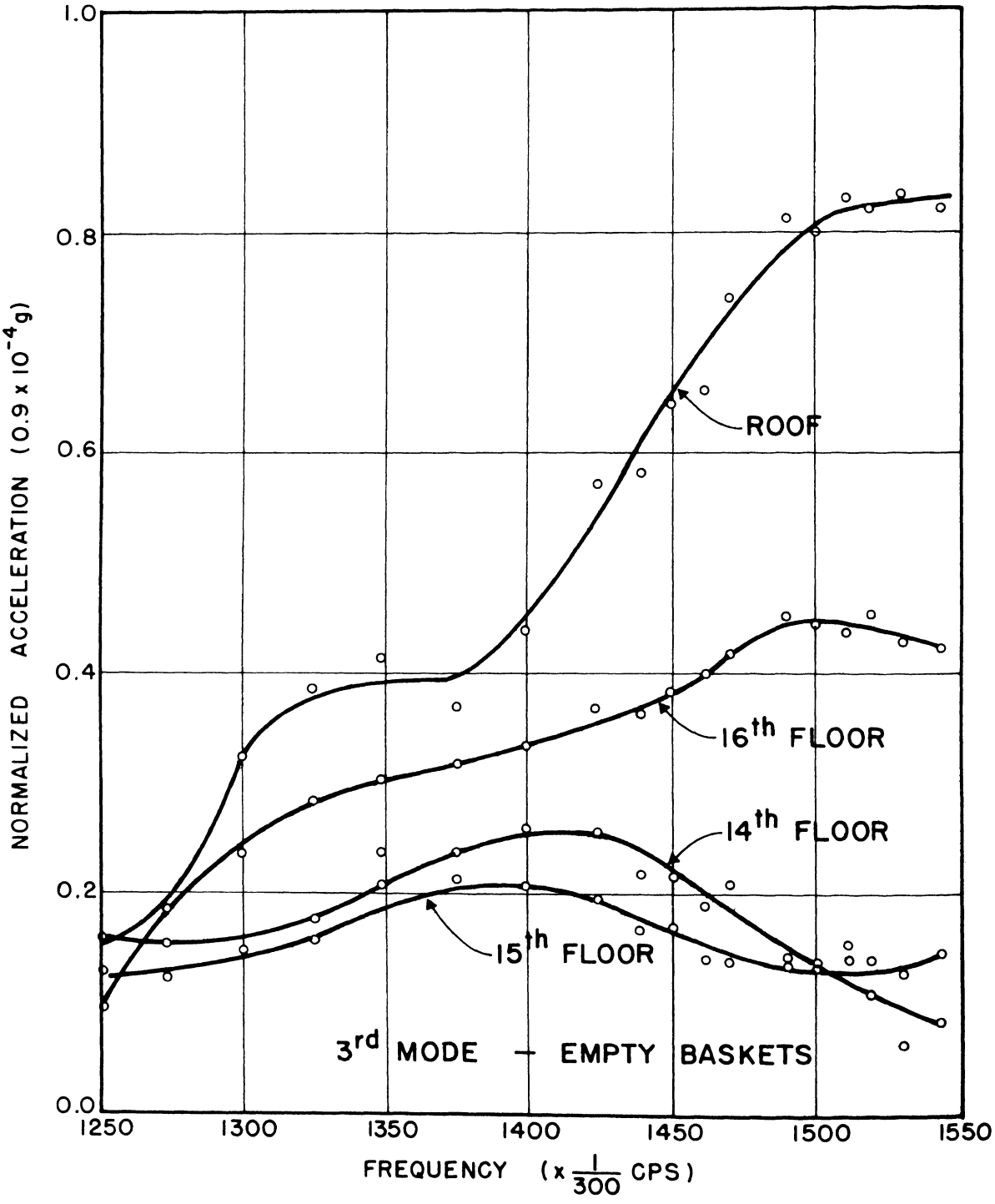

FIG. 3.50 – FREQUENCY RESPONSES, COLUMN B, E–W, FALL 1965 I

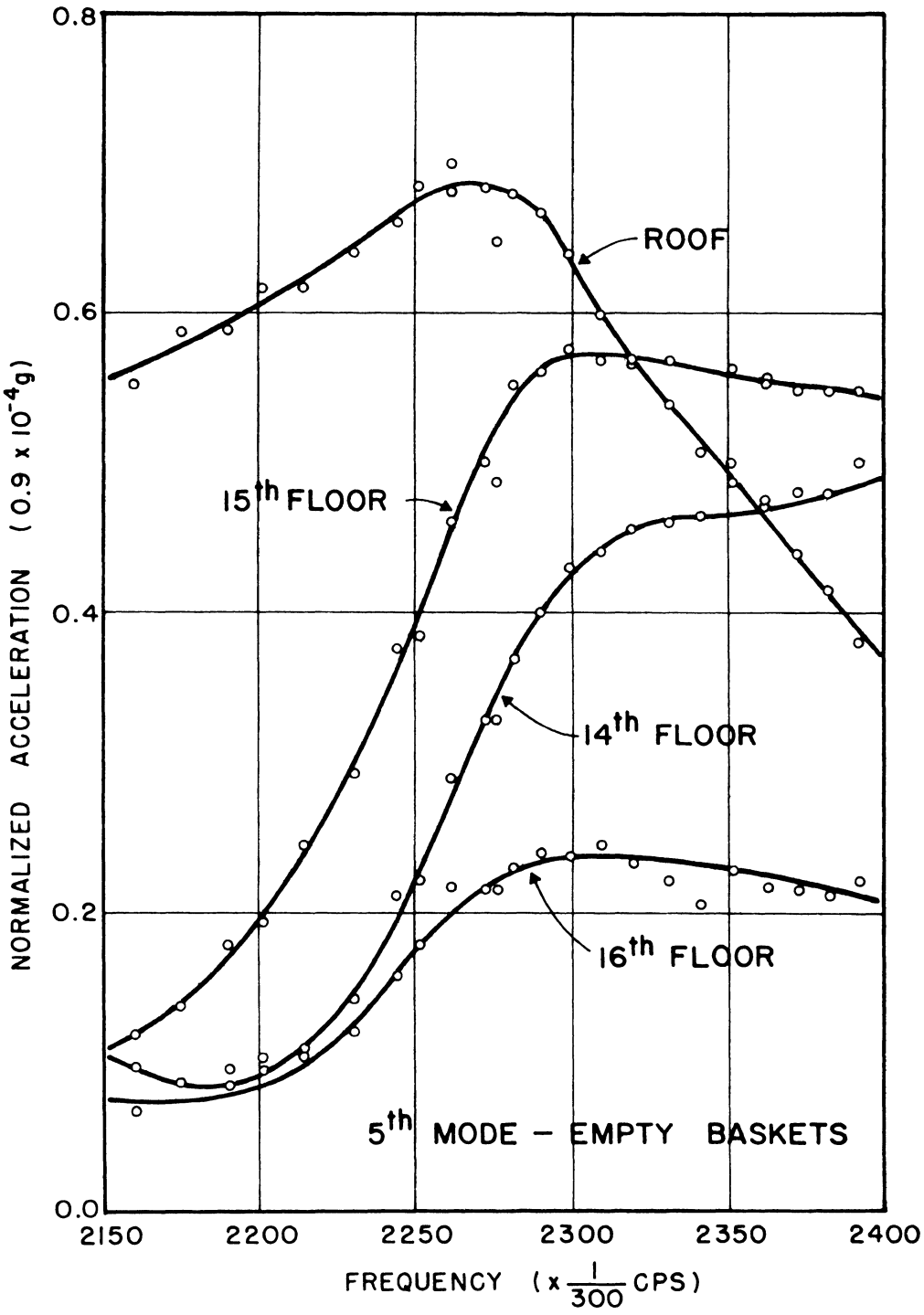

FIG. 3.51 – FREQUENCY RESPONSES, COLUMN B, E–W, FALL 1965 I

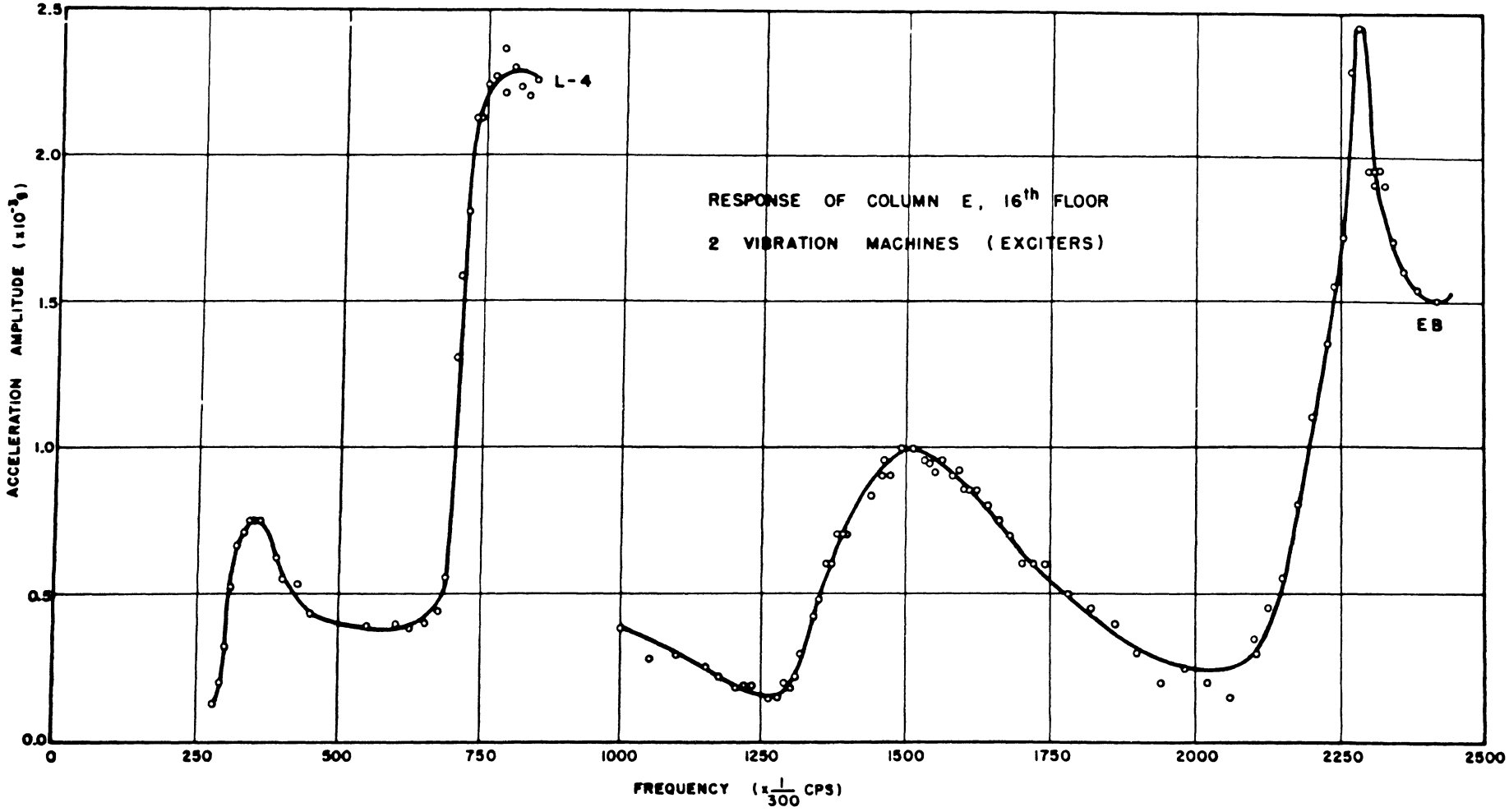

FIG. 3.52

ACCELERATION FREQUENCY RESPONSES, N–S FALL 1965 I

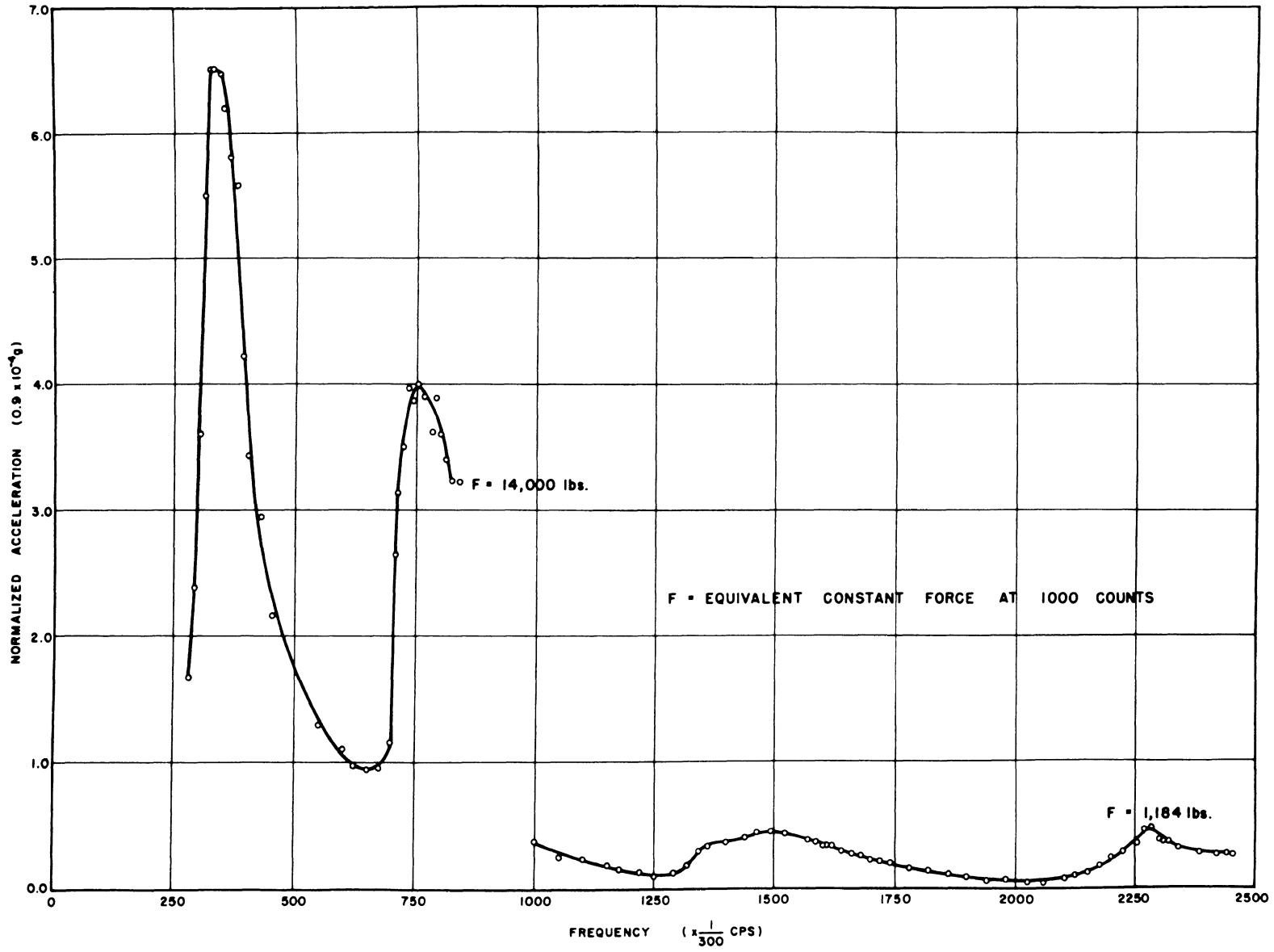

FIG. 3.53

NORMALIZED ACCELERATION FREQUENCY RESPONSE, N–S, FALL 1965 I

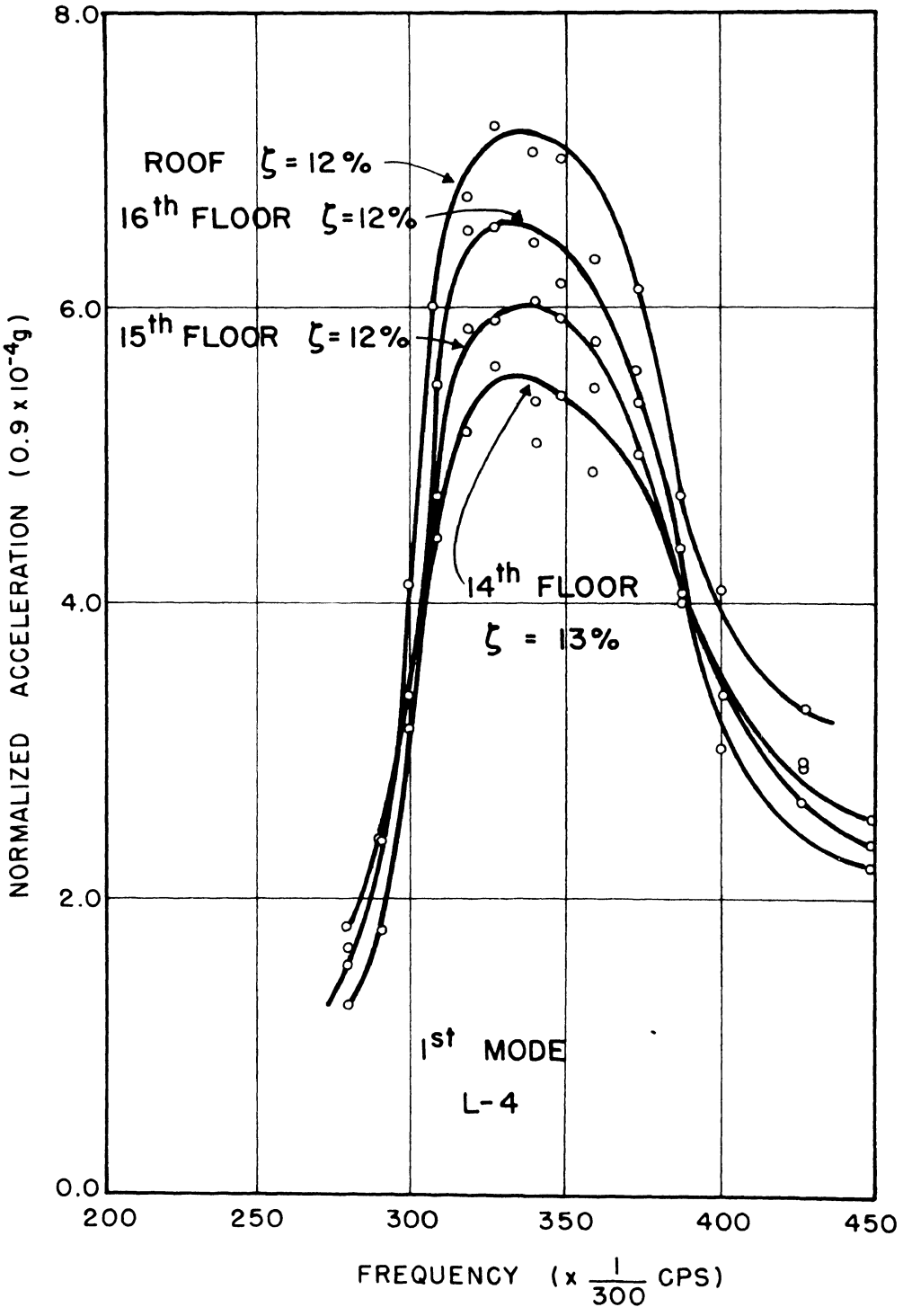

FIG. 3.54 – FREQUENCY RESPONSES, COLUMN E, N–S, FALL 1965 I

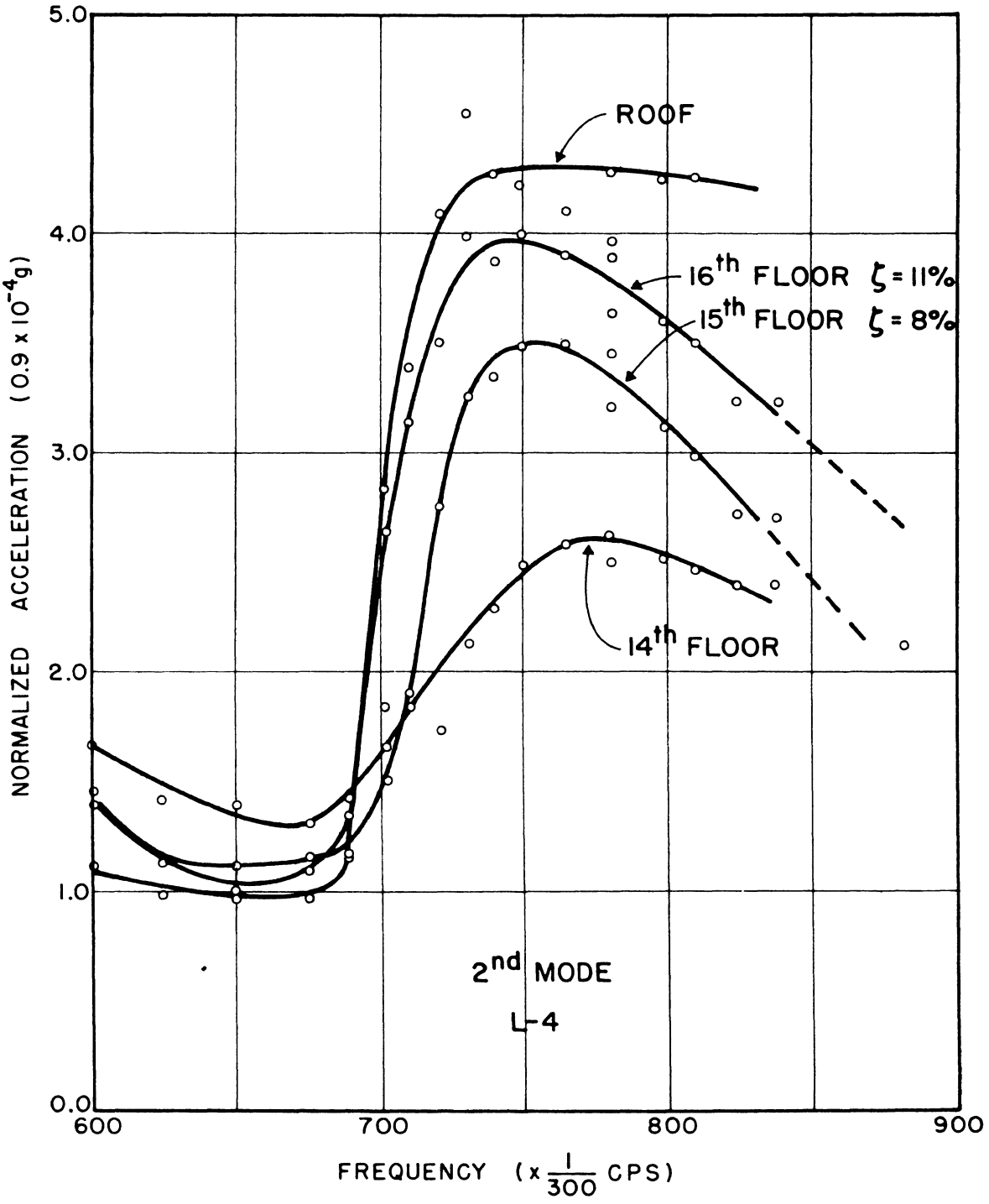

FIG. 3.55 – FREQUENCY RESPONSES, COLUMN E, N–S, FALL 1965 I

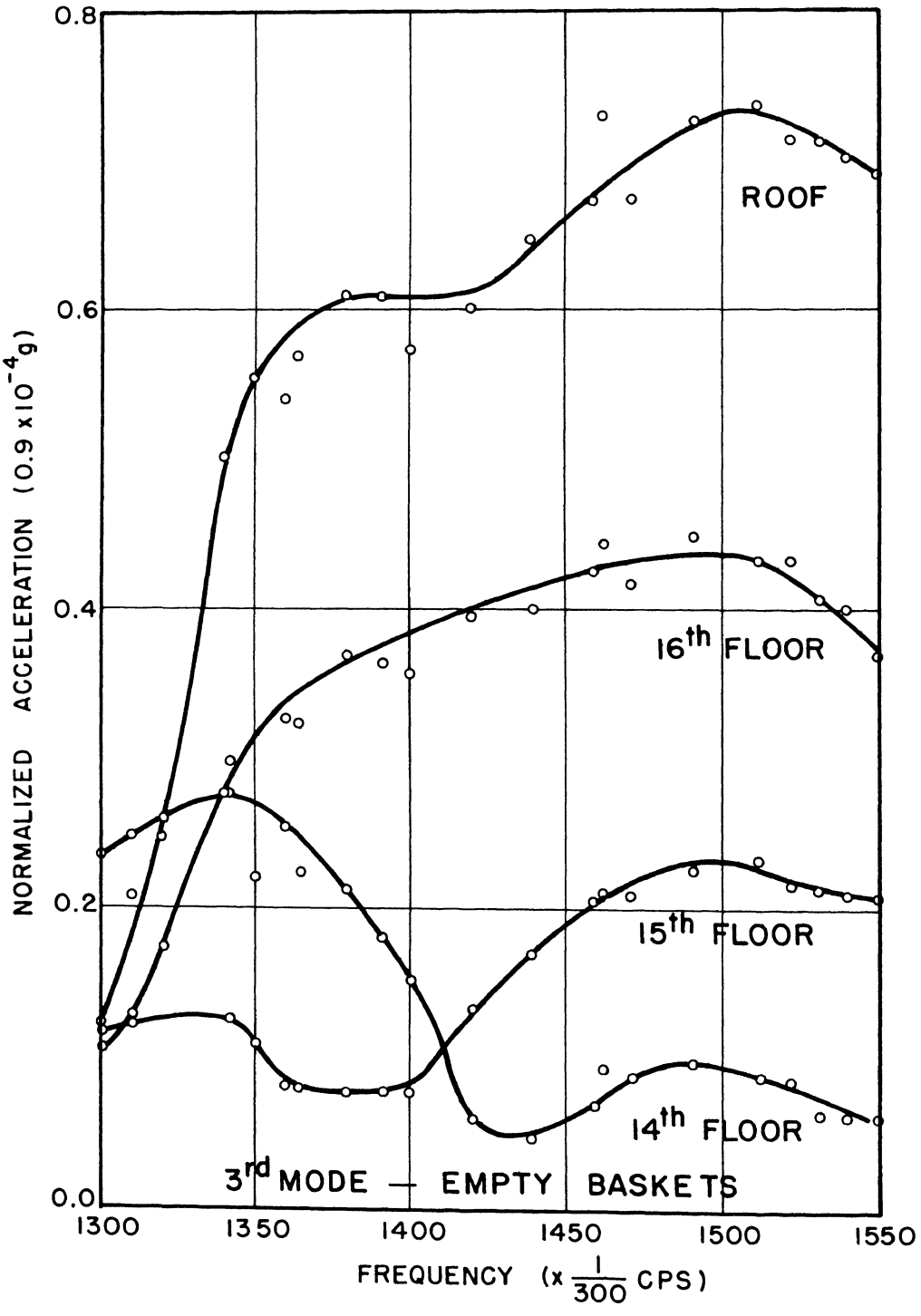

FIG. 3.56 — FREQUENCY RESPONSES, COLUMN E, N–S, FALL 1965 I

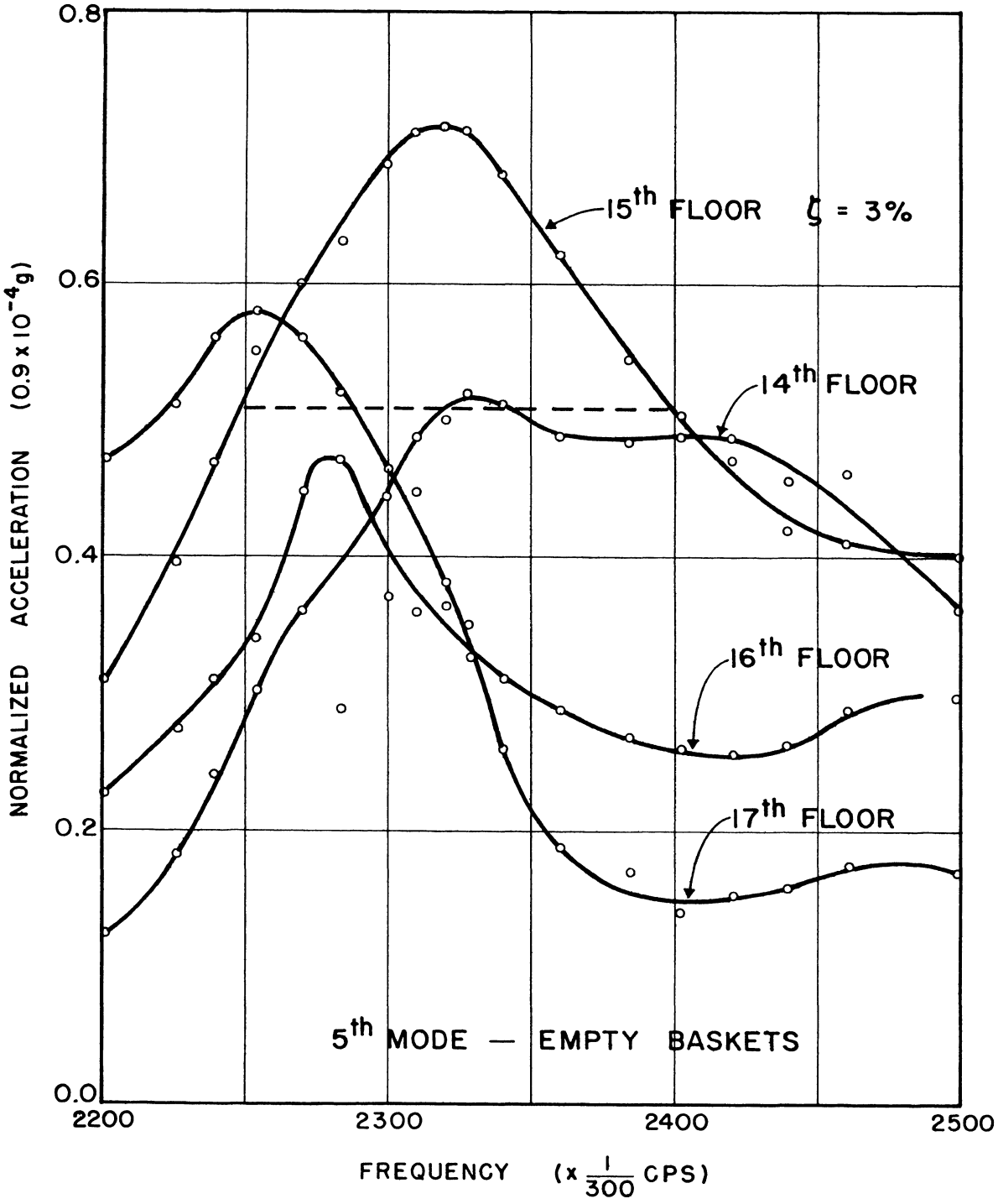

FIG. 3.57 – FREQUENCY RESPONSES, COLUMN E, N–S, FALL 1965 I

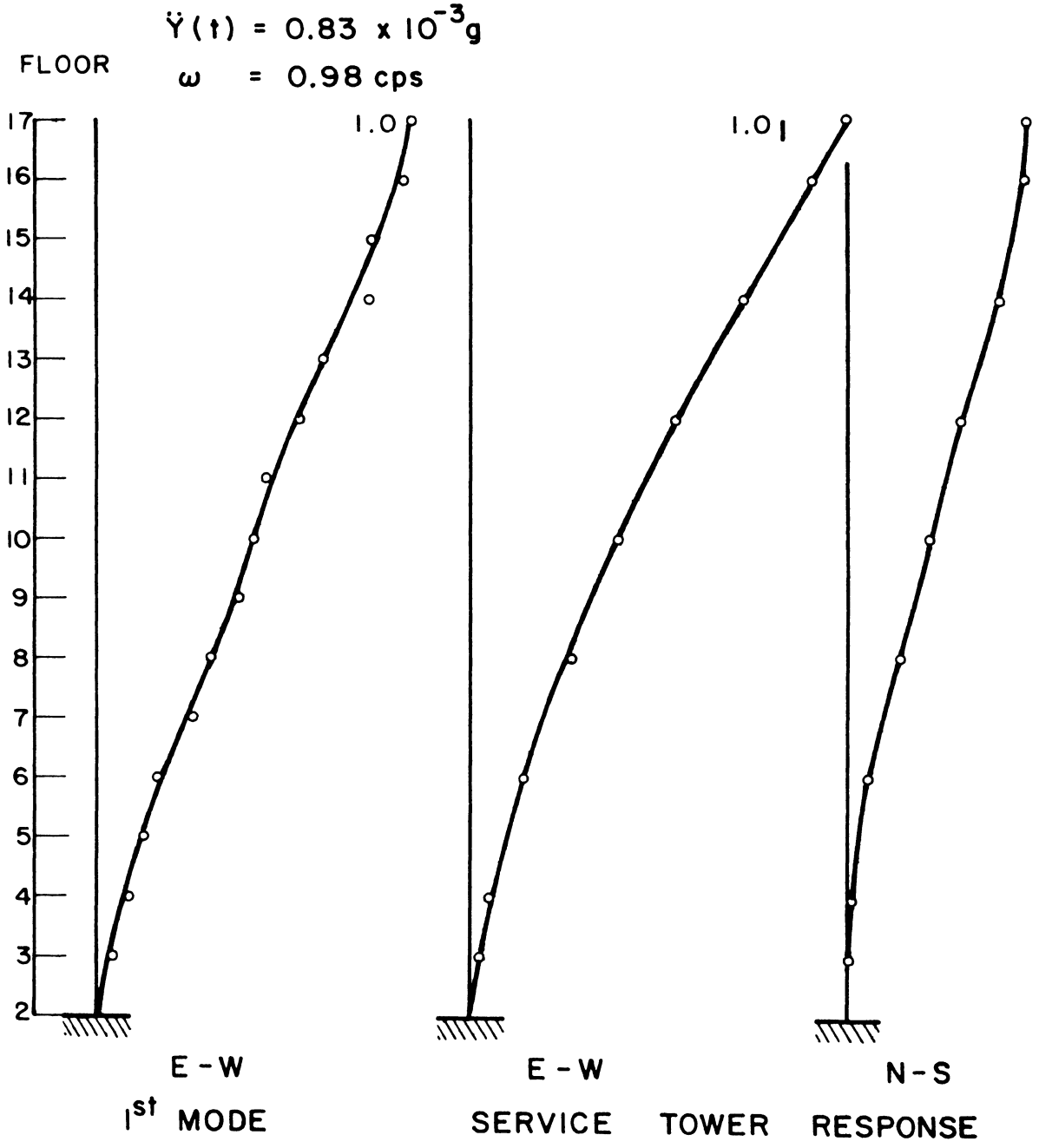

FIG. 3.58 – FIRST MODE SHAPE E–W, AND SIMULTANEOUS RESPONSE OF SERVICE TOWER, FALL 1965 I

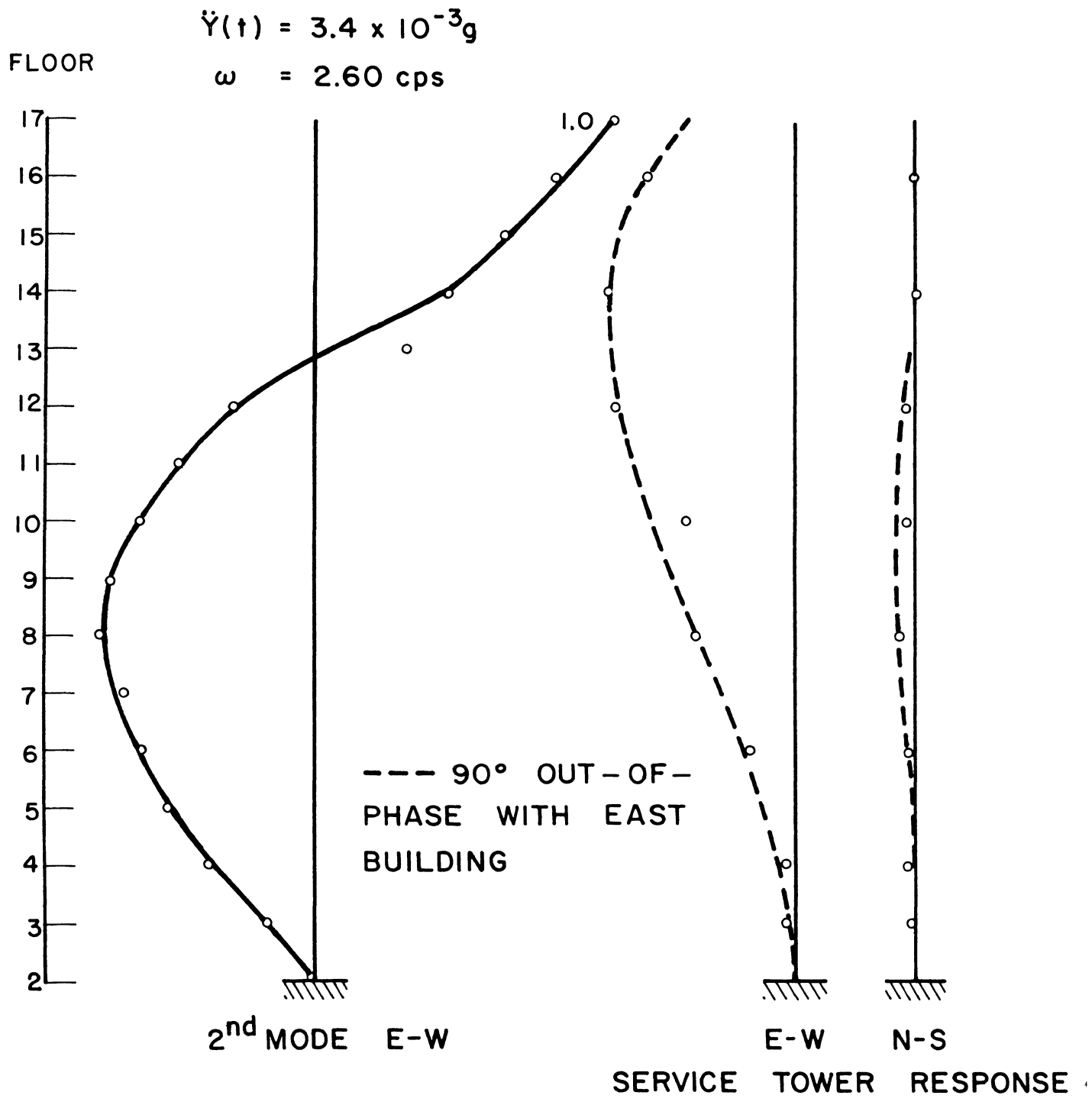

FIG. 3.59 – SECOND MODE SHAPE E–W, AND SIMULTANEOUS RESPONSE OF SERVICE TOWER, FALL 1965 I

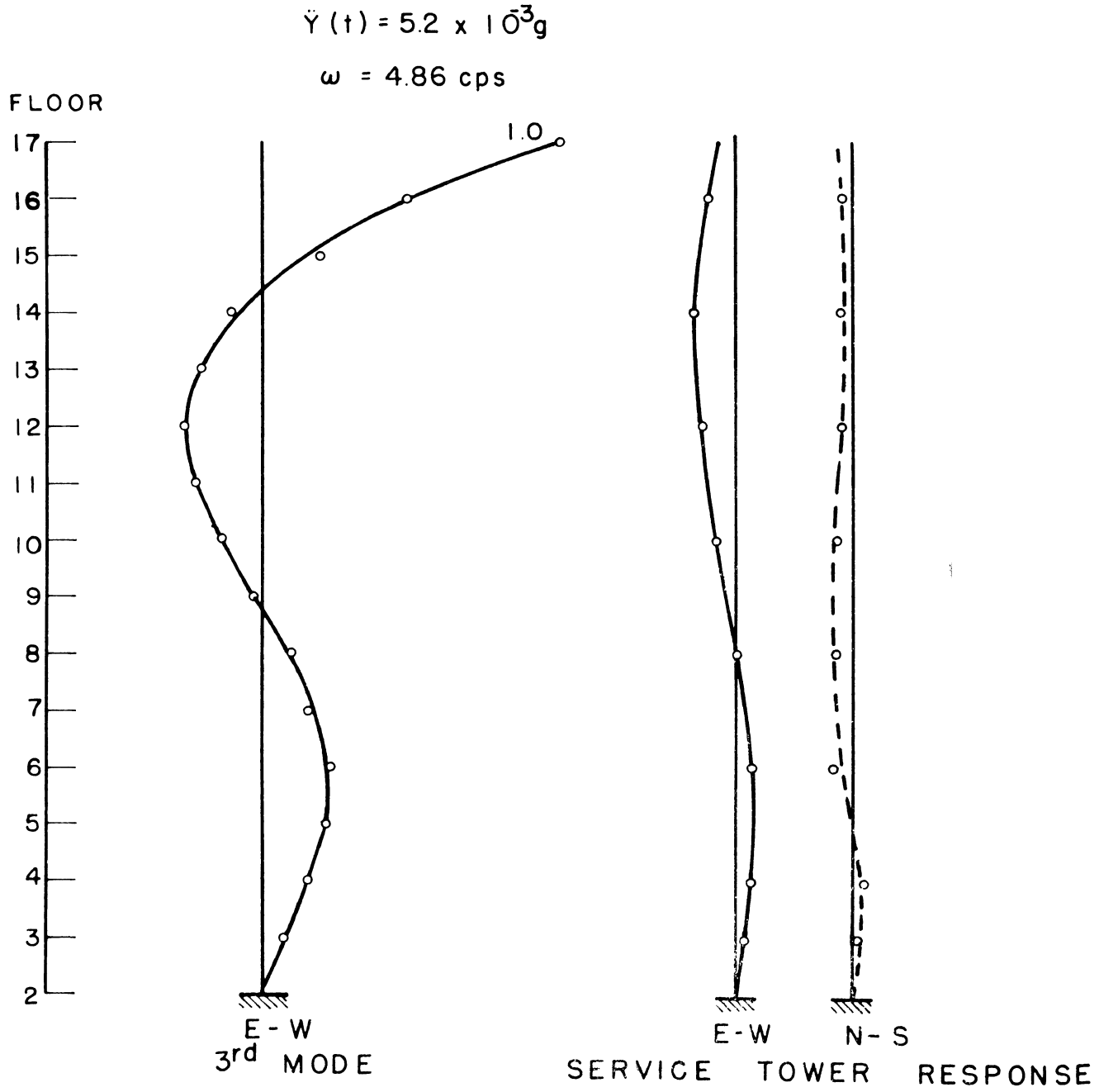

FIG. 3.60 – THIRD MODE SHAPE E–W, AND SIMULTANEOUS RESPONSE OF SERVICE TOWER, FALL 1965 I

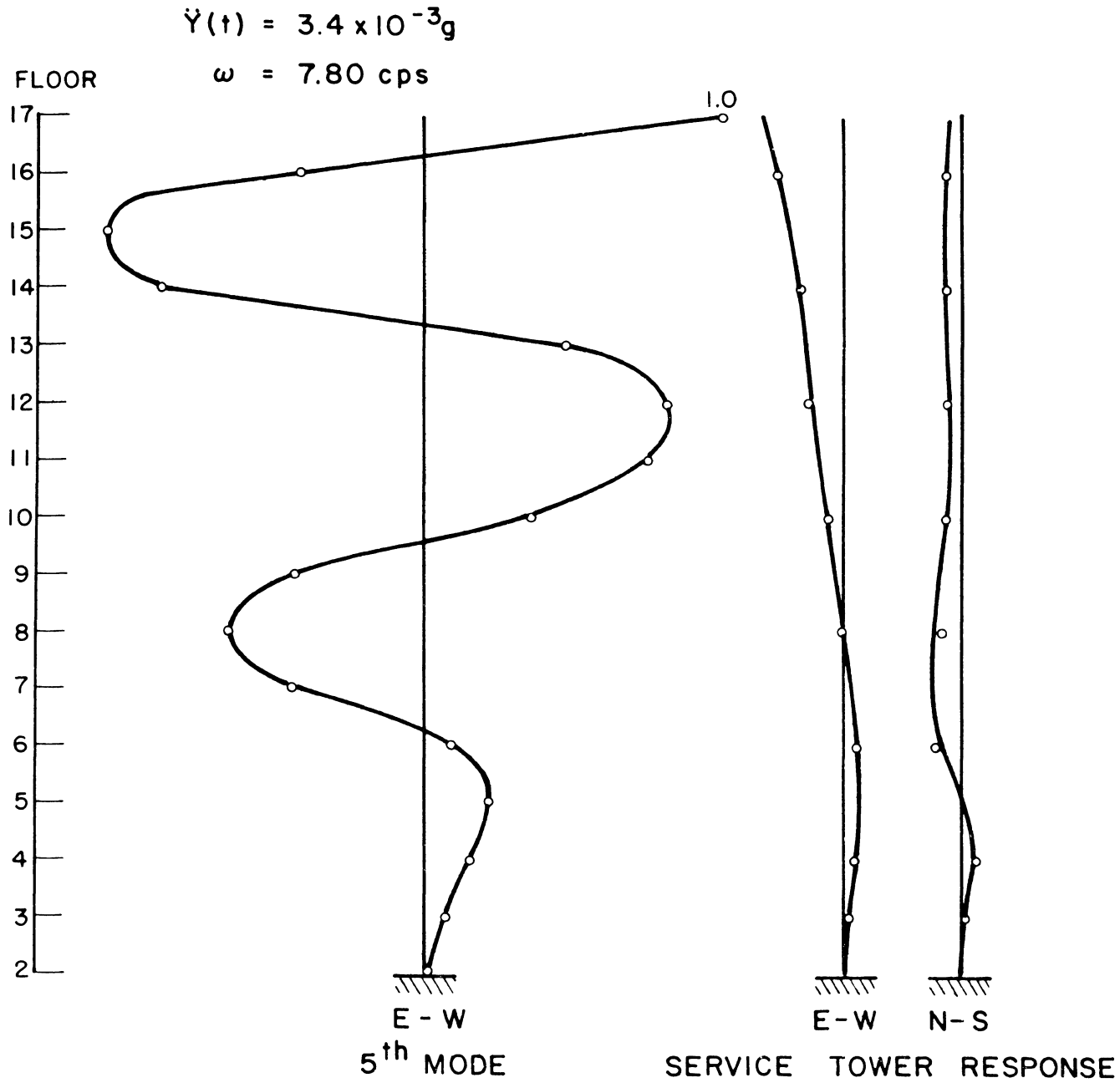

FIG. 3.61 – FIFTH MODE SHAPE E–W, AND SIMULTANEOUS RESPONSE OF SERVICE TOWER, FALL 1965 I

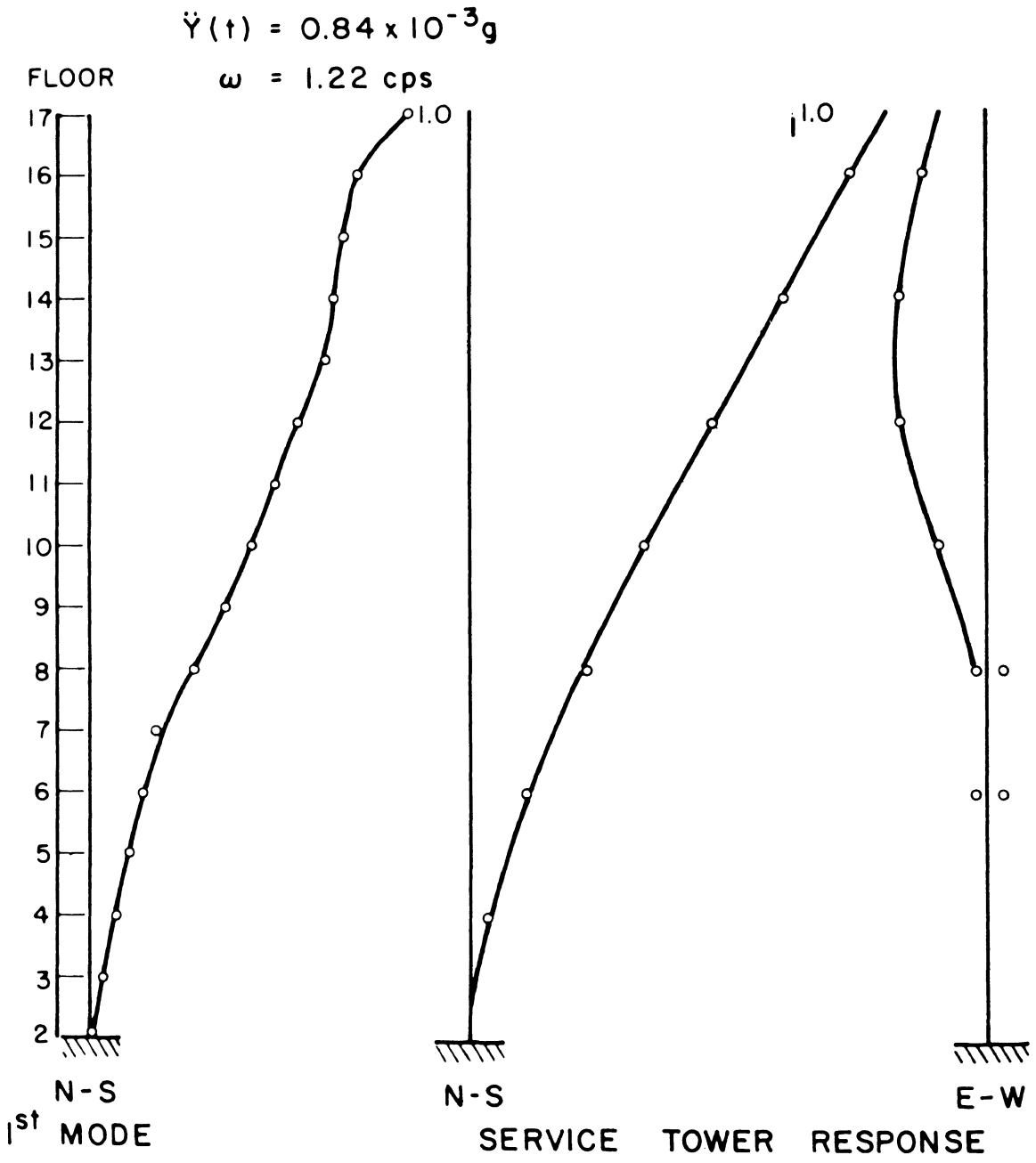

FIG. 3.62 – FIRST MODE SHAPE N–S, AND SIMULTANEOUS RESPONSE OF SERVICE TOWER, FALL 1965 I

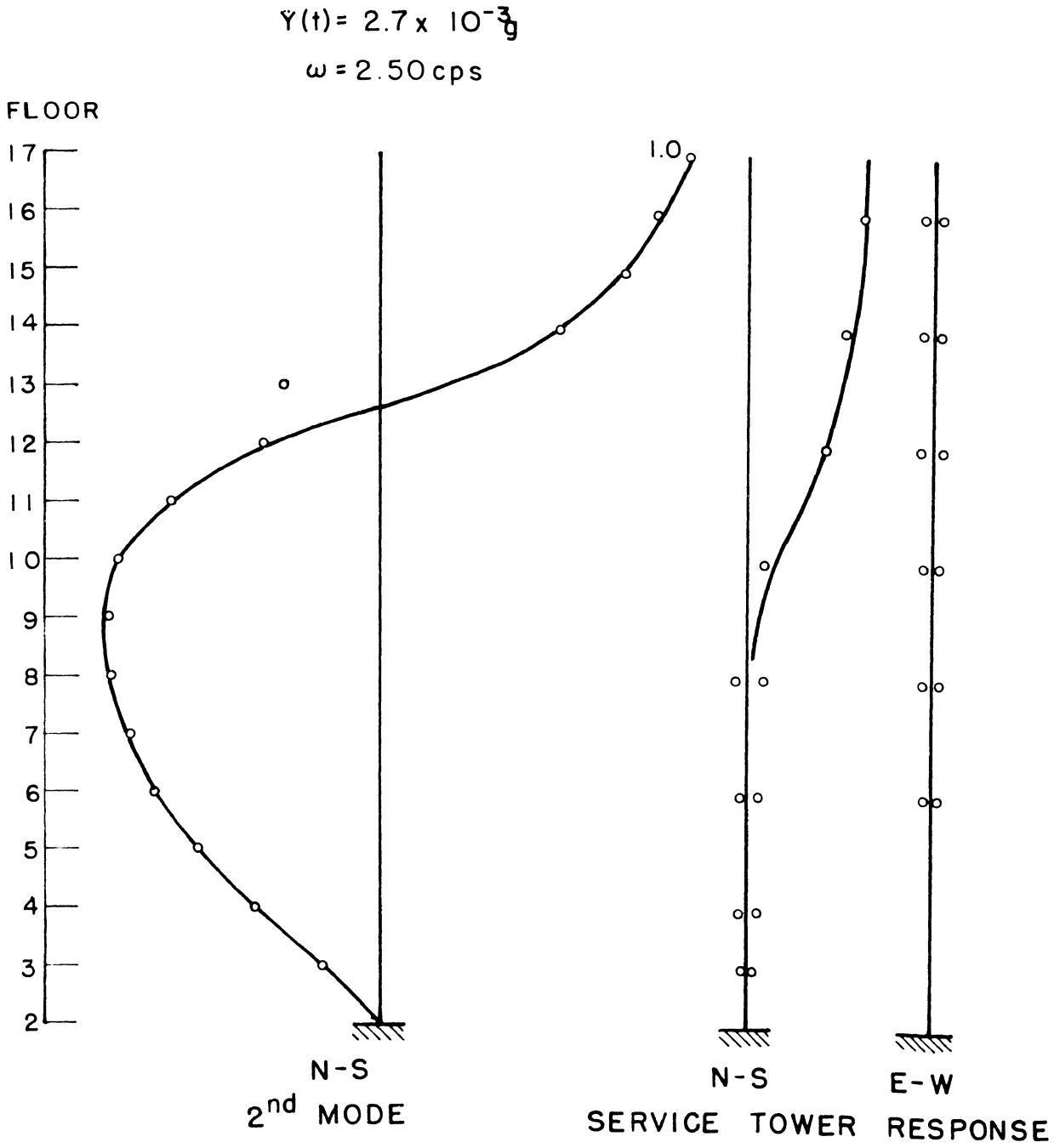

FIG. 3.63 – SECOND MODE SHAPE N–S, AND SIMULTANEOUS RESPONSE OF SERVICE TOWER, FALL 1965 I

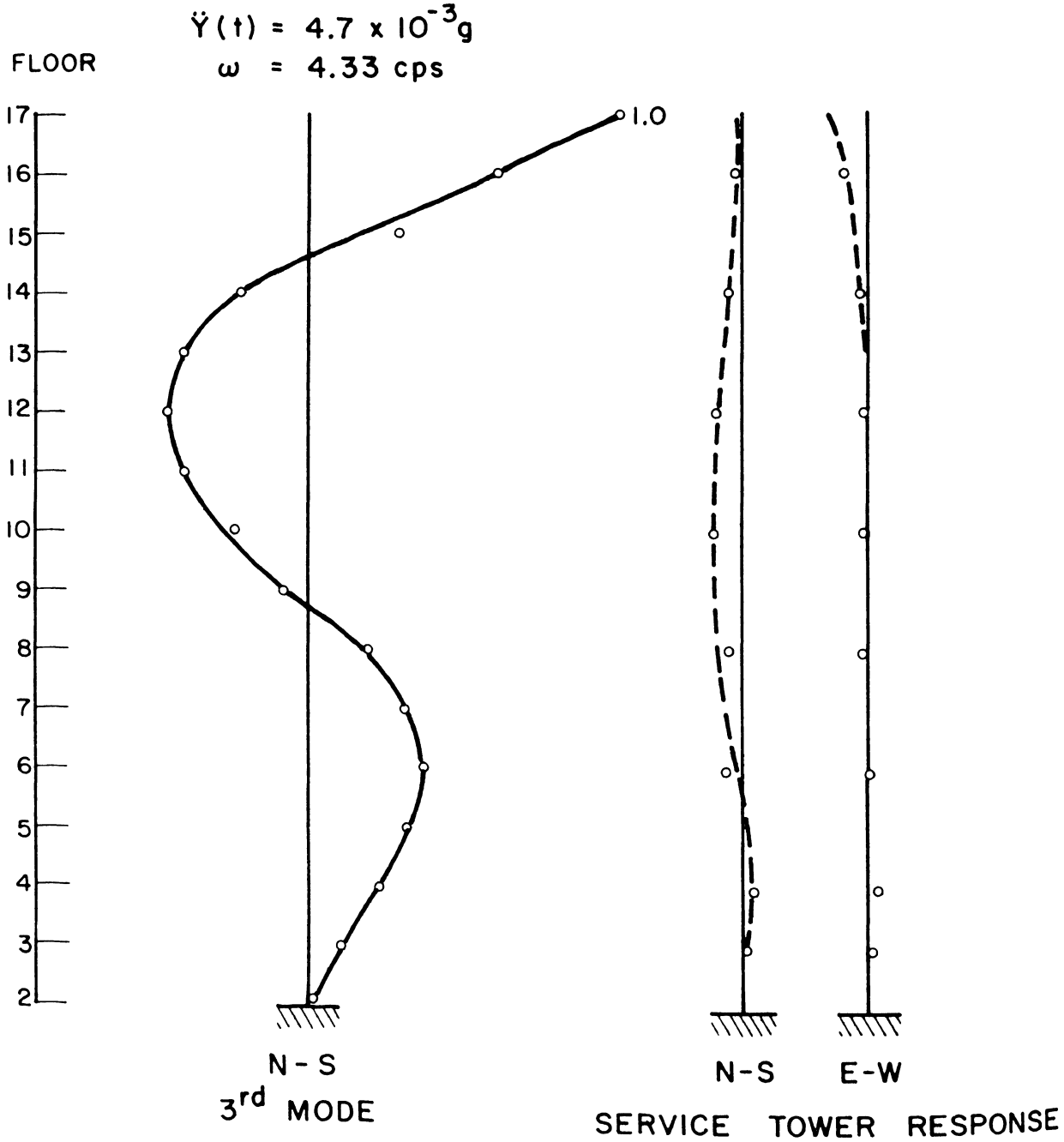

FIG. 3.64 – THIRD MODE SHAPE N–S, AND SIMULTANEOUS RESPONSE OF SERVICE TOWER, FALL 1965 I

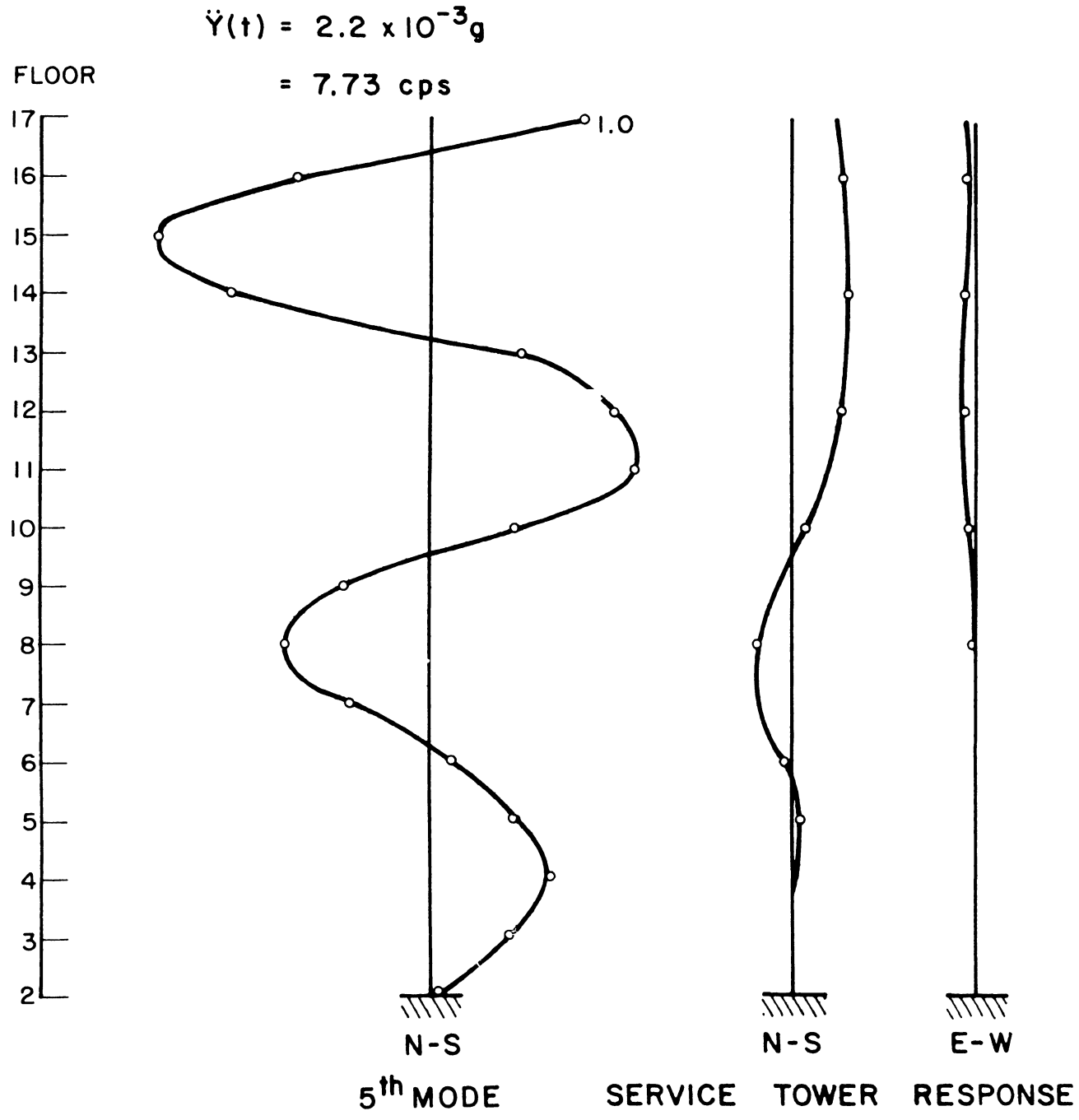

FIG. 3.65 – FIFTH MODE SHAPE N–S, AND SIMULTANEOUS RESPONSE OF SERVICE TOWER, FALL 1965 I

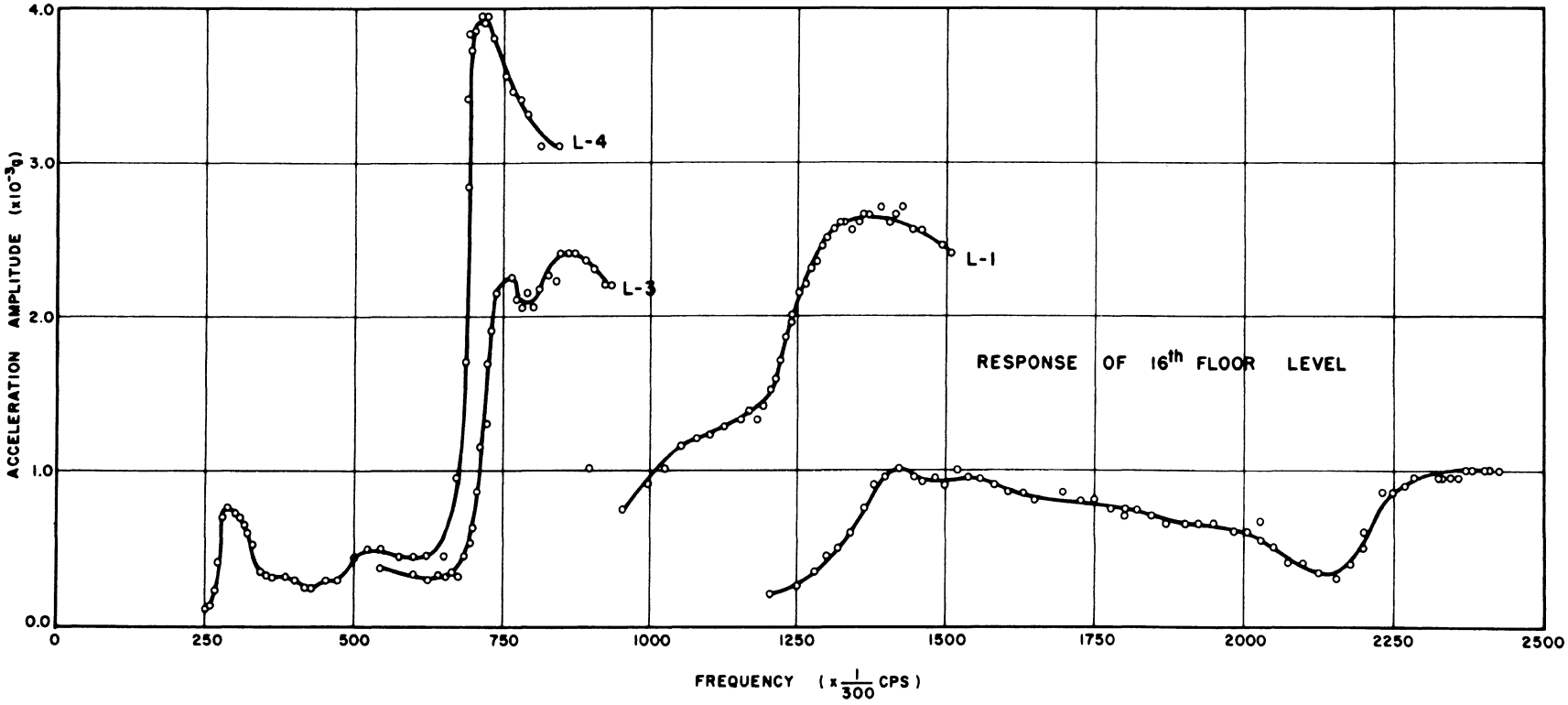

FIG. 3.66

ACCELERATION FREQUENCY RESPONSES WITH GREASE PLATE SANDWICHES IN PLACE, COL. B, E–W, FALL 1965 II

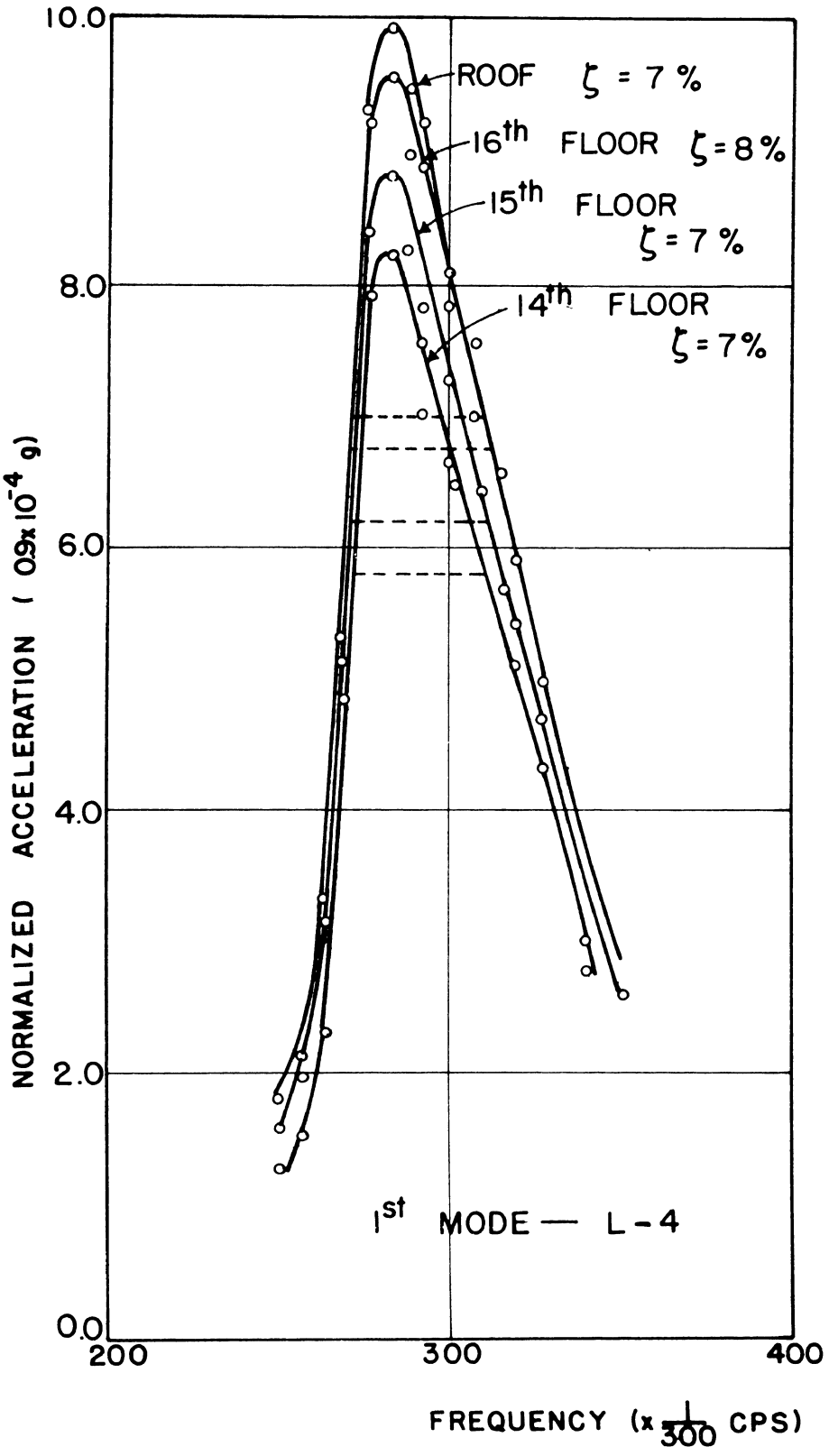

FIG. 3.67 – FREQUENCY RESPONSES WITH GREASE PLATE SANDWICHES IN PLACE, COLUMN B, E–W, FALL 1965 II

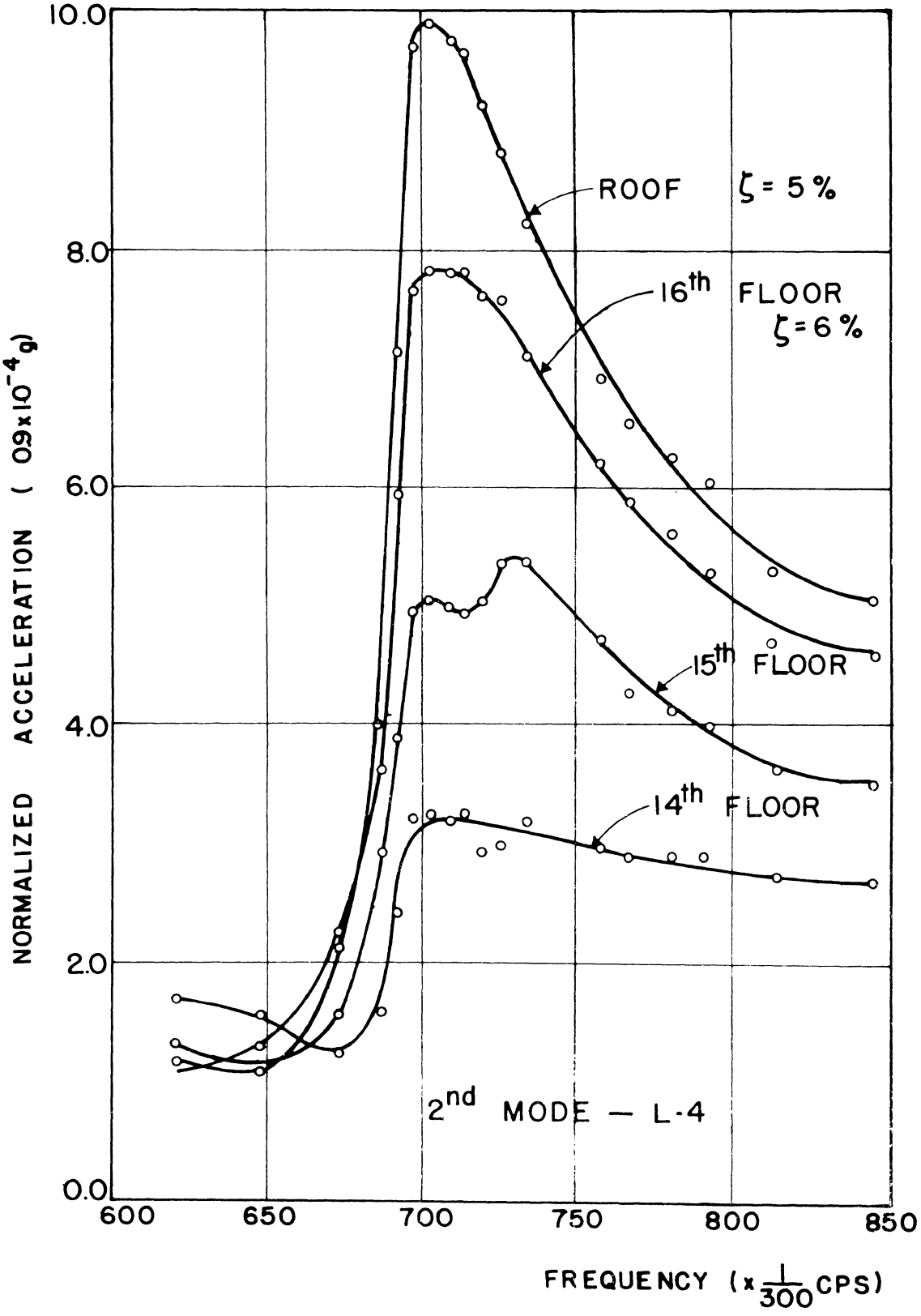

FIG. 3.68 – FREQUENCY RESPONSES WITH GREASE PLATE SANDWICHES IN PLACE, COLUMN B, E–W, FALL 1965 II

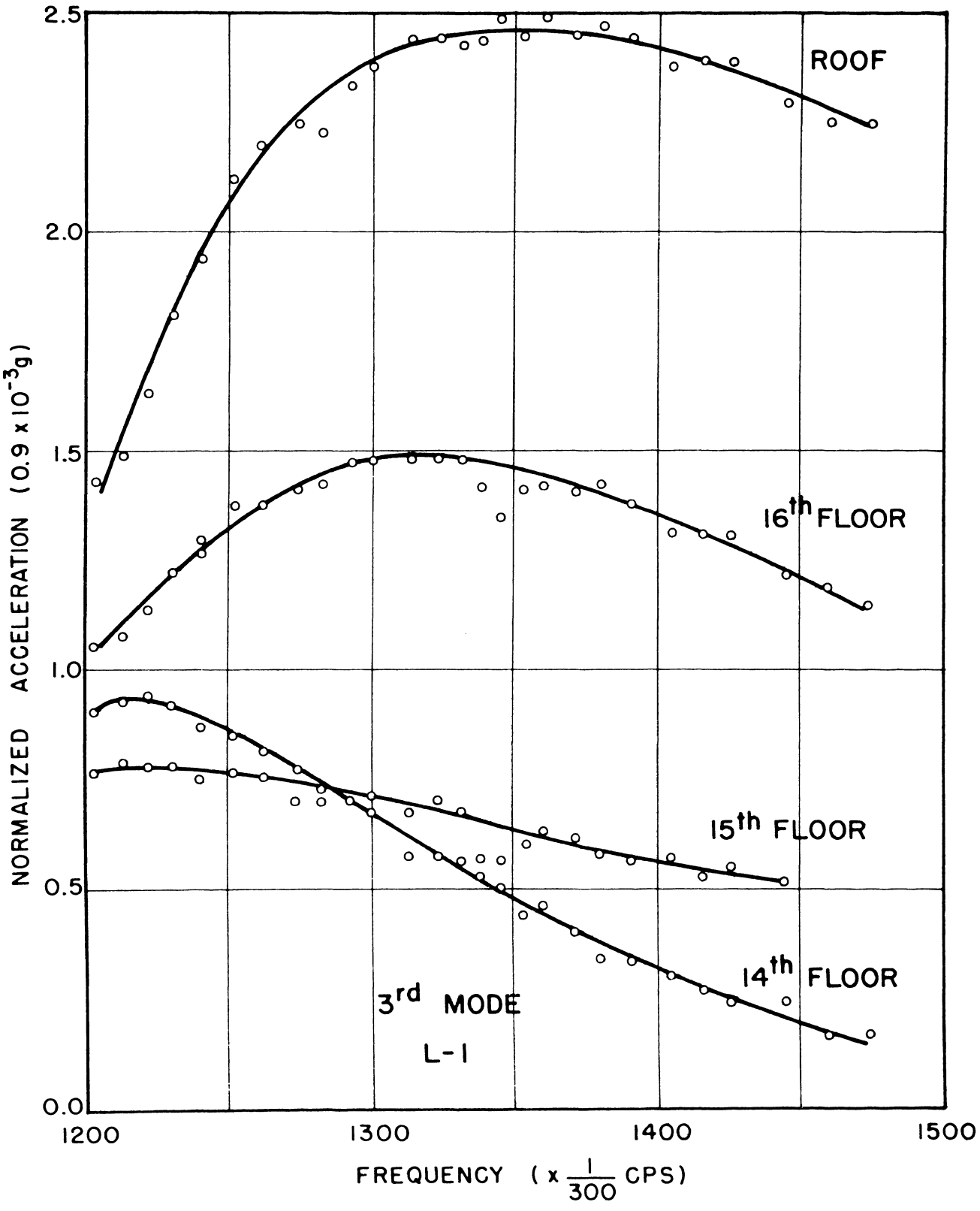

FIG. 3.69 – FREQUENCY RESPONSE WITH GREASE PLATE SANDWICHES IN PLACE, COL. B, E–W, FALL 1965 II

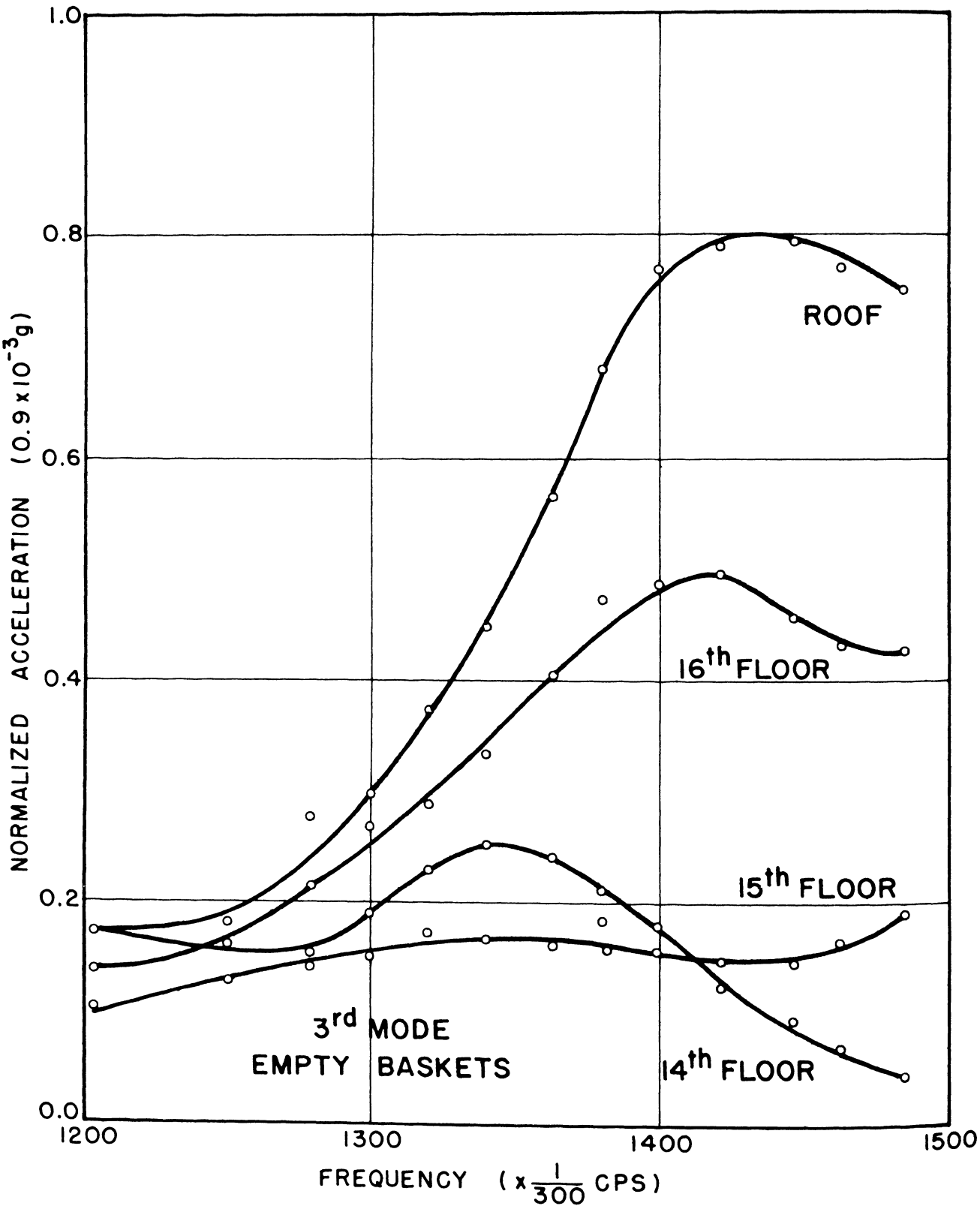

FIG. 3.70 – FREQUENCY RESPONSE WITH GREASE PLATE SANDWICHES IN PLACE, COL. B, E–W, FALL 1965 II

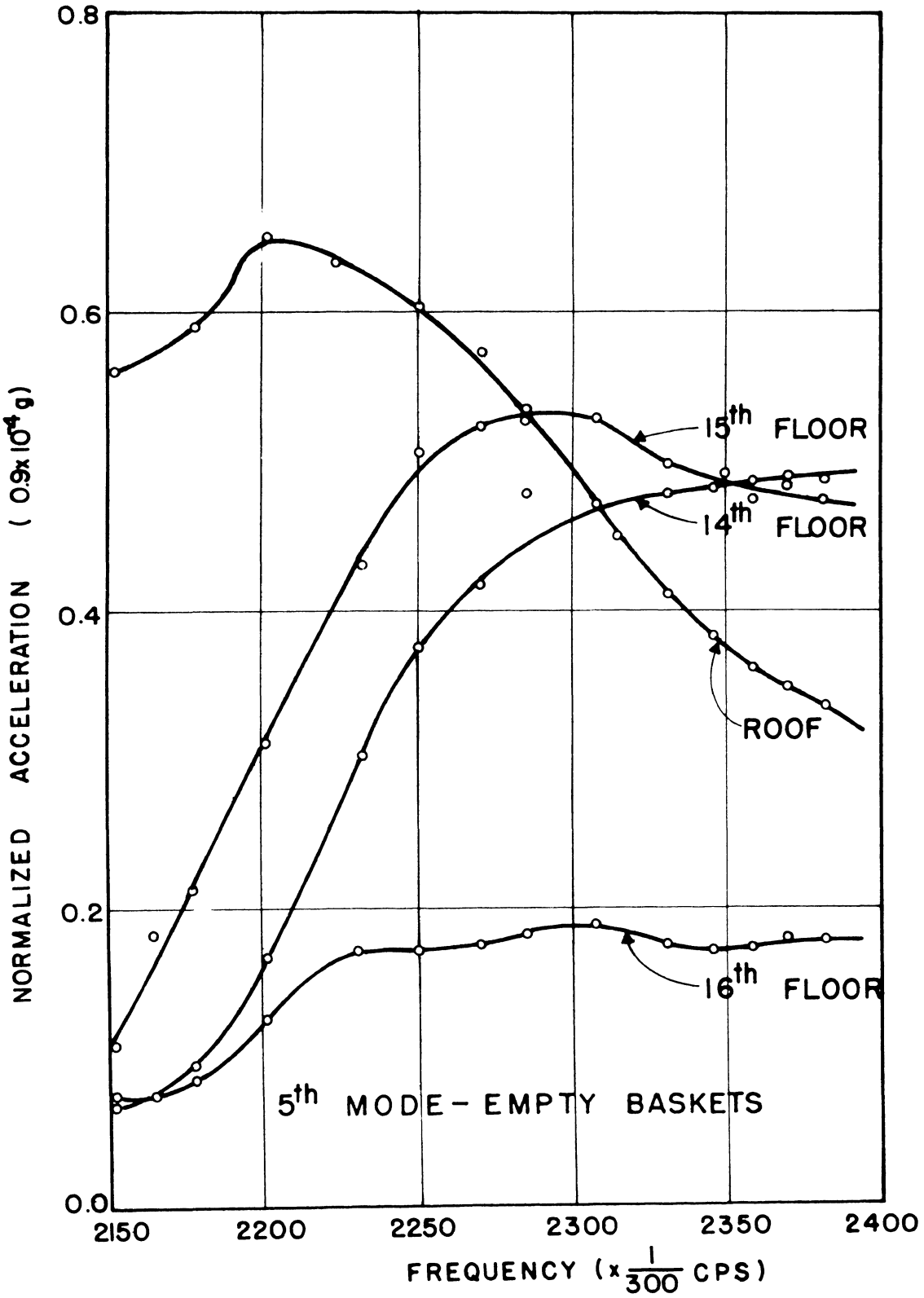

FIG. 3.71 – FREQUENCY RESPONSES WITH GREASE PLATE SANDWICHES IN PLACE, COL. B, E–W, FALL 1965 II

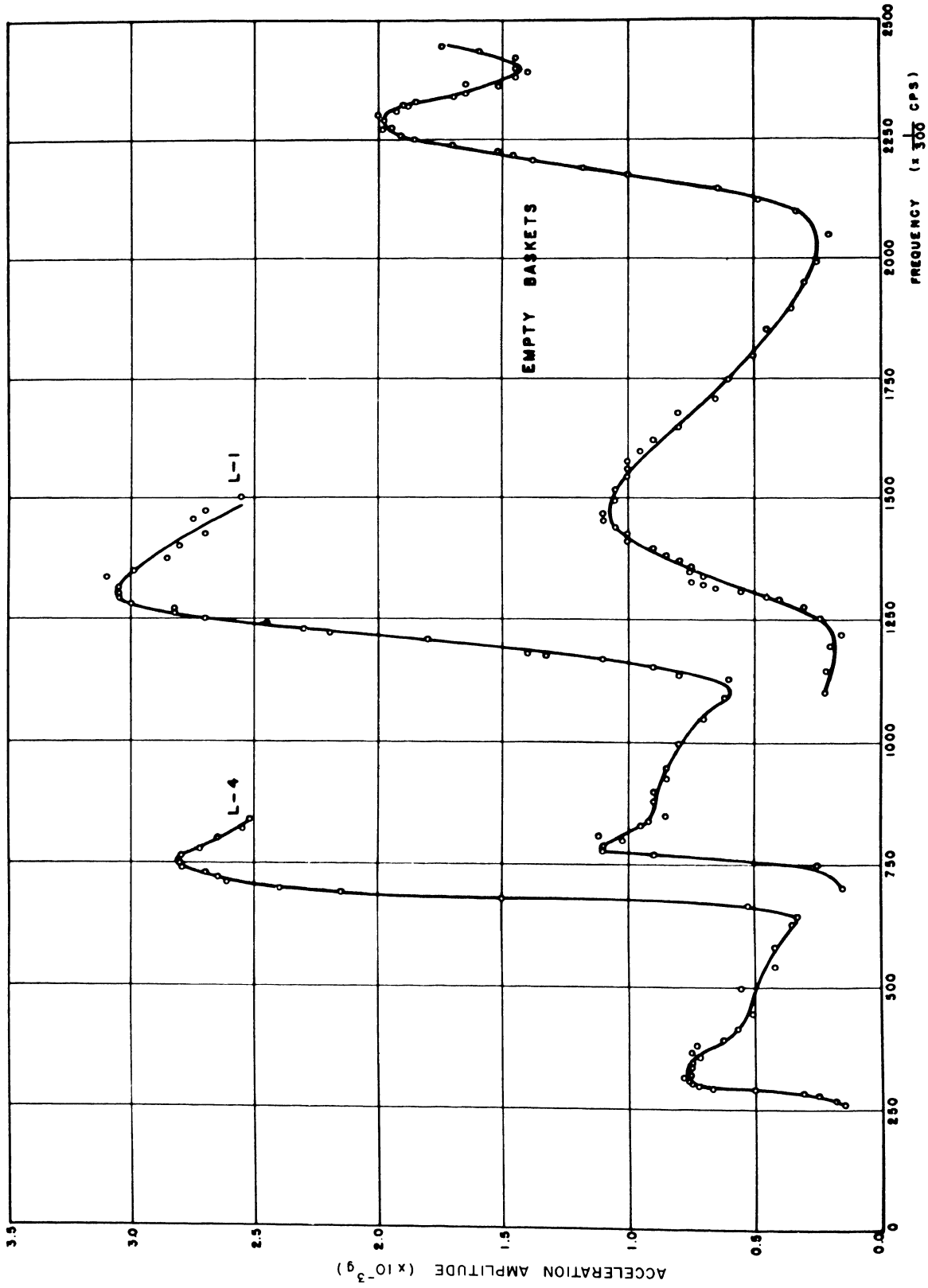

ACCELERATION FREQUENCY RESPONSES WITH GREASE PLATE SANDWICHES IN PLACE, N–S

FIG. 3.72

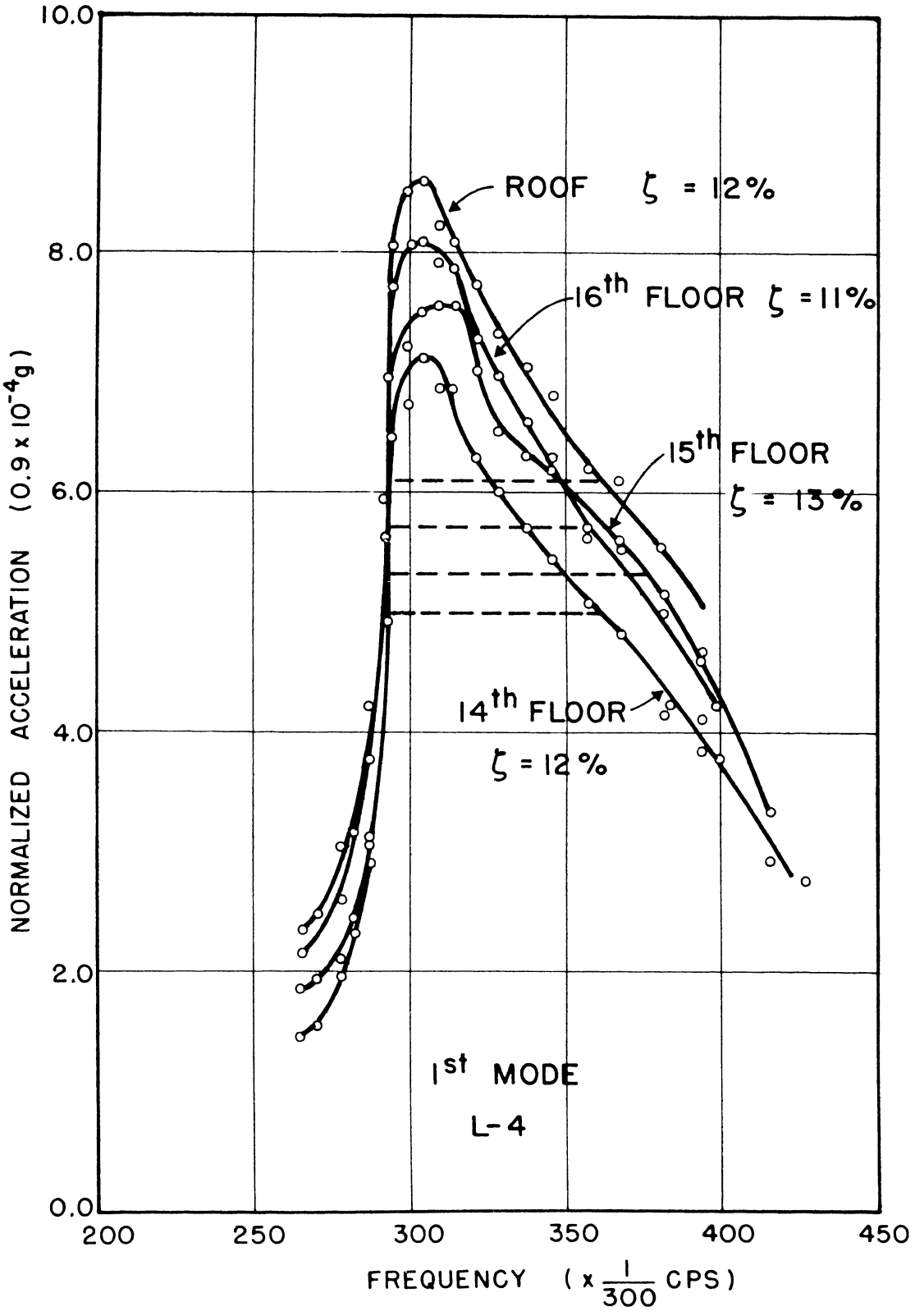

FIG. 3.73 – FREQUENCY RESPONSES WITH GREASE PLATE SANDWICHES IN PLACE, COL. E, N–S, FALL 1965 II

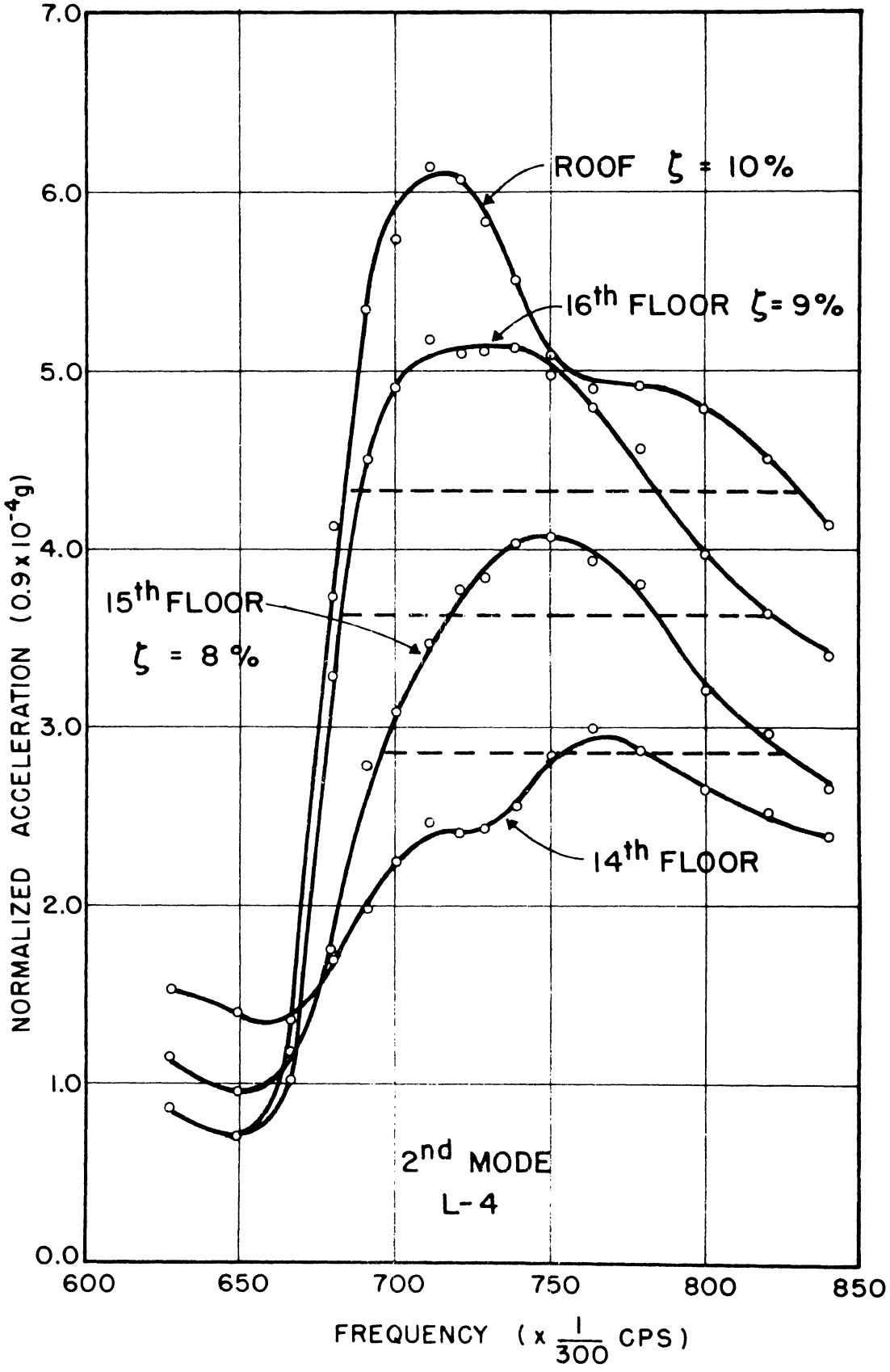

FIG. 3.74 – FREQUENCY RESPONSES WITH GREASE PLATE SANDWICHES IN PLACE
COL. E, N–S, FALL 1965 II

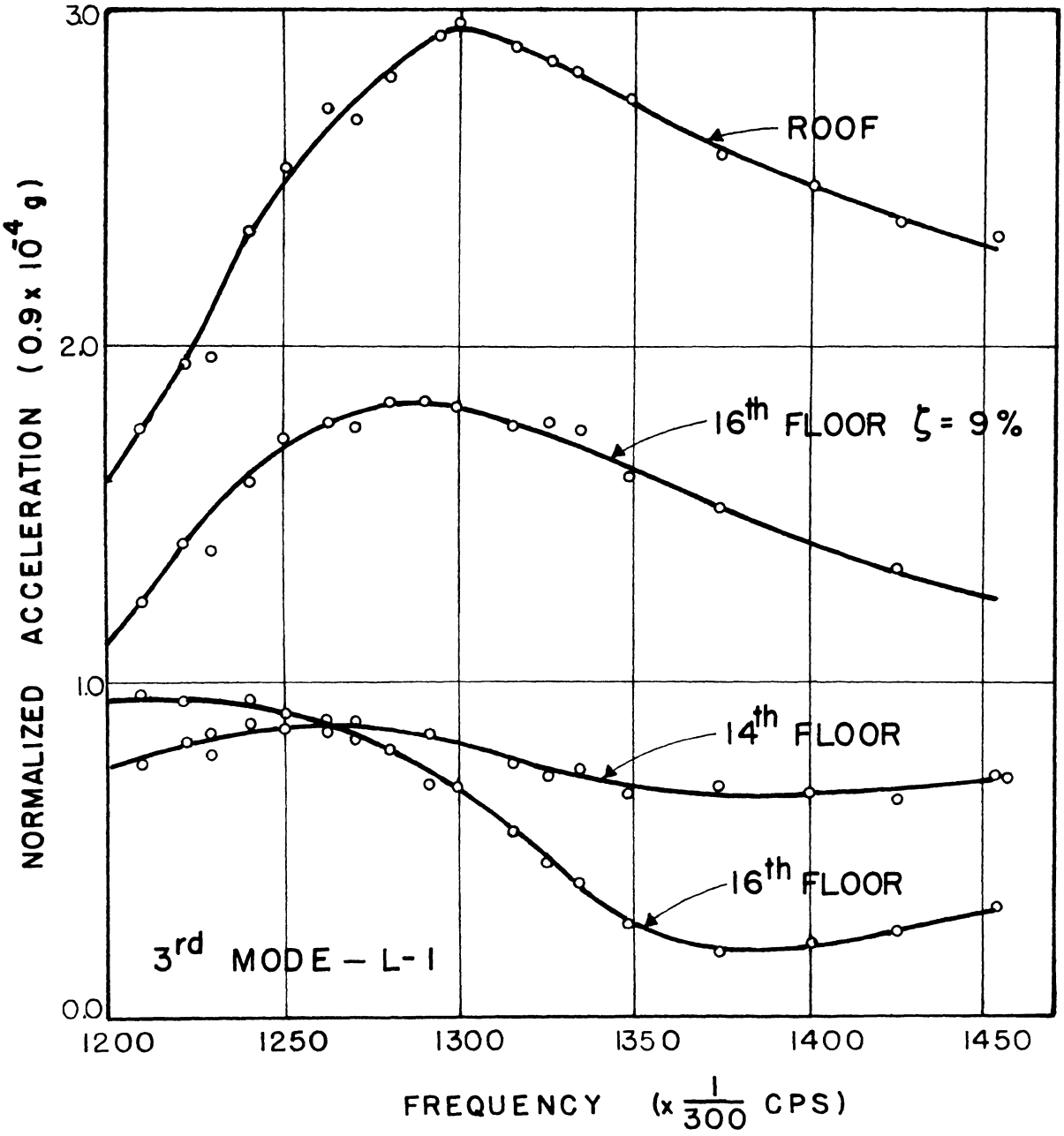

FIG. 3.75 – FREQUENCY RESPONSE WITH GREASE PLATE SANDWICHES IN PLACE, COL. E, N–S, FALL 1965 II

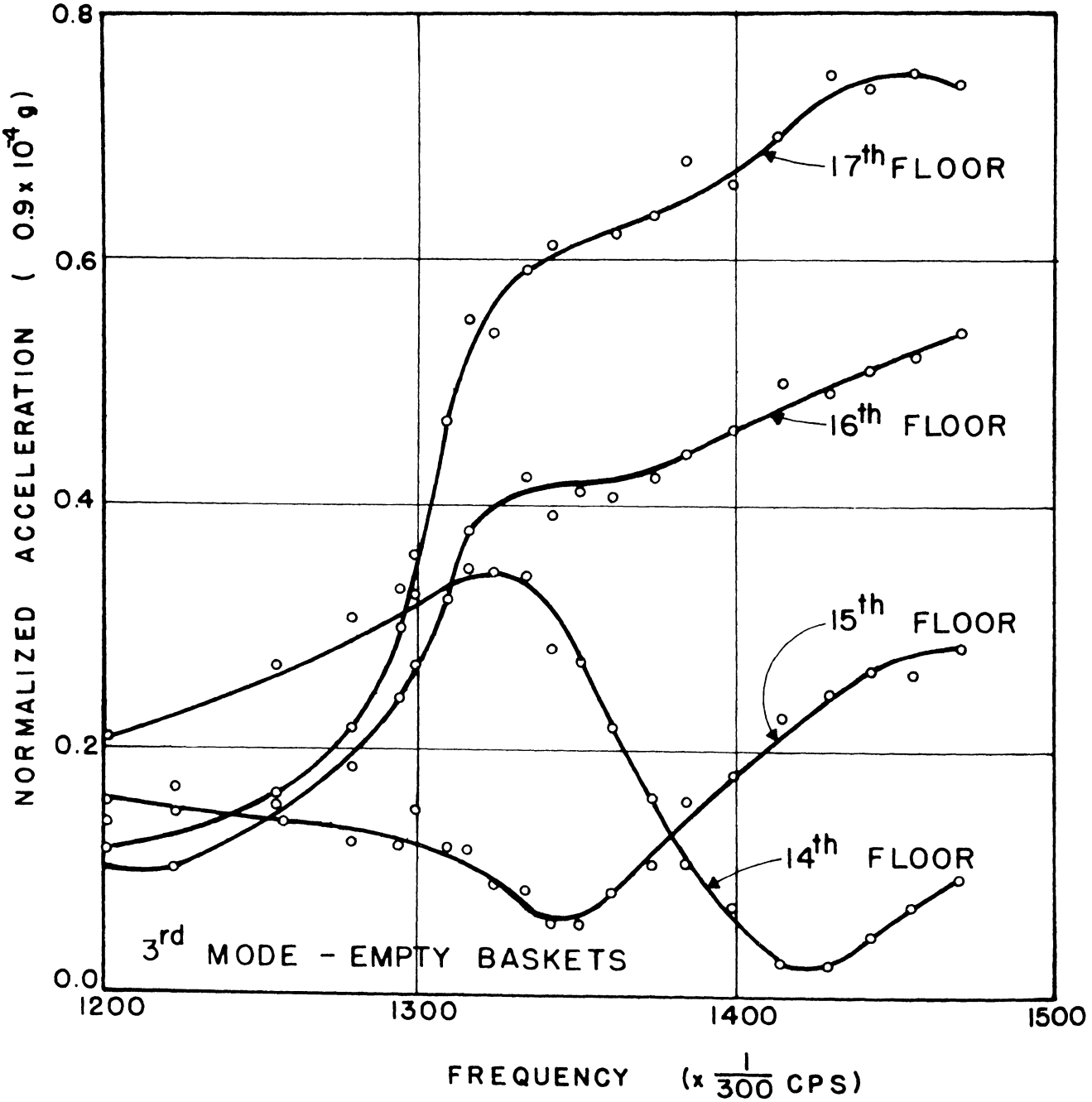

FIG. 3.76 – FREQUENCY RESPONSE WITH GREASE PLATE SANDWICHES IN PLACE, COL. E, N–S, FALL 1965 II

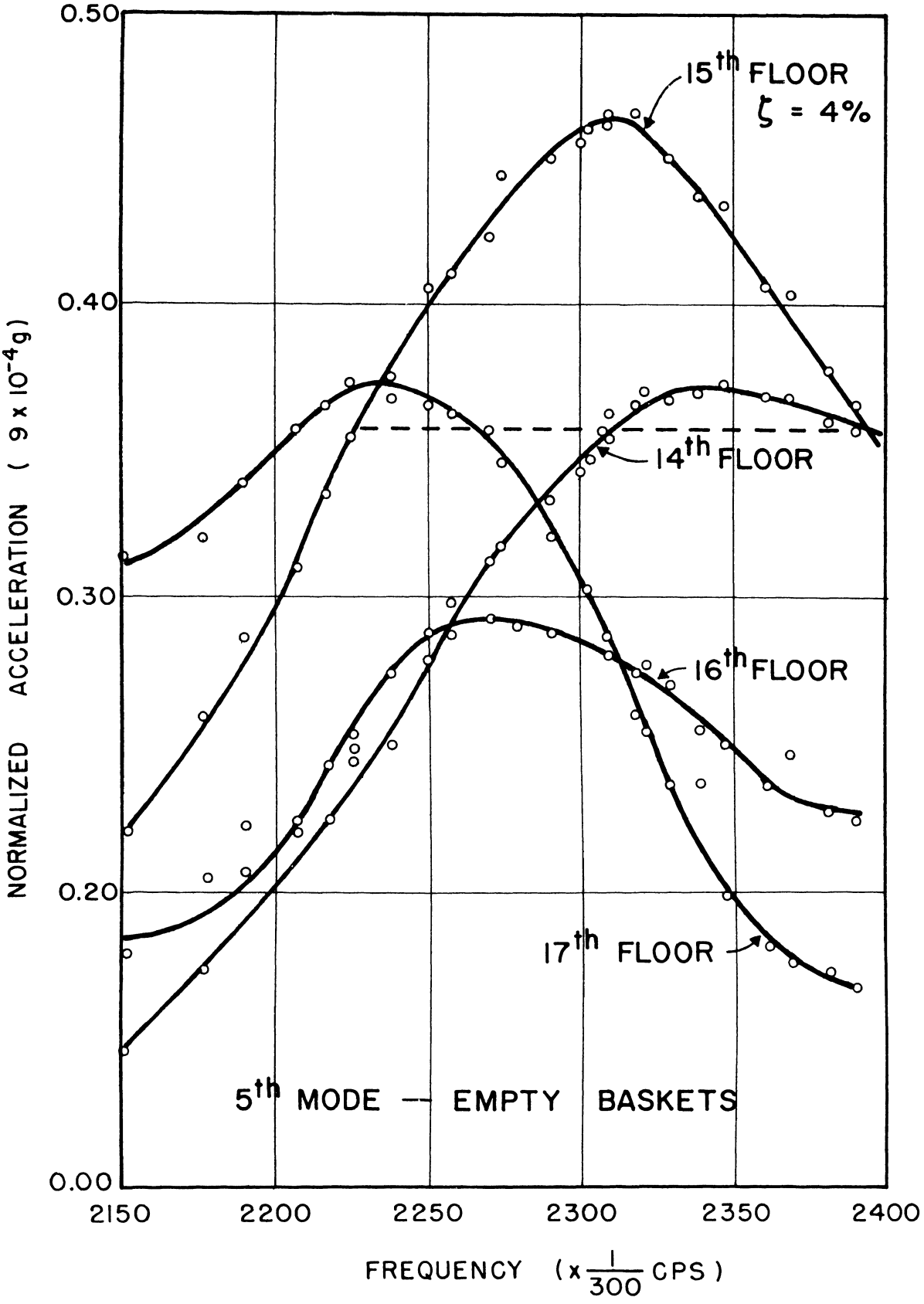

FIG. 3.77 – FREQUENCY RESPONSES WITH GREASE PLATE SANDWICHES IN PLACE, COL. E, N–S, FALL 1965 II

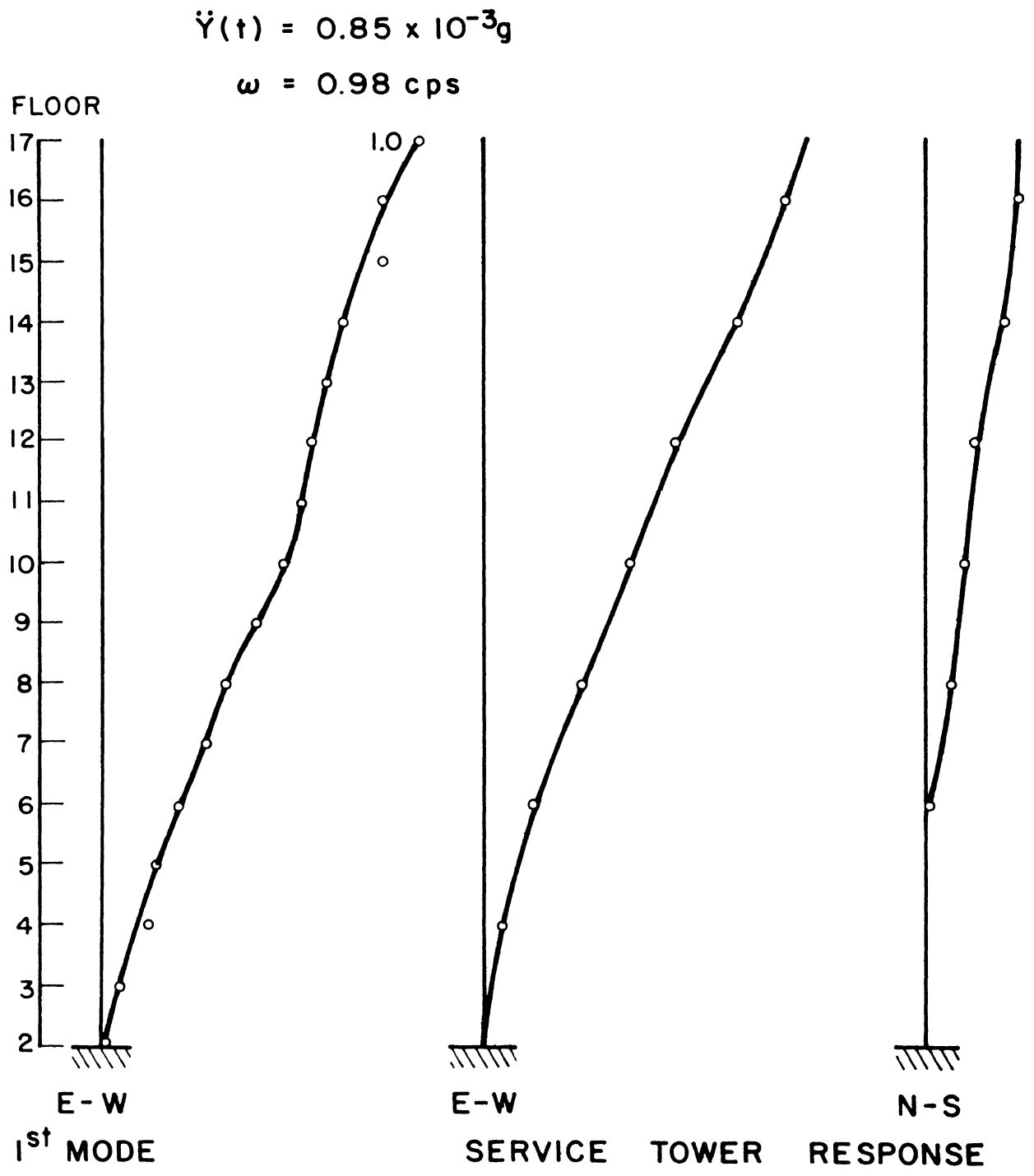

FIG. 3.78 – FIRST MODE SHAPE E–W, AFTER INSERTION OF GREASE PLATE SANDWICHES, FALL 1965 II

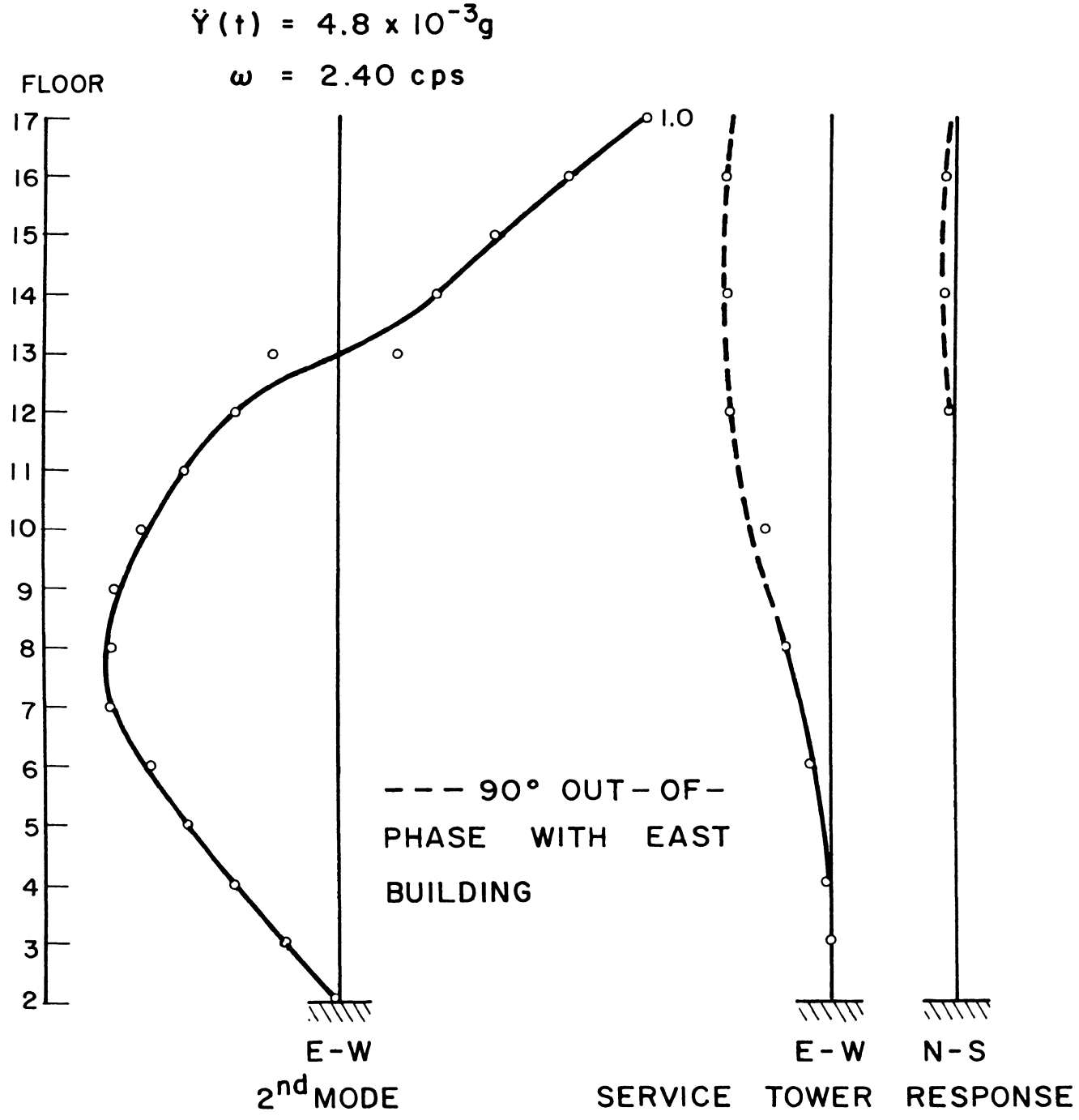

FIG. 3.79 – SECOND MODE SHAPE E–W, AFTER INSERTION OF GREASE PLATE SANDWICHES, FALL 1965 II

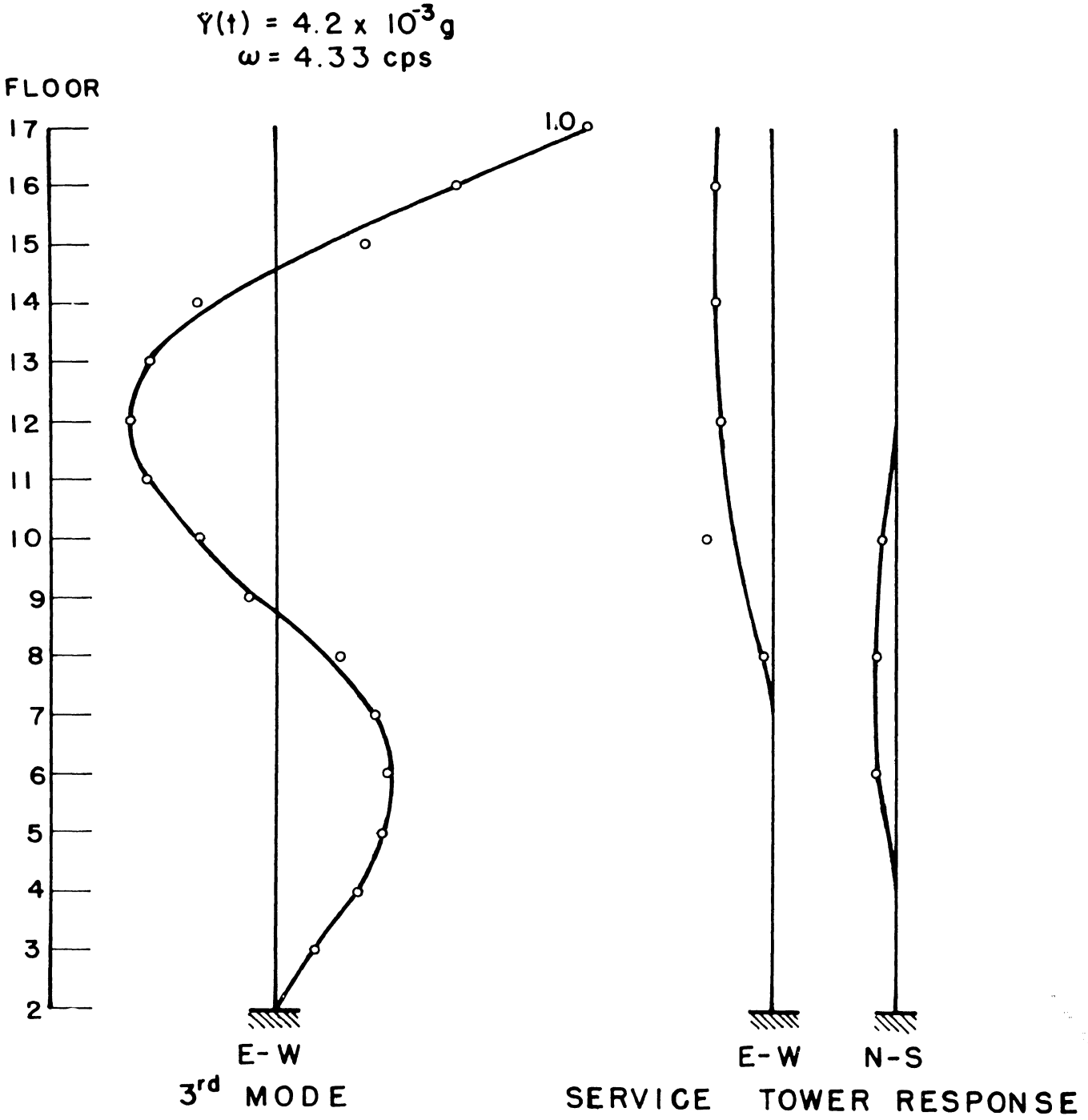

FIG. 3.80 – THIRD MODE SHAPE E–W, AFTER INSERTION OF GREASE PLATE SANDWICHES, FALL 1965 II

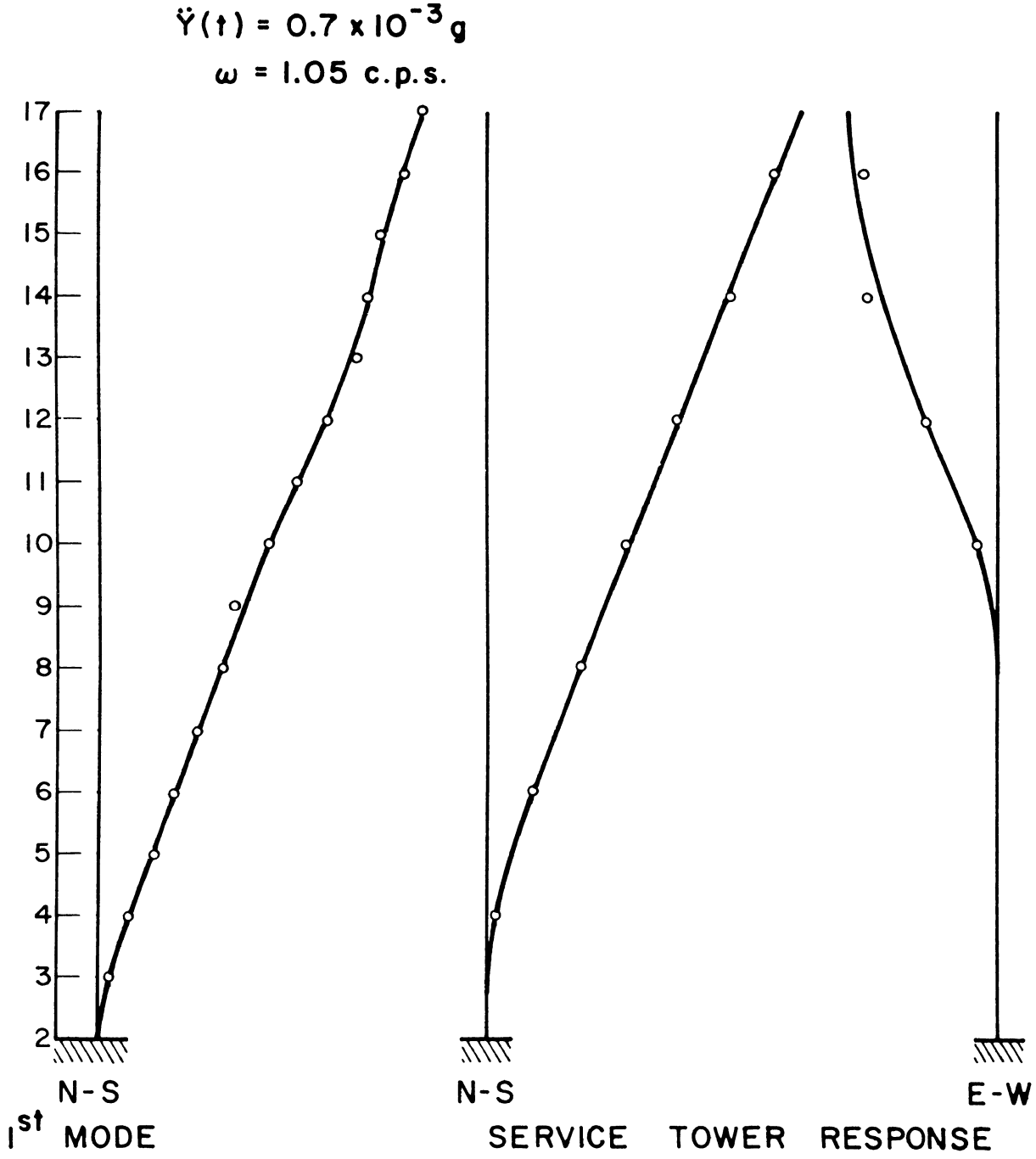

FIG. 3.81 – FIRST MODE SHAPE N–S, AFTER INSERTION OF GREASE PLATE SANDWICHES, FALL 1965 II

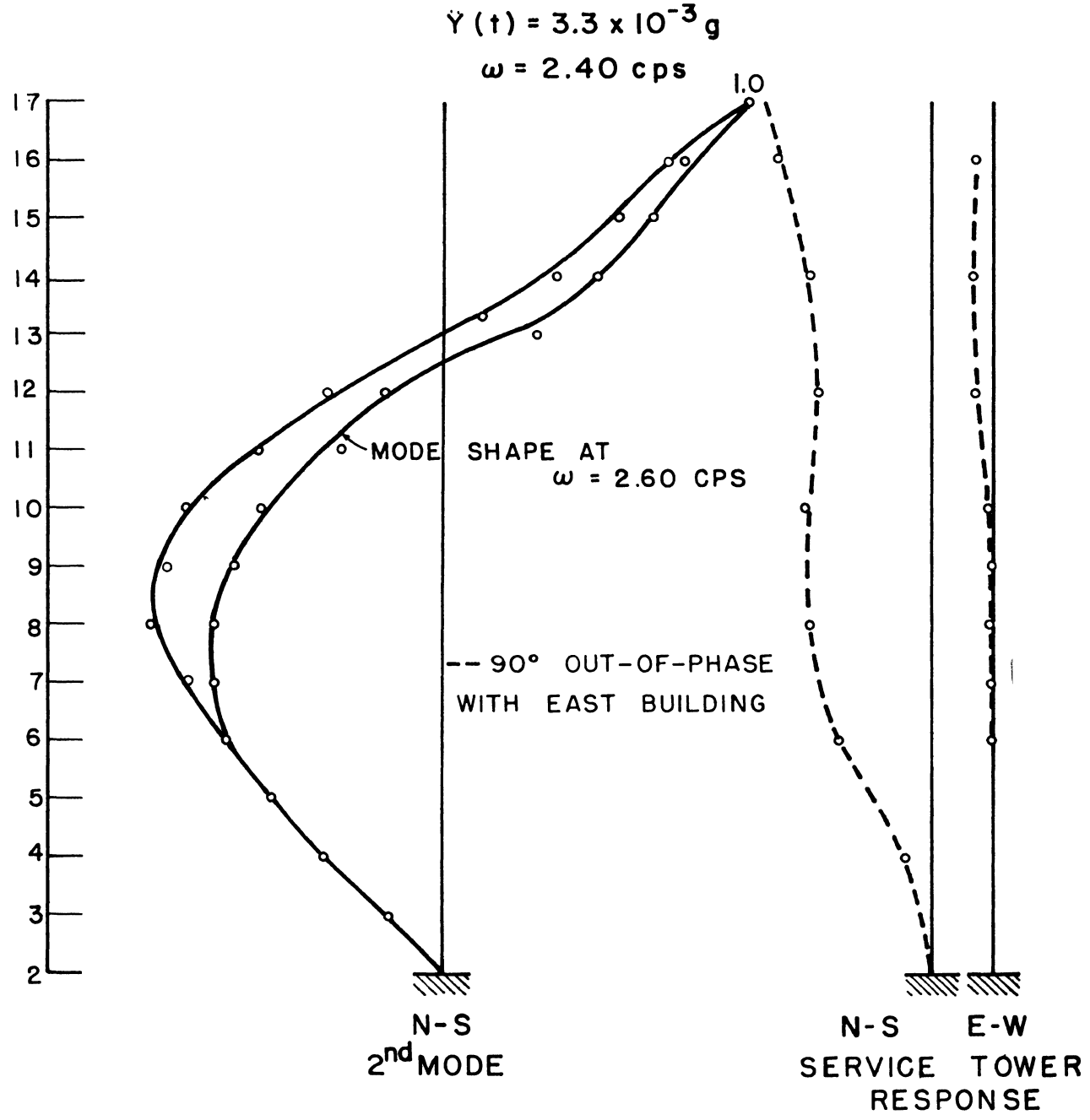

FIG. 3.82 – SECOND MODE SHAPE N–S, AFTER INSERTION OF GREASE PLATE SANDWICHES, FALL 1965 II

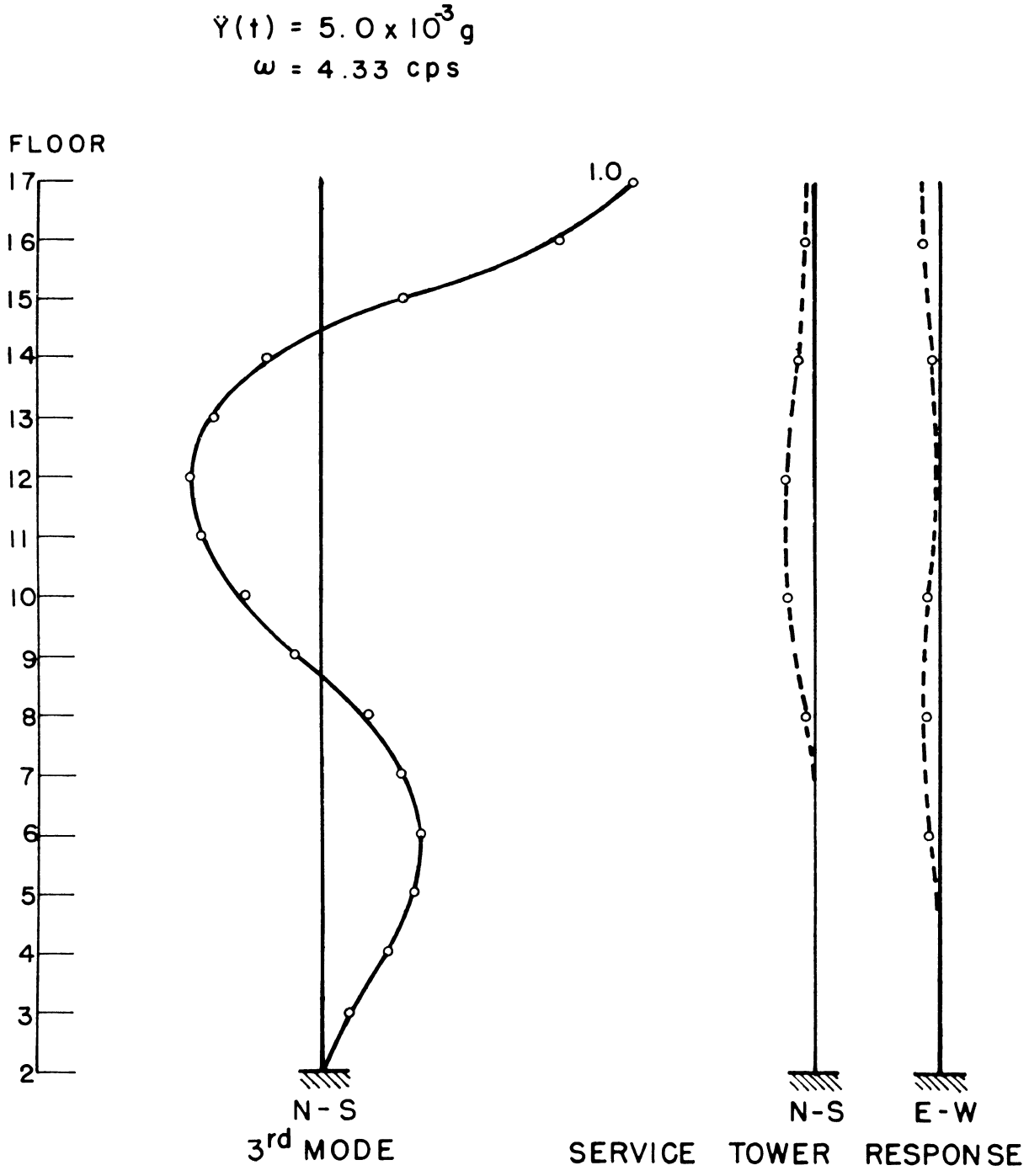

FIG. 3.83 – THIRD MODE SHAPE N–S, AFTER INSERTION OF GREASE PLATE SANDWICHES, FALL 1965 II

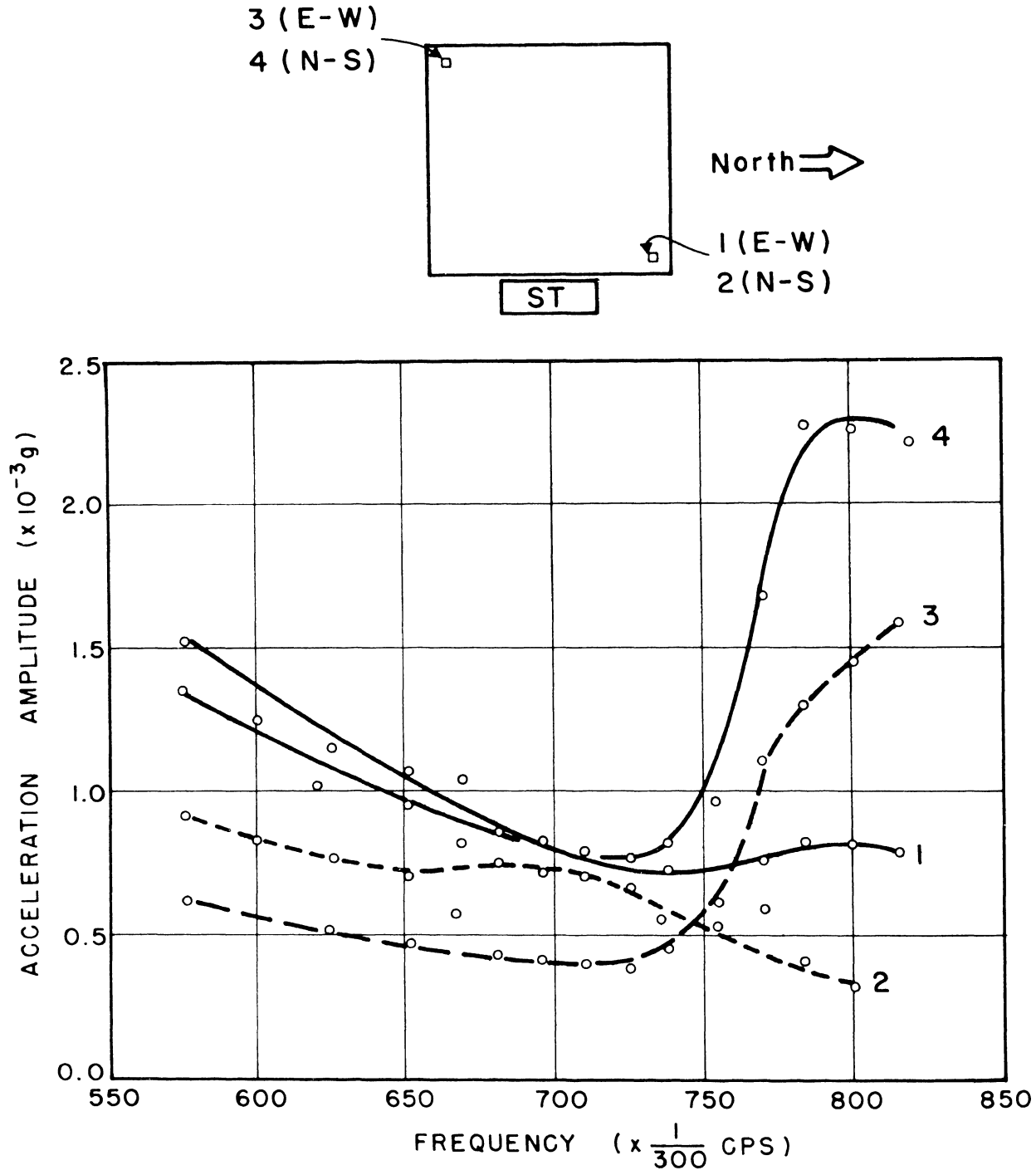

FIG. 3.84 – TORSIONAL RESPONSE: 1st MODE; FALL 1965 II

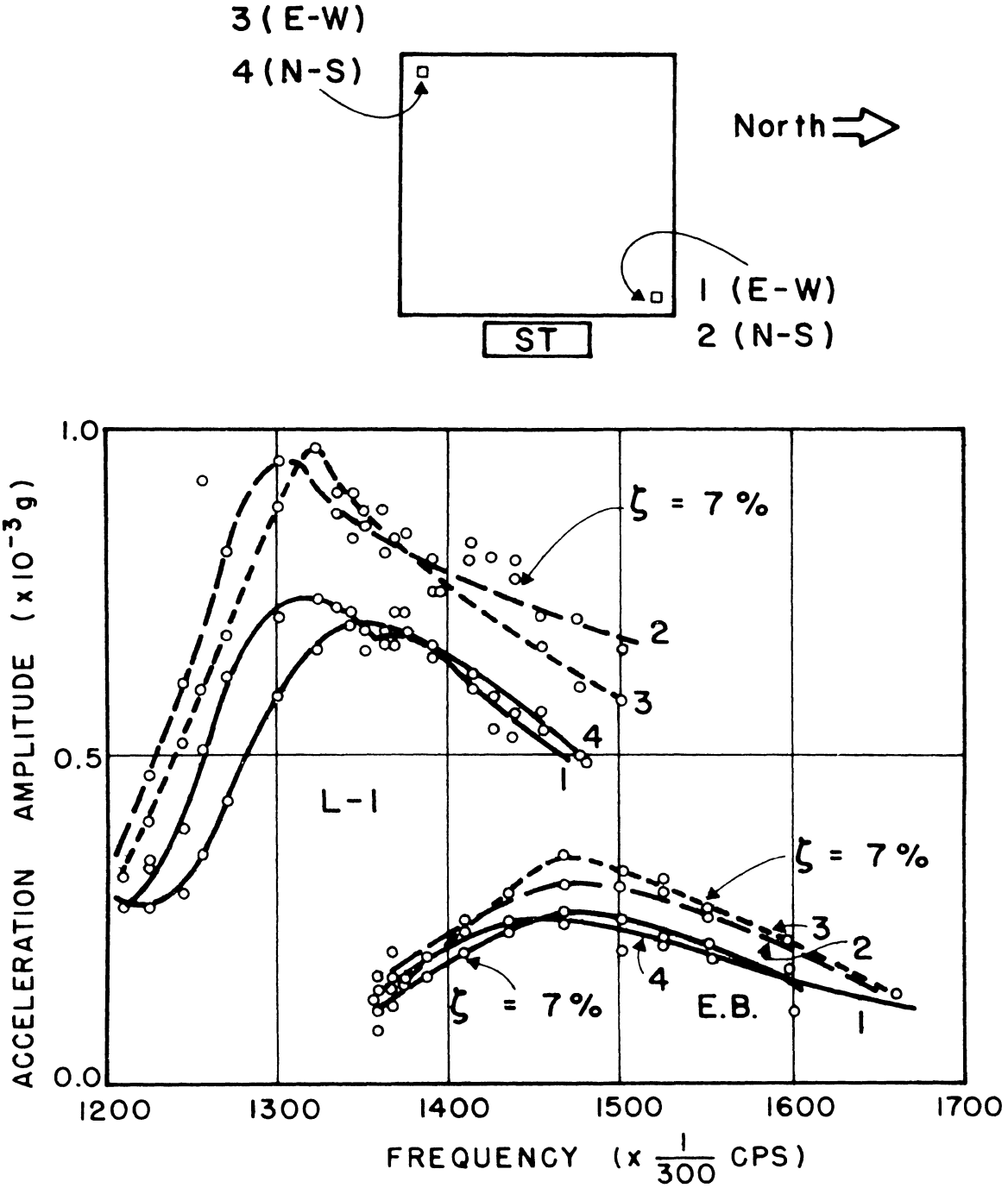

FIG. 3.85 – TORSIONAL RESPONSE, FALL 1965 II

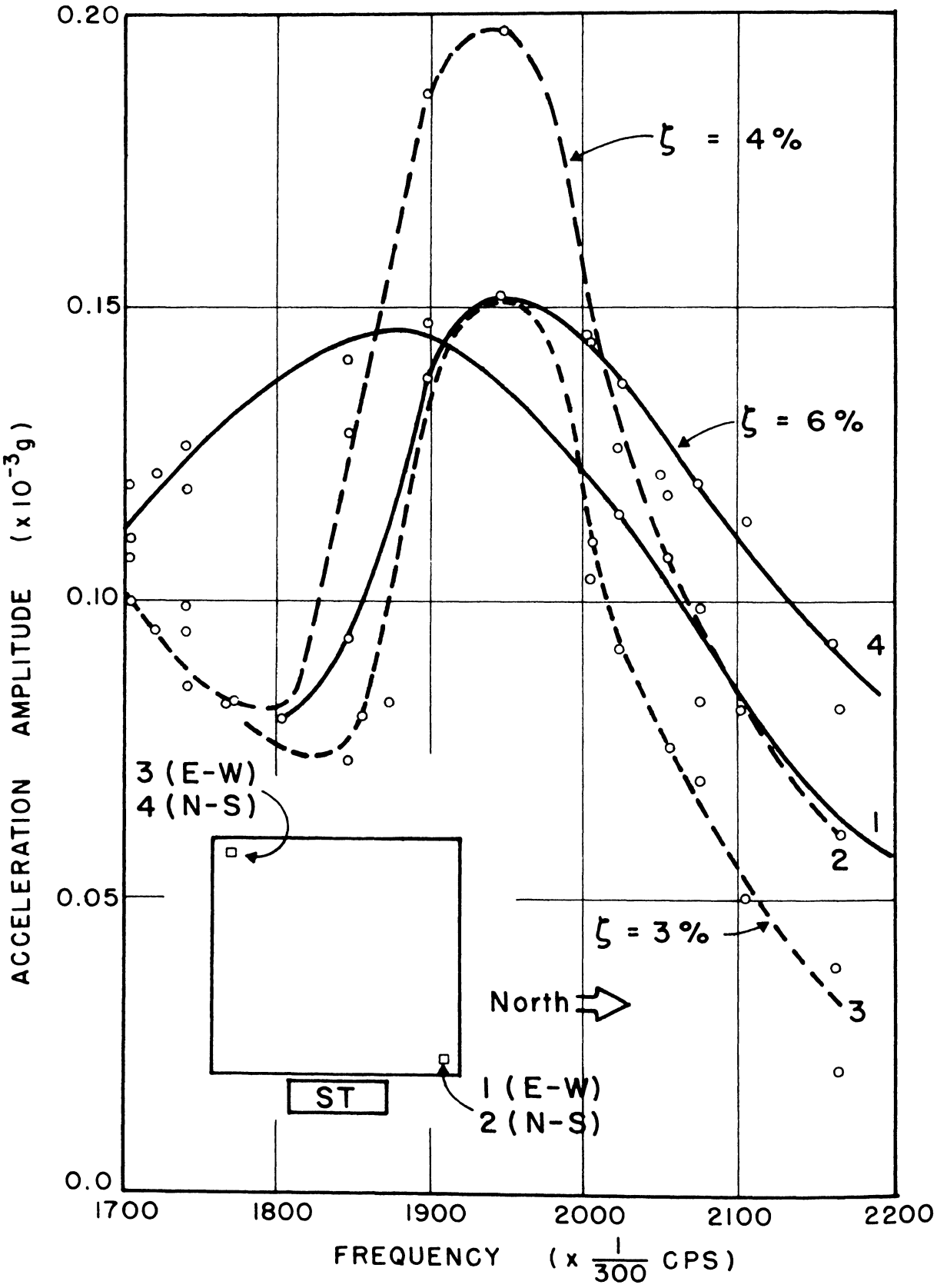

FIG. 3.86 – TORSIONAL RESPONSE, FALL 1965 II

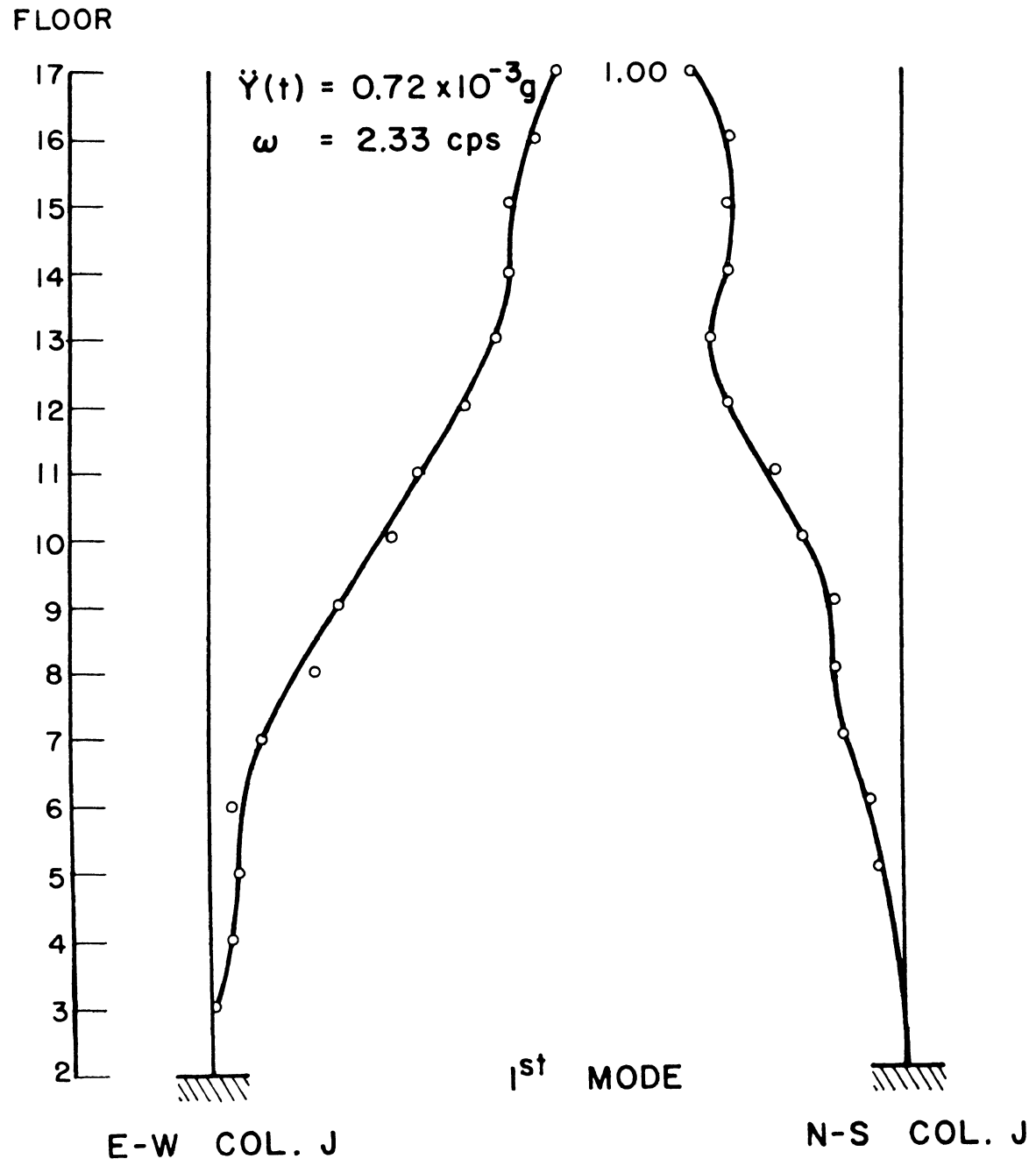

FIG. 3.87 – FIRST TORSIONAL MODE SHAPE, FALL 1965 I

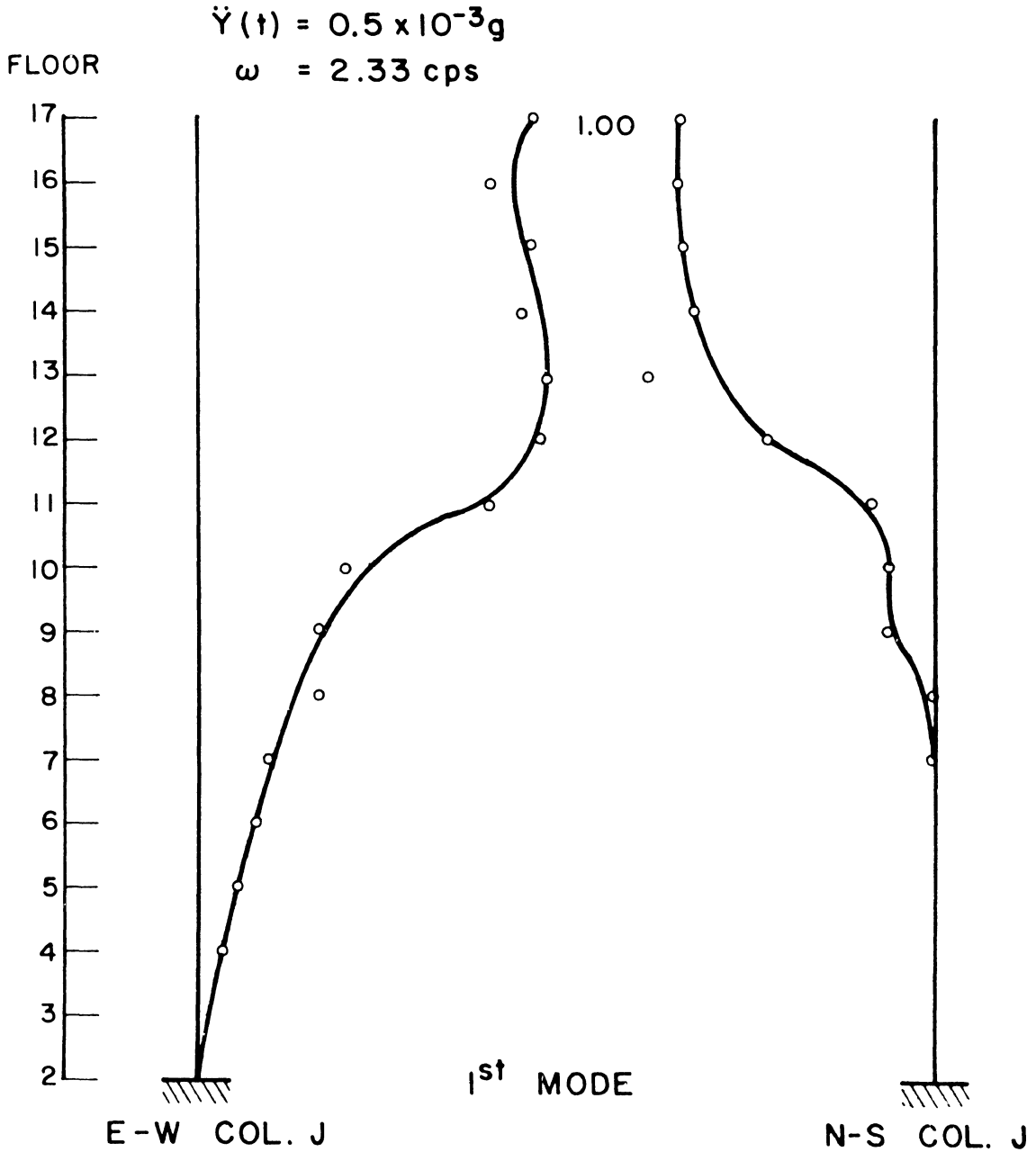

FIG. 3.88 – FIRST TORSIONAL MODE SHAPE, FALL 1965 II

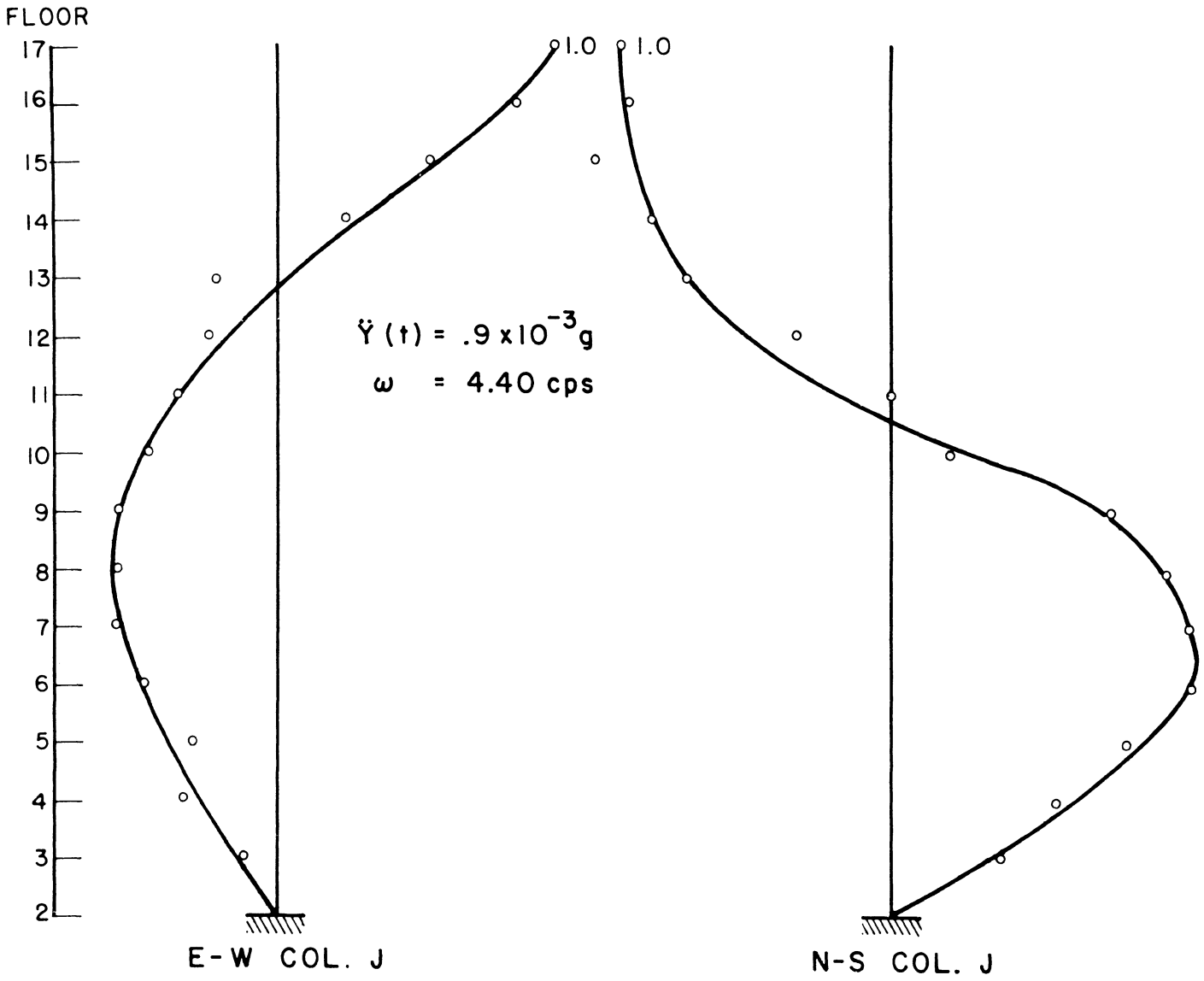

FIG. 3.89

SECOND TORSIONAL MODE SHAPE AFTER INSERTION OF GREASE PLATE SANDWICHES

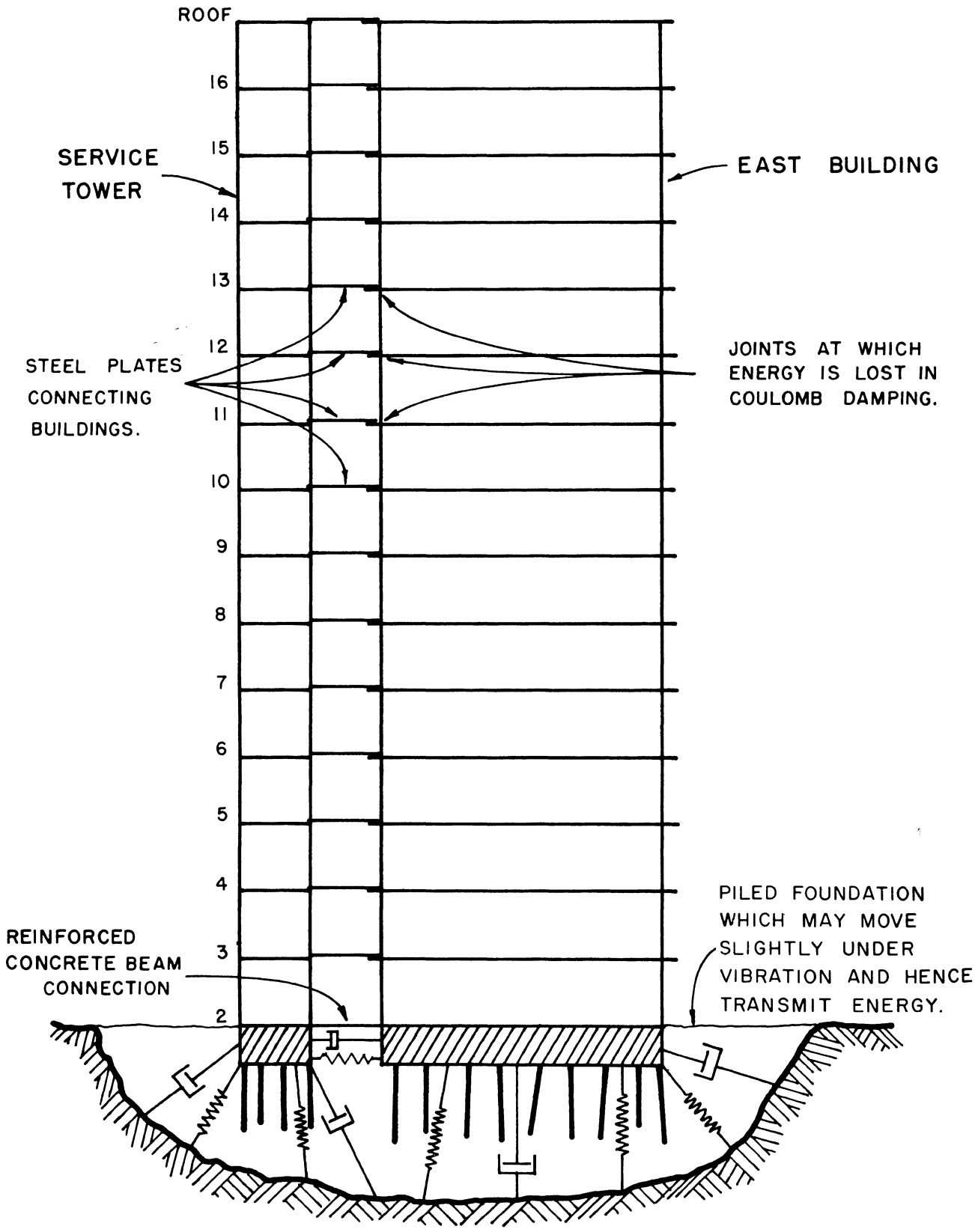

FIG. 3.90 – DIAGRAMMATIC MODEL OF STRUCTURAL SYSTEM AFTER SUMMER 1964

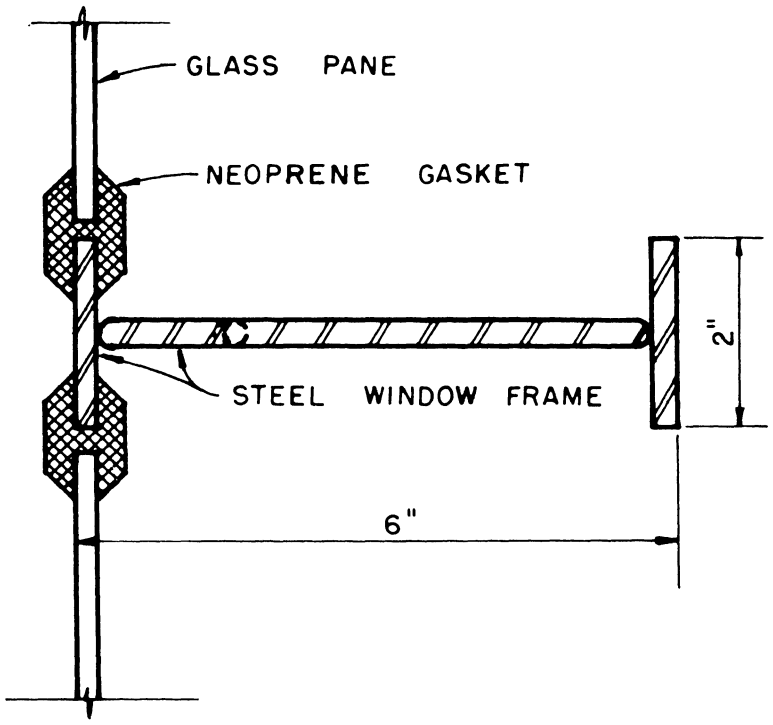

FIG. 3.91 – NEOPRENE GASKETS

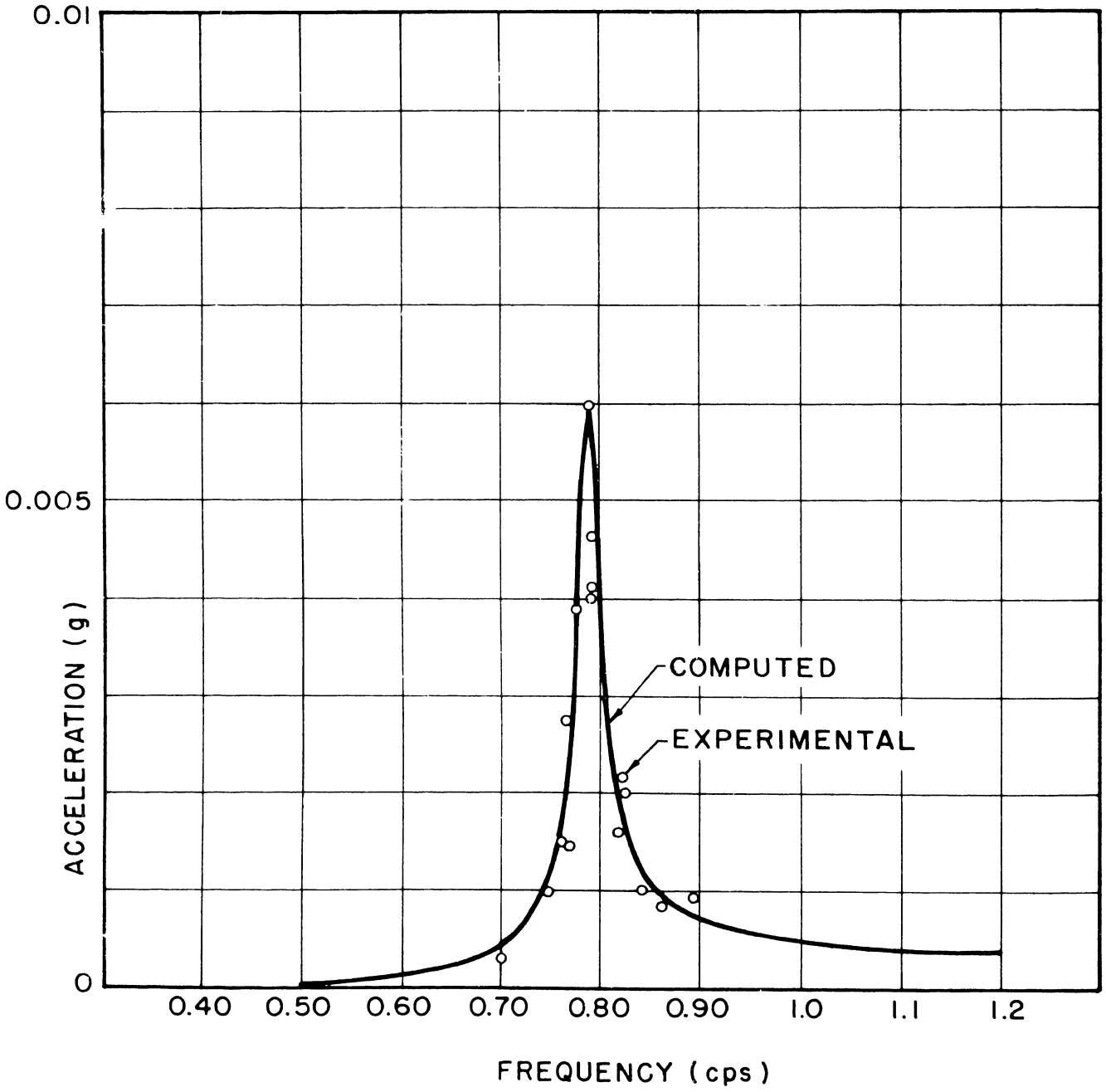

$f_{exp.}$ = 0.85 cps

$f_{com.}$ = 0.786 cps

FIG. 4.1 – FIRST MODE FREQUENCY RESPONSE, E–W DIRECTION

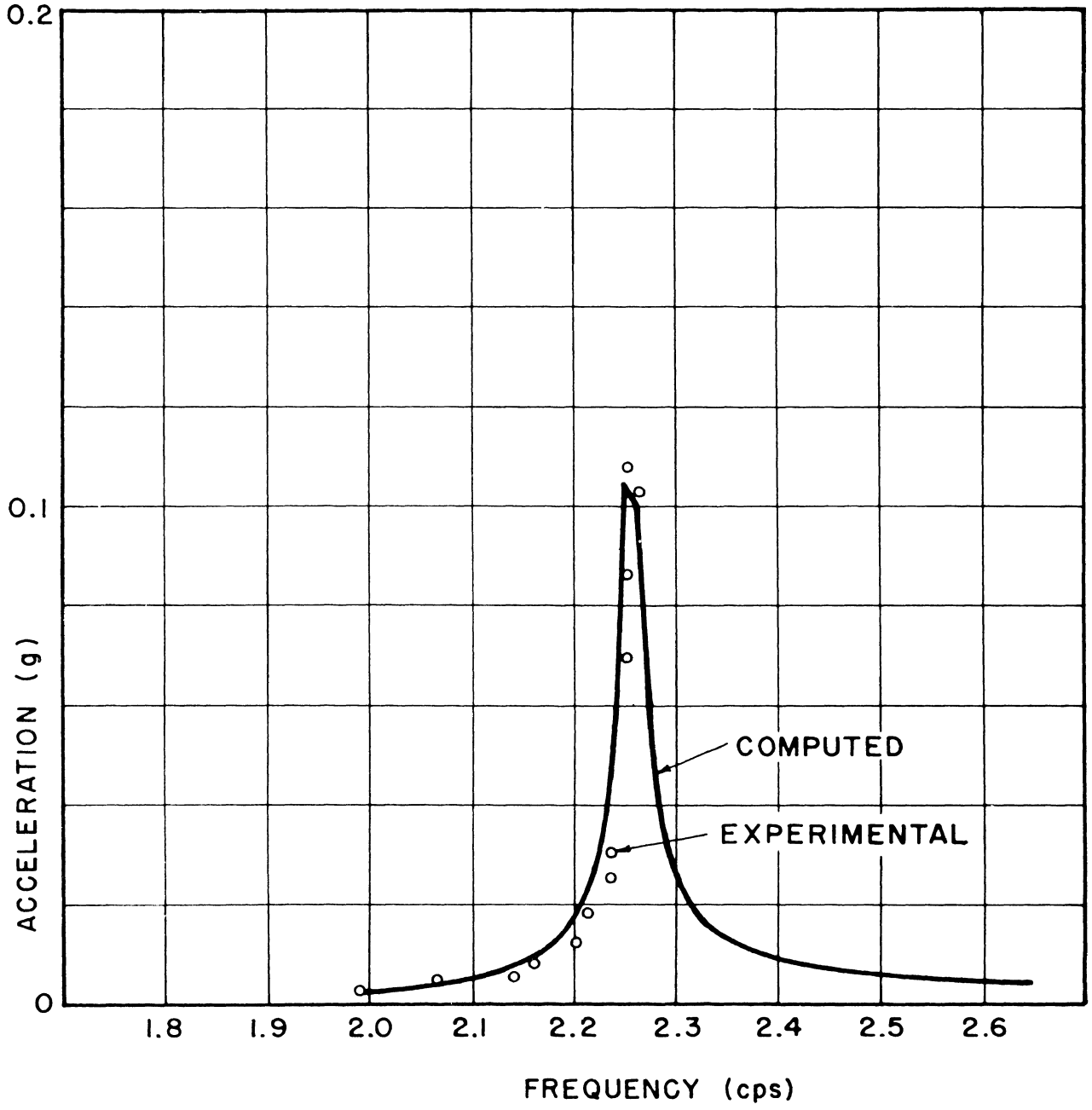

FIG. 4.2 – SECOND MODE FREQUENCY RESPONSE, E–W DIRECTION

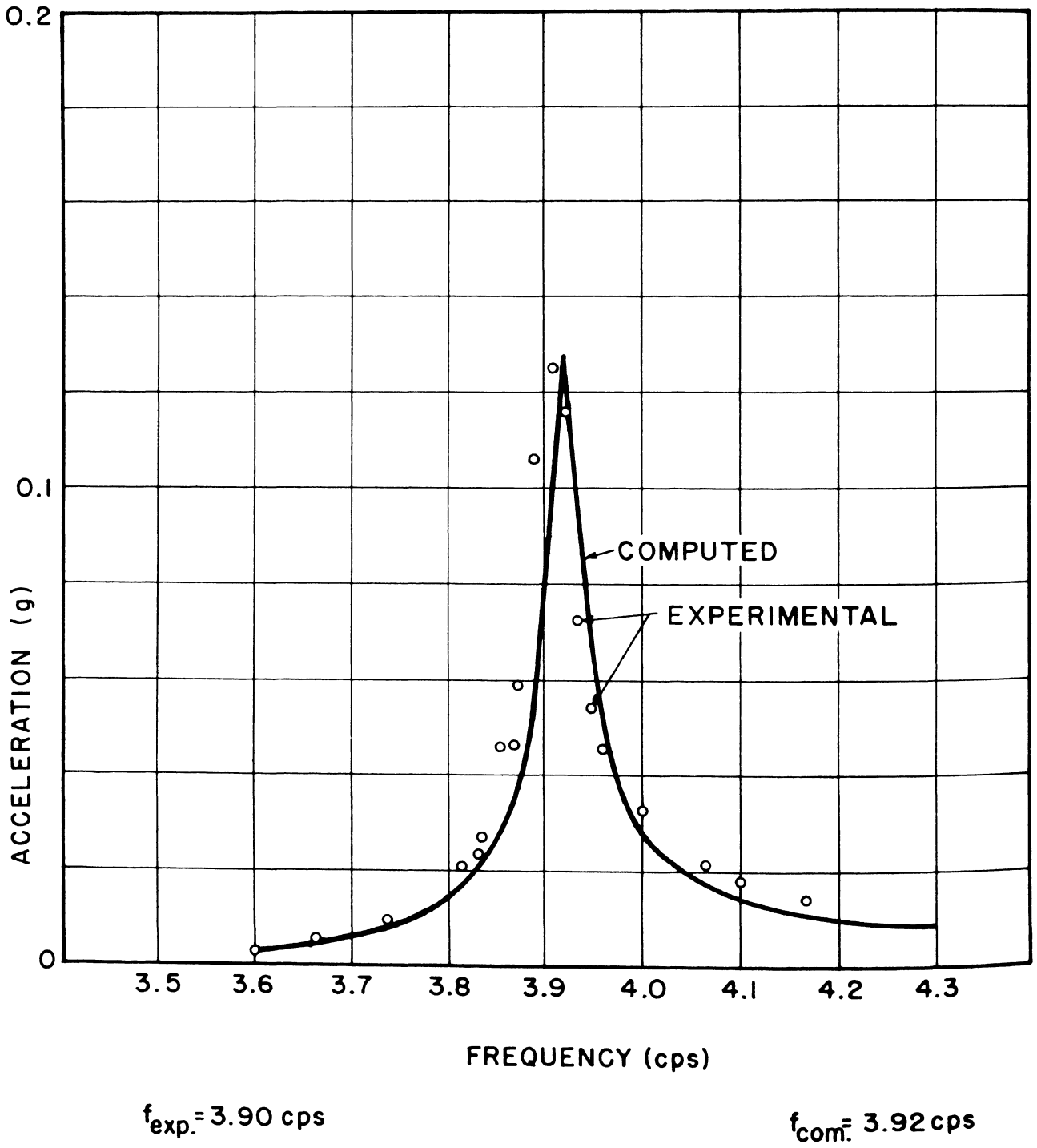

FIG. 4.3 – THIRD MODE FREQUENCY RESPONSE, E–W DIRECTION

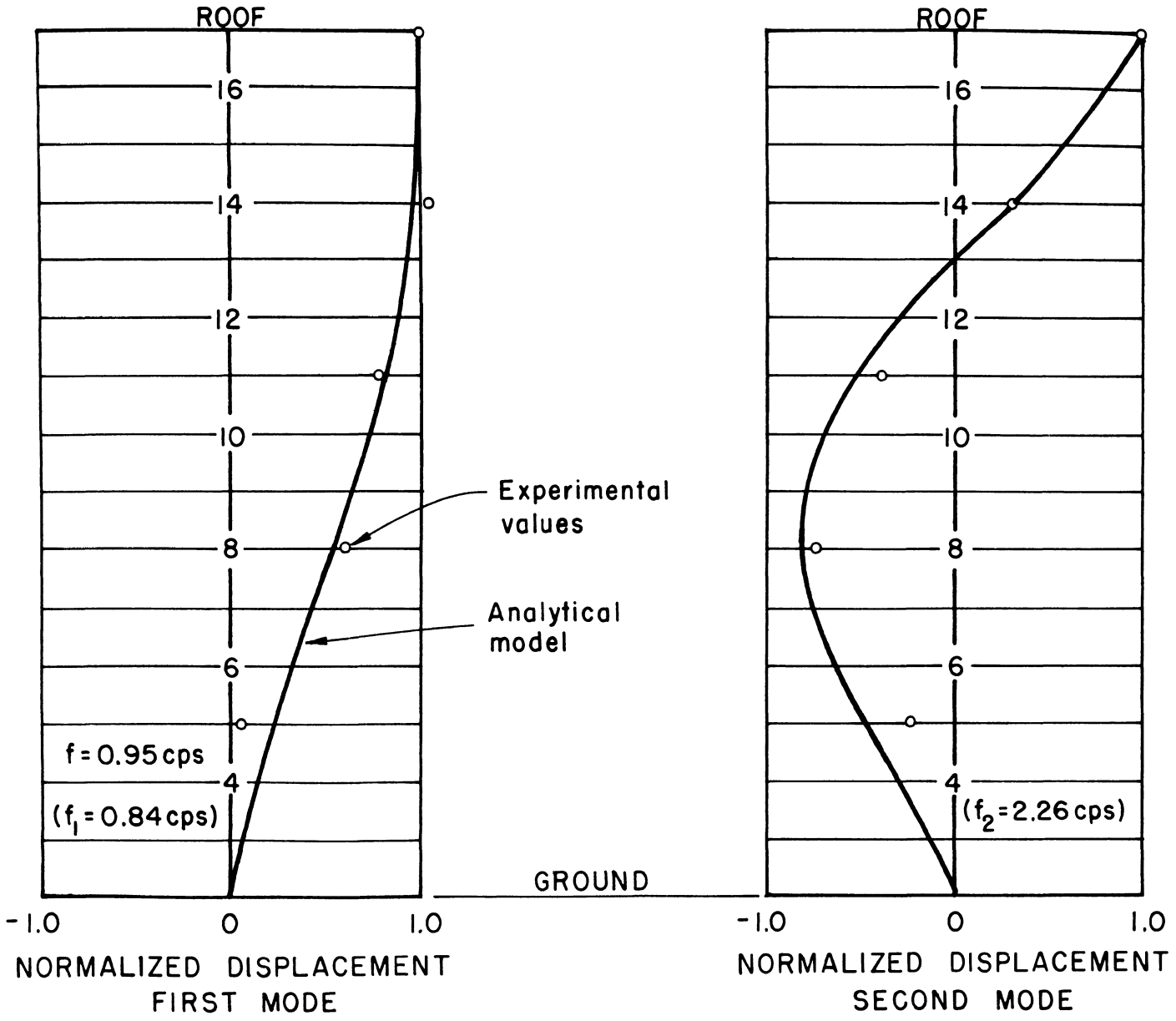

FIG. 4.4

MODE SHAPES OF MODEL AND PROTOTYPE

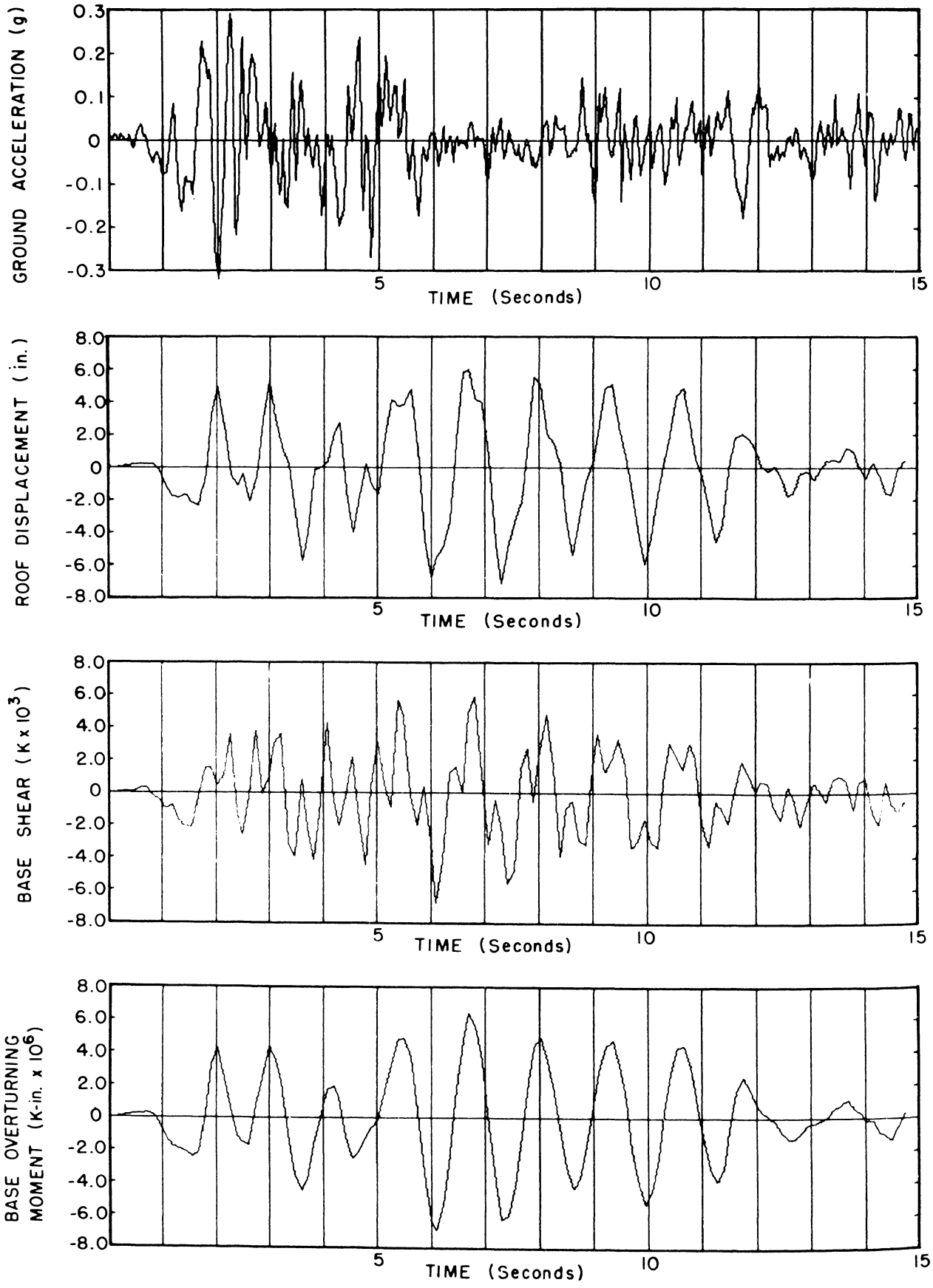

FIG. 4.5 – RESPONSE OF SUMMER 1964 MODEL TO EL CENTRO EARTHQUAKE

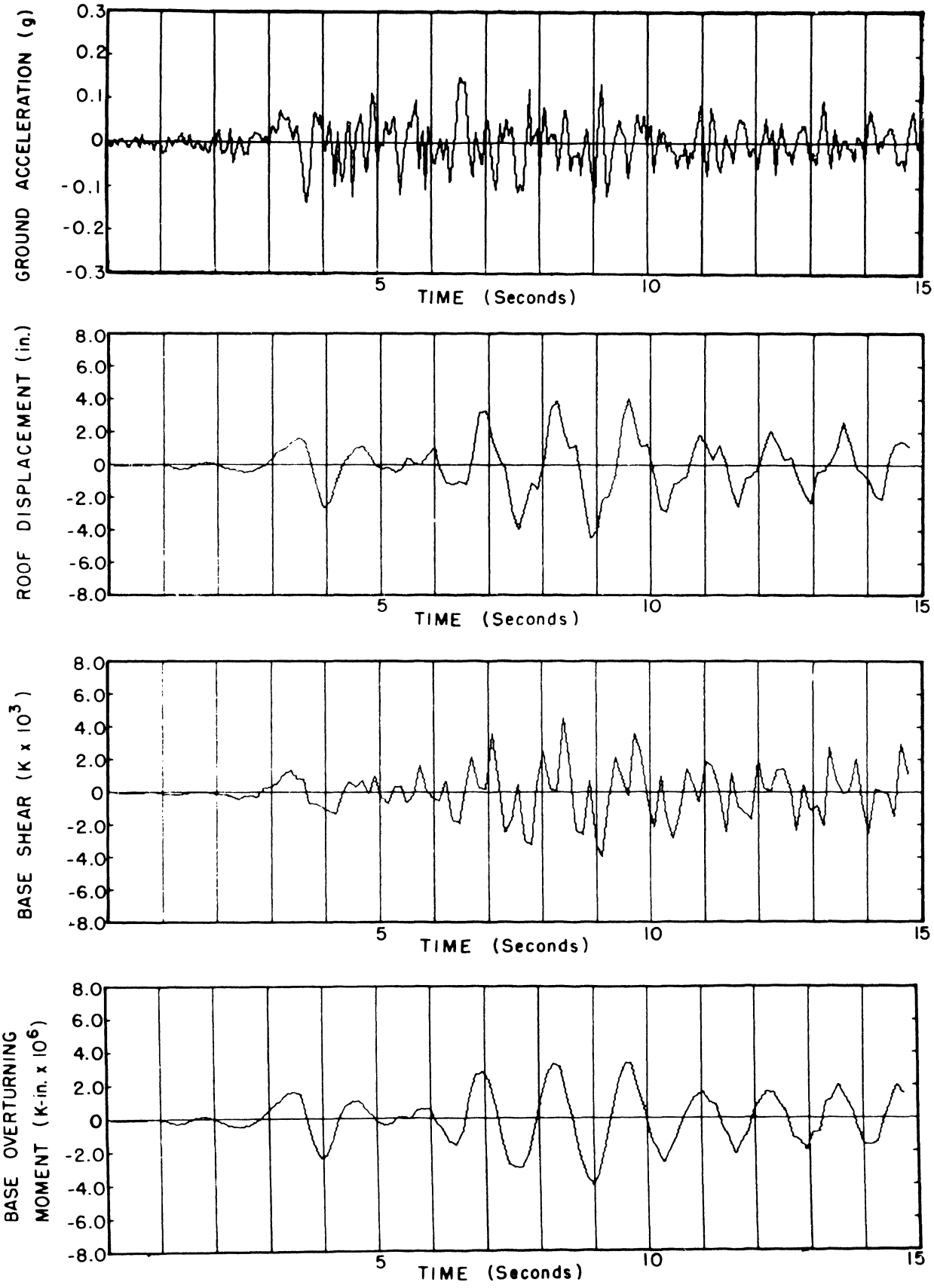

FIG. 4.6 – RESPONSE OF SUMMER 1964 MODEL TO TAFT EARTHQUAKE

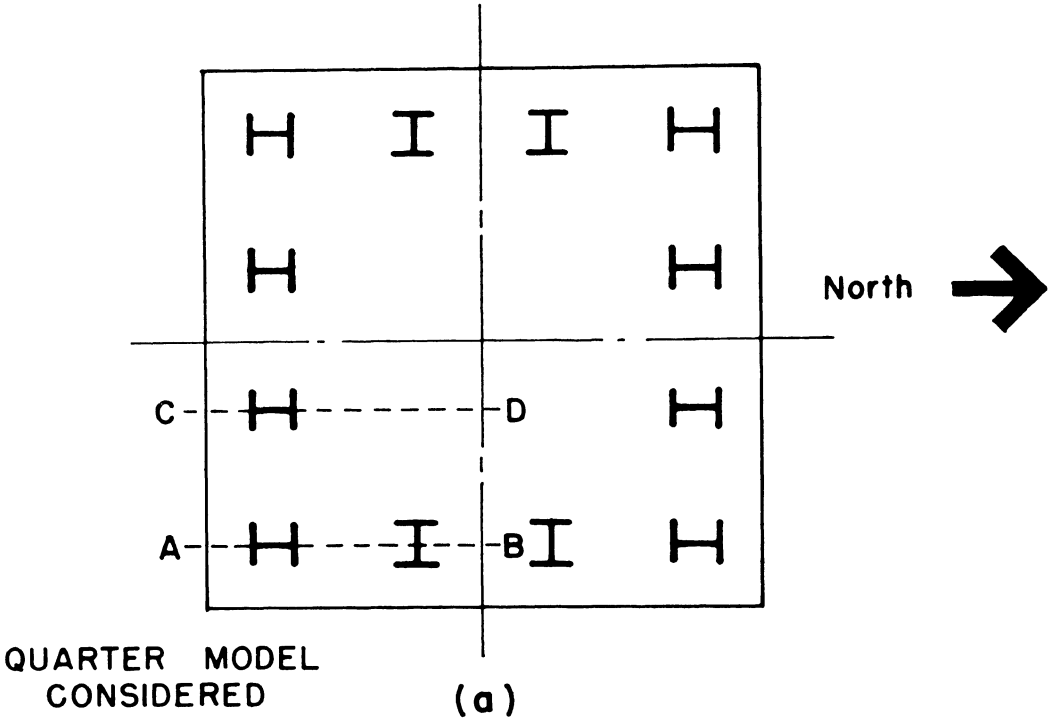

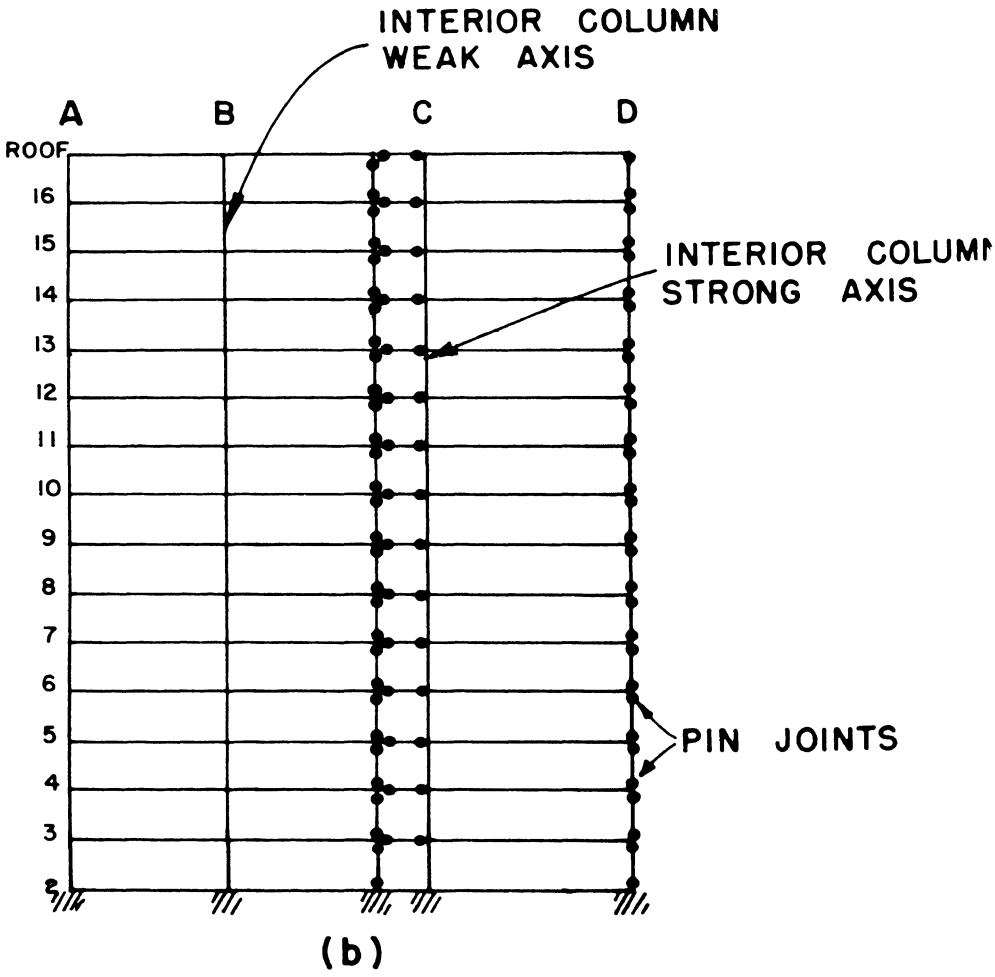

FIG. 4.7 – EQUIVALENT PLANE FRAME OF QUARTER MODEL

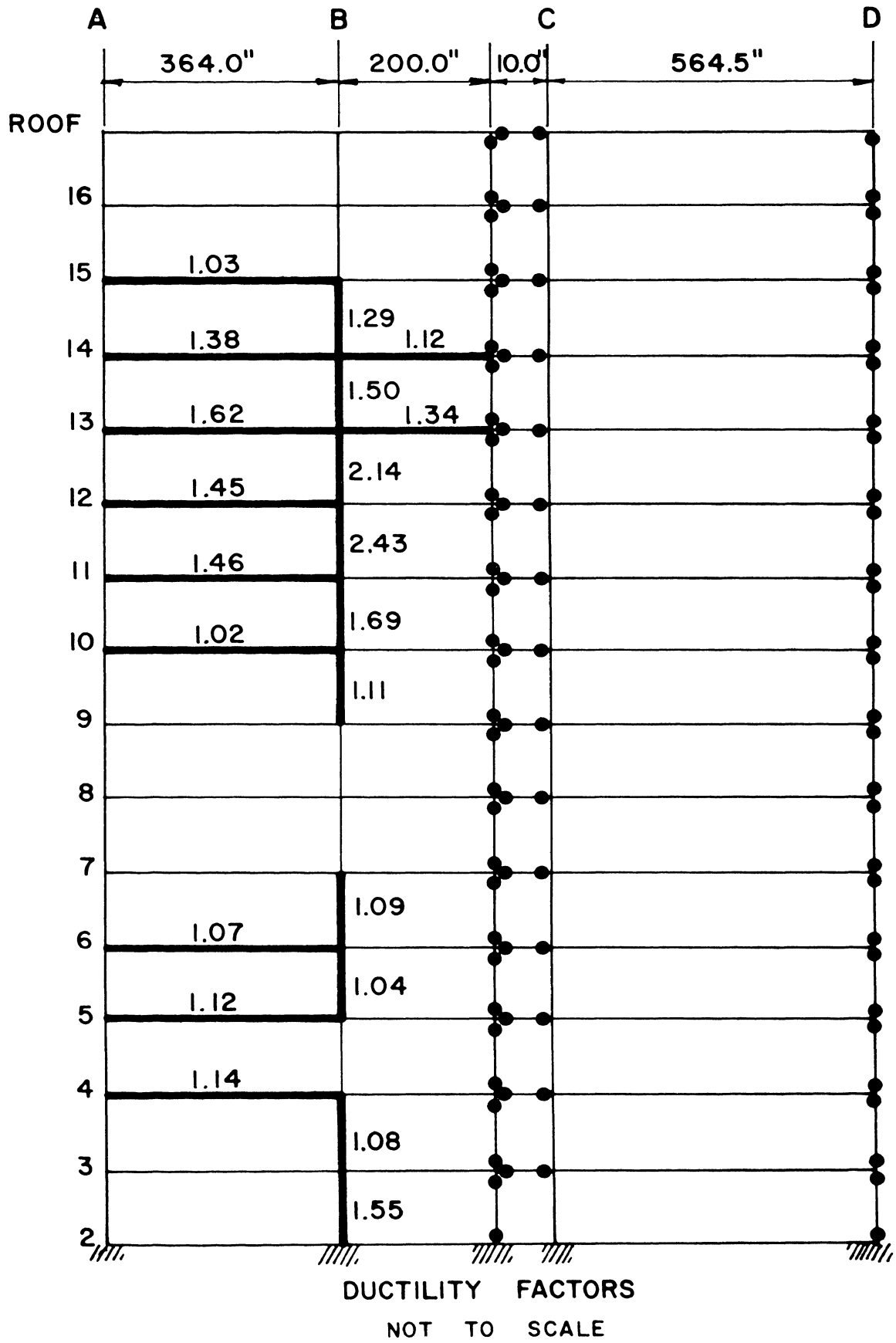

FIG. 4.8 – YIELD MECHANISM OF EAST BUILDING WITH ZERO DAMPING, EL CENTRO EARTHQUAKE

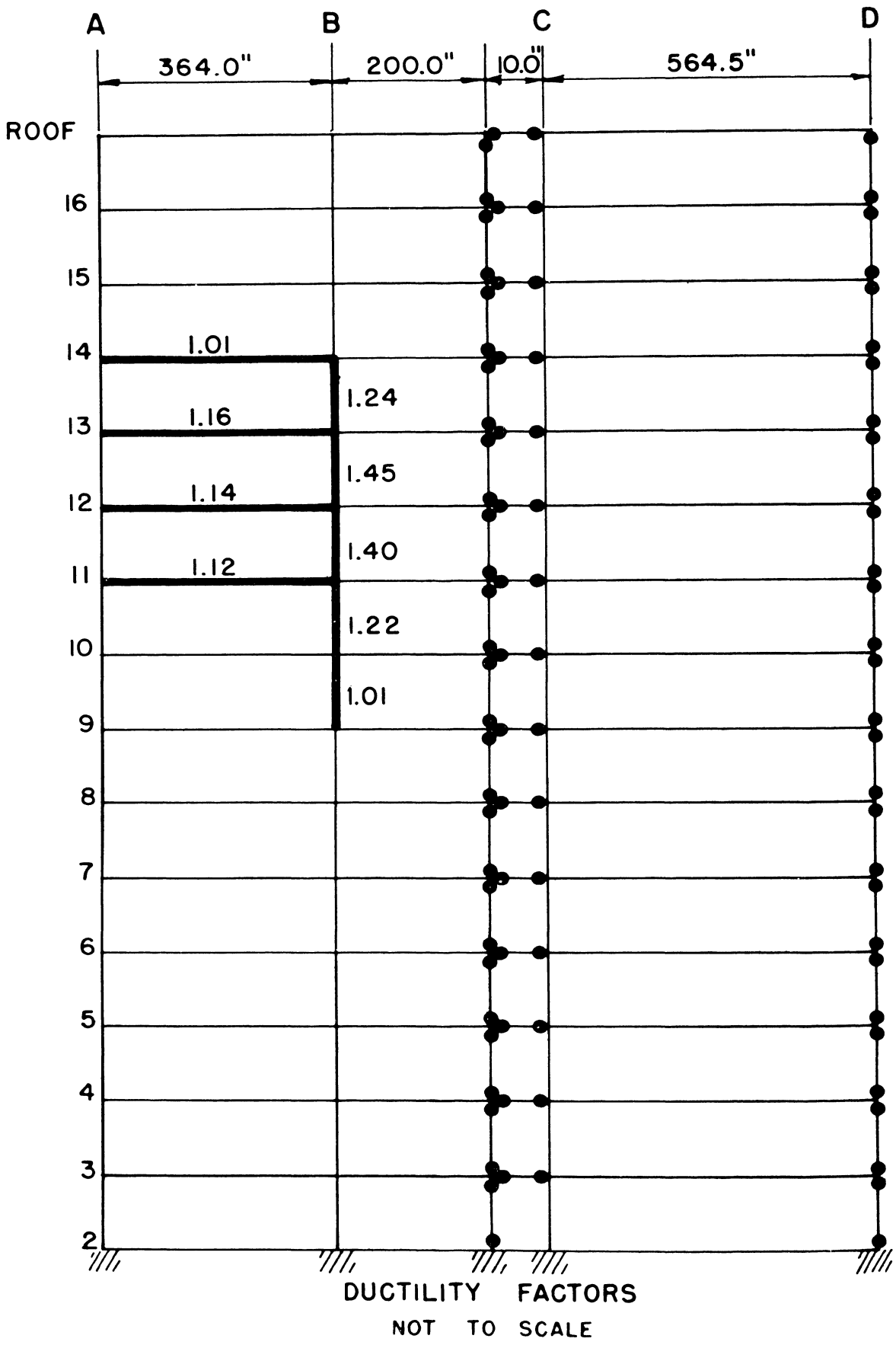

FIG. 4.9 – YIELD MECHANISM OF EAST BUILDING WITH 5% CRITICAL DAMPING IN 1st MODE. 1.30 x EL CENTRO EQ.

BULLETINS

Steel Research for Construction

No. 1 Current Paving Practices on Orthotropic Bridge Decks
Battelle Memorial Institute, October, 1965

No. 2 Strength of Three New Types of Composite Beams
A. A. Toprac, October, 1965

No. 3 Research on and Paving Practices for Wearing Surfaces on Orthotropic Steel Bridge Decks, Supplement to Bulletin 1
Battelle Memorial Institute, August, 1966

No. 4 Protection of Steel Storage Tanks and Pipe Underground
Battelle Memorial Institute, May, 1967

No. 5 Fatigue Strength of Shear Connectors
R. G. Slutter and J. W. Fisher, October, 1967

No. 6 Paving Practices for Wearing Surfaces on Orthotropic Steel Bridge Decks, Supplement to Bulletins 1 and 3
Battelle Memorial Institute, January, 1968

No. 7 Report on Investigation of Orthotropic Plate Bridges
D. Allan Firmage, February, 1968

No. 8 Deformation and Energy Absorption Capacity of Steel Structures in the Inelastic Range
T. V. Galambos, March, 1968

No. 9 The Dynamic Behavior of Steel Frame and Truss Buildings
Dixon Rea, J. G. Bouwkamp and R. W. Clough, April, 1968

Committee of Structural Steel Producers • Committee of Steel Plate Producers

american iron and steel institute

150 East 42nd Street, New York, N. Y. 10017